HAL
open science

# General Synthesis Report of the Different ADS Design Status. Establishment of a Catalogue of the R&D needs

G. Rimpault, Patrick Richard, L. Mansani, F. Frogheri, A. Woaye-Hune, S. Ehster-Vignoud, S. Larmignat, A. Mueller, J.L. Biarotte, C. Artioli, et al.

## To cite this version:

G. Rimpault, Patrick Richard, L. Mansani, F. Frogheri, A. Woaye-Hune, et al.. General Synthesis Report of the Different ADS Design Status. Establishment of a Catalogue of the R&D needs. [Contract] EURATOM. 2010. hal-01084509

**HAL Id: hal-01084509**

**https://hal.science/hal-01084509**

Submitted on 19 Nov 2014

**HAL** is a multi-disciplinary open access archive for the deposit and dissemination of scientific research documents, whether they are published or not. The documents may come from teaching and research institutions in France or abroad, or from public or private research centers.

L'archive ouverte pluridisciplinaire **HAL**, est destinée au dépôt et à la diffusion de documents scientifiques de niveau recherche, publiés ou non, émanant des établissements d'enseignement et de recherche français ou étrangers, des laboratoires publics ou privés.

# SIXTH FRAMEWORK PROGRAMME
# EURATOM
# Management of Radioactive Waste

| | |
|---|---|
| Project acronym: | EUROTRANS |
| Project full title: | EUROpean Research Programme for the TRANSmutation of High Level Nuclear Waste in an Accelerator Driven System |
| Contract no.: | FI6W-CT-2004-516520 |

| | |
|---|---|
| Domain: | *DM1DESIGN* |
| Workpackage N°: | *WP1.1* |
| Identification N°: | *D1.70* |
| Type of document: | *Deliverable* |
| Title: | *General Synthesis Report of the Different ADS Design Status. Establishment of a Catalogue of the R&D needs.* |
| Dissemination Level: | *PU* |
| Reference: | *CEA/DEN/CAD/DER/SPRC/LEDC/RT 10-2* |
| Status: | *Final* |

| | Name | Partner | Date | Signature |
|---|---|---|---|---|
| written by: (*) | G. Rimpault | CEA | 15/7/2010 | |
| WP leader: (*) | G. Rimpault | CEA | 15/7/2010 | |
| DM leader: (*) | D. De Bruyn | SCK•CEN | 16/7/2010 | |
| IP leader: (*) | J. U. Knebel | KIT | - | |

(*) when relevant

CONTRACT N°: FI6W-CT-2004-516529

FP6

ISSUE CERTIFICATE

# EUROTRANS

## EUROpean Research Programme for the TRANSmutation of High Level Nuclear Waste in an Accelerator Driven System

**Domain N°:** *DM1 DESIGN*

**Workpackage N°: WP1.1**

**Identification N°: D1.70** **Revision: 0**

## General Synthesis Report of the Different ADS Design Status. Establishment of a Catalogue of the R&D needs.

**Dissemination Level:** *PU*

**Issued by:** *CEA*

**Reference:** *CEA RT/DEN/DER/SPRC/LEDC/10-2*

**Status:** *Final*


**Summary:**

The EUROTRANS Integrated Project had the goal to demonstrate the possibility of nuclear waste transmutation/burning in Accelerator Driven Systems (ADS) at industrial scale.

A Pb-cooled ADS for the European Facility on Industrial scale Transmuter (ETD/EFIT) has been designed with a back-up solution based on an He cooled ADS.

As an intermediate step towards this industrial-scale prototype, an eXperimental Transmuter based on ADS concept (ETD/XT-ADS) able to demonstrate both the feasibility of the ADS concept and to accumulate experience on U-free fuel.

The two machines (XT-ADS and Pb-cooled EFIT) have been designed with sufficient details to allow definition of the critical issues as regards design, safety and associated technological and basic R&D needs. The different designs fit rather well with the technical objectives fixed at the beginning of the project.

The superconducting LINAC accelerator has been clearly assessed as the most suitable concept for the three reactors in particular with respect to the stringent requirements on reliability. R&D needs are focused on critical components (injector, cryomodule) long term testing.

The design of the different ADS has been performed in view of what is reasonably achievable pending the completion of R&D programmes. Pending questions associated to technology gaps have been identified through the different appropriate R&D work programmes and a Catalogue of the R&D needs has been established.


| | RESPONSIBLE Name/Company/Signature | WP LEADER Name/Company/Signature | DM CO-ORDINATOR Name/Company/Signature |
|---|---|---|---|
| Name | G. Rimpault | G. Rimpault | D. De Bruyn |
| Company | CEA | CEA | SCK-CEN |
| Date | 5/8/2010 | 5.8.2010 | 5.8.2010 |
| Signature | | | |

| | |
|---|---|
| Direction de l'Énergie Nucléaire<br>Direction du Centre de Cadarache<br>Département d'Études des Réacteurs<br>Service de Physique des Réacteurs et du Cycle<br>Laboratoire d'Etudes et Développements des Cœurs | CEA/DEN/CAD/DER/SPRC/LEDC<br>DO 2 14/01/10<br>10PPMU000003<br>diffusé le : 14/01/10 |


# Rapport Technique DEN

## *General Synthesis Report of the Different ADS Design Status. Establishment of a Catalogue of the R&D needs.*

Référence

SPRC/LEDC/RT 10-2

## Authors


G. Rimpault, P. Richard (CEA), L. Mansani, F. Frogheri (ANSALDO), A. Woaye-Hune, S. Ehster-Vignoud, S. Larmignat (AREVA), A. Mueller, J.-L. Biarrotte (CNRS), C. Artioli, G. Glinatsis (ENEA), M. Schikorr, D. Struwe, W. Maschek (FZK), D. De Bruyn, D. Maes, G. Van den Eynde,V. Sobolev(SCK•CEN), J. Wallenius (KTH), A. Guertin (Subatech), Carmen Angulo (Tractebel Engineering)

with contributions from

G. Granget, F. Delage, S. Leray (CEA), C. Fazio (FZK), E. Gonzales (CIEMAT)

**Commissariat à l'Énergie Atomique**

**Centre : CADARACHE**

**Adresse de l'unité émettrice : DER/SPRC Bâtiment 230A**
**13108 SAINT PAUL LEZ DURANCE CEDEX - FRANCE**

**Tél. : 04.42.25.26.05** **Fax : 04.42.25.75.95** **Courriel : sprcledccad@cea.fr**

**Établissement Public à caractère Industriel et Commercial**

**RCS Paris B 775 685 019**



***This document refers to work being performed by scientists and institutions involved in IP EUROTRANS, as well as the financial support of the European Commission through the contract FI6W-CT-2004-516520.***

| NIVEAU DE CONFIDENTIALITÉ | | | | |
|---|---|---|---|---|
| DO | DR | CCEA | CD | SD |
| X | | | | |

| PARTENAIRES/CLIENTS | ACCORD | TYPE D'ACTION |
|---|---|---|
| ***European Commission*** | ***Contract FI6W-CT-2004-516520*** | 6th Frame Work Programme |

| RÉFÉRENCES INTERNES CEA | | | |
|---|---|---|---|
| DIRECTION D'OBJECTIFS | DOMAINE | PROJET | EOTP |
| DISN | R4G | ASYIN | A-ASYIN-03-02 |
| JALON | INTITULÉ DU JALON | DÉLAI CONTRACTUEL DE CONFIDENTIALITÉ | CAHIERS DE LABORATOIRE |
| - | - | - | - |

| SUIVI DES VERSIONS | | | |
|---|---|---|---|
| INDICE | DATE | NATURE DE L'ÉVOLUTION | PAGES, CHAPITRES |
| 0 | 15/07/10 | Emission initiale | |
| | | | |

| | NOM | FONCTION | VISA | DATE |
|---|---|---|---|---|
| **RÉDACTEUR** | G. Rimpault | Expert Sénior | | 15/7/2010 |
| **VÉRIFICATEUR** | P. Richard | Ingénieur | | 21/07/10 |
| **APPROBATEUR** | B. Fontaine | Chef de Laboratoire | | 22/07/10 |
| **ÉMETTEUR** | JP. Grouiller | Chef de Service | pr | 04/08/2010 |

*This document refers to work being performed by scientists and institutions involved in IP EUROTRANS, as well as the financial support of the European Commission through the contract FI6W-CT-2004-516520.*

**KEY WORDS MOTS CLEFS**

Transmutation, EUROTRANS, ADS Design

**RÉSUMÉ / CONCLUSIONS**

This document is a General Synthesis Report of the Different ADS Design Status being designed within the EUROTRANS Integrated Project; an FP6 European commission partially funded programme. This project had the goal to demonstrate the possibility of nuclear waste transmutation/burning in Accelerator Driven Systems (ADS) at industrial scale.

The focus is on a Pb-cooled ADS for the European Facility on Industrial scale Transmuter (ETD/EFIT) with a back-up solution based on an He cooled ADS.

As an intermediate step towards this industrial-scale prototype, an eXperimental Transmuter based on ADS concept (ETD/XT-ADS) able to demonstrate both the feasibility of the ADS concept and to accumulate experience when using dedicated fuel sub-assemblies or dedicated pins within a MOX fuel core has been also studied.

The two machines (XT-ADS and Pb cooled EFIT) have been designed in a consistent way bringing more credibility to the potential licensing of these plants and with sufficient details to allow definition of the critical issues as regards design, safety and associated technological and basic R&D needs. The different designs fit rather well with the technical objectives fixed at the beginning of the project in consistency with the European Roadmap on ADS development.

For what concerns the accelerator, the superconducting LINAC has been clearly assessed as the most suitable concept for the three reactors in particular with respect to the stringent requirements on reliability. Associated R&D needs have been identified and will be focused on critical components (injector, cryomodule) long term testing.

The design of the different ADS has been performed in view of what is reasonably achievable pending the completion of R&D programmes. The way the EUROTRANS Integrated Project has been organised with other domains than the DM1 Design being specifically devoted to R&D tasks in support to the overall ETD/EFIT and ETD/XT-ADS design tasks has been helpful. The other domains were centred on the assessment of reactivity measurement techniques (DM2 ECATS), on the development of U-free dedicated fuels (DM3 AFTRA), on materials behaviour and heavy liquid metal technology (DM4 DEMETRA) and on nuclear data assessment (DM5 NUDATRA). Pending questions associated to technology gaps have been identified through the different appropriate R&D work programmes and a Catalogue of the R&D needs has been established.

Finally, the work within the EUROTRANS integrated project has provided an overall assessment of the feasibility at a reasonable cost for an ADS based transmutation so that a decision can be taken to launch a detailed design and construction of the intermediate step Experimental ADS now already launched within the 7$^{th}$ FP programme under the name of Common Design Team (CDT).

*This document refers to work being performed by scientists and institutions involved in IP EUROTRANS, as well as the financial support of the European Commission through the contract FI6W-CT-2004-516520.*

# BORDEREAU D'ENVOI

| Date : 31/03/2010 | N/Réf : | CEA/DEN/CAD/DER/SPRC<br>RT SPRC/LEDC 10-2<br>Indice 0 |
|---|---|---|
| Destinataires : | | |
| | Nombre | Observations |
| | | *Diffusion du document complet (transmis par courriel sous format PDF)* |
| **SCK.MOL** | | |
| D. DE BRUYN | 1 | Avec issue certificate<br>Pour diffusion interne EUROTRANS |
| **DEN/SAC/DISN/R4G** | | |
| J. ROUAULT | 1 | |
| **DEN/SAC/DISN/R4G** | | |
| P. ANZIEU | 1 | |
| **DEN/DER** | | |
| A. ZAETTA | 1 | |
| G. WILLERMOZ | 1 | |
| **DEN/DER/SPRC** | | |
| D. GIBIAT | 1 | Portail documentaire SPRC e-doc |
| **DEN/DER/SESI** | | |
| Ph DARDE | 1 | |
| C. RENAULT | 1 | |
| **DEN/SPEX/LPE** | | |
| J.C. BOSQ | 1 | |
| F. MELLIER | 1 | |
| Ch. JAMMES | 1 | |
| Ch. DESTOUCHES | 1 | |
| **DEN/DER/SESI/L4G** | | |
| F. VARAINE | 1 | |
| P. RICHARD | 1 | |
| G. GRANGET | 1 | |
| **DEN/DER/SESI/LE2S** | | |
| D. PLANCQ | 1 | |
| JF PIGNATEL | 1 | |
| T. CADIOU | 1 | |
| **DEN/DEC/SESC** | | |
| F. DELAGE | 1 | |
| P. JACKY | 1 | |
| S. PILLON | 1 | |

*This document refers to work being performed by scientists and institutions involved in IP EUROTRANS, as well as the financial support of the European Commission through the contract FI6W-CT-2004-516520.*

# BORDEREAU D'ENVOI (Suite)

| Date : 31/03/2010 | N/Réf : | CEA/DEN/CAD/DER/SPRC<br>RT SPRC/LEDC 10-2<br>Indice 0 |
|---|---|---|
| Destinataires : | | |
| | Nombre | Observations |
| | | *Diffusion du document complet (transmis par courriel sous format PDF)* |
| **DSM/IRFU/ShN**<br>S. LERAY | 1 | |
| **DSM/DAPNIA/SACM**<br>R. GOBIN | 1 | |
| **DEN/DTN/DIR**<br>Ch. LATGE | 1 | |
| **DEN/DTN/STPA/LTRS**<br>F. BEAUCHAMP | 1 | |
| **DEN/DENS/DPC/SCCME/LECNA**<br>F. BALBAUD | 1 | |
| **DEN/DMN/SRMA/LA2M**<br>J. HENRY | 1 | |
| **DEN/DPC/SCCME/LECNA**<br>JL. COUROUAU | 1 | |
| **DEN/ITESE**<br>F. LEGEE<br>G. MATHONNIERE | 1<br>1 | |
| | | *Diffusion 5 premières pages* |
| DEN/SAC/DISN/R4G | 1 | |
| DEN/CAD/DEC | 1 | |
| DEN/CAD/DER | 1 | |
| DEN/CAD/DER/SESI | 1 | |
| DEN/CAD/DER/SPEX | 1 | |
| DEN/GRE/DER/SSTH | 1 | |

*This document refers to work being performed by scientists and institutions involved in IP EUROTRANS, as well as the financial support of the European Commission through the contract FI6W-CT-2004-516520.*

# SUMMARY

**1. INTRODUCTION AND SCOPE ..... 11**

**1.1 ADS UNDERLYING OBJECTIVES ..... 12**
**1.2 PERSPECTIVES ON PARTITIONING &TRANSMUTATION ..... 12**
1.2.1 ORIGIN OF NUCLEAR WASTE ..... 12
1.2.2 RADIO-TOXICITY ..... 15
**1.3 FUEL CHOICES ..... 16**

**2. DESCRIPTION OF THE ETD ACCELERATOR ..... 20**

**2.1 BEAM CHARACTERISTICS ..... 20**
2.1.1 ACCELERATOR GENERAL PERFORMANCES ..... 20
2.1.2 RELIABILITY AND AVAILABILITY ..... 20
2.1.3 OPERATION ..... 21
2.1.4 ACCELERATOR BEAM TIME STRUCTURE FOR DYNAMIC REACTIVITY MEASUREMENTS ..... 22
**2.2 THE REFERENCE ADS ACCELERATOR ..... 22**
2.2.1 THE LINAC FRONT-END ..... 23
2.2.2 THE INDEPENDENTLY-PHASED SC LINAC ..... 24
2.2.3 THE FINAL BEAM TRANSPORT LINE ..... 26
2.2.4 RELIABILITY-ORIENTED DESIGN ..... 26
2.2.5 TOLERANCE TO RF FAULTS IN THE SC LINAC ..... 27
2.2.6 RELIABILITY ANALYSIS AND DISCUSSION ..... 28
2.2.7 CONCLUSION ON THE ACCELERATOR DESIGN ..... 28
**2.3 RATIONALE FOR THE MAXIMUM ALLOWABLE NUMBER OF BEAM TRIPS ..... 29**
2.3.1 METHODOLOGY ..... 29
2.3.2 PHENIX OPERATION AND ALLOWABLE NUMBER OF SCRAM ..... 29
2.3.3 OPERATING TRANSIENTS AND DAMAGE THROUGH FATIGUE AND/OR FATIGUE-CREEP ..... 30
2.3.4 STRUCTURE INTEGRITY DUE TO BEAM TRIPS ..... 31
2.3.4.1 Main components ..... 31
2.3.4.2 Fuel Elements ..... 32
2.3.5 PERSPECTIVES FOR THE MAXIMUM ALLOWABLE BEAM TRIPS ..... 34

**3. DESCRIPTION OF THE 395 MWTH PB-COOLED EFIT ..... 37**

**3.1 CHOICE OF COOLANT TEMPERATURES ..... 37**
**3.2 EFIT-PB CORE DESIGN ..... 39**
3.2.1 DESIGN APPROACH ..... 39
3.2.2 CORE DESCRIPTION ..... 41
3.2.3 DECAY HEAT GENERATION. ..... 43
3.2.4 SUMMARY OF THE CERCER CORE DESIGN ..... 44
3.2.5 THE CERMET CORE DESIGN VARIANT ..... 44
**3.3 EFIT-PB PRIMARY SYSTEM ..... 46**
3.3.1 MAIN LAY OUT DESCRIPTION ..... 46
3.3.2 REACTOR VESSEL AND INTERNAL STRUCTURE ..... 50

*This document refers to work being performed by scientists and institutions involved in IP EUROTRANS, as well as the financial support of the European Commission through the contract FI6W-CT-2004-516520.*

3.3.2.1 Reactor Vessel and Support System ..... 50
3.3.2.2 Internal structure ..... 51
3.3.3 STEAM GENERATOR AND PRIMARY PUMP SUB-ASSEMBLY ..... 51
3.3.3.1 Steam generator Unit ..... 51
3.3.3.2 Primary coolant pumps ..... 52
**3.4 DECAY HEAT REMOVAL SYSTEM ..... 56**
3.4.1 DHR 1 SYSTEM: DIRECT REACTOR COOLING (DRC) SYSTEM ..... 56
3.4.2 MOLTEN LEAD-DIATHERMIC OIL HEAT EXCHANGER (DIP COOLER, DHX) ..... 56
3.4.3 AIR-DIATHERMIC OIL VAPOUR CONDENSER (AVC) ..... 57
3.4.4 ISOLATION CONDENSER SYSTEM ..... 58
**3.5 THE TARGET UNIT ..... 63**
**3.6 INTEGRATED COOLANT PURIFICATION UNIT ..... 65**
**3.7 PRIMARY SYSTEM CHEMISTRY CONTROL ..... 65**

**4. DESCRIPTION OF THE 400 MWTH HE-COOLED EFIT ..... 68**

**4.1 DESIGN OBJECTIVES AND CRITERIA CONSIDERED IN THE EFIT-HE DESIGN ..... 68**
**4.2 PLANT CHARACTERISTICS ..... 68**
4.2.1 DEFINITION OF INLET/OUTLET TEMPERATURES – POWER CONVERSION CYCLE ..... 69
4.2.2 FUEL CLADDING ..... 70
4.2.3 SUMMARY OF THE MAIN HE EFIT PLANT CHARACTERISTICS ..... 70
**4.3 DESCRIPTION OF THE ACCELERATOR AND SPALLATION TARGET ..... 72**
**4.4 EFIT-HE CORE DESIGN ..... 73**
4.4.1 MAIN SUB-CRITICAL CORE CHARACTERISTICS ..... 73
4.4.2 CORE COMPOSITION ..... 74
4.4.3 HE EFIT CORE PERFORMANCES ..... 75
**4.5 EFIT-HE SYSTEM LAY OUT ..... 79**
**4.6 REACTOR VESSEL AND INTERNALS ..... 81**
4.6.1 THE DIAGRID ..... 81
4.6.2 THE SUPPORT PLATE ..... 81
4.6.3 INNER VESSEL ..... 82
4.6.4 MAIN VESSEL AND COVER HEAD ..... 82
**4.7 HEAT EXCHANGER ..... 82**
**4.8 DHR SYSTEM ..... 83**

**5. DESCRIPTION OF THE 57 MWTH LBE-COOLED XT-ADS (MYRRHA) ..... 86**

**5.1 GENERAL DESCRIPTION OF THE XT-ADS PLANT LAY OUT ..... 86**
**5.2 XT-ADS WINDOWLESS SPALLATION TARGET DESIGN ..... 88**
5.2.1 SPALLATION TARGET BOUNDARY CONDITIONS ..... 88
5.2.2 SPALLATION LOOP LAYOUT ..... 89
5.2.3 FREE SURFACE AND RECIRCULATION ZONE ..... 90
5.2.4 LBE AS COOLANT AND TARGET MATERIAL ..... 90
5.2.5 PUMPING OPTIONS ..... 90
5.2.6 VACUUM SYSTEM ..... 91
5.2.7 DESIGN SUPPORT STUDIES ..... 91
5.2.8 MHD PUMP DEFINITION ..... 91

*This document refers to work being performed by scientists and institutions involved in IP EUROTRANS, as well as the financial support of the European Commission through the contract FI6W-CT-2004-516520.*

5.2.9 TARGET NOZZLE ..... 92
5.2.10 HEAT DEPOSITION ..... 93
5.2.11 THERMAL-HYDRAULICS ..... 93
5.2.12 BEAM TARGET INTERACTION ..... 94
5.2.13 SAFETY ANALYSIS ..... 94
**5.3 PRIMARY SYSTEM ..... 94**
5.3.1 SAFETY CONSTRAINTS ..... 94
5.3.2 DESCRIPTION OF THE PRIMARY LOOP ..... 96
5.3.3 HEAT EXCHANGERS ..... 97
5.3.4 PRIMARY PUMPS ..... 98
5.3.5 PRIMARY SYSTEM AUXILIARIES ..... 98
**5.4 SECONDARY SYSTEM ..... 99**
**5.5 DECAY HEAT REMOVAL SYSTEM ..... 101**
**5.6 REACTOR VESSELS, COVER AND DIAPHRAGM ..... 101**
**5.7 CORE SUPPORT STRUCTURE ..... 102**
**5.8 IN-VESSEL FUEL STORAGE ..... 102**
**5.9 IN-VESSEL FUEL HANDLING MACHINES ..... 103**
**5.10 CORE DESIGN ..... 104**
5.10.1 PRESENTATION OF THE CORE DESIGN ..... 104
5.10.2 CRITICALITY AND SOURCE CALCULATIONS ..... 107
5.10.3 IRRADIATION CAPABILITIES ..... 109

**6. SAFETY EVALUATION OF THE ETD CONCEPTS ..... 113**

**6.1 SAFETY STATUS OF EFIT-PB PLANT ..... 113**
6.1.1 SUBCRITICALITY MARGIN ASSESSMENT ..... 113
6.1.2 EFIT-PB SAFETY GUIDELINES ..... 113
6.1.3 EFIT-PB ULOF TRANSIENT STUDIES ..... 114
6.1.4 OTHER EFIT-PB TRANSIENT STUDIES ..... 116
6.1.5 OVERALL EFIT-PB SAFETY STUDIES SUMMARY ..... 118
**6.2 SAFETY STATUS OF EFIT-HE PLANT ..... 121**
6.2.1 EFIT-HE SAFETY APPROACH AND PLOF TRANSIENT STUDIES ..... 121
6.2.2 OTHER EFIT-HE TRANSIENT STUDIES ..... 130
6.2.3 EFIT-HE SAFETY STUDIES SUMMARY ..... 132
6.2.4 PLANT BEHAVIOUR UNDER TRANSIENT CONDITIONS ..... 132
6.2.5 CORE SAFETY FEATURES ..... 133
**6.3 SAFETY STATUS OF XT-ADS PLANT ..... 134**
6.3.1 SAFETY APPROACH FOR THE XT-ADS PLANT ..... 134
6.3.2 XT-ADS ULOF TRANSIENT STUDIES ..... 135
6.3.3 XT-ADS OTHER DBC AND DEC TRANSIENT STUDIES ..... 138
6.3.4 XT-ADS OVERALL SAFETY ASSESSMENT STUDIES ..... 141

**7. CONSISTENCY OF THE DIFFERENT CONCEPTS WITH THE ETD OBJECTIVES ..... 144**

**7.1 EFIT-PB DESIGN ..... 144**
7.1.1 CURRENT FEATURES ..... 144
7.1.2 POTENTIAL FOR DESIGN OPTIMISATION ..... 147

*This document refers to work being performed by scientists and institutions involved in IP EUROTRANS, as well as the financial support of the European Commission through the contract FI6W-CT-2004-516520.*

**7.2 EFIT-HE DESIGN ..... 149**
**7.3 XT-ADS DESIGN ..... 151**

**8. STRUCTURAL INTEGRITY/ROBUSTNESS ..... 155**

**8.1 EFIT-PB DESIGN ..... 155**
**8.2 EFIT-HE DESIGN ..... 158**
8.2.1 DHR DESIGN STRATEGY ..... 158
8.2.2 EFIT-HE DESIGN ROBUSTNESS ..... 160
**8.3 XT-ADS DESIGN ..... 160**
8.3.1 EFIT & XT-ADS COMMON CHARACTERISTICS ..... 160
8.3.2 CHANGES COMPARED TO MYRRHA DRAFT 2 DESIGN ..... 161
8.3.3 DOSE RATES OF THE CORE BARREL AND THE UPPER GRID PLATE AND RECOMMENDATIONS ..... 162
8.3.4 XT-ADS CORE SUPPORT STRUCTURES ..... 163
8.3.5 FUEL CLADDING ..... 165
8.3.6 RECOMMENDATIONS TOWARDS CDT ..... 165

**9. ECONOMICS ..... 167**

**9.1 XT-ADS COST ..... 167**
**9.2 EFIT-PB COST ..... 168**
**9.3 ECONOMIC TRENDS ..... 169**
**9.4 RELIABILITY/AVAILABILITY ..... 170**

**10. OPTION VALIDATION STATUS (R&D NEEDS) ..... 172**

**10.1 RELATED R&D ACTIVITIES ON THE LINAC ACCELERATOR ..... 172**
10.1.1 R&D ACTIVITIES ON THE INJECTOR ..... 172
10.1.2 R&D ACTIVITIES ON THE MAIN SUPERCONDUCTING LINAC ..... 174
10.1.3 CONCLUSION ON ACCELERATOR R&D NEEDS ..... 175
**10.2 DM2 ECATS (EXPERIMENTAL ACTIVITIES ON THE COUPLING OF AN ACCELERATOR, A SPALLATION TARGET AND A SUB-CRITICAL BLANKET) ..... 177**
10.2.1 PLANT DESIGN REQUIREMENTS AND EXPERIMENTAL OBJECTIVES ..... 177
10.2.2 THE YALINA EXPERIMENTS ..... 177
10.2.3 THE RACE EXPERIMENTS ..... 180
10.2.4 THE GUINEVERE EXPERIMENTS ..... 183
10.2.5 CONCLUSION ON ADS MONITORING AND ACCELERATOR-CORE COUPLING ..... 185
**10.3 DM3 AFTRA (ADVANCED FUELS FOR TRANSMUTATION SYSTEMS ) ..... 189**
10.3.1 TRU FUEL PERFORMANCE ASSESSMENT AT NORMAL OPERATION CONDITIONS. ..... 189
10.3.2 FUEL SAFETY ASSESSMENT ..... 189
10.3.3 IRRADIATION TESTS ..... 190
10.3.4 OUT-OF-PILE MEASUREMENTS ..... 190
10.3.5 CONCLUSION ON U-FREE FUEL ..... 191
**10.4 DM4 DEMETRA (DEVELOPMENT AND ASSESSMENT OF STRUCTURAL MATERIALS AND HEAVY LIQUID METAL TECHNOLOGIES FOR TRANSMUTATION SYSTEMS) ..... 193**
10.4.1 OBJECTIVES ..... 193

*This document refers to work being performed by scientists and institutions involved in IP EUROTRANS, as well as the financial support of the European Commission through the contract FI6W-CT-2004-516520.*

10.4.2 MATERIALS CHARACTERISATION ..... 193
10.4.3 IRRADIATION STUDIES ..... 196
10.4.4 HLM QUALITY CONTROL ..... 197
10.4.5 THERMAL-HYDRAULICS ..... 197
10.4.6 CONCLUSION ON PB AND LBE RELATED TECHNOLOGY ..... 200
**10.5 DM5 NUDATRA (NUCLEAR DATA FOR TRANSMUTATION) ..... 203**
10.5.1 OBJECTIVES OF DM5 NUDATRA ..... 203
10.5.2 UNCERTAINTY PROPAGATION AND DATA NEEDS OF ETD ADVANCED FUEL CYCLES ..... 203
10.5.3 MEASUREMENTS AND EVALUATIONS OF CROSS SECTIONS ..... 204
10.5.4 HIGH ENERGY EXPERIMENTS AND MODELLING ..... 206
10.5.5 DECAY HEAT IN MA LOADED CORES ..... 209
10.5.6 CONCLUSION ON DM5 NUDATRA ..... 210
**10.6 R&D NEEDS SYNTHESIS ..... 212**
**10.6.1 PB-COOLED SYSTEMS ..... 212**
10.6.1.1 Structural materials ..... 212
10.6.1.2 Thermal-hydraulics ..... 212
10.6.1.3 Reactor Components ..... 213
10.6.1.4 Instrumentation and coolant chemistry control ..... 214
**10.6.2 GAS-COOLED SYSTEMS ..... 215**
10.6.2.1 Main Components : RPV and primary circuit ..... 215
10.6.2.2 Neutronics ..... 216
10.6.2.3 Core Thermal-hydraulics ..... 216
10.6.2.4 Tools for compressor/circulator modelling and studies: a multi-scale approach ..... 217
10.6.2.5 Helium instrumentation: ..... 217
**10.6.3 LBE-COOLED SYSTEMS ..... 218**

**11. GENERAL CONCLUSIONS ..... 220**

**11.1 MOTIVATION OF THE OVERALL IP EUROTRANS PROJECT ..... 220**
**11.2 DESIGN:EFIT-PB ..... 220**
**11.3 DESIGN: EFIT-HE ..... 223**
**11.4 DESIGN: XT-ADS ..... 224**
**11.5 ACCELERATOR ..... 226**
**11.6 SPALLATION TARGET ..... 227**
**11.7 SAFETY ANALYSIS ..... 227**
**11.8 COST ANALYSIS ..... 228**
**11.9 PERSPECTIVES ..... 229**

**12. ACKNOWLEDGEMENTS ..... 230**

*This document refers to work being performed by scientists and institutions involved in IP EUROTRANS, as well as the financial support of the European Commission through the contract FI6W-CT-2004-516520.*

# 1. INTRODUCTION AND SCOPE

The development of the ADS (for Accelerator Driven Systems) is motivated by the potential which have these machines to reduce the volume and the radiotoxicity of the nuclear waste and more particularly of minor actinides generated by the operation of existing pressurized water reactors. This reduction of the volume and the radio-toxicity of such nuclear waste is obtained by transmutation and incineration (i.e. fission) of minor actinides into less active isotopes or shorter-lived by-products.

The overall EUROTRANS integrated project had the goal to demonstrate the possibility of nuclear waste transmutation/burning in Accelerator Driven Systems (ADS) at industrial scale [1.1]. The domain DESIGN, within it, had the task to provide the pre-design of the European Transmutation Demonstrator (ETD) able to achieve such task.

The focus during this FP6 European commission partially funded programme is on a Pb-cooled ADS for the European Facility on Industrial scale Transmuter (ETD/EFIT) with a back-up solution based on an He cooled ADS in continuity with the PDS-XADS 5$^{th}$ FP project [1.2]. It takes credit from the roadmap on Partitioning & Transmutation of the Technical Working Group [1.3] and the FP6 Project PATEROS (P&T European Roadmap for Sustainable Nuclear Energy) [1.4]

As an intermediate step towards this industrial-scale prototype, an eXperimental Transmuter based on ADS concept (ETD/XT-ADS) able to demonstrate both the feasibility of the ADS concept and to accumulate experience when using dedicated fuel sub-assemblies or dedicated pins within a MOX fuel core has been also studied. The possibility of irradiating these dedicated sub-assemblies in conditions which are representative of the ETD/EFIT (after both concepts have been pre-designed) has then be one of the major tasks of these ETD/XT-ADS studies.

The two machines (XT-ADS and EFIT) have been designed in a consistent way bringing more credibility to the potential licensing of these plants. As part of this objective, synergies between both designs have been identified with their respective particular objectives in mind.

The definition of the detailed missions of the different ADS once settled, it has been of primarily importance to design these machines keeping in mind what is reasonably achievable and the conditions under which the design optimization can proceed. The EUROTRANS Integrated Project has been organized in different domains with DM1 Design defining the overall ETD/EFIT and ETD/XT-ADS designs while the others were specifically devoted to R&D tasks. These tasks were centered on the assessment of reactivity measurement techniques (DM2 ECATS), on the development of U-free dedicated fuels (DM3 AFTRA), on materials behavior and heavy liquid metal technology (DM4 DEMETRA) and on nuclear data assessment (DM5 NUDATRA).

The XT-ADS design has been proceeding with margins taking into account the uncertainties associated to the knowledge of the material boundary limits. The ETD/EFIT design has been proceeding with a similar approach but with material boundary limits defined without uncertainties given the expected time of the construction of the plant i.e. in twenty five years. These constraints have been defined at the start of the project [1.2] anticipating some R&D results to come and part of the objective of this document is to review these constraints on the light of the different work progresses of EUROTRANS IP and and the remaining R&D to be performed prior to the construction of the different plants.

This part of the document (Chapter 1) gives a justification to the ADS development for nuclear waste transmutation purposes and their overall general requested characteristics.

It then goes to define the main design aspects of the different plants, the constraints under which the different design works have proceeded in view of their optimizations and, in particular, the material boundary conditions.

Chapter 2 is related to the ETD accelerator description and its reliability.

*This document refers to work being performed by scientists and institutions involved in IP EUROTRANS, as well as the financial support of the European Commission through the contract FI6W-CT-2004-516520.*

Chapters 3 to 9 are bound to evaluate the different ETD/EFIT designs in view of their respective objectives. This part includes the possible improvements or refinements, the optimization could proceed in view of possible strategic choices among conflicting constraints.

Chapter 10 makes a status of the R&D i.e. review the different constraints which have been used for designing the different plants and list the R&D still required to achieve the licensing of the plant.

Chapter 11 concludes this document including the degree of feasibility of the plants and their costs.

## 1.1 ADS underlying objectives

The spent fuel discharged from nuclear power plants constitutes the main contribution to nuclear waste. At present, approximately 2500 tons of spent fuels are produced annually in the EU, containing about 25 tons of plutonium and 3.5 tons of the "minor actinides" neptunium, americium, and curium and 3 tons of long-lived fission products.

These radioactive by-products, although present at relatively low concentrations in the spent fuel, are a hazard to life forms when released into the environment. A measure of the hazard of these elements is provided by the toxicity and in particular the radiotoxicity arising from their radioactive nature rather than their chemical form. The radiotoxicity of the fission products dominates the total radiotoxicity during the first 100 years. Thereafter, their radiotoxicity decreases and reaches the reference level after about 300 years. The long-term radiotoxicity is dominated by the actinides, mainly by the plutonium and americium isotopes. The reference radiotoxicity level is reached by spent nuclear fuel only after periods of more than 100,000 years.

This is the basis of the motivation for partitioning and transmutation programmes worldwide, and for the development of dedicated burner reactors such as Accelerator Driven Systems (ADS) as one possible strategy for the reduction of the volume and radio-toxicity of such wastes. In particular, the major actinide plutonium and the Minor Actinides (MAs) such as neptunium, americium and curium together with some of the more radio-active and volatile/hydrogenous long-lived fission products (LLFPs) such as 135cesium, 129iodine and 99technicium pose the greatest hazards from the point of view of radio-toxicity and proliferation risk. One possible solution offered is transmutation and/or incineration (i.e. fissioning) of the waste into less active isotopes or short-lived by-products in a nuclear reactor [1.5].

## 1.2 Perspectives on Partitioning &Transmutation

ADS can play a very important role in the P&T perspective and allows a very high level of radio-toxicity reduction.

It has been demonstrated, that same radio-toxicity reduction could be reached by a strategy implementing an electro-nuclear system of advanced fast reactors (AFR), which would provide the same level of radio-toxicity reduction performance as a double strata system. The competitiveness and full feasibility is still under investigations and furthermore, the consequence it has on the economic of the whole fuel cycle is of major concern. Because of this and as the build-up of a fast reactor park has encountered some delays; the major alternative route using ADS appears attractive enough to be further developed. At the R&D level, the ADS development offers many common characteristics with critical systems with fast spectrum and the decision on one or the other route will at the end become a public/political decision.

Therefore it is important to proceed with the R&D and a stepwise demonstration of the technology and of the ADS system, for an industrial prototype implementation around 2035 and a full industrial large scale deployment starting around 2045.

### 1.2.1 Origin of Nuclear Waste

Most of the reactors operative in the world today are thermal spectrum reactors such as LWRs (Pressurised Water Reactors) or Russian VVERs, BWRs (Boiling Water Reactors), AGRs (Advanced CO2 Gas

*This document refers to work being performed by scientists and institutions involved in IP EUROTRANS, as well as the financial support of the European Commission through the contract FI6W-CT-2004-516520.*

Reactors), and CANDU D2O types. Some fast spectrum reactors of the sodium or lead-bismuth eutectic cooled type are also in operation but constitute less than one percent of the total worldwide operating fleet.

The currently dominant 'open' fuel cycle in which uranium fuel is irradiated and then discharged for re-processing (i.e. separation and subsequent storage) before direct replacement with new uranium fuel has resulted in the gradual accumulation of large quantities of highly radioactive or fertile materials in the form of depleted uranium, plutonium, MAs and LLFPs.

Some of the separated products from reprocessed fuels have already been utilised in the past in the form of MOX (Mixed Pu/U Oxide) fuels, but as yet, not in sufficient quantities to significantly slow down the steady accumulation of these materials in storage.

Table 1.1 below shows a typical PWR discharge inventory [1.6] of the long-lived waste products.

Table 1.1: Part of discharge inventory from 900 MWe Uranium (3.7% 235U) fuelled PWR after a burnup of around 40 GWd/t and a cooling period of 5 years. All units are kg/TWhe.

| Higher actinides | | MAs | | LLFPs | |
|---|---|---|---|---|---|
| U | 3000 | Np | 1.8 | $^{99}$Tc | 2.9 |
| Pu | 33 | Am | 1.7 | $^{129}$I | 0.7 |
| - | | Cm | 0.16 | $^{135}$Cs | 1.7 |

There are other elements produced in-reactor via fissions or capture processes etc, but these are mainly either short-lived (and therefore pose no long term problem following a cooling period during which they may transmute to stable or less active isotopes) or stable. $^{99}$Tc, $^{129}$I and $^{135}$Cs represent the largest contribution to the radiotoxicity of all LLFPs produced in a typical uranium fuelled reactor [1.7].

The total mass of fuel in the reactor quoted in table 1.1 would typically be around 72 tons (~157 assemblies x 0.46 t/ass'). This would give annual discharge totals for the non-uranic elements in table 1.1 of around 200kg of plutonium, 11kg of neptunium, 10kg of americium and 1kg of curium. Additionally, the amounts of LLFPs of interest resulting from fissioning of heavier elements would be around 17kg of $^{99}$Tc, 4kg of $^{129}$I and 10kg of $^{135}$Cs and around another 20 –30 kg of other fission products [1.6].

The situation envisioned for the medium term future is a situation in which spent fuel have been accumulated the operation of PWR plants over a period of 50 years.

This current situation most common in Europe uses PWRs to burn UOX fuels which are then reprocessed to produce MOX fuel. About nine UOX PWR sub-assemblies are required to fabricate a MOX PWR sub-assembly. This situation is mainly driven by the fact that this enable to reduce significantly the number of sub assemblies to store in repositories. The reprocessing of MOX PWR sub assemblies is envisaged at the moment only for regulatory rules. Storing spent fuel at La Hague is allowed only if the spent fuel is going to be reprocessed. Also to be considered is the fact that with the current situation, plutonium inventory is steadily increasing although at a relative limited pace since PWR using MOX fuel are effectively burning Plutonium. Reprocessing of MOX PWR fuel is however envisaged for the deployment of advanced Generation IV reactors. In this scenario, Plutonium will be going in these advanced Generation IV system but not possibly minor actinides since these would pollute the entire fuel cycle. A dedicated fuel cycle would be a less serious burden and hence minor actinides coming from MOX spent fuel could then be introduced in dedicated ADS. It should be mentioned that at the moment nuclear waste from UOX spent fuel are put into glass. These glasses include also minor actinides but although their final disposal is not finally decided, experts do not envisage seriously retrieving these minor actinides from glasses where they make no harm.

*This document refers to work being performed by scientists and institutions involved in IP EUROTRANS, as well as the financial support of the European Commission through the contract FI6W-CT-2004-516520.*

These ADS will likely be deployed in 30 years which means that the reprocessing will take place only at a time where most of the Pu-241 will have decayed on the Am-241. The scenario briefly described is presented in the following figure 1.1.

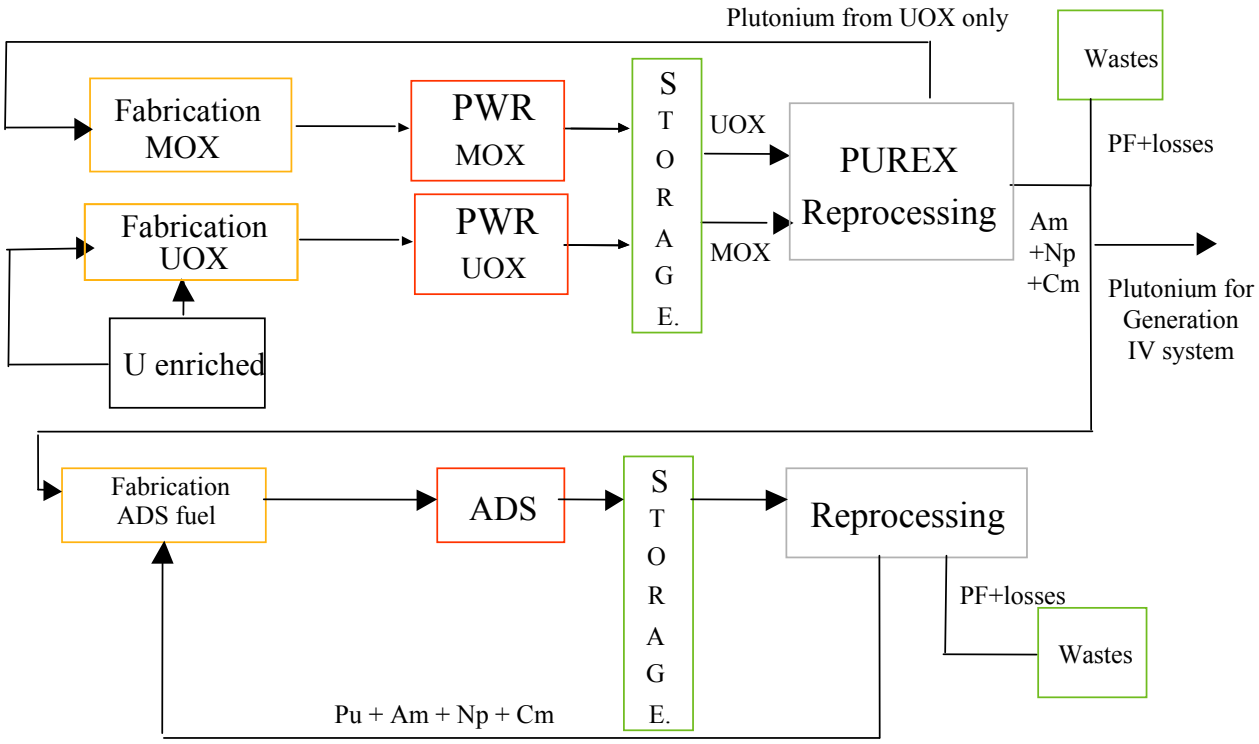


Figure 1.1: Reference Scenario of the burning of minor actinides in ADS

This scenario has been applied to the whole Nuclear Reactor Park in Europe by the PATEROS European Project [1.4]. In this scenario, the advanced PUREX reprocessing is required for the PWR spent fuel, to enable to separate not only Uranium from Plutonium and Plutonium from minor actinides and fission products but also minor actinides from fission products. Some breakthroughs in this field are appearing and it is therefore a limited uncertainty for this scenario. The capability to apply advanced reprocessing on sizable amount of spent fuel from commercial power plants (i.e. LWR) in order to separate Pu and MA has been studied within the FP6 project EUROPART (EUROpean research programme for the PARTitioning of minor actinides from high active wastes issuing the reprocessing of spent nuclear fuels) [1.12] and is now being studied by the FP7 project ACSEPT (Actinide reCycling by SEParation and Transmutation) [1.15].

Therefore, minor actinides will then come from the reprocessing of MOX spent fuel. Minor Actinides are hence coming from a MOX spent fuel reprocessing 30 years after it has been irradiated (likely to be the case since both EFIT and GEN-IV reactors are not ready to operate before). Plutonium used in ADS for the first loading (and eventually for some other cycles if the ADS is not correctly optimised) will be coming also from the MOX spent fuel.

MOX spent fuel have been burnt 45 GWd/t since it the current situation in France (at La Hague reprocessing plant, they have only MOX 40 GWd/t PWR fuel). Note that EPR is designed to host both UOX and MOX fuel S/As which will have a 60 GWd/t out load limit which determines the fuel residence time.

In the EFIT pre-design studies presented here, the core optimisation has been performed with Pu and MA vectors coming from spent fuel: 90% from $UO_2$ cooled down 30 years and 10% from MOX cooled down 15 years, unloaded at 45 GWd/ton, respectively.

*This document refers to work being performed by scientists and institutions involved in IP EUROTRANS, as well as the financial support of the European Commission through the contract FI6W-CT-2004-516520.*

### 1.2.2 Radio-toxicity

In the majority of studies, two main criteria are used to define the degree of significance of the waste produced in-reactor: The total mass (or inventory) of transurania and the subsequent radiotoxicity of that waste. The latter is of direct importance to the human population as a whole and tends to be the primary driving force behind efforts to reduce the growth of existing waste inventories. The radiotoxicity of nuclear waste is defined as the global dose resulting from complete incorporation by the population of the waste product by either ingestion or inhalation and is presently expressed in Sieverts per ton of spent fuel. Note that the Sievert is defined as the amount of ionising radiation required to have the same biological effect as one rad (1 rad=0.01joules/Kg) of high penetration X-rays (equivalent to a 'Gray' for X-rays). A recommended choice of unit is, Sv/TWhe as this unit is a measure of the efficiency (or lack of efficiency) of a core for waste burning (or production). For the typical PWR mentioned above, the plutonium accounts for between 70 and 90% of the total radiotoxicity of the discharge products [1.6] for up to 105 years after storage. Consequently, when defining a complete strategy for the treatment of radioactive waste (i.e. close the fuel cycle), it is of prime importance to consider, simultaneously with the MAs and LLFPs, a programme of recycling plutonium.

The one characteristic that all of the MAs and LLFPs under discussion have in common is their high radiotoxicity inventory. For the MAs, after plutonium, the most toxic is Americium followed by Curium. Neptunium is not particularly radiotoxic in its most common isotope ($^{237}$Np) but can decay to fissile uranium or produce via neutron capture under irradiation the highly active isotope $^{238}$Pu (via $^{237}$Pu), which is a strong alpha emitter, in just a few years. Another possibility is the (n, 2n) reaction giving $^{236}$Pu (via $\beta$ - decay). The subsequent decay of this isotope and its daughters leads to $^{208}$Tl, which is a hard gamma emitter (3.4 MeV). Regarding the radiotoxicity of the LLFPs, it is helpful to compare their activity against that of the main MAs as shown below in Table 1.2.

The Table 1.2 below lists the most prevalent MAs of interest from the uranium fuel cycle together with the most prolific and toxic LLFPs, giving their principle decay modes, energies and dose coefficients.

Table 1.2: General decay data for the main MAs and LLFPs considered

| Isotope | $T_{½}$ (years) | Principal decay modes | Q energy (MeV) | Branching ratio | ($\alpha$, n) n/g/s | nSv/Bq (ICRP-72) |
|---|---|---|---|---|---|---|
| $^{237}$Np | 2.14e6 | $\alpha$ | 4.95 | - | 0.322 | 110 |
| $^{241}$Am | 432.7 | $\alpha$<br>S.F. | 5.64<br>188.1 | ~1<br>1e-12 | 3.17e3 | 200 |
| $^{244}$Cm | 18.1 | $\alpha$<br>S.F. | 5.9<br>191.8 | ~1<br>1.35e-6 | 8.84e4 | 120 |
| $^{99}$Tc | 2.13e5 | $\alpha$ - ($\gamma$) | 0.294±0.002 | - | - | 0.64 |
| $^{129}$I | 1.56e7 | $\alpha$ - ($\gamma$) | 0.19±0.005 | - | - | 110 |
| $^{135}$Cs | 2.3e6 | $\alpha$ - ($\gamma$) | 0.205±0.005 | - | - | 2 |

Although the radiotoxic inventory of the LLFP in spent fuel is lower than that of natural uranium, some of these nuclides ($^{129}$I and $^{99}$Tc) may dominate the dose committment from a failing repository. The calculated doses are however several orders of magnitude below regulatory limits. Therefore, minor actinide transmutation, as studied in EUROTRANS, mainly has two objectives - reducing the heat load of the repository, and reducing the radio-toxic inventory of the long lived high level waste, the latter being of significance when studying human intrusion scenarios.

*This document refers to work being performed by scientists and institutions involved in IP EUROTRANS, as well as the financial support of the European Commission through the contract FI6W-CT-2004-516520.*

## 1.3 Fuel choices

A Uranium-free fuel is necessary for the development of the European Facility for Industrial Transmutation (EFIT) [1.8].

The Domain DM3 (AFTRA) has been responsible for the fuel development within EUROTRANS IP [1.9] In AFTRA, the choice of the different fuel forms and matrices has been done after a ranking procedure based on a number of criteria, ranging from fabrication, reprocessing via economics to safety. Fuel forms comprised composite fuels as CerCer (Ceramic-Ceramic) and CerMet (Ceramic-Metal) and also cores with Zr based solid solution fuels.

The main focus of the ADT (Accelerator Driven Transmuter) fuel development concentrated on the oxide route in line with the European experience.

The DM1 design work concentrated mainly on the CerCer core. Several reasons were behind this choice: MgO is a less absorbing material but CerCer is also better known although its material properties are not as efficient as initially expected. The composite CerCer fuel $(Pu_{0.4},Am_{0.6})O_2$-x – MgO can be manufactured for a lower unit cost but has the disadvantage of a low dissociation temperature.

Within AFTRA the work was focussed on a CerMet core. The composite CerMet fuel $(Pu_{0.5},Am_{0.5})O_{2-x}$ – $^{92}$Mo (93% enriched) [1.10] exhibits higher thermal-mechanical resistance against beam-trips was e.g. an argument for the CerMet choice. Disadvantages include the cost for enrichment of $^{92}$Mo and higher neutron absorption.

Reprocessing of the fuels currently favoured for the EFIT (CerCer and CerMet) has been confirmed within the FUTURE program (5$^{th}$ FP of the EU [1.10]) and the EUROPART program (6$^{th}$ FP of the EU FP6-EURATOM-RADWASTE [1.12]). These innovative fuels are still under scrutiny with the results of the irradiation campaigns which started within EUROTRANS still awaited. Investigations in FUTURE concern the fabrication process and fuel behaviour under nominal and transient conditions (and consequently the material limits are set up according to safety criteria). For what concerns reprocessing, one relies in the findings of the PYROREP program for which Pu-Am are co-extracted from the fission products and the MgO ceramic or light Mo metal. During the fabrication process, missing MA being burnt in the previous cycle are added to the reprocessed fuel. The core is designed to keep the reactivity constant through that process but an adjustment is still possible by using an increased matrix fraction. Still to be solved however – although several possible solutions are existing- is how to keep the MgO ceramic or light Mo metal out of fission products stream and re-use them at the fuel fabrication stage. The scenario envisaged is not put into question with this point but might have an impact on the amount of low waste. Wet reprocessing are discarded for this plant, not because the 2 processes PUREX and DIAMEX lead to separate streams of MA and Pu (quite degraded Pu vector which cannot be of any use for weapons) but because of the fuel heat and radioactivity.

Fabrication represents the potential to fabricate a fuel at an industrial scale with acceptable thermal and mechanical properties, while reprocessing assumes that the fuel will be compatible with industrial reprocessing standards in Europe. These two basic requirements have the consequence that a lower priority is assigned to nitride and metallic fuels. In the 5$^{th}$ FP CONFIRM project [1.11] as well as in the US AFCI project, it has been shown that the fabrication of Am bearing inert matrix nitride fuels with a density above 80% of the theoretical value is difficult due to limitations in sintering temperature. The sodium bond used in fabrication of metallic fuels makes them incompatible with aqueous reprocessing. Furthermore, pyro-chemical reprocessing methods have yet to demonstrate acceptable recovery yields in industrial scale applications.

High concentrations of Minor Actinides and Plutonium in ADS fuels result in: high gamma and neutron emissions and significant production of helium during irradiation. Moreover, coolant, core components and ADS technology bring in other constraints. Therefore, an optimal fuel has to be identified via a wide set of criteria: thermal, mechanical and chemical properties, fabricability, behaviour under irradiation and reprocessibility, as well as neutronic and technological constraints related to the ADS technology and the objective of high transmutation performance.

*This document refers to work being performed by scientists and institutions involved in IP EUROTRANS, as well as the financial support of the European Commission through the contract FI6W-CT-2004-516520.*

CerCer and CerMet composite fuels consisting of particles of $(Pu,MA)O_{2-x}$ phases dispersed in a magnesia matrix or a molybdenum matrix (enriched in $^{92}Mo$) are primary candidates under investigation in Europe within the FP-6 EUROTRANS project due to:

- promising results according to performance, safety and fabricability criteria as well as first experimental feedbacks on $(Pu,Am)O_2$ fabrication and out-of-pile characterizations, gained within the FP5 - FUTURE program (2002-2006);
- strong synergy with R&D programs on transmutation targets;
- broad industrial experience on oxide fuel fabrication for critical reactors.

Nitride-based fuels represent a back-up solution. Indeed, even if their high attractiveness has been confirmed by the results of FP5 - CONFIRM program (2001-2008) and JAEA investigations, our knowledge and technical know-how remains limited. So these fuels are considered at an early stage of development with longer term R&D activities still required.

Regarding CerCer and CerMet fuels, work performed within AFTRA has already provided a wide range of promising results:

- Several cores have been designed, and optima meeting the specification have been found. Preliminary thermo-mechanical calculations of hottest fuel pins (CerMet and CerCer cores with 169 pins per sub-assembly) have given evidence of good performances. Nevertheless, future progresses in gas release phenomena understanding remain essential to provide reliability and accuracy to these first results.
- Safety analyses show that in both CerCer and CerMet cores, the most limiting conditions would come from the T91 clad and safety limits for fuel are not violated. Nevertheless the safety margins for the CerMet are considerably higher.
- FUTURIX-FTA irradiation test which addresses irradiation behaviour of MgO-CerCer and Mo-CerMet fuels under ADS type conditions, and BODEX irradiation test which deals with Helium behaviour in inert matrices, are complete. BODEX PIE are going-on whereas FUTURIX-FTA PIE are planned in the FP-7 FAIFUELS program. The HELIOS irradiation which addresses the effect of temperature and helium release in fuel microstructures is still on-going. Characterizations on a nitride fuel pin irradiated within the CONFIRM program are under investigation.
- Thermal properties of a large range of fresh fuels have been assessed: they highlight the higher thermal stability and thermal conductivity of CerMet compared to CerCer fuels.
- Compatibility tests have pointed out chemical compatibility between $Pu_{0.5}Am_{0.5}O_{2-x}$ and Mo, MgO matrices.
- There is not any interaction between Pb (EFIT coolant) and T91, Mo or MgO compounds.
- Mo (respectively MgO) is compatible with T91 up to 950°C (respectively 550°C). Indeed, dealing with MgO, SEM/EDS analyses performed on 950°C heat treated T91/MgO sandwich, have pointed out the local presence of magnesium in the T91 area in contact with MgO. No change in the aspect or composition of MgO was nevertheless observed.
- Finally, great progress has been made in Pu-Am-O phase diagram investigation, pointing out that Am drives the reduction process in the oxygen sub-stœchiometric domain.

PIE of HELIOS and FUTURIX-FTA fuels scheduled within the FP-7 FAIRFUELS program, will provide in the next years additional data, which are essential to recommend the most promising fuel between $^{92}Mo$-CerMet and MgO-CerCer.

*This document refers to work being performed by scientists and institutions involved in IP EUROTRANS, as well as the financial support of the European Commission through the contract FI6W-CT-2004-516520.*

As a consequence of this selection process, detailed studies were performed on two composite fuel types:

- (Pu,Am)O2-x – $^{Enr}$Mo (CerMet)
- (Pu,Am)O2-x – MgO (CerCer)

where the molybdenum $^{Enr}$Mo of the CerMet fuel is ~ 93% enriched in $^{92}$Mo.

Fabrication of the two preferred candidate fuels has been successfully accomplished in ATALANTE and in the MA-lab within the FUTURIX-FTA project. Solubility tests have been performed on the CerMet fuel, thus confirming the solubility of molybdenum in nitric acid. It is considered that the fabrication of pellets with a matrix content less than 60 vol. % (required fuel content is 45 % for EFIT-He and 55 % for EFIT-Pb with CerCer fuel), and with acceptable thermal and mechanical properties, remains to be proven for both of the pre-selected fuel candidates [1.12].

Modelling of the thermo-mechanical performance under irradiation using the independent fuel simulation codes TRAFIC and MACROS showed that irradiation induced reduction of thermal conductivity of magnesium oxide would lead to unacceptably high fuel temperatures when approaching a target burnup of 30% in the hottest pin. The CerCer fuel should thus be operated at a relative low linear heating rate (< 250 W/cm in the hottest pin). The thermo-mechanical performance modelling of the CerMet fuel has not yet been performed because of missing the important data on degradation of its properties under irradiation.

The most important properties for both CerCer and CerMet fuels proposed by AFTRA domain to start the optimisation design process are presented in the following Table 1.3.

Table 1.3 : U-free fuel characteristics to be considered in ETD/EFIT studies

| Fuel Type<br>Characteristics to be considered | CerCer with MgO matrix | CerMet with light Mo matrix |
|---|---|---|
| Minimum matrix volume fraction | 50% | 50% |
| Practical density | 90% Theoretical Density | 93% Theoretical Density |
| Filling density | 95% | 94% |
| Fuel theoretical density | 11.46 g/cm$^3$ | 11.46 g/cm$^3$ |
| Matrix theoretical density | 3.58 g/cm$^3$ | 9.87 g/cm$^3$ |
| Melting (or dissociating) temperature | 1930 K | 2360 K |
| Maximum operating temperature<br>Cat I (25 % power excursion) | 1650 K | 1850 K |
| Maximum operating temperature Cat II | 1860 K | 2080 K |
| Maximum operating temperature Cat III | 2080 K | 2300 K |
| Isotopic Contents | | Mo (weight): Mo92=92.7%,Mo94=6.23%, Mo95=1.0%, Mo96=0.07%, Mo97=0% |

High temperature tests on the CerCer fuel carried out in the framework of the FUTURIX-FTA experiments has shown that vaporisation of magnesium oxide occurs at T ≈ 2130°K under nitrogen atmosphere. Even though in-pile conditions are somewhat different, and might suppress vaporisation, the calculated eutectic

*This document refers to work being performed by scientists and institutions involved in IP EUROTRANS, as well as the financial support of the European Commission through the contract FI6W-CT-2004-516520.*

melting temperature of the CerCer compound is comparatively low (e.g. $AmO_{2-x}$+MgO forms eutectic with a melting temperature of 1930-2320 K at x = 0-0.5 [1.14]).

The practical density (93% Theoretical Density) for the CerMet fuel is an average of 96 % TD for Mo and 90 % TD for $AnO_{2-x}$ particles. More detailed information such as conductivity as a function of irradiation time, swelling, etc can be found in [1.14]. There is almost no information on the interaction between molybdenum metal and actinide oxides [1.14]. Molybdenum melting point is 2896°K but eutectic point with oxide fuel could possibly occur at 2050 K.

REFERENCES

[1.1] J. Knebel, "Motivation and Strategy of the Integrated Project on Transmutation (IP EUROTRANS)", FZK, 22 October 2003

[1.2] G. Rimpault, Definition of the detailed missions of both the Pb-Bi cooled XT-ADS and Pb cooled EFIT and its gas back-up option, Techn. Report CEA SPRC/LEDC 05-420, December 2005; IP EUROTRANS – DM1 Design – WP 1.1 – Deliverable 1.1, Contract n° FI6W-CT-2004-516520, June 2006.

[1.3] "A European Roadmap for Developing Accelerator Driven Systems (ADS) for Nuclear Waste Incineration", The European Technical Working Group on ADS, ISBN 88-8286-008-6, April 2001

[1.4] P&T European Roadmap for Sustainable Nuclear Energy (PATEROS). Contract Number FP6-036418. http://www.sckcen.be/pateros/

[1.5] OECD/NEA state-of-the-art report (1999) entitled, 'Actinide and Fission Product Partitioning and Transmutation. Status and Assessment Report'

[1.6] J Tommasi et al, 'Long-lived waste transmutation in reactors', Nuclear technology, Vol 111, pg133, 07/95.

[1.7] A Tchistiakov, 'Etude de potentiel de transmutation et des caractéristiques de sûreté d'un système hybride: accélérateur-réacteur sous-critique', Thèse de l'université de Provence, Aix-Marseille I, soutenue le 07/04/1998.

[1.8] "Fuel for the XADS", Document prepared by the FFP subgroup of the TWG on ADS- March 2001

[1.9] F. Delage, Executive Summary of Domain 3 AFTRA of the EUROTRANS IP.

[1.10] S. Pillon, Summary Report of the FUTURE project

[1.11] J. Wallenius, Summary Report of the CONFIRM project

[1.12] EUROpean research programme for the PARTitioning of minor actinides from high active wastes issuing the reprocessing of spent neclear fuels (EUROPART) Contract Number FI6W-CT-2003-508854 (http://www.europart-project.org/scripts/home/)

[1.13] J. Wallenius, Deliverable D3.1.7 of AFTRA IP EUROTRANS

[1.14] R. Thetford, V. Sobolev, Recommended properties of fuel, cladding and coolant for EFIT pre-design, Eurotrans Contract N° FI6W-CT-2004-516520, Deliverable N° 3.4, Draft 0.4. 17 Feb. 2006.

[1.15] Stéphane Bourg, Emmanuel Touron, Concha Caravaca, Christian Ekberg, Emmanuel Gaubert, Clément Hill: ACSEPT: a new FP7-Euratom Collaborative Project in the field of partitioning processes for advanced fuel cycles, ATALANTE 2008 Montpellier (France) May 19-22, 2008

*This document refers to work being performed by scientists and institutions involved in IP EUROTRANS, as well as the financial support of the European Commission through the contract FI6W-CT-2004-516520.*

# 2. DESCRIPTION OF THE ETD ACCELERATOR

## 2.1 Beam characteristics

### 2.1.1 Accelerator general performances

The accelerator is basically a high intensity proton machine, delivering a proton beam on a spallation target. The high energy protons are used in the spallation target to create neutrons by spallation reactions. The produced neutrons in their turn feed the subcritical core. In principle, both cyclotrons as well as linear accelerators are relevant candidates for providing such beams. Because, of several conditions such as the reliability and availability design values and the beam stability, the decision to use a linear accelerator type is to be preferred, as already pointed out within the PDS-XADS project.

Therefore, an accelerator delivering a beam with protons at 600MeV has been designed for the XT-ADS while 800MeV has been chosen for the two EFIT plants. In a window design, higher proton energies are necessary in order to limit the energy deposited in the window. The current choices are consistent with the windowless target option which has been chosen for both plants. However, the experience gained with MEGAPIE gives a strong evidence that a window option might be envisaged even at 600 MeV, and so that the current choices are consistent with both windowless and window type options.

The effective level of beam current intensity has been limited for the XT-ADS to 5 mA and to 20 mA for both EFIT-Pb and EFIT-He as a consequence of appropriate fuel core design and specific fuel cycle.

According to recommendations made within the PDS-XADS Project, when a beam trip of less than 1 second is occurring it is said in the specifications that the system should continue to operate and the expert system should be given the information (from the accelerator and/or the spallation module) so that it does not consider that as an accident which requires a beam interruption. It was decided at first to design the plant to accept a limited number of beam SCRAM (5 per year) and that spurious information from the different experimental devices should be avoided as much as possible. This 1 second limit has been reconsidered at the end of the project (see Section 2.3 for the rationale) and is now of 3 seconds as both the XT-ADS and the ETD/EFIT exhibit large thermal inertia due to the large LBE or Pb pool they offer and margins that exist with the fuel and cladding behaviour during these transients. A fine tuning of the power is not specifically required since the accelerator is designed to deliver a proton current with a maximum 2% fluctuation, that will lead to a maximum 3% change in the power (with the 1% maximum energy fluctuation included).

The accelerator is basically of the Continuous Wave (CW) type. However, a pulsed mode will also be implemented in order to enable the on-line measurement of the sub-criticality level through dynamic measurements. This constraint is a major one as operating the XT-ADS in a safe way requires knowledge of the sub-criticality level at any time.

### 2.1.2 Reliability and availability

The reliability requirements are essentially related to the number of allowable beam trips. Frequently repeated beam trips can significantly damage the reactor structures, the spallation target or the fuel of the sub-critical core and, also, decrease the ADS plant availability. Beam trips of sufficiently large duration would lead to a variation in the plant parameters (thermal power, primary flow, pressure, temperature) or to a plant shutdown. Accelerators are known for sudden interruptions, the duration of which ranging from a few milliseconds to a failure requesting a repair before restart.

The initial recommendations have been revisited at the end of the project. On the basis of current results, the allowable duration of the beam trips is 3 seconds (it was initially of 1 second). However, some complementary R&D is still pending (see Chapter 10.1).

From the point of view of availability (and cost), in the perspective of an industrial application, the tolerable number of long-term beam interruptions should be as low as possible. The number of unexpected shutdown

*This document refers to work being performed by scientists and institutions involved in IP EUROTRANS, as well as the financial support of the European Commission through the contract FI6W-CT-2004-516520.*

for the present nuclear plants dedicated to the electricity production is a few per year (usually 1 or 2). This background leads to limit the number of beam trips to 5 per year.

The shape of the beam footprint can be either a disk or a rectangle and the dimensions of the footprint (diameter or side length) must be stable in a range of ± 10 %.

Finally, it is also worthwhile to point out that the accelerator maintenance policy influences the availability of the XT-ADS. In order to be coherent with the existing maintenance policy on Nuclear Power Plants, it is suitable to avoid the short maintenance periods and to base the maintenance policy on longer periods: once per year during three months appears to be a reasonable value. However, for the XT-ADS, given the rather short cycle length (3 months) a more lenient policy can be chosen.

A summary of accelerator requirements is presented in the following table 2.1.

Table 2.1: Proton Beam General Specifications (revisited figures have been crossed out)

| | **Transmuter demo (XT-ADS / MYRRHA project)** | **Industrial transmuter (EFIT)** |
|---|---|---|
| Proton beam current | 2.5 mA (& up to 4 mA for burn-up compensation) | ~ 20 mA |
| Proton energy | 600 MeV | ~ 800 MeV |
| Allowed beam trips ~~(> 1sec)~~ (> 3sec) number | ~~~ < 5 per 3-month operation cycle~~<br>~ < 10 per 3-month operation cycle | ~ < 3 per year |
| Beam entry into the reactor | Vertically from above | |
| Beam stability on target | Energy: ± 1% - Current: ± 2% - Position & Size: ± 10% | |
| Beam time structure | CW (w/ low-frequency 200μs zero-current beam holes for sub-criticality monitoring) | |

### 2.1.3 Operation

The ADS plant is optimised for operating at nominal power. But, it has also to be capable to operate for long periods at partial load (from around 20% to 100% of the nominal power) without significant penalties. Moreover, during the plant commissioning and after a refuelling in a shutdown state, operations at very low power (< 3%) are required.

This can be achieved by varying the current at the injector in a continuous wave beam (CW linac) accelerator while, for a pulsed mode of operation, it can be achieved also by adjusting the pulse width or the repetition rate. An automatic regulation system will assure the beam stability for operation with stable thermal power.

Fast thermal transients and thermal-mechanical loading of the core are avoided following any power change, so that suitable operating procedures shall also be defined for controlling the beam during the normal XADS start-up and shut-down, and for controlling the XT-ADS rated core power and power level changes as well.

The beam start-up/shut-down sequences, as well as power level changes at rated power conditions, will take into account the thermal transients effects in the overall primary and secondary systems of the XT-ADS, such to make them equivalent to, or close matching, the control rods extraction/insertion driven transients which occur in a standard Nuclear Power Plant.

On the other hand, it is worthwhile to mention that the beam has to be used on a second line, for specific experiments, or for the commissioning. It is especially recommended to install a full-power beam dump for this purpose.

*This document refers to work being performed by scientists and institutions involved in IP EUROTRANS, as well as the financial support of the European Commission through the contract FI6W-CT-2004-516520.*

#### 2.1.4 Accelerator Beam Time Structure for Dynamic Reactivity Measurements

For nominal operation, the accelerator beam will work in CW mode which means a continuous uninterrupted beam without any holes. In this operation mode, the current-to-power indicator will provide the on-line measurement of the reactivity.

Since the proportionality constant in the current-to-power indicator has to be verified regularly, interim reactivity monitoring techniques have to be applied. The exact frequency of this verification has to be determined based the ECATS programme (DM2 of EUROTRANS Project), on operational experience and on the status of current and planned R&D are being presented in chapter 10.2. Based on the MUSE experiments, two possible techniques have been put forward. A third one could be envisaged and tested during the course of the XT-ADS start up experimental programme. DM2 ECATS will finally have to recommend one of them as a reference one taking into account all possible constraints and again the status of current and planned R&D are being presented in chapter 10.2.

These dynamic reactivity measurements require specific beam time structures for the accelerator.

The first technique (PND) is based on the fitting of the prompt neutron population, and is presently the reference one. It is asking for 200μs zero-current beam holes from time to time (typically 1Hz).

The second technique (PNS area method) which is related to the determination of the removal of the total prompt neutron population will require the complete decay of the prompt neutron population and the beginning part of the decay of the delayed neutrons. This implies a much longer hole to be considered. In the MUSE experiments, the considered time scale was seconds. The second technique is envisaged during the fuel loading approach and in that case the beam could work as pulsed source with sharp positive pulses of 1 μs at zero-power.

The third technique (SPJ method) relies in the determination of the delayed neutron amplification. This implies a rather long hole of 200 ms since prompt neutron amplification should disappear. Repeated and well calibrated pulses (duration, sharp decay, …) would be sufficient to get an appropriate accurate measurement. It is not even necessary to operate the accelerator at its full power, but given the experience gained with MUSE programme, a power level much larger than the inherent source is necessary (10 times at least).

Ideally, this SPJ method would be able to measure the reactivity continuously. Since it takes a few hundred microseconds to determine the flux level on the plateau, the SPJ could possibly be used for continuous monitoring. However, acquisition time for good statistics being large, it is not foreseen to use it to trigger the reactor. The advantage of the method is mainly associated to its reduced uncertainty.

## 2.2 The Reference ADS Accelerator

The European ADS concepts requires a high-power proton accelerator operating in CW mode, ranging from 2.4 MW (XT-ADS operation) up to 16 MW for the industrial EFIT. The extremely high reliability requirement (beam trip number) can immediately be identified as the main technological challenge to achieve.

The conceptual design of the accelerator has been developed during the PDS-XADS project [2.1] and further developed during this project for serving the XT-ADS as well as the EFIT with primarily focuses on the improvement of the beam reliability as this is one of the key issues in order to achieve a high availability factor for the transmutation facility [2.2].

*This document refers to work being performed by scientists and institutions involved in IP EUROTRANS, as well as the financial support of the European Commission through the contract FI6W-CT-2004-516520.*

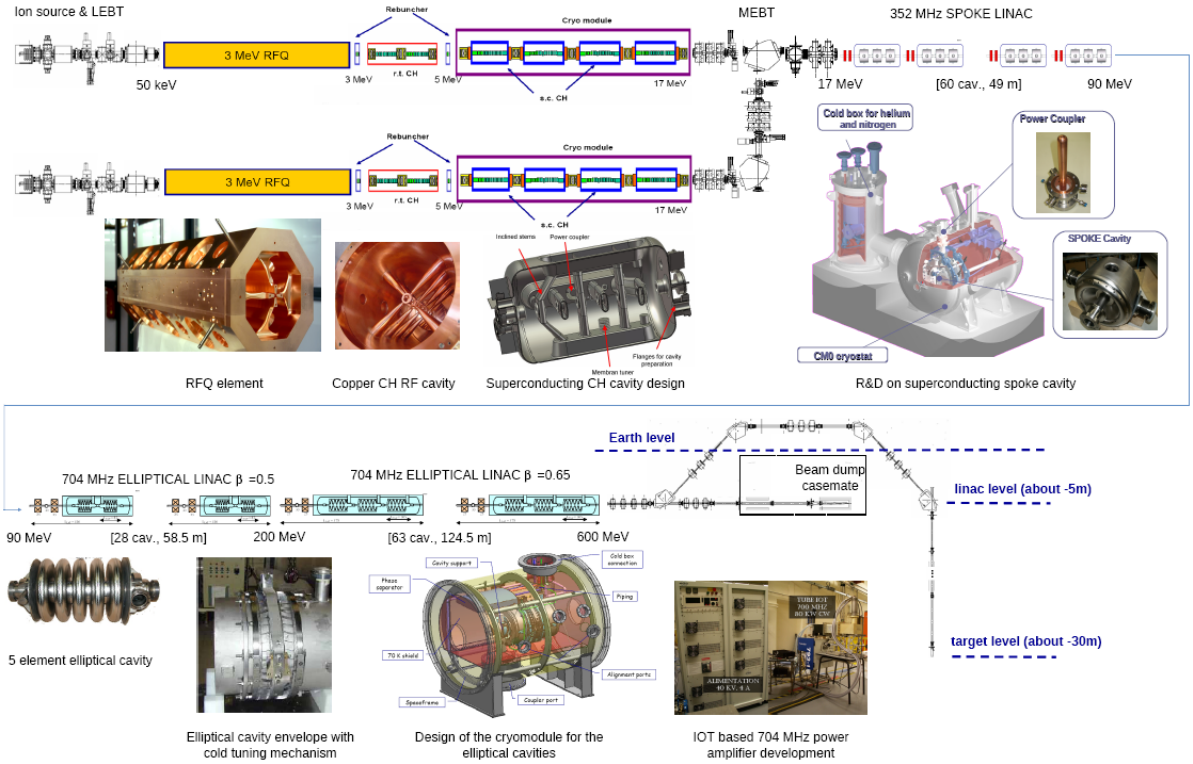


Figure 2.2: European ADS accelerator conceptual scheme.

It is a superconducting linac-based solution (see Figure 2.1), leading to a very modular and upgradeable machine: the same concept remains valid both for the XT-ADS demonstrator and for the industrial scale facility EFIT. Thus, in order to upgrade the XT-ADS accelerator into the EFIT one (namely from 600 MeV to 800 MeV), additional accelerating modules have to be “simply” added at the high-energy end of the beam line to match with the final energy increase, while more powerful RF power stations have to be installed to take into account the higher beam intensity; all other elements remain similar at first order.

Such a solution also brings a high RF-to-beam efficiency thanks to superconductivity (optimized operation cost) and an excellent potential for reliability, both in the main linac, which is designed to be intrinsically “fault-tolerant”, and in the front-end section where a hot stand-by redundant injector with fast switching capability, can be installed if needed. An advanced reference design of this accelerator has been settled during the EUROTRANS project, mainly focusing on the XT-ADS case in the MYRRHA context. The characteristics of this reference accelerator are detailed here after; much more details are available in the final deliverable of WP1.3 (D1.74). This reference accelerator is mainly composed by a 17 MeV injector followed by a 17 to 600 MeV fully superconducting linac with independently-phased cavities. The investment cost for such a XT-ADS machine has been assessed around 240 M€ (manpower and contingencies included, buildings and general utilities excluded).

### 2.2.1 The Linac Front-End

The linac injector is composed of a 50 keV ECR proton source, a short magnetic Low Energy Beam Transport line and a 3 MeV 4-vane copper RFQ operating at 352 MHz.

This RFQ, designed to handle up to 30 mA CW beams with close to 100% transmission for all currents, is about 4.5 metres long, and operates with moderated Kilpatrick factors (~1.7).

*This document refers to work being performed by scientists and institutions involved in IP EUROTRANS, as well as the financial support of the European Commission through the contract FI6W-CT-2004-516520.*

This “classical” injection section is then followed by a more “exotic” but promising energy booster [2.3], that is a combination of normal conducting and superconducting CH (Crossbar H-mode) DTL structures as shown in Figure 2.2, bringing the beam up to 17 MeV.

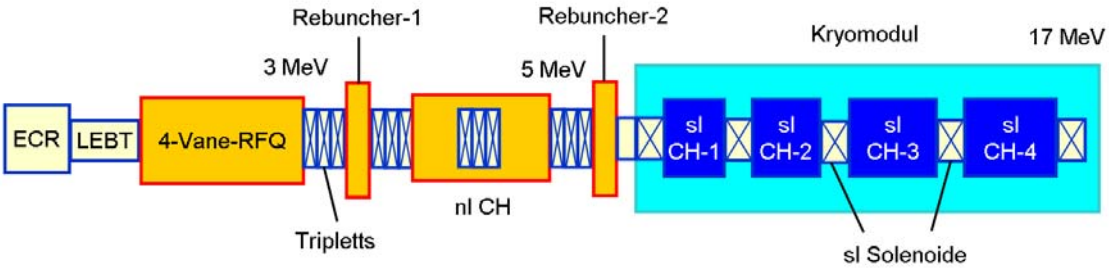


Figure 2.2: The reference linac front-end.

Focusing is ensured by quadrupole triplets and superconducting solenoids inside the cryomodule containing the 4 superconducting CH cavities, and a couple of re-bunchers is used to perform the longitudinal beam adaptation. The design of the DTL structures is based on the KONUS beam dynamics concept [2.4], which allows to exhibit excellent accelerating efficiency at these low energies with a net energy gain of 14 MeV in less than 10 metres, while having very low power consumption in CW operation (Figure 2.3).

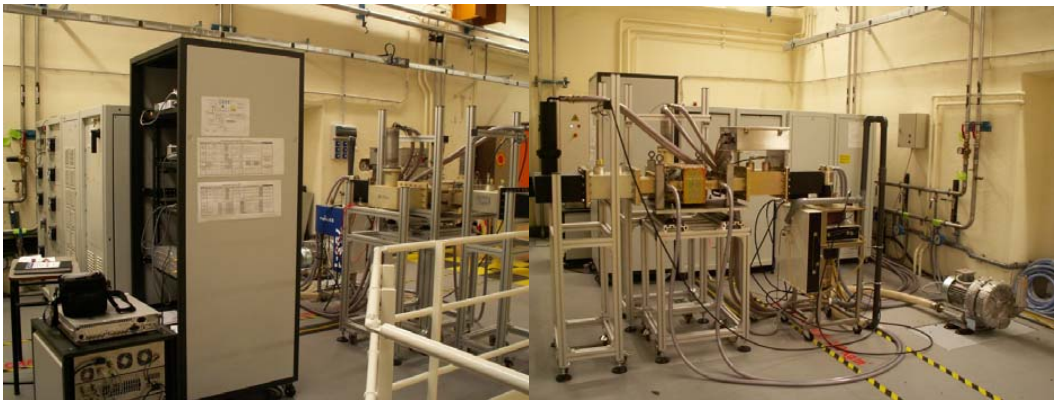

Figure 2.3: View of the RF Power supply setup at Orsay: on the left, the DC power generator as well as the 1 kW amplifier, the interlocks and control closet; on the right, a back view of the IOT with its circulators and all the pipes circuits for air and water cooling.

Multiparticle beam-dynamics simulations of the whole front-end show very good beam behaviour and low sensitivity to errors. Moreover, the proposed solution can cope with various beam currents, with very reasonable emittance growth of about 10% at 5 mA, and 30% at 30 mA. This means that the same machine design can be used for a low current machine (XT-ADS) and for a high current machine (EFIT). Only the RF power and the setting of the re-bunchers have to be adjusted.

In this front-end line, the beam beta-profile is frozen by design, so that any accelerating section failure will inevitably lead to a beam interruption. For this reason and in order to enhance the machine reliability, it is proposed to duplicate the injector (at least the ion source, at most the whole 17 MeV front-end) to provide a hot stand-by injection line able to relieve the main one in case of failure. The detailed design of the corresponding connecting line is still to be worked out.

### 2.2.2 The Independently-Phased SC Linac

From 17 MeV, a fully modular superconducting linear accelerator accelerates the proton beam up to the final energy. This corresponds in the XT-ADS case (600 MeV) to a length of about 240 metres from the ion

*This document refers to work being performed by scientists and institutions involved in IP EUROTRANS, as well as the financial support of the European Commission through the contract FI6W-CT-2004-516520.*

source. The linac is composed of a succession of independently-powered spoke and elliptical cavities with high energy acceptance and moderate energy gain per cavity – low number of cells and conservative accelerating gradients (around 25 MV/m peak fields nominal operation point) – in order to increase as much as possible the tuning flexibility and provide sufficient margins (about 30%) to allow the implementation of fault-recovery scenarios (see dedicated section here after). It has been shown that such a reliability-oriented design choice leads to an about +20% extra-length, which can be considered as “the price to pay” for reliability.

The 600 MeV XT-ADS baseline linac architecture is summarized in Table 2.2. This linac design has been optimized in terms of total length. It is based on the use of regular focusing lattices, with not-too-long cryostats and room-temperature quadrupole doublets in between. Such a scheme provides several advantages: easy maintenance and fast replacement if required, easier magnet alignment at room-temperature and no fringe field issues, possibility to provide easily reachable diagnostic ports at each lattice location, and last but not least, nearly perfect optical lattice regularity (no specific beam matching required from cryostat to cryostat). The beam tuning has been performed with great care: phase advances are limited below 90° per lattice and parametric resonances are avoided, phase advances per meter are tuned as continuous as possible so as to ease the beam matching, and a very safe and constant longitudinal acceptance is kept all along the accelerator, especially at the 350 to 700 MHz frequency jump transition, as recommended in [2.5].

Table 2.2 : XT-ADS Independently-Phased Linac Overview

| **Section number** | **1** | **2** | **3** |
|---|---|---|---|
| Input energy (MeV) | 17.0 | 86.4 | 186.2 |
| Output energy (MeV) | 86.4 | 186.2 | 605.3 |
| Cavity technology | Spoke 352.2 MHz | Elliptical 704.4 MHz | |
| Cavity geometrical β | 0.35 | 0.47 | 0.66 |
| Cavity optimal β | 0.37 | 0.51 | 0.70 |
| Nb of cells / cavity | 2 | 5 | 5 |
| Focusing type | NC quadrupole doublets | | |
| Nb of cavities / cryomodule | 3 | 2 | 4 |
| Total nb of cavities | 63 | 30 | 64 |
| Acc. field (MV/m @ opt. β) | 5.3 | 8.5 | 10.3 |
| Synchronous phase (deg) | -40 to -18 | -36 to -15 | |
| 5mA beam loading / cav (kW) | 1 to 8 | 3 to 22 | 17 to 38 |
| Section length (m) | 63.2 | 52.5 | 100.8 |

This “conservative” optical design leads to very safe beam behaviours, with low sensitivity to mismatched conditions or current fluctuations, and producing very low emittance growths (about 5%). No beam loss is observed in the multi-particle simulations, that have been performed using a 100 000 particles input distribution, coming from the simulation of the 17 MeV full injector, transported and matched through a typical MEBT – not yet optimized – composed of a quadrupole triplet, a quadrupole doublet and 2 re-bunching cavities. The obtained beam envelopes are shown in Figure 2.4 (left).

*This document refers to work being performed by scientists and institutions involved in IP EUROTRANS, as well as the financial support of the European Commission through the contract FI6W-CT-2004-516520.*

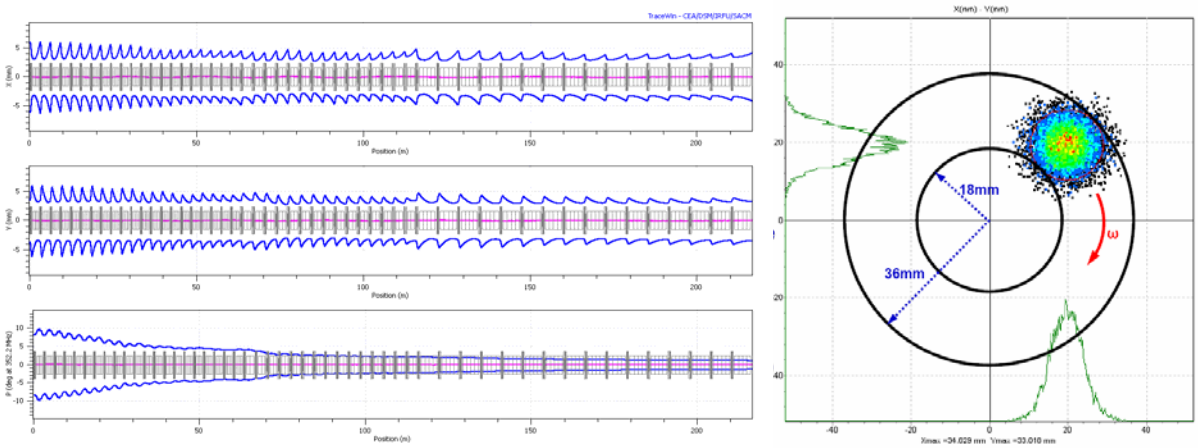


Figure 2.4: (left) 17 – 600 MeV linac 95% beam envelopes;
(right) beam footprint on target.

One has to note that in the 800 MeV EFIT linac case, the very same modular scheme applies, but a third family section is added to cover the 500 to 800 MeV energy range, using 704.4 MHz superconducting elliptical cavities with a geometrical beta of 0.85. This EFIT accelerator is therefore longer by about 75 metres, reaching about 320 metres overall. Due to the higher beam current, more powerful RF amplifiers (4 to 5 times more) are also required for all cavities, leading to beam loading figures up to around 250 kW for the more demanding high-energy cavities (instead of about 40 kW in the XT-ADS case). Another slight change will be of course the total capacity of the cryogenic refrigerator, to be increased from 3.5 kW (XT-ADS case) up to about 6 kW @2K.

### 2.2.3 The Final Beam Transport Line

The objective of the final transport line is to safely inject the proton beam with the specified footprint – donut-shaped – onto the spallation target located inside the reactor (~25 metres deep). The line is composed of two non-dispersive 2×45° achromats, so that the beam spot position and size at the target is independent from energy jitter and spread. In the dispersive region of the last achromat, position and size monitors will be able to provide information on proton energy variations, and to trigger a feedback system. Natural defocusing is used in the last straight line to get the desired beam spot size, and the footprint is then obtained by raster scanning, using a redundant set of fast steering magnets operated at frequencies of 50 to a few hundreds Hz, and acting in the two transverse directions. The obtained beam footprint on target, obtained via multi-particle simulation, is represented on Figure 2.4 (right).

### 2.2.4 Reliability-Oriented Design

As already underlined, the ADS accelerator is expected – especially in the industrial scenario – to have a very limited number of unforeseen beam interruptions per year. This requirement is motivated by the fact that frequently-repeated beam interruptions can induce high thermal stresses and fatigue on the reactor structures, the target or the fuel elements, with possible significant damages especially on the fuel claddings; moreover these beam interruptions dramatically decrease the plant availability, possibly implying plant shut-downs of tens of hours in most of the cases. The initial recommendations concerning these beam trips (for XT-ADS: less than 5 beam trips longer than 1 second per 3-month cycle) have been revisited at the end of the project. A new tentative limit to the allowable beam trips is now proposed for the XT-ADS case: 10 transients longer than 3 seconds per 3-month operation cycle.

To reach such an ambitious goal, reliability-oriented design practices needed to be followed from the early design stage. In particular:

*This document refers to work being performed by scientists and institutions involved in IP EUROTRANS, as well as the financial support of the European Commission through the contract FI6W-CT-2004-516520.*

• “strong design” is needed: every linac main component has to be de-rated with respect to its technological limitation (“over-design”);

• a high degree of redundancy needs to be planned in critical areas; this is especially true for the identified “poor-reliability” components like the linac injector area, which is duplicated, or the RF power systems, where the use of solid-state amplifiers should be considered and investigated as much as possible;

• the accelerator should be able, to the maximum extent, to pursue operation despite some major faults in basic components (“fault-tolerance” capability); it has been shown in [2.6] that a solution based on a modular independently-phased SC linac is indeed capable to easily adapt its nominal tuning in the case of a loss of any RF cavity or power loop unit (see here after).

### 2.2.5 Tolerance to RF Faults in the SC Linac

Because we deal with a non-relativistic proton beam, any RF cavity fault implying beam energy loss will also lead to a phase slip along the linac. It will increase with distance, and thus push the beam out of the stability region: the beam will be completely lost.

To recover such RF faults conditions, the philosophy is to re-adjust the accelerating fields and phases of some non-faulty RF cavities to recover the nominal beam characteristics at the end of the linac, and in particular its transmission, phase and energy. A simple way to perform is to react on the accelerating cavities neighbouring the failing one. This so-called “local compensation method” (see Figure 2.5) has the advantage of involving a small number of elements, and therefore of being able to compensate multiple RF faults in different sections of the machine at the same time.

Beam dynamics simulations show that nominal beam parameters at the target can always be restored using such a retuning method, given the condition that a 20 to 30% rise in accelerating field and RF power can be sustained in the few (4 to 8) retuned elements [2.6]. This method is of course rather demanding in terms of linac length and installed RF power budget, but is on the other hand totally in-line with the ADS over-design criterion, and in any case required to try to reach the required reliability level.

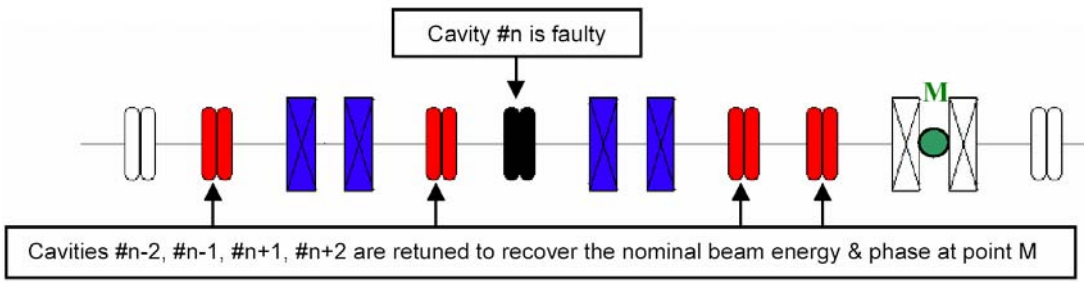


Figure 2.5: The local compensation method.

Transient beam dynamics have been performed to better analyse what happens to the beam during such retuning procedures, keeping in mind that they have to be performed in less than 1 second ideally. A new simulation tool has been developed, based on the TraceWin code [2.7], allowing analysing the effect of time-dependent perturbations on the beam through RF control loop modelling. From this work [2.9], a reference “fast failure recovery scenario” has been defined, that consists in stopping the beam for 1 sec maximum while achieving the retuning. The following sequence (~100ms duration) is proposed:

• the RF fault is detected (or anticipated) via suited dedicated diagnostics and interlocks, and a fast beam shut-down is triggered;

• the new correcting field and phase set-points (previously stored in the low level RF cards’ memory during the commissioning phase) are updated;

*This document refers to work being performed by scientists and institutions involved in IP EUROTRANS, as well as the financial support of the European Commission through the contract FI6W-CT-2004-516520.*

• the failed cavity is quickly detuned (using piezoactuators) to avoid the beam loading effect, and the associated failed RF loop is cut off;

• once steady-state is reached, beam re-injection is triggered.

A conceptual design of a suitable Low Level RF (LLRF) system has been performed [2.9], based on the use of an integrated digital board containing a FPGA chip able to process the feedback control algorithms, several ADCs and DACs to convert the received and produced signals, a RAM memory used to store set-points or save operating parameters, a serial bus to communicate with the general control/command system, and a fast serial bus to communicate with boards of adjacent cavities.

### 2.2.6 Reliability Analysis and Discussion

Two independent integrated reliability analyses have been performed so far to try to estimate the number of malfunctions of the XT-ADS accelerator that could cause beam/plant shutdowns per 3-month operation cycle, and to analyze the influence of MTBFs (Mean Time Between Failures), MTTRs (Mean Time to Repair), and of the whole system architecture on the results.

These studies have been respectively performed by means of a reliability block diagram analysis using the Relex© software [2.10] and by home-made Monte-Carlo simulations [2.11] with slight differences in the hypotheses.

In both cases, the results show that such linacs have a high potential for reliability improvement if the system is properly designed with this particular objective: from about 100 unexpected beam shut-downs per 3-month operation period for a “classical “all-in-series” SC linac, this figure falls around 5 beam interruptions – which is actually the XT-ADS goal – in the case where a second redundant injector stage with fast switching capabilities is used, and when fault-tolerance is included in the independently-phased linac via fast fault-recovery scenarios. Thus, further experimental investigations are necessary to validate the simplified modelling used for such a complex system, and because of the lack of a well-established component reliability figures database.

Having a look at present high-power hadron facilities – like the SNS, not specifically designed for reaching a high reliability – it appears that the experienced number of beam trips longer than 1 second is much higher, by at east one order of magnitude [2.12], showing that there is still a long way to go on this topic. But on the other hand, facilities like ESRF, which is very much concerned by the reliability issue, prove that overall MTBF of several days can already be obtained routinely [2.13], leading to an equivalent of about 20 beam interruptions per 3-month operation.

As a conclusion, it seems at least not completely unrealistic to approach and ultimately reach the ADS accelerator reliability goal. It will imply, as underlined before, to include in the linac design de-rating, redundancy and fault-tolerance, and to have a few years of commissioning and training to identify and fix the weak elements. Approaching the goal “from the other side”, i.e. relaxed specifications on beam trip numbers and their durations by appropriate design measures in the target/reactor system, would also help. Some first steps have been already done in this direction, as mentioned earlier.

### 2.2.7 Conclusion on the Accelerator design

A reliability-oriented superconducting linac has been identified as the reference solution for the European ADS concept, and an advanced design of the machine is proposed for the MYRRHA / XT-ADS project, composed by a 17 MeV injector, possibly doubled, followed by independently-phased modular superconducting cavities with fault tolerance capability. Huge R&D have been performed during the EUROTRANS project, with very successfull results and conclusions. These activities will be pursued within FP7, focusing on several main aspects: design consolidation, investigations on a 176 MHz injector alternative, experiments focused on fault recovery scenarii, and several activities on system optimisation (optimal operating temperature of spoke cavities, RF system optimisation with special focus on solid-state amplifiers at 700 MHz, more detailed and relevant reliability analyses...). The goal would be to be ready for a possible MYRRHA construction phase by 2015.

*This document refers to work being performed by scientists and institutions involved in IP EUROTRANS, as well as the financial support of the European Commission through the contract FI6W-CT-2004-516520.*

## 2.3 Rationale for the Maximum Allowable Number of Beam Trips

### 2.3.1 Methodology

The allowable beam trips in an ADS should make a compromise between an efficient and reliable subcritical reactor and a reasonable cost of an accelerator.

At the beginning of the project, the order of magnitude of the allowable duration of the beam trips was set to 1 second with two frequency values being defined for longer trips followed by reactor shutdowns:

- the objective for the accelerator designers is 5 shutdowns per year or less;
- the objective for the reactor designers is to sustain at least 50 shutdowns per year.

These initial values have been revisited taking into account experience of the PHENIX plant design and operation ($P_{nom}$ = 568 $MW_{th}$). The experience thermal effects induced by the reactor starts and shutdowns can be compared to the effect of the proton beam trips in XT-ADS and EFIT in spite of their smaller sizes and differences in the main systems. Studies have been done for demonstrating the possibility of keeping the structure integrity of the plant but also of the fuel cladding under repeated beam trips. A new tentative limit to the allowable beam trips is now proposed – 10 quick transients / 3 months - with an assessment of the potential risks that the XT-ADS will face if the accelerator misses that goal.

### 2.3.2 Phenix operation and allowable number of SCRAM

The safety dossier of Phenix includes limits for the number of normal, quick and emergency (SCRAM) stops of the plant. The definition of these categories is given in the following:

- Normal stop (NS): It is the reference stop. It induces little constraints on the structures. It takes several hours (8 hours approximately) before the control rods are being fully dropped.
- Quick stop (QS): For relaxing the mechanical load changes on the potentially the most damaged structures, the QS procedure has been modified in 2001. The initial QS procedure was the following one: Simultaneous descent in a motorized mode of the 6 control rods at the 1.4 cm/s speed during 210 seconds and the introduction of a negative reactivity of at least 2000 pcm.
- Emergency stop (ES) : gravity fall of the 6 control rods which is equivalent to at least 3600 pcm in approximately 700 ms distributed as follows (logical: 30 ms, de-energizing of the magnetic reels and start of the moving element: 170 ms, drop time in 500 ms).

The maximum number of allowable operating transients for PHENIX (150 000 hours hence 20 years) was set to 2000 start up and normal or inadvertent stops. A value of 200 number of ES stops was quoted for this machine for its entire life; the maximum permitted number for both together QS and ES is 800.

*This document refers to work being performed by scientists and institutions involved in IP EUROTRANS, as well as the financial support of the European Commission through the contract FI6W-CT-2004-516520.*

In the following table, one presents what has been really achieved during the 20 years of operation of the PHENIX plant.

Table 2.3 Effective Number of Transients during PHENIX operation

| Transient | Effective Number Of Transients | Frequency for 1000 hours of operation | remarks |
|---|---|---|---|
| Start Up | 500 | 4 | < 30% forecast (relative to the operating hours) |
| Normal Stop (NS) | 200 | 1.25 | < 25% forecast (relative to the operating hours) |
| Quick Stop (QS) | 200 | 2.3 | < 35 % forecast (relative to the operating hours) |
| Emergency Stop (ES) | 100 | | |

One can notice that the number of the allowable transients has not been reached in PHENIX reactor in any of categories.

The values cited above yields for PHENIX reactor 40 permitted abnormal (emergency and quick) stops per year or 10 quick transients for a period of 3 month equivalent to one cycle of XT-ADS. This is lower than 50 shutdowns per year foreseen as the objective for the XT-ADS reactor designers in deliverable D1.1 [1.2]. However, the designed life time of XT-ADS is at least twice longer than that initially planned for PHENIX, therefore supplementary analysis should be performed for irreplaceable components of the XT-ADS reactor.

### 2.3.3 Operating transients and damage through fatigue and/or fatigue-creep

The changes of operating conditions (start, stop, variation of power, etc….) in a nuclear plant induce modifications on the mechanical loads and hence on the stress of the important structures according to their impact (speed, amplitude) and of the coolant inertia. These mechanical load variations contribute to the increase in the structure damage by fatigue or fatigue-creep if the temperatures are sufficiently high.

The codes used for calculating the integrity of the structures of the fast neutron power reactors like RCC-MR and RCC- MX are codes which now include material data for irradiation effects. Today the RCC-MX 2008 and RCC-MR 2007 are now more complete than rules RAMSES II, specific to the strongly irradiated structures (hexagonal tubes, sheaths), for the dimensioning of the irradiated structures. However, some innovative materials being studied for use in ETD, such as FMS T91, do not have any irradiation effect included in these codes yet.

The approach taken by PHENIX designers to define the number of allowable quick or emergency stops is very much based on a demonstration that a restricted number of stops is acceptable and that periodic checks of the components is not leading to any degradation of the plant integrity. However, the experience has shown that this process has led to the replacement of some initially designed components by less sensitive ones and also in the end has led to a reduction of its life time.

Detailed studies have been done to quote the impact of any transients on the various structures. During the course of maintenance periods of Phenix, it was discovered that some components were not easily supporting fast transients (in particular heat exchangers) and their designs were changed to better accept these transients. The detailed feedback of these regular checks is not freely available since it has an

*This document refers to work being performed by scientists and institutions involved in IP EUROTRANS, as well as the financial support of the European Commission through the contract FI6W-CT-2004-516520.*

economical aspect but it should be quoted that margins which exist are subject to appropriate design and associated proof of maintaining the integrity of its various components.

In order to keep the rate of temperature change in various structures of PHENIX during a start up within allowed limits, the time required to start or restart the rector after a SCRAM (ES) is 22 hours. (It could be reduced to 14 hours, if the design of some components of the plant would be modified in order to reduce the thermal stresses). The longer part in this period is the initial power increase from zero to 15% of nominal power. At that level of power, the temperature of most of structures is at about nominal level (except the fuel). The coolant flow is increased while increasing the power. The neutron doubling time for the start up procedure of a critical core (which does not exist in an ADS) is not a constraint for the start up procedure hence the transferability to XT-ADS is valid. However, the lower inertia of the XT-ADS core has to be taken into account in the restart procedure. The possibility of maintaining the primary system temperature during a transient for a given time by reducing the amount of heat to be extracted from the core might enlarge the time of acceptance of the accelerator failure.

### 2.3.4 Structure Integrity due to Beam trips

#### 2.3.4.1 Main components

JAEA has performed thermal transient analyses to investigate the effects of beam trips on the reactor components, with the objective of formulating ADS design considerations, and to determine the requirements for accelerator reliability. These analyses were made on the thermal responses of three parts of the reactor components; the beam window, the inner barrel and the reactor vessel. The results indicate that the acceptable frequency of beam trips ranges from 50 to $2.5 \times 10^4$ times per year, depending on the beam trip duration and component [2.14].

These findings were supported by a work performed by Areva [2.15] in the course of the PDS-XADS project. He quoted the final statements: “For the lead-bismuth eutectic cooled ADS, limitations are likely to be imposed by the structures exposed to the fluctuating free level, such as the main vessel, which require detailed thermal-hydraulic and structural analyses.

Beam trips with time duration of less than about 10 s would have no effect on the reactor structures. A number of allowable beam trips of significant duration for the reactor structures of 5000 is a reasonable target value for accelerator designers.”

These JAEA [2.14] and Areva statements [2.15] are leading to much larger values than the provisional values taken at the beginning of the project and those taken for PHENIX as seen in the previous section.

More recently a work performed by SCK-CEN did attempt to find the number of allowed beam trips [2.18]. The lifetime estimation was performed according to the RCC-MR code, calculating strain amplitude ($\Delta\varepsilon$) resulting from beam trips (from stresses in 3 main directions or from von Mises stress), assessing the maximum allowed number of cycles (N) during life time according to $\Delta\varepsilon$-N curves and related tables. Since, figures and tables are only available for unirradiated T91 and AISI 316L, a safety factor of 10 is taken, which is the usual recommended practice.

This work has been performed for the cladding (T91), the core barrel (ASI 316L), the core support plate (T91), the spallation loop (T91), the diaphragm (AISI 316 L) and other structures (T91). It distinguishes various durations of beam trips < 10 seconds; from 10 seconds to 5 minutes and > 5 minutes.

*This document refers to work being performed by scientists and institutions involved in IP EUROTRANS, as well as the financial support of the European Commission through the contract FI6W-CT-2004-516520.*

Table 2.4 Recommendations for the maximum number of allowable beam trips

| Trips | Allowed Number | |
|---|---|---|
| | / cycle | /year |
| < 10 seconds | 800 | 2500 |
| 10 seconds – 5 minutes | 80 | 250 |
| > 5 minutes | 8 | 25 |

These results are very much dependent on the assumptions being taken i.e. the fact that erosion, corrosion and LBE embrittlement has not yet been taken into account. Also, constant temperature in the cold plenum during beam trip transient was assumed. However, in order to make provisions for these assumptions, a supplementary safety factor of 10 has been applied.

The results of these three studies (Areva [2.15], SCK•CEN [2.18] and JAEA [2.14]) are devoted to experimental ADS and do not fit with the PHENIX plant safety dossier for which values of 2000 stops (normal, quick and emergency ones) are quoted for its entire life of 20 years. For what concerns the emergency stops (SCRAM) values of 200 and the quick stops of 600 are quoted for its entire life of 20 years (i.e. 10 SCRAM/year and 30 QS/year).

The reason of such differences is not related to the way irradiation has been taken into account since the approach is the usual practice in these matters. However, it must be noticed that although the damage dose on the core barrel and the support plate is sufficiently low [2.14]; no safety margins have been taken and the integrity of these components is bound to periodic scrutiny. Hence, it is rather surprising that such margins exist with XT-ADS when those specific problems which might arise due to the use of LBE at low temperature (and which make the study comparable to PHENIX operation) might lead to extra concerns. It is the case in particular for LBE erosion, corrosion and steel embrittlement. Probably the approach taken by specialists to define the number of allowable stops in PHENIX is very much based on a demonstration that a restricted number is acceptable and on the desired availability of the reactor rather than defining from studies the maximum allowable number of stops. Therefore the PHENIX recommendations might be considered only as an indication of the minimum permitted number of the quick transients for the XT-ADS reactor case: 10 transients per cycle of 3 months. However, specific problems which might arise due to the use of LBE in XT-ADS at low temperature might lead to extra concerns. It is the case in particular for LBE erosion, corrosion and steel embrittlement.

#### 2.3.4.2 Fuel Elements

One of the crucial parts of a nuclear plant during quick and emergency stops remains fuel rods, which operate at higher temperature gradients, radiation doses and coolant velocity than any other component. In order to insure better response of a fuel rod to fast transients (including the beam trips), at least two effects should be avoided during its residence time in the core of XT-ADS: a strong pellet-cladding mechanical interaction (PCMI) and embrittlement of the cladding by liquid LBE coolant. A mild PCMI is allowed in power plants at normal operation conditions; the stresses built by it are permanently relieved by the cladding creep. The danger appears at fast overpower excursions and when the cladding becomes brittle.

In spite the fact that the linear heating rates and the fuel temperature gradients in the XT-ADS fuel pins are not very high at normal operation conditions compared to those in the well-known experimental and power sodium fast reactors, they are sufficient, however, for fuel pellets cracking in the radial and, in lesser extent, in the circumferential direction in a majority of the fuel pins already at the first start of the reactor. Consequently the fuel pellet effective gaps reduce for 30-40 % (depending on the initial radial temperature gradient in the pellets) due to relocation of the pellet fragments.

*This document refers to work being performed by scientists and institutions involved in IP EUROTRANS, as well as the financial support of the European Commission through the contract FI6W-CT-2004-516520.*

At the beginning of fuel life the following quick reactor shutdowns followed by subsequent power recovery result only in a very small secondary cracking which is rapidly saturated with the repeating of this transient. The thermal stresses generated within the pellet fragments by the repeated ramps are not sufficient to initiate their cracking. A partial healing of micro-cracks may happen due to irradiation assisted diffusion, despite of relatively low temperature. In this case the new ramps can reinitiate the cracking.

With an increase in the fuel burnup the pellet swelling, induced by the fission products (solid and gaseous) and fission gas release become more and more important; both depend on temperature. At low fuel temperature a large fraction of the fission gases and solid fission products remain within the fuels matrix enhancing swelling. In the beginning this effect is compensated by the irradiation induced densification. At higher burnup the swelling dominates and this results in the gap reduction [2.20]. At further burnup increase the release of fission product starts and the rate of swelling decreases. It is important to note that a part of fission gases is accumulated on the fuel grain boundaries, within micro-pores and in the micro-cracks. In the case of a rapid cooldown followed by a heat-up this part can initiate the secondary cracking of the fuel pellet fragments, but also a burst release of the fission products. So, the gas pressure will increase and a bit more fuel pellet fragments may appear. The next transients in a short time will not have the same effect (the fission gas from the grain boundaries have already released and the mechanical stresses have been relaxed. A mild PCMI can appear if the designed gap was insufficiently wide.

Reliability of predictive capabilities for the fuel pin mechanics behaviour under these operation conditions is dependent on knowledge of the fuels materials and the clad materials behaviour dependent on burnup and damage dose. During the rapid cool down of the cladding the closed gap conditions increase the risk of built-up of a large fuel to clad contact pressures approaching to the yield stress limits for the irradiated T91 clad material. This danger was also indicated in the report of R. Dagan *et al*. (FZK) [2.17], where the results of modelling were presented for a particular case.

During the design of fuel and development of the core management scheme for XT-ADS the main attention was paid to avoiding PCMI during the expected fuel residence time. B. Arien (SCK•CEN) [2.22] modelled the thermal response of the XT-ADS hottest fuel rod to beam trips followed by restarts in 1, 2, 5 and 10 s at BOL. It was shown that the gap remains open in all four cases. In order to approach to an acceptable fuel management scenario, modelling of the thermomechanical behaviour of the XT-ADS crucial rods was performed taking into account the initial cracking of the fuel pellets [2.18]. The obtained results show that it is possible to avoid PCMI during 7-8 cycles.

The detailed thermomechanical modelling of the effect related to multiple ramps and relevant experiments under realistic load conditions and for fuel pin conditions representative for the irradiation state at the end of the foreseen residence time in the XT-ADS should still be done. If the respective experimental observation can be retraced theoretically it might be feasible to find better multi-batch fuel reload strategies which reduce the risk of the fuel pin failures as consequence of too frequent beam trips. In the mean-time one can use physically sound models benchmarked on the results of relevant experimental results available in the literature on the oxide fuel cracking at power ramps, while remaining on the conservative side concerning the number of allowable beam trips.

The current experiments show that lead-bismuth environment is also a catalyst for increasing the risk of early unintended clad rupture. The oxide layer, which protects the cladding material from direct contact with lead, can be damaged by several processes, in particular due to the differences in terms of mechanical and thermal properties (e.g. ductility, thermal expansion coefficient, thermal conductivity). At normal operation the damaged zone in the oxide layer is expected to rapidly recover due to oxygen dissolved in the coolant. However, in the case of a high rate of the cladding creep, observed at rather high stresses, the rate of this self-healing is not sufficient to cover the increasing damaged spot.

The analysis of the creep test results [2.21] revealed several important surface phenomena, which lead to different behavior of the specimens tested in LBE compared with the specimens tested in air:

- oxide scale breaking and crack propagation;
- liquid metal - steel interaction at the crack tips;
- dissolution of the steel components [2.17].

*This document refers to work being performed by scientists and institutions involved in IP EUROTRANS, as well as the financial support of the European Commission through the contract FI6W-CT-2004-516520.*

The weight, with which these phenomena influence the specimen behavior during creep to rupture tests in LBE, depends on the value of the applied stress. At high stress, and therefore high strain, the crack propagation process is accelerated and mostly controlled by the reduction of the surface energy due to Pb and Bi absorption on the steel surface. At low stress and low strain, this process is delayed due to the competing mechanism of healing the oxide scale cracks. This means that, by increased numbers of thermal shocks, the oxide layer, which protects the cladding material against corrosion, may be cracked if sufficiently large thermomechanical stresses will be generated during a transient. In this situation the probability of the direct contact between the Pb-Bi coolant and T91 cladding material and their interaction (corrosion and embrittlement) increase. However, it should be noticed that the experimental results were obtained by A. Jianu, G. Müller, A: Weisenburger, *et al*. [2.21] at the Pb-Bi coolant temperature of 550 °C and stresses 140-220 MPa, and the authors pointed out that "*Normal operating conditions of nuclear systems components, cooled with LBE do not foresee stress levels similar to those*" and that "*The threshold stress, below which LBE has no influence on the creep properties, must be examined. Below this level, the data obtained during creep tests in air can be extrapolated to estimate the creep behaviour of the specimens exposed to LBE*." At lower stresses the effect of the self-healing of the oxide layer on the cladding surface remains dominant. According to estimations performed in [2.18] the highest stresses in the T91 cladding of XT-ADS in the absence of PCMI are less than 50 MPa during all normal operation time, i.e. far below the lowest level considered in [2.21]. Nevertheless, this effect has to be studied in more details and the technology of the cladding protection must be proven for the XT-ADS conditions.

To address in a quantitative manner this issue whose importance cannot be questioned, a new set of experiments is planned exclusively for thermal shocks under different stress conditions and within lead-bismuth environment. With these dedicated experiments planned at the Material Institute in FZK, the range of allowable number of beam trips will be determined more precisely with conclusions forecast in March 2010. The test will be directly aimed to the integrity of the oxide layer over the clad under those load conditions.

### 2.3.5 Perspectives for the maximum allowable beam trips

It was foreseen already at the beginning of the project that the objective of a maximum of 5 beam trips longer than 1 second per cycle (3 months) will be revisited at the end of the project. JAEA values for a similar project are giving some serious reasons to revisit the target value.

The preliminary values were taken based on the experience of PWR and FR plants (especially PHENIX). It appears that current practices in defining the maximum limits in normal, quick and emergency stops is bound to preliminary mechanical studies but also very much to an iterative process between design and periodic verifications of the various components. Hence, the consequence of a bad prediction in the induced stress of quick or emergency stops is either leading to the replacement of a component (Heat Exchanger for instance) with an associated reduction of the plant availability or a reduction in the plant life time.

Hence, increasing the maximum number of beam trips is not an issue which has minor consequences on the plant operation. Current studies show that some margins exist – but the core barrel, the support plate and the fuel pins need further studies. For the fuel pins the main critical points are the avoiding by design the PCMI and the potential danger of the cladding embrittlement by LBE coolant. In March 2010, tests planned in FZK will be directly aimed to the integrity of the oxide layer over the clad under those load conditions. However, fuel assemblies could be replaced with an impact on the plant availability and the fuel cycle cost. To address in a quantitative manner this issue whose importance cannot be questioned, a new set of experiments is planned exclusively for thermal shocks under different stress conditions and within lead-bismuth environment. With these dedicated experiments, the range of allowable number of beam trips will be determined more precisely.

At the moment, increasing the number of allowable beam trips up to 10 beam trips/cycle of three months (based on specs of PHENIX) and allowed delay of the beam restart up to 3 seconds seems possible at least at the start of the operation of the XT-ADS plant (temporarily) with a potential added risk on the availability of the plant and with the requirement to use an adequate scenario of the fuel reloading. It will require periodic scrutiny to address safety concerns. If the FZK experiments will provide some margins on

*This document refers to work being performed by scientists and institutions involved in IP EUROTRANS, as well as the financial support of the European Commission through the contract FI6W-CT-2004-516520.*

the fuel side, then the possibility of relaxing the limits might be coming from beam trips of longer length provided the inertia is sufficiently long to recover a significant power after beam trip. In beam trips (between 3 seconds and 5 minutes) an adequate plant operating system is required to reduce the secondary coolant flow (and this as soon as possible after the beam trip in order to avoid LBE freezing) and to keep the primary coolant (and the main components of the primary system and vessel) at the operating conditions.

Finally, the objective to keep the number of beam trips to an absolute minimum is mandated also by the need to guarantee the availability of the machine, a point which will be covered in Chapter 3.4.

REFERENCES

[2.1] J-L. Biarrotte et al, “A reference accelerator scheme for ADS applications”, Nucl. Instr. and Meth. In Phys. Res. A 562 (2006), pp. 565-661.

[2.2] J-L. Biarrotte et al., “Accelerator R&D for the European ADS demonstrator”, Proc. PAC2009, Vancouver, Canada.

[2.3] C. Zhang et al, “Conceptual studies for the EUROTRANS front-end”, Proc. PAC2007, Albuquerque, USA.

[2.4] U. Ratzinger and R. Tiede, “Status of the HIIF RF linac study based on H-mode cavities”, Nucl. Instr and Meth. in Phys. Res. A 415 (1998), pp. 229-235.

[2.5] R. Duperrier et al., “Frequency jump in an ion linac”, Phys. Rev. ST Accel. Beams 10, 084201 (2007).

[2.6] J-L. Biarrotte & al., “Beam dynamics studies for the fault tolerance assessment of the PDS-XADS linac design”, Proc. HPPA 2004, Daejeon, Korea.

[2.7] http://irfu.cea.fr/Sacm/logiciels/index.php

[2.8] J-L. Biarrotte, D. Uriot, “Dynamic compensation of an rf cavity failure in a superconducting linac”, Phys. Rev. ST – Accel. & Beams, Vol. 11, 072803 (2008).

[2.9] O. Piquet et al., “VHDL analysis and synthesis”, Eurotrans DEL n°1.66 (CEA), 2008.

[2.10] L. Burgazzi, P. Pierini, “Reliability studies of a high-power proton accelerator for accelerator-driven system applications for nuclear waste transmutation”, Reliability engineering & systems safety, Vol. 92, n°4 (2007), pp. 449-463.

[2.11] R. Brucker et al, “Integrated reliability analysis of the Eurotrans accelerator”, Eurotrans DEL n°1.69 (Empres. Agrup.), 2009.

[2.12] J. Galambos et al., “Commissioning strategies, operations and performance, beam loss management, activation, machine protection”, Proc. ICFA HB 2008, Nashville, USA.

[2.13] L. Hardy et al., “Operation and recent developments at the ESRF”, Proc. EPAC 2008, Genoa, Italy.

[2.14] H. Takei, K. Tsujimoto., N. Ouchi., H. Oigawa,M. Mizumoto, K. Furukawa, Y. Oigawa, Y. Yano “Comparison of beam trip frequencies between estimation from current experimental data of accelerators and requirement from ADS transient analyses” HPPA5 workshop proceedings mol Belgium, May 2007.

[2.15] Benoît Giraud, Luciano Cinotti, Brian Farrar, “PRELIMINARY ENGINEERING REQUIREMENTS ON ACCELERATORS FOR ADS”,

[2.16] Y. Romanets et al., Report D1.54 IP EUROTRANS « Evaluation of Radiation Damage and Circuit Activation of XT-ADS”

*This document refers to work being performed by scientists and institutions involved in IP EUROTRANS, as well as the financial support of the European Commission through the contract FI6W-CT-2004-516520.*

[2.17] R. Dagan M. Schikorr, A. Weisenburger, " Estimation of Permissible Beam Trips for Sub Critical Systems", draft document.

[2.18] D. Maes, V. Sobolev, B. Arien, D. Lamberts, P. Baeten "MYRRHA; Preliminary results on BEAM TRIPS ", draft document

[2.19] "The SAS4A LMFBR Accident Analysis Code System", ANL/RAS 83-38, Rev.2, February 1988.

[2.20] K. Lassmann, F Hohlfeld, The revised URGAP-model to Describe the Gap Conductance Between Fuel and Cladding, Nucl. Eng. Design, 103 (1987) 215-221.

[2.21] A. Jianu, G. Müller, A: Weisenburger, A. Heinzel, C. Fazio, V. Markov, A. Kashtanov, Creep to rupture tests of T91 steel in flowing Pb-Bi eutectic melt at 550° C. Accepted for publication, Journal of nuclear materials 2009.

[2.22] B. Arien, "Possible mitigation of the beam trip effects", Presentation, Coordination Meeting of WP1.1 of FP7 CDT, Brussels, 8 July 2009.

*This document refers to work being performed by scientists and institutions involved in IP EUROTRANS, as well as the financial support of the European Commission through the contract FI6W-CT-2004-516520.*

# 3. DESCRIPTION OF THE 395 MWTH PB-COOLED EFIT

## 3.1 Choice of coolant temperatures

The ETD/EFIT lead (Pb) cooled reactor will be deployed within a nuclear park in which it will produce part of the electricity. In order to limit the burden of such a plant (it is more expensive than existing LWR power plant), the reactor has been designed to produce electricity with rather good efficiency. This has been achieved operating the primary coolant cycle with rather high output temperature. The lead coolant offers such possibility with three orders lower bismuth activation than LBE. With the lead coolant inlet and outlet temperatures of respectively 400°C and 480°C, a thermal efficiency of ~40% can be reached with the superheated vapour secondary circuit, taking into account electricity required by pumps (from both the primary circuit and the secondary ones) but without deducing the power required for the accelerator.

The core pressure drop has been limited to improve the efficiency of the plant, however, other considerations associated to decay heat removal in transient events and to elevation of the plant have been also an incentive to design the core with a pressure drop below 1 bar.

The decision for such lead inlet and outlet operating temperatures implies some consequences on the water secondary circuit input and output temperatures and these should be sufficiently high to limit the possibility of freezing the lead coolant in either ordinary transients or in accidental conditions.

The corrosion/erosion resistance of the cladding material is very much linked to the thermal hydraulic conditions within the sub-assembly, especially to the temperature level, to the temperature drop across the core, to the content of dissolved oxygen and to the coolant velocity. Long term operation of the existing T91 cladding in Pb-flow is limited to 500 °C under optimal oxygen control conditions and to the average channel speed of 2.0 m/s. However, using T91 cladding with the current limitation would make the margin to the coolant outlet temperature rather small and hence the possibility of increasing the power density rather small.

In the current strategy of R&D acquisition, the XT-ADS and EFIT operating temperatures, as suggested by ANSALDO [3.11], are set in an increasing challenging order and hence appear reasonable for achieving the final goal.

The figure 3.1 shows that a window type spallation target is not possible in a EFIT-Pb plant since its operating temperature would be too high for an irradiated material to withstand the mechanical constraints built in the window proposed design. This, hence, favours a design of windowless target. For the XT-ADS plant, the windowless choice is very much a decision ensuring consistency with the EFIT-Pb plant and window target might be feasible (provided 600 MeV is not too small for keeping the energy deposition within acceptable limits).

The required material technology behind all these considerations has been studied by the DEMETRA domain; the achieve progresses and R&D still to be done are reported in Chapter 10.4.

*This document refers to work being performed by scientists and institutions involved in IP EUROTRANS, as well as the financial support of the European Commission through the contract FI6W-CT-2004-516520.*

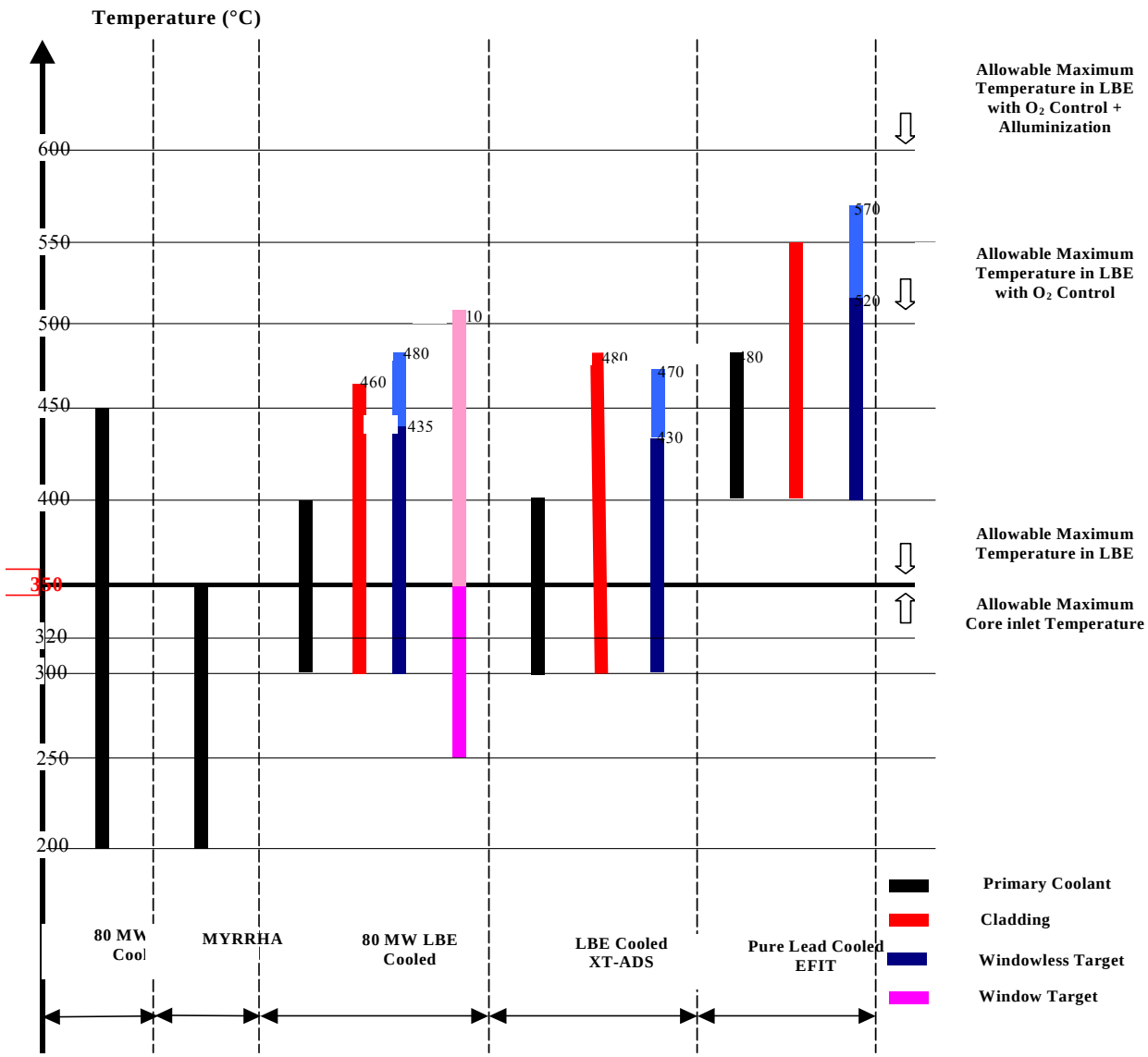


Figure 3.1: ETD/XT-ADS and ETD/EFIT operating temperatures

The current upper temperature limit for a long term operation of the T91 cladding is set to 550°C (it can be secured with the help of the GESA coating technology still under scrutiny) which would make the margin to the coolant outlet temperature rather small and hence the possibility of increasing the power density rather limited.

*This document refers to work being performed by scientists and institutions involved in IP EUROTRANS, as well as the financial support of the European Commission through the contract FI6W-CT-2004-516520.*

What is already known about the T91 steel and the Fe, Al based coatings are the following:

- the maximum allowable temperature for the T91 limited by resistance to creep rupture strength (without considering irradiation and HLM) is 550 °C for the stresses induced by full release of fission gas at 10 at.% FIMA burnup in the adopted design of the fuel pin .
- the oxide layer that forms on the T91 surface by dissolved in Pb oxygen is a protection against direct contact with Pb only in the several interval of oxygen content. Therefore, the Pb environment should be oxygen controlled. Above 500°C, a protection with FeAl based coating has been envisaged. This coating is thought to be stable in Pb under controlled oxygen up to 600 – 650 °C [10.4.3]. However, the long-term stability and the resistance to temperature transients of the oxide layer and the coating should be tested.

The behaviour of T91 irradiated in a neutron field is expected to be similar to the other 9Cr1Mo steel already tested in Phénix (France) up to about 90 dpa at about 450 °C and in USA up to 204 dpa at 400 °C, where the level of hardening and embrittlement in the range 400-550°C is less important with respect to the low temperature (T<400°C) results, which are obtained from other irradiation experiments (see BOR-60 and BR2 MTR (T< 300°C)). However, the above statement needs to be proved by the PIE Phénix campaign and may be by supplementary irradiation tests. In the curent EFIT design the clad damage limit of 130 dpa was adopted. As said before the maximum Pb speed is set to 2m/s to limit the corrosion/erosion of the cladding to few µm for a whole residence time.

At this step it was assumed that the maximum damage on non-replaceable components should remain below 2 dpa except for the pressure vessel for which it should remain below 0.1 dpa for the entire plant lifetime. However, this assumption has still to be confirmed by future thermomechanical calculations and tests.

Other material boundary constraints are reported in [3.1]. In addition to that, the use of advanced materials such as $Ti_3SiC_2$ a ceramic material used for the pump placed in the hot leg seems to be able to withstand the rather hot Pb temperature but its mechanical properties should be justified by appropriate experiments.

## 3.2 EFIT-Pb core design

### 3.2.1 Design Approach

In designing the EFIT reactor core, starting from the selected materials and the goals to be reached, the core design has been conducted with the several considerations [3.1] developed hereafter.

Positive Pu breeding gain (increase of Pu mass) has to be avoided. The use of U-free fuel helps in that matter since no Pu is being produced through U238 capture but production of Pu through Cm decay should also balance the Pu disappearance through fission and capture. Since the final fission balance is in any case 42 kg/$TWh_{th}$, (a consequence of the fact that there is a relationship between energy produced and material destroyed though fissions; related to the fact that one fission produces 200MeV). The design aim is hence to achieve a ~42 kg/$TWh_{th}$ for the MA balance and ~0 kg/$TWh_{th}$ for the Pu balance.

Starting from given Pu and MA vectors [1.2], a preliminary ratio of MA nuclides to all nuclides, that brings about a burn up reactivity swing of a few hundreds pcm/cycle or less ($\Delta K \approx 100$ pcm/cycle) without burning or breeding Pu, is determined. For the case of $\Delta K \approx 0$ and Pu breeding ratio ≈ 1, this means that reactor operation, intended as combined operation of sub-critical core and spallation neutron source, takes place at constant proton beam current over each cycle and that, at the end of each fuel cycle, the new fuel can be fabricated by adding fresh MA only to the reprocessed fuel of the previous cycle. The choice of Pu breeding ratio ≈ 1 implies that Pu has to be brought in the ADS fuel cycle only for the first fuel loading. To obtain the optimum transmutation rates and Pu breeding ratio ≈ 1, a content in Pu of 45.7%, defined as the ratio (in weight) between the amount of its nuclides and the sum of them with MA (= total fuel), has been used for the

*This document refers to work being performed by scientists and institutions involved in IP EUROTRANS, as well as the financial support of the European Commission through the contract FI6W-CT-2004-516520.*

EFIT core loaded with the selected CerCer (MgO matrix) composite fuel and ≤40 % Pu for the EFIT core loaded with the CerMet (Mo matrix) composite fuel [3.17].

The number of the FAs at the required Pu content, enough to obtain the optimum transmutation rate, which assures the design constraint of (sub)criticality level of $K_{eff}$ ~ 0.97, defines also the power level of the core. To maximize the average HM power density, that is to maximize the MA fission rate, power distribution radial flattening techniques are needed.

Beyond the general statement related to the thermodynamic efficiency of the plant, there is another reason requiring power distribution radial flattening techniques: to minimize the spread of the FAs outlet temperature. Since inert matrix volume fractions lower than 50% are needed to warrant the integrity of the composite CerCer and CerMet fuels under irradiation, it has been chosen to increase the fuel pin diameter in the core peripheral FAs with CerCer in order to increase the fuel volume fraction; in the case of CerMet thicker fuel pins are used with different volume fractions of Mo matrix. This means that, with a constant MA to Pu ratio, the power distribution radial flattening is achieved through the use of fuel pins of different sizes and composition.

Since EFIT is a hybrid reactor controlled by the spallation neutrons, it must be ensured that the core remains always sub-critical, without having to rely on shutoff or control rods. The margin to criticality is an important requirement for the core definition that leads, eventually, to define core size and reactor power.
This approach led to assume a margin of 0.016 ΔK to criticality. This figure includes allowance for measurement errors, required at DBC, akin to standard practice for light water reactors. $K_{eff}$ shall hence not exceed 0.984 at any time during DBC. It is further assumed that a thinner margin is acceptable for DEC, owing to their postulated very low frequency, and that $K_{eff}$ shall not be greater than 0.95 during refuelling or Target Unit removal for replacement. Figure 3.2 below illustrates safety criteria, showing that at no time $K_{eff}$ shall move into the red regions, which represent the margins to criticality allocated to the three above mentioned conditions. The green region covers the range of $K_{eff}$ allowed for normal operation. The yellow regions cover the excursion ranges of $K_{eff}$ predicted by the transient analyses for DBC and DEC respectively. Because completion of design is outstanding and the transient analyses will follow, both regions are depicted, but not figured out. As starting point for the design $K_{eff}$ = 0.97 has been preliminary assumed for EFIT as the maximum value for the nominal full power conditions (upper limit of the green region).

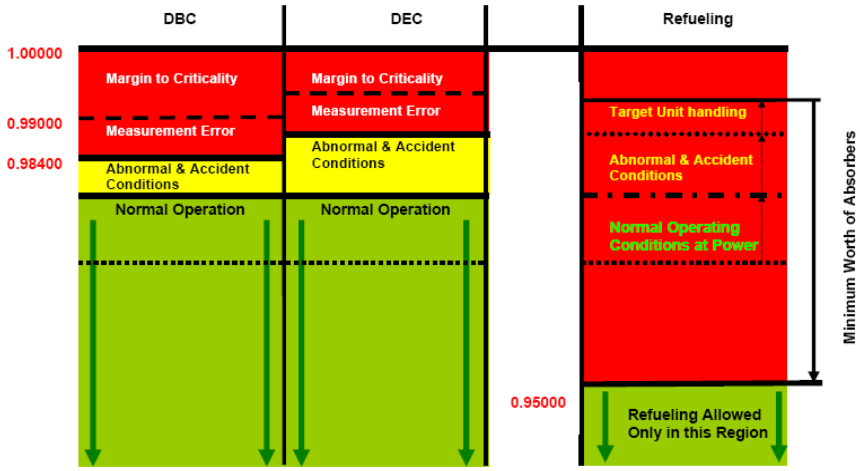


Figure 3.2: Reactivity criteria for ETD/EFIT safe

Evidence of the achievement of such constraints is given in chapter 6.1.

*This document refers to work being performed by scientists and institutions involved in IP EUROTRANS, as well as the financial support of the European Commission through the contract FI6W-CT-2004-516520.*

### 3.2.2 Core description

The EFIT core is designed for a thermal power of about 400 MW, aiming at transmutation performance and radial power flattening. In order to flattening the radial power distributions, a 3 fuel zone core has been selected. In case of the core loaded with CerCer fuel, the intermediate zone is loaded with fuel containing 50 vol. % MgO matrix and suitable pin diameter and pitch (to maximize the power density and to minimize the core pressure losses). In the inner zone the fuel content is lowered increasing the MgO content up to 57 vol. % and in the outer zone, the fuel has the same composition of intermediate zone but with increased pin diameter to increase the total fuel amount. This permits to work with a high maximum and average power density (max for each homogeneous zone 98.7, 94.5 and 95.6 W/cm$^3$ and homogeneous average 70,7 W/cm$^3$ = 303.1 W/cm$^3$ for the fuel material) and, as a consequence, high burn up (about 78,3 MWd/kg HM after 3 years of operation).

The specific burning rate (mass of fissioned MA per TWh$_{th}$ generated energy) is around 42 kg MA/TWh, "42-0 approach". The selected U-free oxide fuel in a MgO matrix has permitted to obtain a MAs and Pu burn up of 13.9% and 0.7% respectively for the 3 year cycle (see Figure 3.3 below).

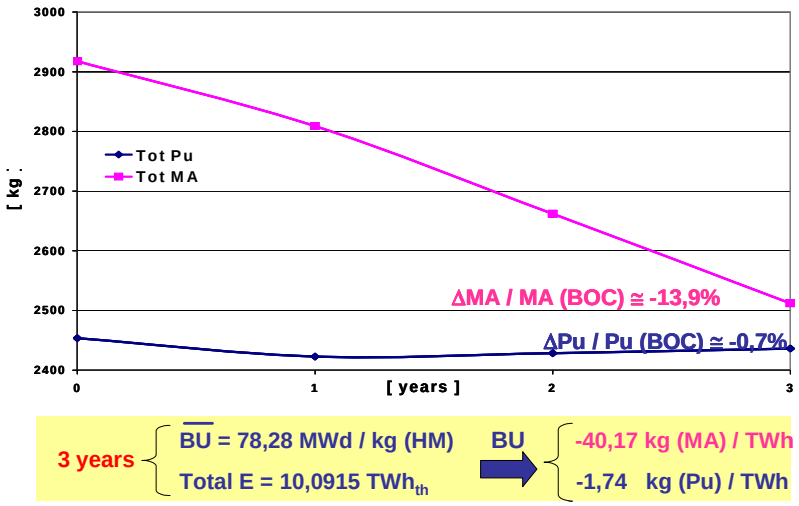


Figure 3.3: Pu and MA Burn Up

The core includes 180 fuel assemblies (FA); 42 inner FAs (type 1), 62 intermediate FAs (type 2), 72 outer FAs (type 3) and 242 dummy assemblies.

The 3 zones and the fuel pellets are described in Figures 3.4 and 3.5

*This document refers to work being performed by scientists and institutions involved in IP EUROTRANS, as well as the financial support of the European Commission through the contract FI6W-CT-2004-516520.*

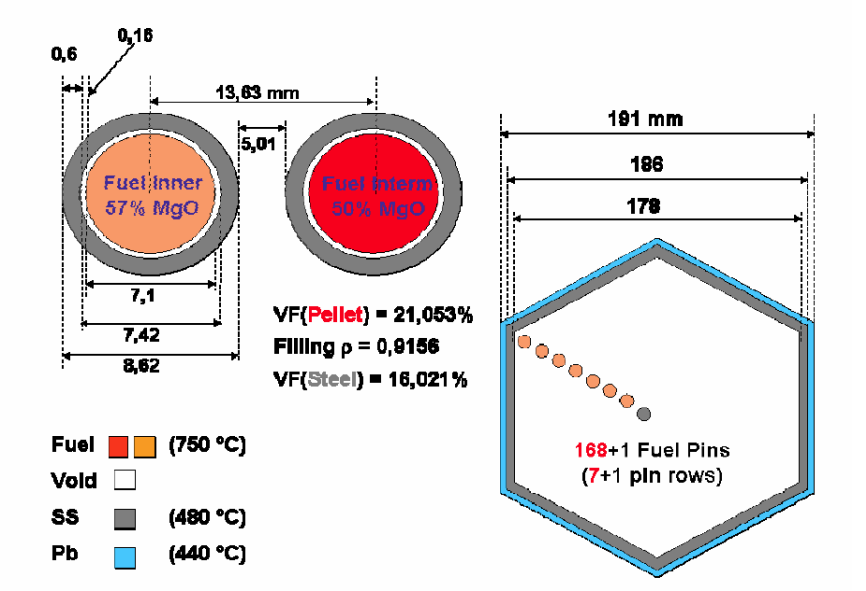


Figure 3.4: Fuel pins and assembly geometry for inner and intermediate zones

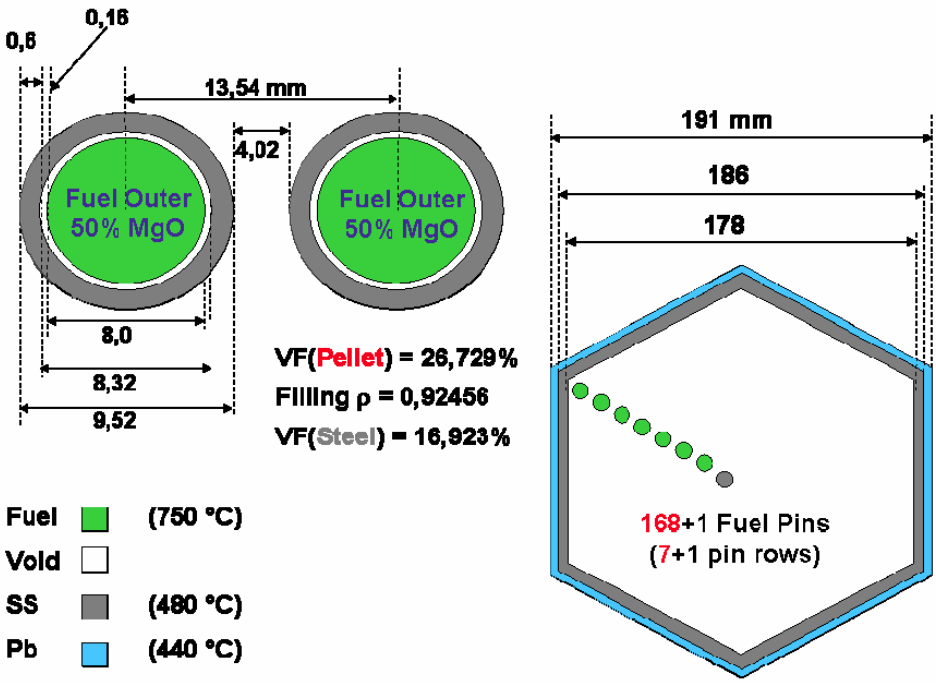


Figure 3.5: Fuel pins and assembly configuration for outer zone

A large number of detailed analyses have been performed concerning the reactivity levels, the power distribution, the power and transmutation optimisation techniques, the burn up behaviour [3.1], the reactivity

*This document refers to work being performed by scientists and institutions involved in IP EUROTRANS, as well as the financial support of the European Commission through the contract FI6W-CT-2004-516520.*

coefficients [3.3], the decay heat production [3.4], the neutron damage evaluation, the materials activation [3.5], thermal hydraulic steady-state and transients analyses [3.6], fuel pin thermo-mechanical and FA fluid-induced vibration behaviours [3.7], etc.

The 3-zone EFIT-CerCer (MgO) Pb-cooled core configuration is characterised by a sub-criticality level (ERALIB-1/JEF-2.2 deterministic approach results) of 2913 pcm at the BOC and of 2710 pcm at the EOC. The 209 pcm of burn up reactivity swing per year was confirmed by the Monte Carlo evaluations using the JEFF 3.1 neutronic cross-sections libraries.

The low importance of the neutron source (0.52) is one of the consequences of the large dimensions of the spallation module (high neutron source leakage).

The impact of the nuclear data in the sub-criticality level (about 1000 pcm of $\Delta K_{eff}/K_{eff}$ discrepancy between MCNP/JEFF 3.1 and ERANOS/ERALIB-1 - JEF 2.2 results) is clearly identified as something to be reduced prior to the construction of the plant (see NUDATRA section).

### 3.2.3 Decay Heat Generation.

A consequence of the high MA content in the fuel is that four independent Decay Heat Removal loops are provided in the EFIT reactor, in order to remove the decay heat towards the atmosphere by natural convection. Actually, the decay heat of MA loaded fuels is approximately 30% higher than the MOX one for short and intermediate times, decreasing (slightly) according to the $^{242}$Cm decay constant (162 days half-life) [3.4]. It was found that the total decay heat is substantially due to the contribution of Cm, which is present in the fresh fuel by an amount of few per cents, less than 3%.

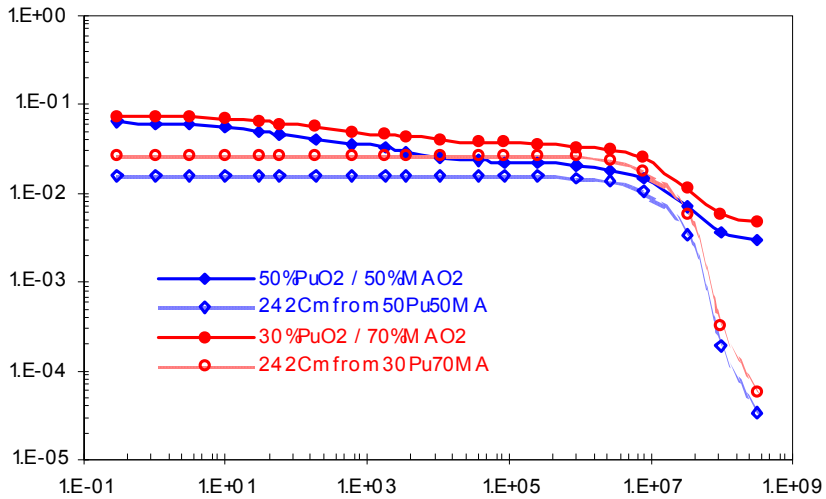


Figure 3.6**:** Normalized decay heat and $^{242}$Cm contribution.

Analysing the mass balance of the different Cm isotopes, a remarkable build up of the $^{242}$Cm isotope is observed, decaying by $\alpha$-mode with Q-value of 6.216 MeV. Figure 3.6 shows the total decay heat and the $^{242}$Cm contribution (normalized to the "deployed power"). An important aspect, from the reactor design point of view, is the long term reliability of the decay heat removal components.

*This document refers to work being performed by scientists and institutions involved in IP EUROTRANS, as well as the financial support of the European Commission through the contract FI6W-CT-2004-516520.*

### 3.2.4 Summary of the CERCER core design

The 3-zone EFIT-CERCER (MgO) / Pb-cooled core configuration meets the established goals satisfying the design constraints. The MA transmutation (fission), via a U-free lead cooled sub-critical system, has been demonstrated to be promising by the EFIT concept based on the “42-0” transmutation rate strategy. At the same time, the 3-zone core design leads to a sufficiently flat radial power profile, allowing acceptable peak pin fuel and cladding temperatures.

At long term the MAOx fuel decay heat, and less for the MOX fuel, is essentially due to the actinides decay rather than the fission products decay. MA decay heat is dominant during the first 3 years. Because of the high decay heat of MAs, the EFIT reactor needs an effective and “long-time” reliable way to evacuate residual power.

The hard neutron spectrum, consequence of the above choices, which contributes to the strong positive reactivity worth of the coolant void effect, involves also relatively high neutron irradiation damages on some components. After 20 years of full power irradiation the Pb coolant activity rises (in average) at about $10^{11}$ Bq/kg.

### 3.2.5 The CerMet core design variant

An important advantage of the CerMet (Mo-matrix) fuel lies in its high thermal conductivity [3.21]. An increase of the pin diameter or even an upgrade of the core to higher power densities and higher ratings is possible. Assuming similar pin and subassembly geometries and Pu/MA ratios as the CerCer (MgO) core revealed that the transmutation rate for MAs was less in the CerMet core [3.22]. However, much better thermal physical properties of CerMet make a design with thicker pins (corresponding to a higher fuel volume fraction) possible to improve the transmutation efficiency without loss of the outstanding safety advantages of the CerMet [3.20]. The designed CerMet three-zone core satisfies the EFIT general and specific requirements and is adapted to the EFIT overall plant design. The ‘42-0 condition’ has been slightly relaxed for obtaining a good MA transmutation rate and achieving a low reactivity swing [3.19]. The core is displayed in Figure 3.7.

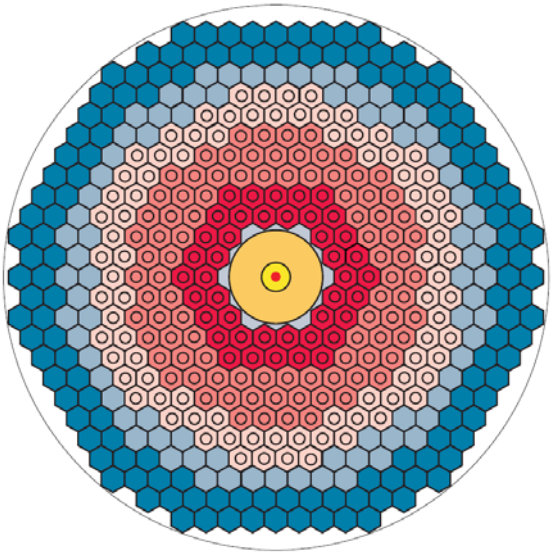

Figure 3.7: Cross plane of current AFTRA 3-zone core with CerMet fuel (core zones 1-2-3 in red with decreasing intensity)

*This document refers to work being performed by scientists and institutions involved in IP EUROTRANS, as well as the financial support of the European Commission through the contract FI6W-CT-2004-516520.*

The higher Mo neutron absorption (CerMet) than MgO one (CerCer) is compensated by its higher conductivity which enables bigger pins and hence a higher fuel volume fraction. In Table 3.1, major design data for the CerCer and CerMet core are displayed.

| | CERCER fuel | | CERMET fuel | |
|---|---|---|---|---|
| | Inner + Intermediate | Outer | Inner + Intermediate | Outer |
| Number of Pin per S/A | 169 | | 91 | |
| Number of Pin rows per SA | 7 | | 5 | |
| Pin outer Diameter (cm) | 0.862 | 0.952 | 1.267 | 1.399 |
| Pitch to Rod Ratio | 1.58 | 1.42 | 1.46 | 1.31 |
| Pitch (cm) | 1.363 | 1.354 | 1.846 | 1.834 |
| Cladding Thickness (cm) | 0.06 | | 0.06 | |
| Pellet/Cladding Gap (cm) | 0.016 | | 0.016 | |
| Pellet Diameter | 0.71 | 0.8 | 1.115 | 1.247 |
| Coolant Fraction | 60.8% | 53.9% | 55.7% | 47.7% |

Table 3.1 Major Design Data of the CerCer and CerMet core

Reactivity feedback coefficients are very similar in magnitude anticipating similar behaviour.

The two designs are compared for their transmutation performance of MAs (Tables 3.2 and 3.3)

| Element | m BOL (kg) | m EOL (kg) | Δm (kg) | Δm (kg/TWh$_{th}$) |
|---|---|---|---|---|
| U | 0 | 4 | 4.4 | 0.44 |
| Np | 113 | 100 | -13.8 | -1.37 |
| Pu | 2454 | 2415 | -38.8 | -3.84 |
| Am | 2679 | 2195 | -483.4 | -47.77 |
| Cm | 125 | 232 | 106.6 | 10.54 |
| ***TOTAL*** | ***5371*** | ***4946*** | ***-425.0*** | ***-42.00*** |

Table 3.2 Transmutation rate between BOL and EOL (CerCer fuel 1098 fpd – 384 MWth)

| Element | m BOL (kg) | m EOL (kg) | Δm (kg) | Δm (kg/TWh$_{th}$) |
|---|---|---|---|---|
| U | 0 | 5 | 4.7 | 0.46 |
| Np | 183 | 172 | -11.4 | -1.12 |
| Pu | 2324 | 2391 | 66.9 | 6.61 |
| Am | 4336 | 3741 | -595.3 | -58.83 |
| Cm | 203 | 313 | 110.5 | 10.92 |
| ***TOTAL*** | ***7047*** | ***6622*** | ***-424.5*** | ***-41.95*** |

Table 3.3 Transmutation rate between BOL and EOL (CerMet fuel 1098 fpd – 384 MWth)

The core characterizations for the latest EFIT-Pb core designs are hence:

- CerCer fuel (MgO matrix):
  (1) The keff value obtained at BOC (0.9655) fits with the safety requirements;
  (2) The source efficiency $\varphi^*$ is about 0.64 over the equilibrium cycle;
  (3) The Beam intensity is about 19 mA over the equilibrium cycle;
  (4) At BOC, maximum global form factor (fax x frad) is 1.79 (inner core) and
  (5) The transmutation rate is about -42 kg/TWhth of heavy nuclei, with production of Cm (10.5 kg/ TWhth).

*This document refers to work being performed by scientists and institutions involved in IP EUROTRANS, as well as the financial support of the European Commission through the contract FI6W-CT-2004-516520.*

- CerMet fuel (Mo92 matrix):
  (1) The keff value obtained at BOC (0.9655) fits with the safety requirements;
  (2) The source efficiency $\varphi^*$ is about 0.47 over the equilibrium cycle;
  (3) The beam intensity is about 22 mA over the equilibrium cycle and
  (4) The transmutation rate is about -42 kg/TWhth of heavy nuclei, with production of Pu (6.6 kg/ TWhth) and Cm (10.9 kg/ TWhth).

## 3.3 EFIT-Pb primary system

### 3.3.1 Main Lay out description

The configuration of the primary system [3.11] is pool-type. The pool concept allows containing all the primary coolant within the Reactor Vessel, thus eliminating all problems related to out-of-vessel transport of the primary coolant. The pool design has important beneficial features, including a simple low temperature boundary containing all primary coolant, the large thermal capacity of the coolant in the primary vessel, a minimum of components and structures operating at the core outlet temperature.

The primary circuit is designed for effective natural circulation, i.e. relatively low pressure losses and driving force brought about by the core mid plane elevation arranged wide below the mid plane of the steam generators or, in case of emergency decay heat removal, the mid plane of the DHR dip coolers.

The speed of the primary coolant is kept low by design (less than 2 m/s), in order to limit the erosion. Wherever this cannot be complied with, e.g. at the tip of the propellers blades, the relative speed is kept lower than 10 m/s and appropriate construction materials are selected for qualification (among them, the machinable Ti3SiC2). Protection of structural steel against corrosion is ensured, in general, by controlled activity of oxygen dissolved in the melt and additional coating for the hotter structures. Wherever stagnation of the primary coolant is predicted, e.g. within dummies, provisions ensure a minimum coolant flow.

The primary system of EFIT (Figures 3.8 and 3.9) is composed of the structures and components in contact with molten lead. The main components are [3.12][3.13]:

- Reactor vessel and internal structures
- Core
- Steam Generating Units (SGU),
- Primary Pumps (PP),
- The safety-related DHR 1 (Direct Reactor Cooling (DRC)) system,
- The safety-related DHR 2 System: Isolation Condenser System
- Target Unit,
- Filter Units.

.

*This document refers to work being performed by scientists and institutions involved in IP EUROTRANS, as well as the financial support of the European Commission through the contract FI6W-CT-2004-516520.*

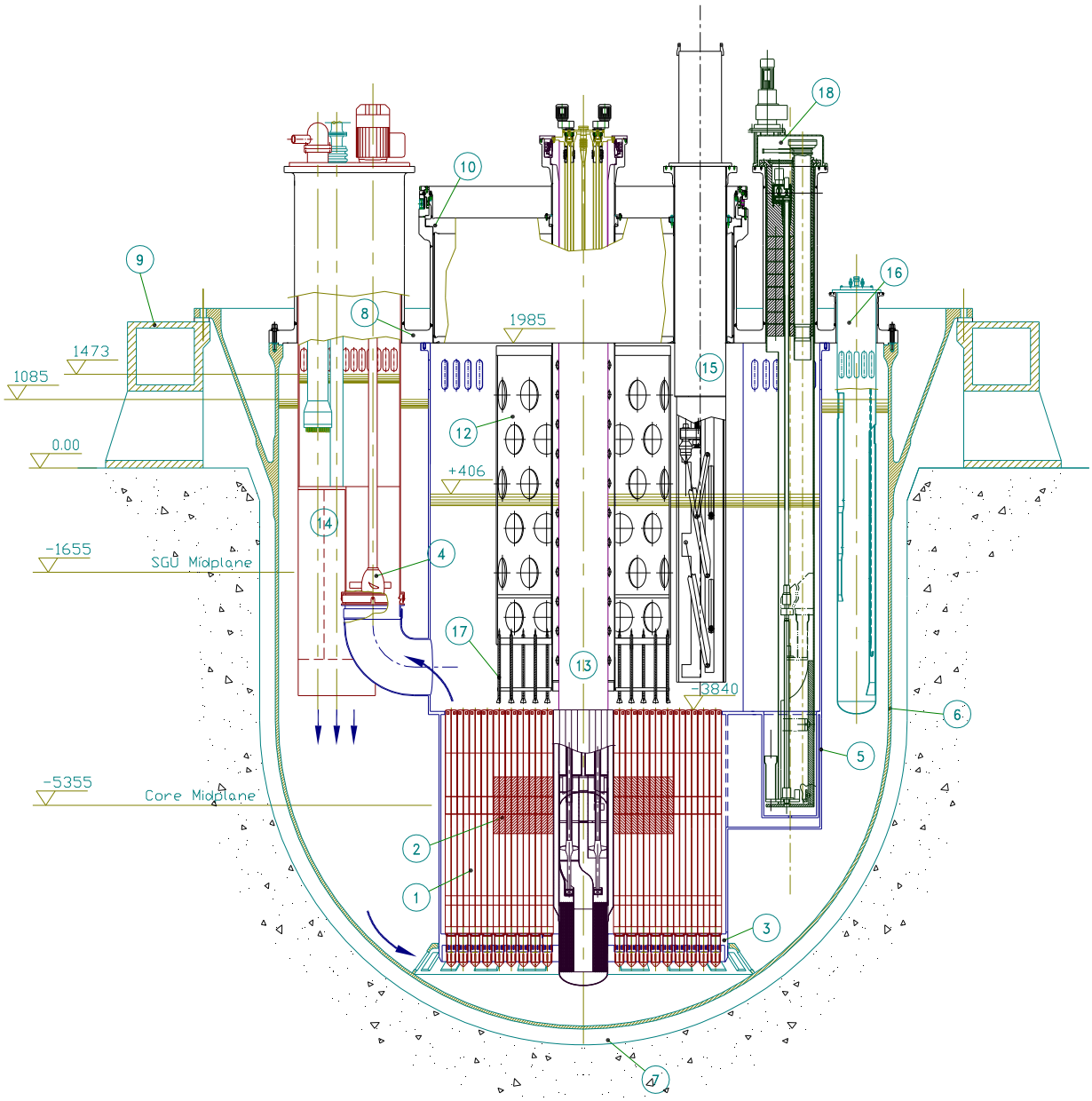


[1 Reactor Core; 2 Active Zone; 3 Diagrid; 4 Primary Pump; 5 Cylindrical Inner Vessel; 6 Reactor Vessel; 7 Reactor Cavity; 8 Reactor Roof; 9 Reactor Vessel Support; 10 Rotating Plug; 11 Thermal Shielding; 12 Above Core Structure: 13 Target Unit; 14 Steam Generator Unit; 15 Fuel Handling Machine; 16 Filter Unit; 17 Core Instrumentation; 18 Rotor Lift Machine; 19 DHR 1 Dip Cooler]

Figure 3.8: Reactor Block – Vertical section

*This document refers to work being performed by scientists and institutions involved in IP EUROTRANS, as well as the financial support of the European Commission through the contract FI6W-CT-2004-516520.*

The lead coolant flow path has been studied in details so that it answers operating and safety concerns (see below Chapter 6.1). Within the sub-assembly, hot lead is pumped into the enclosed pool above the PP and SGU and driven shell-side downwards across the SGU helical-tube bundles into the cold pool. At normal steady-state operation, the free level of the hot pool inside the casing is higher than the free level of the cold pool outside that is higher, in turn, than the free level of the hot pool above the core enclosed by the inner vessel. In case of loss of service power to all level-keeping PP, there would be no need to rely on their mechanical inertia to continue for a while the forced circulation, because the available head would ensure the prompt onset of the natural circulation, and hence preserve the safety function of core cooling since the very beginning of the transient. The loss of a PP would bring about reverse flow in the affected sub-assembly and merely create a temporary core by-pass flow without seriously affecting the function of core cooling. Holes are provided on the upper part of the casing for creating a common, large reactor cover gas plenum and ensure overflow of surging coolant in case of SG tube rupture accident.

The main process parameters of EFIT are reported in Table 3.4 [3.12]

*This document refers to work being performed by scientists and institutions involved in IP EUROTRANS, as well as the financial support of the European Commission through the contract FI6W-CT-2004-516520.*

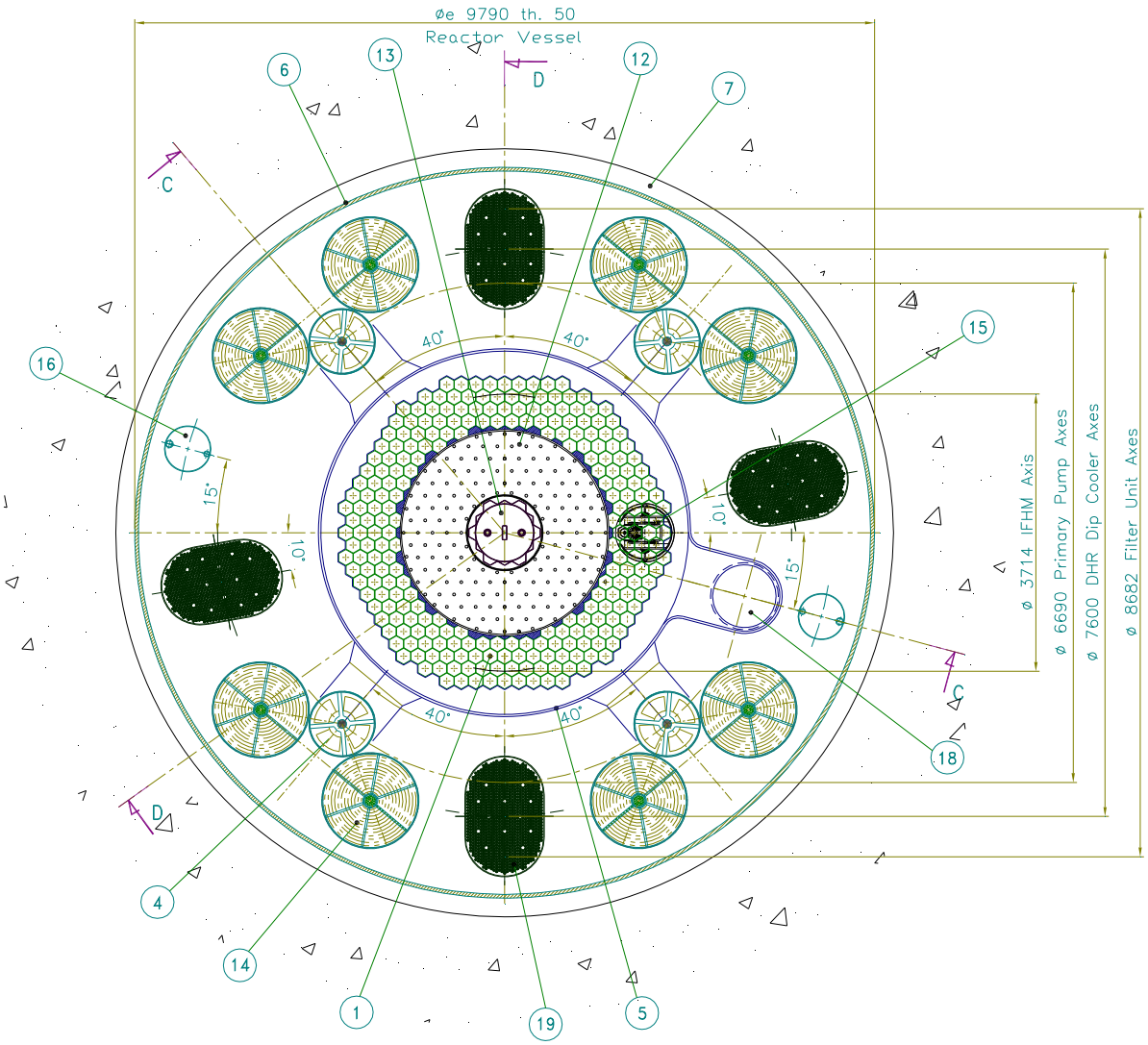


[1 Reactor Core; 2 Active Zone; 3 Diagrid; 4 Primary Pump; 5 Cylindrical Inner Vessel; 6 Reactor Vessel; 7 Reactor Cavity; 8 Reactor Roof; 9 Reactor Vessel Support; 10 Rotating Plug; 11 Thermal Shielding; 12 Above Core Structure: 13 Target Unit; 14 Steam Generator Unit; 15 Fuel Handling Machine; 16 Filter Unit; 17 Core Instrumentation; 18 Rotor Lift Machine; 19 DHR 1 Dip Cooler]

Figure 3.9 : Reactor Block – Horizontal section

*This document refers to work being performed by scientists and institutions involved in IP EUROTRANS, as well as the financial support of the European Commission through the contract FI6W-CT-2004-516520.*

Table 3.4 EFIT main process parameters

| Parameter | Value |
|---|---|
| Reactor thermal power, design capability | 416 MW |
| Proton beam power, max (800 MeV, 20 mA) | 16 MW |
| Current reactor power | 408 MW |
| Power sources | |
| • Fission | 395 MW |
| • Proton Beam (800 MeV, 16.3 mA) | 13 MW |
| • Primary and Target Unit Pumps | ≈0.5 MW |
| Primary coolant flow rate, total | 36,000 kg/s |
| Across the core | |
| • Fuel assemblies | 33,300 kg/s |
| • Fuel Assemblies by-pass leakage | 650 kg/s |
| • Dummies and Neutron Absorbers | 550 kg/s |
| Core by-pass flow | |
| • Across the HX of the Target Unit | 1500 kg/s |
| Primary circuit pressure loss | 1.37 bar |
| Core (mass flow rate 33300 kg/s) | 0.7 bar |
| Pump duct (mass flow rate 9000 kg/s) | 0.27 bar |
| Steam Generating Unit (mass flow rate 4500 kg/s) | 0.4 bar |
| Core inlet temperature | 400 °C (margin of 72.6 K to the melting point of lead) |
| Core outlet temperature, mean | 480 °C |
| Feed water mass flow rate | 250 kg/s |
| Feed water Inlet Temperature | 335 °C (margin of 7.6 K to the melting point of lead) |
| Steam Outlet Temperature | 450 °C (116.4 K superheating) |
| Steam Outlet Pressure | 140 bar (a few K sub-cooling at SG inlet) |

### 3.3.2 Reactor Vessel and Internal Structure

#### 3.3.2.1 Reactor Vessel and Support System

The Reactor Vessel [3.13], [3.14] (Figure 3.8) is a welded structure without nozzles, made of a cylindrical shell with hemispherical bottom head and top Y-piece, both branches of which terminate with a flange. The conical, outer branch is flanged to, and hangs from, the Annular Structure anchored to the civil structure of the Reactor Cavity, whereas the inner branch supports the reactor roof. The Reactor Vessel is supported by an Annular Structure. The Annular Box is joined to the base circular plate by 24 gussets regularly spaced. Base plate is fixed on the concrete.

Main dimensions of the vessel are summarized below:

- Vessel inner Diameter = 9690 mm
- Vessel height = 10895 mm
- Vessel current part thickness = 50 mm

*This document refers to work being performed by scientists and institutions involved in IP EUROTRANS, as well as the financial support of the European Commission through the contract FI6W-CT-2004-516520.*

- Vessel Y joint zone thickness = 80 mm
- Skirt Y joint zone thickness = 80 mm
- Skirt current part thickness = 50 mm
- Gusset thickness = 300 mm

The Reactor Roof is a fixed metal plate made up of a Fixed Roof and a Rotating Plug. It is connected to the Reactor Vessel and supports all main components of the primary system. The Fixed Roof is a mechanical welded structure. The Rotating Plug is a welded structure. It is located on the Fixed Roof. The connection between these components is gastight, and it is part of the Reactor Containment in both operating modes, static configuration on the Reactor Roof during normal Reactor operation and rotation during fuel handling operations. It is made of the following parts:

#### 3.3.2.2 Internal structure

The Internal Structure is located inside the Reactor Vessel and hangs from the Fixed Plate of the Reactor Roof (Figure 3.8). The functional parts welded together are the following ones:

- Bottom Support: The Internal Structure ends at the bottom with a short cylindrical support, which engages with the support welded to the Reactor Vessel Bottom during installation and maintenance operations. In normal operation no connection between Internal Structure and Reactor Vessel exists.
- Diagrid: It is a very thick perforated plate with a large hole on its axis to centre the bottom of the target unit. The holes allow positioning all the fuel assemblies, and they are shaped to receive the subassembly spike with a little clearance. The diagrid holes have a conical shape to facilitate the assembly spike insertion, and to accommodate the assembly transition cone.
- Inner Vessel with upper core restraint plate: it has the following main functions: separates the Core Region and the above Core Volume from the Downcomer, houses the Core, the Above Core Structure and the In Vessel Fuel Handling System, limits the Core Assemblies oscillations due to seismic accelerations. The Inner Vessel is welded to the upper side of the diagrid. It ends with a flange by which it is connected to the fixed plate of the Reactor Roof. The Inner Vessel delimitates two distinct plena: a lower plenum between diagrid and core restraint plate (and assembly heads), where the main primary coolant flow path takes place and an upper plenum of almost stagnant primary coolant, formed by an upstanding of larger cross section than the lower part of the Inner Vessel, welded to the core restraint plate and connected to the Reactor Roof by means of a flange.
- Elbow connections: they are welded on the upper part of the cylindrical inner vessel and allow the connection with the suction pipe of the primary pumps that are engaged in the piston seal.

### 3.3.3 Steam Generator and Primary Pump Sub-Assembly

The SG-PP_SA (Steam Generator and Primary Pump Sub-Assembly) [3.12], [3.13] is an integral part of the primary loop, i.e. from pump suction to steam generator outlet. It is made of two Steam Generator Units (SGU) and one Primary Pumps (PP) arranged between the SGU, all included in a casing supported by, and hung from, the reactor vessel roof (Figure 3.10). It is designed to carry out both functions of hot coolant circulation and power heat transfer.

#### 3.3.3.1 Steam generator Unit

The Steam Generator Unit is a contra-flow heat exchanger, whose size is 52 MW, with eight units per station. The SGU is a vertical unit with an inner and an outer shell. The primary coolant flows downwards shell-side through the inner shell and the annulus between inner and outer shell. The tube bundle is made of

*This document refers to work being performed by scientists and institutions involved in IP EUROTRANS, as well as the financial support of the European Commission through the contract FI6W-CT-2004-516520.*

U-tubes, the inlet legs of which are straight inside the inner shell. After the U-turn, the outlet tube legs are helical inside the annulus and become straight again at the exit of the annulus. Inlet tube plate is located below the helical tube. Outlet tube plate is located in the pool above PP and SGU. Both the plates are below the free level of lead.

The steam generator should be as compact as possible, in order to reduce its overall dimension and weight and, as a consequence, to minimize the reactor vessel size.

The main geometrical characteristics are listed in Table 3.5. The main functional calculated parameters are shown in Table 3.6.

The capability of a restriction orifice, inserted at the inlet of the tube bundle, where the water is still in sub-cooled conditions, to prevent any oscillation of mass flow rate among the different tubes, has been verified. The supposed orifice causes a pressure drop of 0.5 MPa at the mass flow rate of 32.16 kg/s. The diameter of the orifice causing such a pressure drop is 3 mm.

#### 3.3.3.2 Primary coolant pumps

The pumps are designed to operate at 480°C and to supply the coolant at a rate of 9000 kg/s (3098 $m^3$/h). Their most important part is the impeller, the circumferential speed of which is limited to 10 m/s. The speed of flowing lead relative to the rotating propeller blades shall be limited by design. Such operating conditions can give rise to problems associated with erosion-corrosion and cavitation wear as well as with the high stresses in the working parts of the pump. These problems should to a certain extent obviated by the engineering solution found in the development of the pump design. It ensures cavitation-free operation of the pump, which allows drawing on the operational experience of facilities with lead under erosion conditions in selection of materials. The pumps are specified to operate at the temperature of the hot plenum and to provide the total static head that makes up most of the driving force of the natural circulation of the primary loop, at steady-state and during transients, when the temperature of the hot plenum changes with the core power.

On the basis of the required head-capacity operating point an axial flow pump has been selected. This pump is a high-capacity, low-head pump, normally designed for flows greater than 450 $m^3$/h and heads of 15 m or less.

The pumps, installed vertically with fluid fed from the bottom, draw the lead from the hot plenum at the core outlet to the Steam Generators inlet. The high coolant velocity relative to the pump impeller requires the selection of an adequate construction material and its qualification. A suitable candidate is the innovative ceramic material $Ti_3SiC_2$. Some experimental activities of the 6$^{th}$ FP deal with testing of this candidate material. When technological search of the impeller material will be successful, additional experimental activities will be devoted to the development of the pump unit itself.

The pump performances are reported in Table 3.7. The head required to the pump is 1.37 bar with a mass flow rate of 9000 kg/s at a lead temperature of 480 °C. This value of head is comprehensive of:

- pressure drop of the core at the mass flow rate of 33300 kg/s: 0.7 bar
- pressure drop of the Steam Generator at the mass flow rate of 4500 kg/s: 0.4 bar
- pressure drop of the pump duct at the mass flow rate of 9000 kg/s: 0.27 bar

*This document refers to work being performed by scientists and institutions involved in IP EUROTRANS, as well as the financial support of the European Commission through the contract FI6W-CT-2004-516520.*

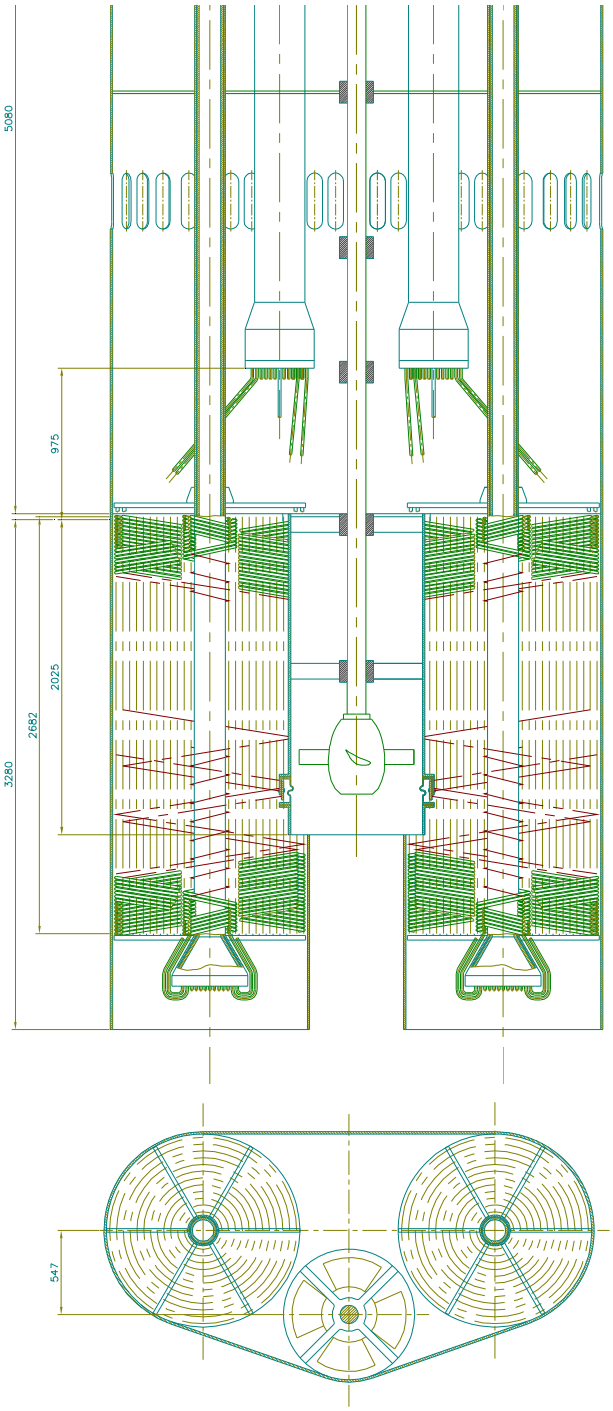


**Figure 3.10: Primary Pump-Steam Generator Assembly (1 Pump and 2 Steam generators)**

*This document refers to work being performed by scientists and institutions involved in IP EUROTRANS, as well as the financial support of the European Commission through the contract FI6W-CT-2004-516520.*

| SGU 52 MW -14 MPa | | |
|---|---|---|
| **Shell geometry** | **EOL** | **BOL** |
| Inner diameter of the inner shell [mm] | 180 | 180 |
| Outer diameter of the inner shell [mm] | 200 | 200 |
| Inner diameter of the outer shell [mm] | 1256 | 1256 |
| **Tube bundle geometry** | **EOL** | **BOL** |
| Tube OD [mm] | 17.46 | 17.46 |
| Tube ID [mm] | 14.158 | 14.158 |
| Transverse pitch of the helical tubes [mm] | 44.0 | 44.0 |
| Longitudinal pitch of the helical tubes [mm] | 24.0 | 24.0 |
| Total number of parallel tubes | 126 | 126 |
| Number of rows of tubes (transverse respect to the lead flow) | 12 | 12 |
| Length of the helical tube [m] | 24.343 | 20.783 |
| Height of the helical-tube bundle [m] | 2.682 | 2.29 |
| Oxide layer thickness side lead [µm] | 40 | |
| Oxide layer thickness side water [µm] | 10 | |
| Outside exchanging surface [$m^2$] | 168.1 | 168.1 |
| Inside exchanging surface [$m^2$] | 136.3 | 136.3 |
| Cross flow section lead side [$m^2$] | 0.742 | 0.742 |
| Cross flow section water side [$m^2$] | 0.0198 | 0.0198 |

**Table 3.5: SGU Main Geometric Characteristics**

*This document refers to work being performed by scientists and institutions involved in IP EUROTRANS, as well as the financial support of the European Commission through the contract FI6W-CT-2004-516520.*

| Thermal Power [MW] | 52 (100%) | | 41.6 (80%) | | 31.2 (60%) | |
|---|---|---|---|---|---|---|
| **LEAD** | **EOL** | **BOL** | **EOL** | **BOL** | **EOL** | **BOL** |
| Hot temperature [°C] | 480 | 480 | 464 | 464 | 448.6 | 448.6 |
| Cold temperature [°C] | 400 | 400 | 400 | 400 | 400 | 400 |
| Mass Flow Rate [kg/s] | 4483 | 4483 | 4483 | 4478 | 4418 | 4418.9 |
| Velocity [m/s] | 0.575 | 0.575 | 0.573 | 0.573 | 0.565 | 0.565 |
| Frictional Pressure Loss [kPa] | 20.3 | 20.3 | 20.3 | 20.3 | 19.7 | 19.7 |
| **Water-Steam** | | | | | | |
| Outlet Pressure [bar (a)] | 140.00 | 140.00 | 140.00 | 140.00 | 140.00 | 140.00 |
| Inlet Pressure [bar (a)] | 144.32 | 144.53 | 143.08 | 143.13 | 141.98 | 142.07 |
| Inlet Temperature [°C] | 335.00 | 335.00 | 335.00 | 335.00 | 335.00 | 335.00 |
| Outlet Temperature [°C] | 450.0 | 463.7 | 443.0 | 450.2 | 431.3 | 435.4 |
| Mass Flow Rate [kg/s] | 32.16 | 31.32 | 26.08 | 25.71 | 20.04 | 19.87 |
| Inlet Water Velocity [m/s] | 2.573 | 2.507 | 2.089 | 2.060 | 1.067 | 1.593 |
| Outlet Steam Velocity [m/s] | 32.531 | 32.808 | 25.911 | 26.036 | 19.274 | 19.33 |
| Pressure Loss [kPa] | 432 | 453. | 308 | 313 | 198 | 207 |
| Water mass inside the tubes [kg] | 36.8 | 30.02 | 31.19 | 24.56 | 24.46 | 19.33 |
| Steam Mass inside the tubes [kg] | 32.2 | 31.52 | 32.09 | 30.48 | 32.03 | 31.55 |
| | | | | | | |
| Average transversal temperature difference [°C] | 80.0 | 71.3 | 71.6 | 65.5 | 61.9 | 56.11 |

**Table 3.6: SGU main functional characteristics**

| | Impeller characteristics |
|---|---|
| Impeller speed | 200 rpm |
| Required NPSH | 1.5 |
| Outside diameter (tips diameter | 0.850 m |
| Hub diameter | 0.5695 m |
| Hub ratio | 0.67 |
| Number of vanes | 4 |
| Blades profile | NACA 23012 |
| Velocity in suction pipe | 1.6 m/s |
| Maximum axial velocity through the pump | 2.75 m/s |
| Max velocity relative to the impeller blade | 9.4 m/s |
| Power required | ~165 kW |

**Table 3.7 Primary Pump Definition**

*This document refers to work being performed by scientists and institutions involved in IP EUROTRANS, as well as the financial support of the European Commission through the contract FI6W-CT-2004-516520.*

## 3.4 Decay heat removal system

Three systems [3.12][3.13] contribute to the Decay Heat Removal (DHR) function in EFIT:

- the non safety-grade water/steam system (Steam Generators)
- the safety-related DHR 1 system: Direct Reactor Cooling (DRC) system
- the safety-related DHR 2 system: Isolation Condenser

Following reactor shutdown, the non safety-grade water/steam system is used for the normal decay heat removal. In case of unavailability of the water/steam system, the DHR1 or DHR2 system is called upon.

The two safety systems shall be diverse and each system shall fulfill its Intended Function (Principle of independence). Moreover, each system shall be redundant to face the single failure criteria on the purpose to practically eliminate the complete failure of the decay heat removal function. Each system is able to extract 100% of the decay heat (2 x 100%). In the future, the Probabilistic Risk Assessment (PRA) method can be used to confirm the overall architecture.

The two systems are diverse between them. In fact:

- DHR1 relays on dip coolers immersed in the primary system;
- DHR2 relays on isolation condenser connected to the secondary side of the Steam Generators

Each of the two systems is redundant because is made of four independent loops and 3 out 4 are sufficient to fulfill the decay heat removal function. The common mode failure is avoided because each system is made of different components and operating fluid.

### 3.4.1 DHR 1 System: Direct Reactor Cooling (DRC) System

The Direct Reactor Cooling system has two functions:

- Safety-grade decay heat removal function during accident conditions;
- Cooling function of the upper portion of the reactor vessel during normal operation

The DRC System is composed of four identical loops (3 loops out of 4 are sufficient to perform the DHR intended functions). The main components of the loop are: a molten lead-diathermic oil heat exchanger (dip cooler, DHX); an air-diathermic oil vapor condenser (AVC) with stack chimney.

In case of unavailability of the water/steam system, the DRC system is called upon to passively enhance its performance and remove decay heat to specification. At start of the emergency condition, lead enters the DHX at higher temperature and flow rate, driven by the larger density difference between the cold shell-side leg and the hot outside leg, and oil starts to vaporize massively, speeded to circulate at higher flow rate by the large hydrostatic head between vaporizing and return legs of the loop. A recirculation ratio of more than four times the once-through vapor rate is achieved, having installed the oil vapor separator and condensate drum at the appropriate level above the DHX.

### 3.4.2 Molten lead-diathermic oil heat exchanger (dip cooler, DHX)

The dip cooler DHX exhibits lead-oil tubes which are straight bayonet-tubes, with the tube bundle contained within a vertical shell. A bayonet tube consists of a pair of concentric tubes, the outer of which has the bottom end sealed by a cap to provide the inversion of flow from downward to upward. Both the outer and inner tubes extend from separate stationary tube plates directly into the reactor vessel. It will be noted that the surface of the outer tube is the main heat transfer surface.

*This document refers to work being performed by scientists and institutions involved in IP EUROTRANS, as well as the financial support of the European Commission through the contract FI6W-CT-2004-516520.*

The DHX sizing has been carried out assuming that only three out of the four DRC loops are available. Because the design core decay heat power is 20 MW, i.e., the decay heat generated three minutes after reactor shutdown, the power to be removed by one DRC loop is 6.67 MW and the DHR design capability of the four DRC loops is 26.6 MW.

The main geometrical characteristics of the DHX are listed in the Table 3.8 below.

| | |
|---|---|
| total cross sectional area | 1.42 $m^2$ |
| perimeter of the outer shell | 3867 mm |
| height of the inlet windows | 600 |
| cross flow section of the inlet windows | 2.3 $m^2$ |
| cross flow section lead side | 0.754 $m^2$ |
| outer diameter of the outer tubes | 30 mm |
| inner diameter of the outer tubes | 27 mm |
| outer diameter of the inner tube | 21.3 mm |
| inner diameter of the inner tubes | 18.3 mm |
| number of tubes | 931 |
| exchanging length of each tube | 3000 mm |
| installed length of each tubes | 3600 mm |
| tube pitch | 40 mm |
| outside exchanging surface of the outer tube | 263 $m^2$ |
| outside exchanging surface of the inner tube | 187 $m^2$ |
| cross flow section of the inner tubes | 0.244 $m^2$ |
| cross flow section of the annulus | 0.201 $m^2$ |
| material of the inner tube | AISI 316 steelT91 |
| material of the outer tube | T91 (18S) steel |

**Table 3.8 main geometrical characteristics of the DHX**

### 3.4.3 Air-diathermic oil Vapour Condenser (AVC)

The oil vapour condenser is made of a bundle of straight finned tubes, connected vertically at both ends to headers, and of ancillary equipment. The tube bundle is cooled by transverse flow of atmospheric air induced by a stack chimney operating in natural draft.

The separator receives, via the vaporization leg, the oil-vapour oil mixture produced in the dip cooler. It separates the oil vapour from the oil. The oil vapour flows towards the condenser, while the oil flows back to the dip cooler via the return leg. The condensed oil drum is interposed between the outlet condenser header and the separator. It avoids the entrance of the nitrogen - pushed outside the bundle by the vapour oil - to arrive to the separator. The nitrogen header is connected with the upper ends of tubes placed in front of the tube bundle and has the duty to collect and store aside at ambient temperature the nitrogen gas displaced from the tube bundle during the phases in which the AVC is called to operate. The oil vapour separator and the condensed oil drum are shown in Figure 3.11 half filled with oil with hydraulically connected liquid oil plena. The AVC tubes parameters are summarized in the Table 3.9 below.

*This document refers to work being performed by scientists and institutions involved in IP EUROTRANS, as well as the financial support of the European Commission through the contract FI6W-CT-2004-516520.*

| | |
|---|---|
| **Tube bundle (1 module)** | |
| Number of row in the direction of the air flow | 5 |
| Number of tubes per row | 128 |
| Total number of tubes | 640 |
| Transversal pitch | 90 mm |
| Longitudinal pitch | 90 mm |
| **Tube Dimensions** | |
| Tube OD | 19.0 mm |
| Tube ID | 16.0 mm |
| Length | 3 m |
| Tube material | T91 (18S) steel |
| **Fins** | |
| Fin type | plate, aluminium |
| Number of fins per unit length of tube | 440/m |
| Fin height | 16 mm |
| Fin thickness | 0.3 mm |
| **Heat transfer surface** (1 module) | |
| Inner surface of the tubes | 96 $m^2$ |
| Extended outer surface of the tubes | 3112 $m^2$ |
| Cross sectional inner flow area | 0.128 $m^2$ |
| **Air-Side Pressure Loss** | |
| Pressure loss for an air mass flow rate of 50 kg/s | 13.2 Pa |
| **Stack Chimney** | |
| Cross sectional area in the tube bundle zone | 34.5 $m^2$ |
| Net cross sectional area in the tube bundle zone | 25.6 $m^2$ |
| Cross sectional area after the tube bundle | 12.0 $m^2$ |
| Height above the tube bundle | 15 m |

**Table 3.9** AVC tubes parameters

### 3.4.4 Isolation condenser system

The Isolation Condenser System consists of four independent sub systems, each of them comprehensive of (see figure 3.11):

- One heat exchanger (isolation condenser), constituted by a vertical tube bundle with an upper and lower horizontal header
- One water pool, where the isolation condenser is sub merged.
- One storage water tank
- One condensate isolation valve (to meet the single failure criteria this function shall be performed at least by two parallel valves)
- Four safety valves

Besides, a large common pool feeds the four single pools.
The isolation condenser is connected to a pair of steam generators:

- The main steam line of a pair of steam generators is connected to the upper header of the isolation condenser.

*This document refers to work being performed by scientists and institutions involved in IP EUROTRANS, as well as the financial support of the European Commission through the contract FI6W-CT-2004-516520.*

- The lower header of the isolation condenser is connected to the main feed water line of a pair of steam generators. The condensate isolation valve is placed on this connection.

The connection between the steam line and the condenser upper header is open both in stand-by and operation conditions. Slope of the isolation condenser steam line is towards the main steam line to permit the return of the condensate due to the heat losses in the line. The condensate isolation valve between the condenser lower header and the feed water line is closed when the system is in stand-by, and opened when the system is called to operate. The opening of the condensate isolation valve causes the draining of the condensate to the steam generator. The isolation condenser tubes and headers become empty and their internal cold surface starts to condensate the steam coming from the steam generator and hence to transfer heat to the cold pool water. The steam condensing causes a pressure reduction which calls other steam from the steam generator. The condensed steam drains from the condenser by gravity to the steam generator. A condensate level is established in the condensate return line. The condensate level should be below the lower header of the isolation condenser: In this way the whole surface of the isolation condenser can contribute to the condensation of the incoming steam. A water tank is provided to each sub system in the condensate return line, below the condensate isolation valve.
The Isolation Condenser System has been designed to remove 20 MW, which is the heat decay after 3 minutes after the accident. The main parameters of each condenser are listed in the Table 3.10 below.

**Table 3.10** Main parameters of individual condenser

| | |
|---|---|
| Upper and lower header | |
| External Diameter | 560 mm |
| Thickness | 60 mm |
| Length | 1200 mm |
| Material | Inconel 600 |
| Tube bundle | |
| Number of tube | 36 |
| Average active tube length | 2000 mm |
| Tube external diameter | 50.8 mm |
| Tube thickness | 2.3 mm |
| pitch along the longitudinal header direction | 106 mm |
| pitch along the header horizontal diameter | 200 mm |
| material | Inconel 600 |
| Condenser connection piping | |
| Steam inlet | Ø 168.3 x 10.97 (6” sch 80) |
| Water condensate outlet | Ø 168.3 x 10.97 (6” sch 80) |

*This document refers to work being performed by scientists and institutions involved in IP EUROTRANS, as well as the financial support of the European Commission through the contract FI6W-CT-2004-516520.*

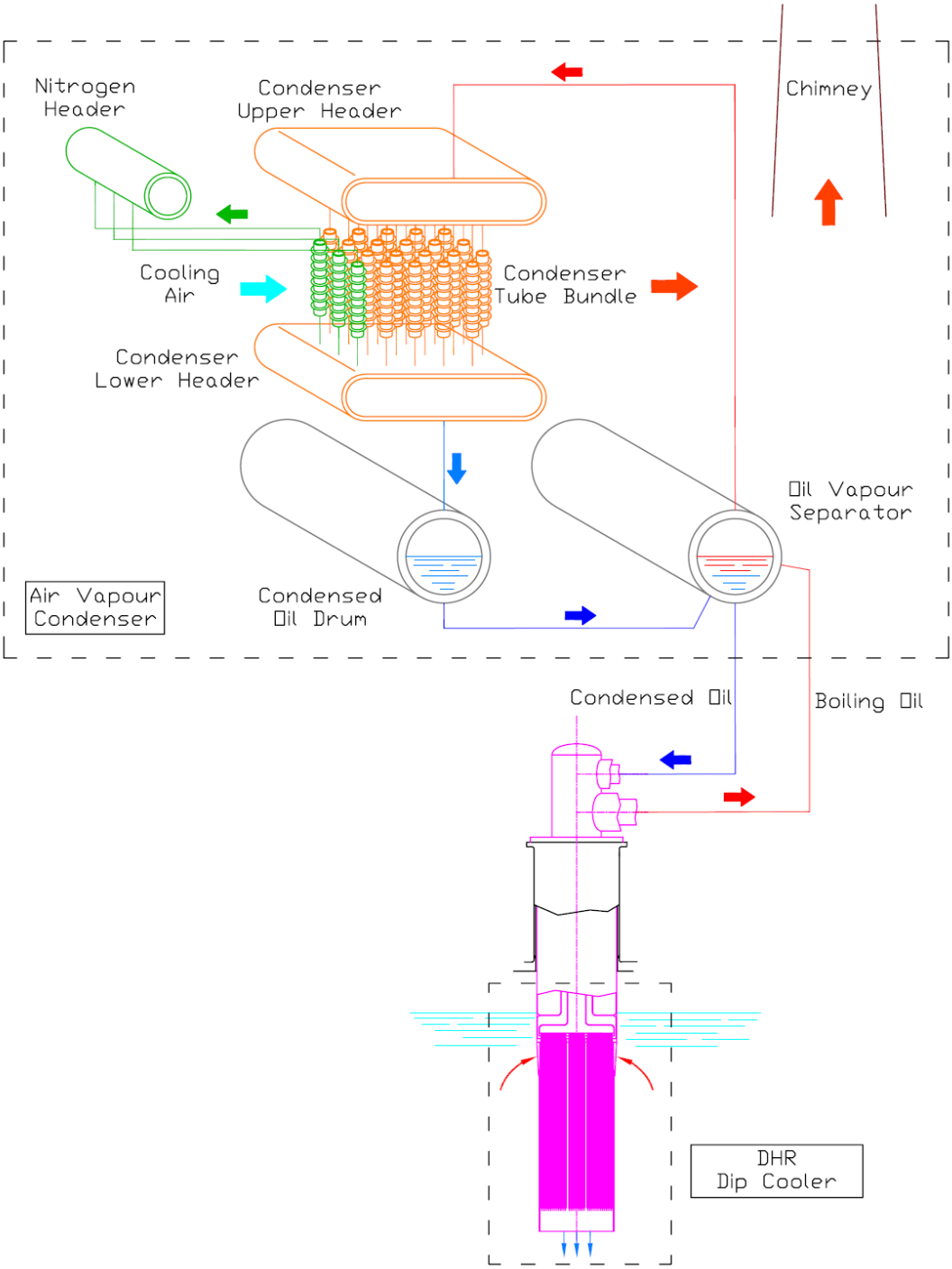


**Figure 3.11: DHR 1: Direct reactor Cooling System (one out of four loops)**

*This document refers to work being performed by scientists and institutions involved in IP EUROTRANS, as well as the financial support of the European Commission through the contract FI6W-CT-2004-516520.*

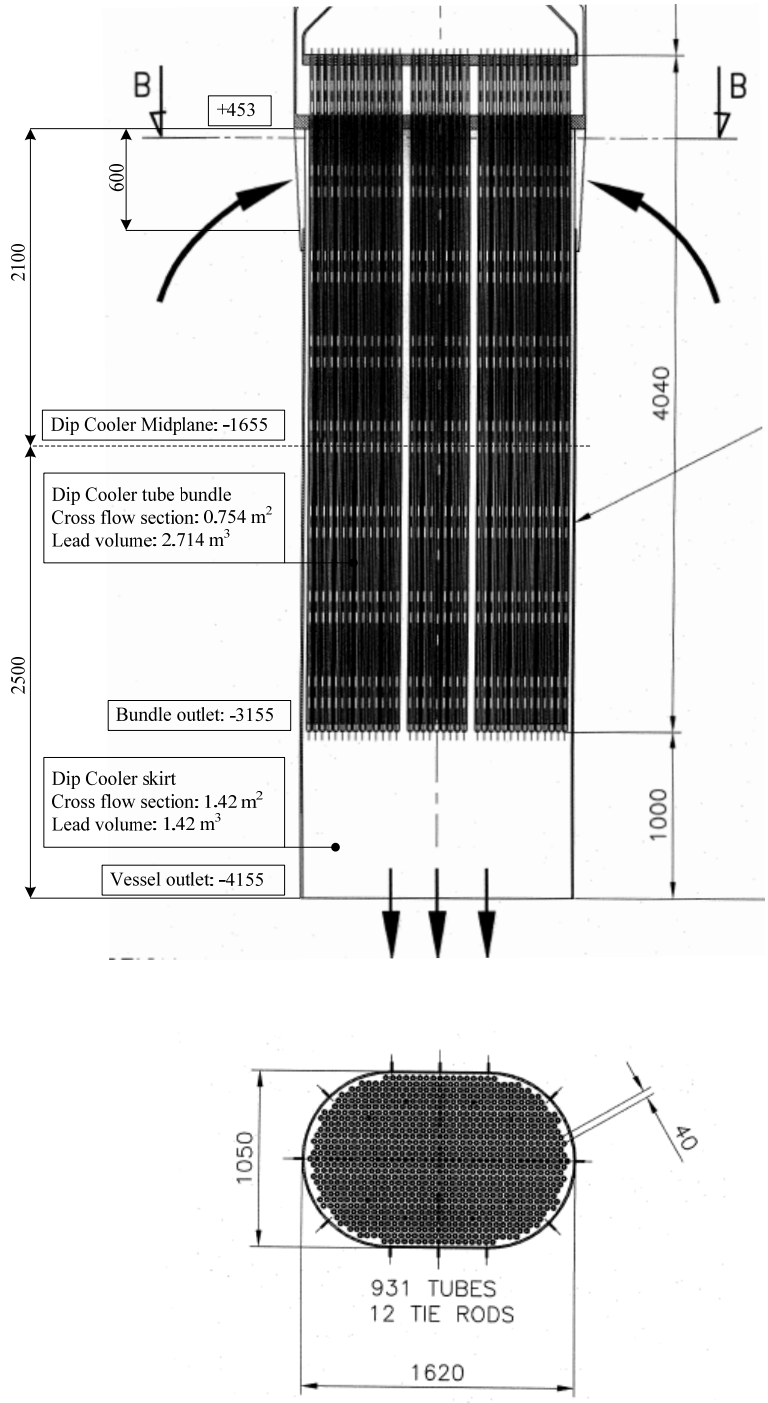


**Figure 3.12: Dip Cooler Geometry**

*This document refers to work being performed by scientists and institutions involved in IP EUROTRANS, as well as the financial support of the European Commission through the contract FI6W-CT-2004-516520.*

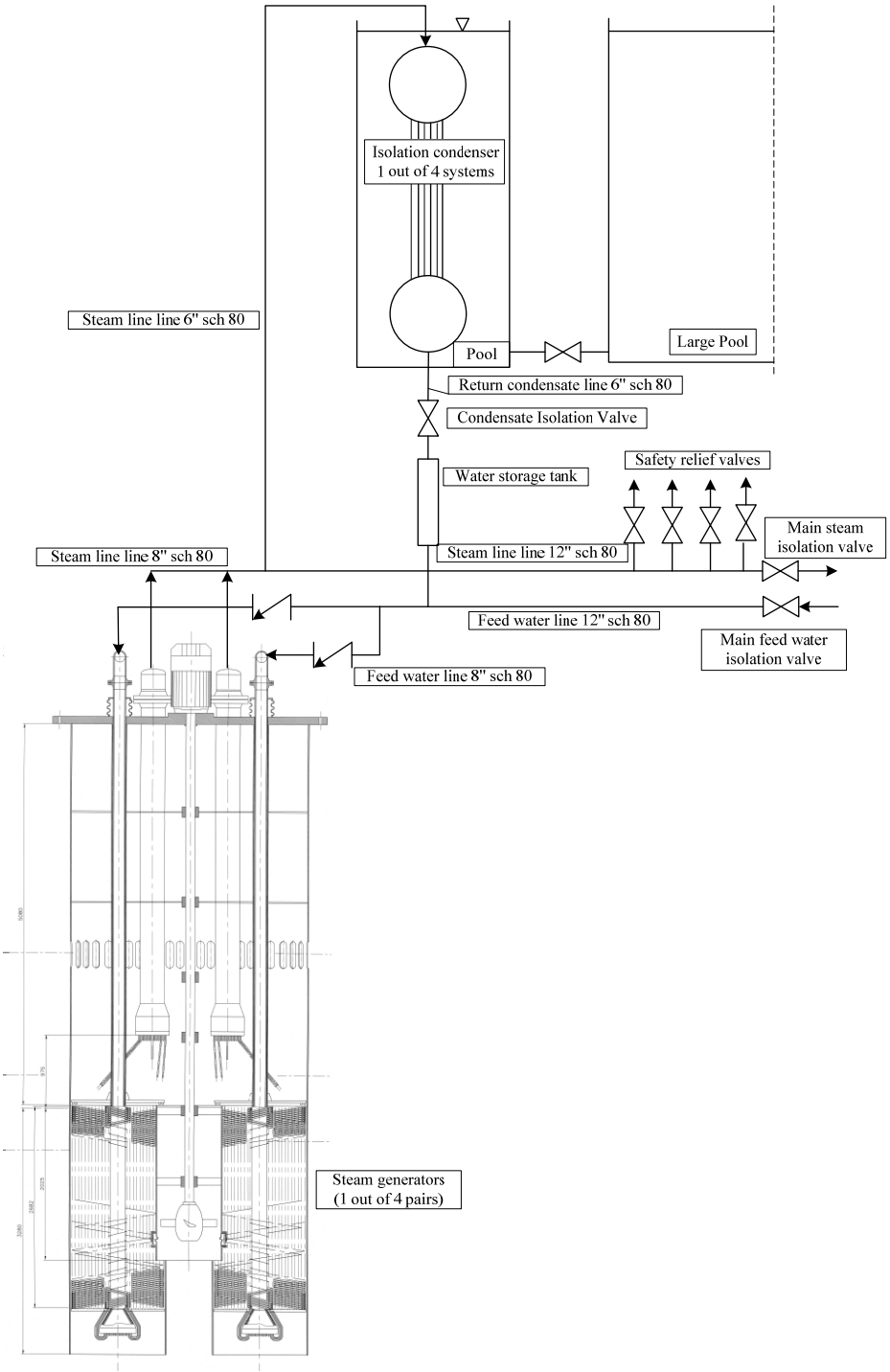


**Figure 3.13: Isolation Condenser scheme**

*This document refers to work being performed by scientists and institutions involved in IP EUROTRANS, as well as the financial support of the European Commission through the contract FI6W-CT-2004-516520.*

## 3.5 The Target Unit

The spallation target unit [3.12], [3.13] is a mechanical component which provides the driving neutron source and constitutes the mechanical-functional interface between the high power proton accelerator and the subcritical fuel core pooled inside the lead cooled primary system.

Centred at the core axis, the Target Unit is of cylindrical shape of about outline 13 to 14 m length and 0,8 m diameter. The Target Unit is hung and connected, by the upper part, at a flanged upstand welded on the reactor roof and is kept at the bottom through insertion into a hole at the centre of the diagrid.

In the windowless target unit configuration (see scheme in Figure 3-14) the lead free surface is exposed to vacuum. The beam impinges directly on lead, which is forced to circulate by means of a pumping system made of two propellers which thrust the lead flow in series arrangement. The propellers are driven by two long hollow shafts (ten meters about) connected to motors located above the reactor roof. In case of failure of one pump, the series configuration enables the second propeller to supply enough flow and to prevent boiling off of lead in the spallation zone.The lead is forced to flow tube-side in the heat exchanger located about 1 m beneath the core mid-plane, at about the level of the fuel assembly feet. In the heat exchanger, heat is transferred to a core by-pass stream of primary coolant which flows shell-side.

The cooled target lead returns the spallation region, which is shaped as a slanted duct of rectangular cross-section with the free surface exposed to vacuum. Lead is accelerated to maximum speed in the middle of the duct (its throat), where the protons beam impinges on the target. The proton beam is driven by magnets to sweep, in alternate up and down motion perpendicular to the direction of the fluid flow, a 140 mm wide path (the throat of the slanted duct is 180 mm wide) across the centre line of the target. The proton beam, relatively to the lead free surface, travels therefore zig zag and impinges always on fresh target. The target flow speed at the free surface is kept high enough in order to limit the deposited energy per unit mass of fluid and hence not to overheat it and keep moderate its evaporation rate into the evacuated beam pipe.

Part of the cold lead stream is diverted upstream of the spallation zone into calm zones located on both sides of the duct, where any foreign particles can settle by gravitation and be segregated from the lead bulk. In this manner, besides preventing foreign matter from affecting the spallation neutron yield, risks of fouling the outer wall of the heat exchanging tubes are also minimised.

The segregation of the spallation products must be achieved inside the EFIT reactor containment, since the beam transport line connecting the accelerator complex to the target unit penetrates the reactor containment and cannot be credited to act as safety barrier against activity release into the environment. This segregation function is addressed, during normal operation, by the use of absorbing and trapping systems for the exhausts leaving the free surface of the spallation zone. Besides ensuring the high vacuum level required in the beam pipe, the spallation exhausts purification system also prevents the migration from inside to outside the reactor building of any radiotoxicity escaping the beam line.

Radiation streaming (mainly constituted by neutron flux) towards the reactor roof may occur through the beam pipe and the gap between propeller shaft and support. In order to limit the streaming through the beam pipe, its circular cross section of 50 mm ID at the top becomes square (50X50 mm) over a transition piece and wider at the bottom with rectangular 50x180mm cross section, enough, with clearance, to allow the specified beam scan travel (140 mm across the centre line of the flowing target lead). The radial gap between propeller shaft and support has been reduced by implementing an appropriate thickening of the outer dynamic void-sealing guard thimble.

The maximum flow velocity of less than 2m/s in the spallation region is considered adequate for keeping erosion by flowing lead low while avoiding overheating the target, particularly at the free surface, where the temperature is predicted not to trespass 520°C. This implies to protect with aluminium coating (GESA treatment) the structural steel that in normal operating conditions has a temperature above 500°C.

*This document refers to work being performed by scientists and institutions involved in IP EUROTRANS, as well as the financial support of the European Commission through the contract FI6W-CT-2004-516520.*

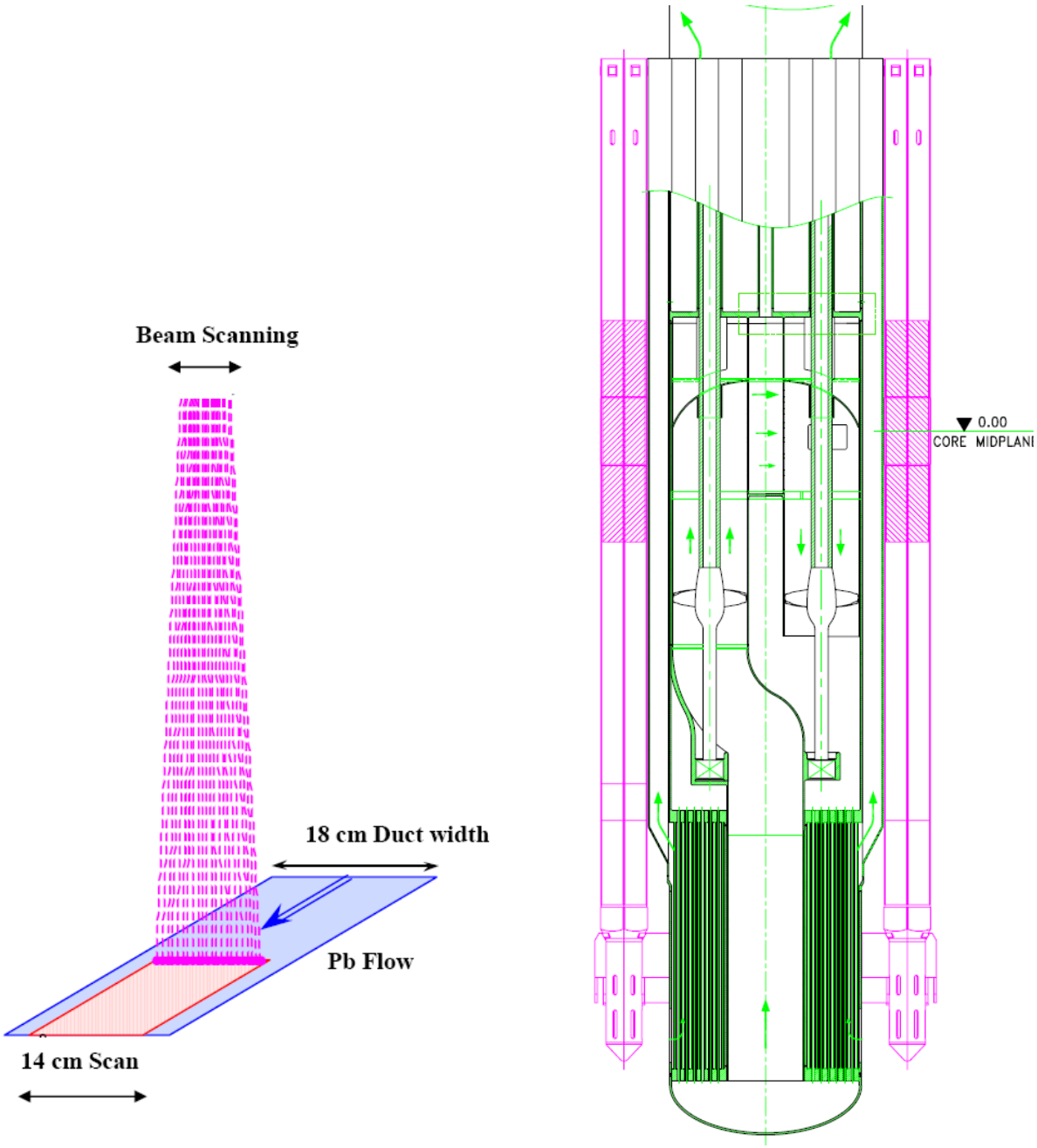


**Figure 3.14: Scheme of Proton Beam zig-zag travel and Target Unit**

*This document refers to work being performed by scientists and institutions involved in IP EUROTRANS, as well as the financial support of the European Commission through the contract FI6W-CT-2004-516520.*

## 3.6 Integrated coolant purification unit

Removal of contaminants from the coolant and the loop, mainly oxide particles which may affect the safety, particularly during maintenance or in case of accidental leakages into the environment, is required at least down to limits, which are reasonably achievable. Basing on information available at present, an in-vessel purification system for the EFIT reactor pool can be limited to the installation of two free-surface Filter Units with a reactor lifetime capacity.

The method chosen for removal oxide particles [3.12] consists in trapping the particles in the free-surface filter by means of gravitational separation (settling). This method is based on the fact that the density of lead in the operating temperature range is much higher than the density of most contaminants.

The filter unit has cylindrical shape of 0.6 m ID and 5 m length, closed at the bottom end and hung to the reactor roof.

It is able to suck about 5 liters/s lead and loose slag floating on the free surface. The lead stream is induced to flow into the filter, driven by an Ar-lift pump, through a 2 x 40 cm vertical slot followed by a 0.1 m ID inlet pipe. The height of the inlet slot is dimensioned, with margins, to cope with the variable free level of lead, that is minimum at cold shutdown (400°C). The lead speed in the pipe is specified to be at least 0.5 m/s, that is approximately the rising speed of gas bubbles in stagnant lead, in order to ensure the entrainment of any solid particles. The bottom part of the inlet pipe has three equally-spaced, about equal-flow ports: the bottom end and two ports as radial lead entrances. This entrance arrangement aims at creating in the filter plenum three zones of increasing speed in order to give the smaller particles that would be otherwise entrained in the lower, higher-speed zone and carried away in the riser, the chance to settle.

## 3.7 Primary system chemistry control

Prevention of corrosion-erosion of the austenitic structural steels in contact with the lead melt is made by maintaining a continuous, compact metal oxide film adherent to the metal substrate of the structures. This implies the presence of dissolved oxygen in the melt.

The range, at nominal operating conditions, of the dissolved oxygen concentration in equilibrium with the oxygen gas above the melt and, hence, with the hydrogen partial pressure in the cover gas of a given humidity, is specified in the following [3.16].

The temperature of the primary coolant of EFIT varies cyclically between the upper mean temperature $T_c$ = 480 °C at the core outlet and a lower temperature $T_f$ = 400 °C at the core inlet. The argon gas as cover gas plenum above the melt, interfaces both hot and cold lead and therefore the control of the dissolved oxygen, via its partial pressure in the gas phase can be carried out more conveniently at the upper temperature.

The allowable activity field for the lead melt and, therefore the reference diagram for the EFIT facility, is reported in the figure 3.15 below.

*This document refers to work being performed by scientists and institutions involved in IP EUROTRANS, as well as the financial support of the European Commission through the contract FI6W-CT-2004-516520.*

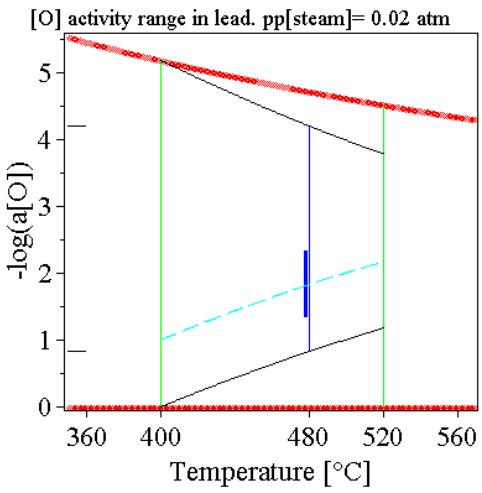


**Figure 3.15: Reference diagram for the EFIT facility for the allowable activity field of the lead melt**

The lower iso-concentration curve represents the variation of the *a*[*O*] vs T, actually of –log(*a*[*O*]) vs T, that corresponds to a constant $C_{[O]}$ in the Lead melt equal to the $C_{[O],s}$ at $T_f$. Thus lead oxide precipitation would occur only below $T_f$.

The upper iso-concentration curve represents the variation of the oxygen activity that corresponds to a constant $C_{[Fe]}$ equal to $C_{[O],s}$ at $T_f$. Thus, if a dissolved iron activity *a*[*Fe*] would be defined as for the oxygen activity at 400 °C *a*[*Fe*] would be equal to 1 and the %wt oxygen in the melt would have reached its minimum value any further decrease of the dissolved oxygen would have to be recovered by dissolution of the stochiometric amount of magnetite.

These two activity limits, identified by the intersection of the two black iso-concentration curves with the $T_c$ isotherm line, define the theoretically allowable range (thin blue segment on Diagram) for the oxygen activity control at $T_c$.

REFERENCES

[3.1] R Thetford, V Sobolev, "Recommended properties of fuel, cladding and coolant for EFIT ", EUROTRANS CONTRACT No.: FI6W-CT-2004-516520, DM3/Workpackage 3.1/Deliverable No.: 3.4 (ver. 1.0), issued by SERCO Assurance, 11 May 2006.

[3.2] C. Artioli, G. Glinatsis, C. Petrovich, M. Sarotto, Specification for the EFIT Core and Fuel Element, DM1/Workpackage 1.2.4/Deliverable 1.06, rev. 1, issued by ENEA, 10 Nov. 2006.

[3.3] C. Artioli, G. Glinatsis, C. Petrovich, M. Sarotto, EFIT Core Reference Cycle Analysis and Reactivity Coefficients, DM1 / Workpackage 1.2.4/Deliverable 1.36, rev. 0, issued by ENEA, 18 Jun. 2008.

[3.4] G. Glinatsis, Decay Heat Investigation of U-free Transmuter Cores Dedicated Fuels, ENEA Technical Note FPN–P9EH-004, 05 Jun, 2007.

[3.5] G. Glinatsis, C. Petrovich, Evaluation of Radiation Damage and Circuit Activation of EFIT, DM1/Workpackage 1.2.4/Deliverable 1.38, rev. 0, issued by ENEA, 25 Mar. 2008.

[3.6] G. Glinatsis, EFIT-MgO/Pb Core Design Reactivity Coefficients. IP-EUROTRANS DM1 General Meeting. Ansaldo Nucleare, Genova, 02-03 Apr, 2008.

*This document refers to work being performed by scientists and institutions involved in IP EUROTRANS, as well as the financial support of the European Commission through the contract FI6W-CT-2004-516520.*

[3.7] M. Schikorr, EFIT Core Thermal Hydraulics, DM1/Workpackage 1.2.4/Deliverable 1.37, rev. 0, issued by FZK, 23 Oct. 2008.

[3.8] G. Glinatsis, C. Artioli, C. Petrovich, M. Sarotto, Reactivity Coefficients and Uncertainty Evaluations on the EFIT Core Neutron Design. Physor'08, Interlaken, Switzerland, September 14-19, 2008.

[3.9] C.Artioli, et al., Optimization of the Minor Actinides transmutation in ADS: The European Facility for Industrial Transmutation EFIT-Pb concept, ACCAPP'07, Pocatello, Idaho, USA, 30 July – 2 August, 2007.

[3.10] "Safety Concepts of the 400MWth-Class EFIT Accelerator Driven Transmuter and Considerations for Further Developments", ICENES'2009, Ericeira, Portugal, 29th June – 3rd July, 2009

[3.11] EUROTRANS 121 SMFX 006, Rev. 0 Specification for the EFIT Primary System (D1.4)

[3.12] EUROTRANS 121 SMFX 007, Rev. 1 Main Components Functional Sizing of EFIT (D1.24)

[3.13] ANSALDO EUROTRANS 121 DMMX 009, Rev. 0 Main Components Assembly Drawings of EFIT (D1.26)

[3.14] FPN – P9EH – 016, Rev. 0 EFIT Core Design Summary Report (D1.58)

[3.15] EUROTRANS 121 TMLX 008, Rev. 0 Main Vessel and Support System Thermo-Mechanical Sizing of EFIT (D1.25)

[3.16] EUROTRANS 121 SIPX 010, Rev. 0 Primary System Chemistry Control Technical Specification of EFIT (D1.46)

[3.17] Barbensi Andrea, Corsini Giovanni, Mansani Luigi, Artioli Carlo, Glinatsis Georgios, "EFIT: the european facility for industrial transmutation of minor actinides", AccApp'07 Conference, Pocatello, Idaho, July 30 – August 02, 2007, pp. 885 – 892.

[3.18] C. Artioli, H. Aït Abderrahim, G. Glinatsis, L. Mansani, C. Petrovich, M. Sarotto, M. Schikorr, "Optimization of the minor actinides transmutation in ADS: the european facility for industrial transmutation EFIT-pb concept", AccApp'07 Conference, Pocatello, Idaho, July 30 – August 02, 2007, pp. 560 – 567.

[3.19] Carlo Artioli, "Minor Actinides burning in the 42-0 Concept: The EU "EFIT" (European Facility for Industrial Transmutation) ADS" International Conference on Peaceful Uses of Atomic Energy, New Delhi, September 29 - October 1, 2009

[3.20] A. Rineiski, X.-N. Chen, W. Maschek, V. Sobolev, W, Uyttenhove, J. Wallenius, A. Fokau, F. Delage, "Comparison of the neutronic performances of the ETD reference core loaded with the selected TRU-fuels from BOL to EOL", EUROTRANS CONTRACT No.: FI6W-CT-2004-516520, DM3/Workpackage 3.1/Deliverable N° 3.3, 30 March 2010.

[3.21] W. Maschek X. Chen, A. Rineiski, C. Matzerath Boccaccini, J. Wallenius, M. Eriksson, V. Sobolev, B. Arien, P. Smith, R. Thetford, J.P. Ottaviani, S.Pillon, D. Haas, Fuel Recommendation for EFIT based on Transient Analyses. Deliverable D3.9, IP EUROTRANS, Contract N°: FI6W-CT-2004-516520, EURATOM FP6, May 200.

[3.22] X.-N Chen, A. Rineiski, P. Liu, C. Matzerath Boccaccini, W. Maschek, V. Sobolev, "Design and Neutronic Calculations of CERMET AFTRA-EFIT (ADT-400)", 5th Coordination Meeting of DM3 AFTRA IP EUROTRANS, 24-25 October 2007, Petten, Netherlands.

*This document refers to work being performed by scientists and institutions involved in IP EUROTRANS, as well as the financial support of the European Commission through the contract FI6W-CT-2004-516520.*

# 4. DESCRIPTION OF THE 400 MWTH HE-COOLED EFIT

## 4.1 Design Objectives and Criteria Considered in the EFIT-He Design

The design of the He-cooled EFIT took as far as possible benefits from other programmes dealing with gas-cooled reactors. Both the background of the XADS studied within the 5th FP [4.1] and the GCFR studies currently on-going within the 6th FP [4.2] were particularly considered. Consequently, some parts and/or components were largely inspired by the design proposed in those Projects.

In the PDS-XADS Project, the possibility to implement a solid target with a "cold" window has been shown as the key point for ADS feasibility ([4.3], [4.4])..

The design objectives for EFIT-He [4.4] are very much the same than the EFIT-Pb i.e.

- An objective of efficiency of the Minor Actinides (MAs) transmutation of 42 kg/TWhth
- The lowest possible variation of $K_{eff}$ during the fuel cycle
- A rather flat distribution of power: radial form factor < 1.4; axial form factor < 1.32
- A core pressure loss lower than 1 bar

but the design criteria are different [4.6] since the plant is using He rather than Pb as a coolant:

- A linear power density limited to 180 W/cm (objective to limit the fuel temperature at a relatively low level)
- The limits on the acceptable temperatures for cladding: < 1200°C, under nominal operation ; < 1600 °C, in transient conditions (cat. IV)
- A gas pressure in the fuel plenum limited to 50 bar at the End Of Life (EOL)
- A maximum helium speed of 100 m/s.

## 4.2 Plant Characteristics

On the basis of the above mentioned objectives and criteria, several characteristics of the EFIT-He have been estimated or bounded early in the course of the Project. They deal with :

- The thermal power of the facility ;
- The beam characteristics ;
- The inlet/outlet temperatures of the core ;
- The fuel type.

At this stage of the plant description, it is worth pointing out that the choice of the fuel has already been made at the very beginning of the EUROTRANS Project within the frame DOMAIN 3 AFTRA. The rationales for this choice are presented in Chapter 1.3.

More particularly for the EFIT-He design, one must note that only the CerCer fuel pellet, made of $((Pu, Am)O_{2-x}$ embedded in a MgO matrix, is considered [4.7]. Under this consideration, only the fuel cladding choice is discussed hereafter.

The plant power is the result of an optimation process which should take into account the Transuranian (TRU) loading for achieving significant MA burning/transmutation, the size of the spallation module, the power flattening and the safety related options. Given the main design choices of the plant lay out, a core with a power in the range of about 300 to 600 MW(th) seems to be appropriate to meet these requirements. Such an ADS system could be loaded with about 5 to 12 tons of TRUs, and that a transmutation of about 80 to 140 kg per year could be obtained".

The plant power was, thus, set to 400 $MW_{th}$ which appeared as a good compromise between the plant size and the external source efficiency.

The LInear ACcelerator (LINAC) concept was chosen for the two EFIT concepts. Rationales for this choice are presented in chapter 2.

*This document refers to work being performed by scientists and institutions involved in IP EUROTRANS, as well as the financial support of the European Commission through the contract FI6W-CT-2004-516520.*

This kind of machine allows producing protons with energy up to 1 GeV. As a consequence of compromise between spallation neutron efficiency and cost, the characteristics of the proton beam were set to values of: 800 MeV and 20 mA [4.6] from the very beginning of the studies.

### 4.2.1 Definition of inlet/outlet Temperatures – Power Conversion Cycle

In order to limit the R&D work and in order to be coherent with the GFR design options, an indirect supercritical CO2 with re-compression cycle was proposed for the EFIT-He concept. This conversion cycle is schematically shown in Figure 4.1.

The technology of the conversion cycle being defined, the core inlet/outlet temperatures were optimised in order to maximise the power conversion efficiency. The detailed calculations are presented in the report in references [4.6] and [4.8].

The objective of this work helped to define a power cycle that complies with the reactor requirements and that returns a plant net efficiency, before the accelerator electrical power is deducted, of better than 40%.

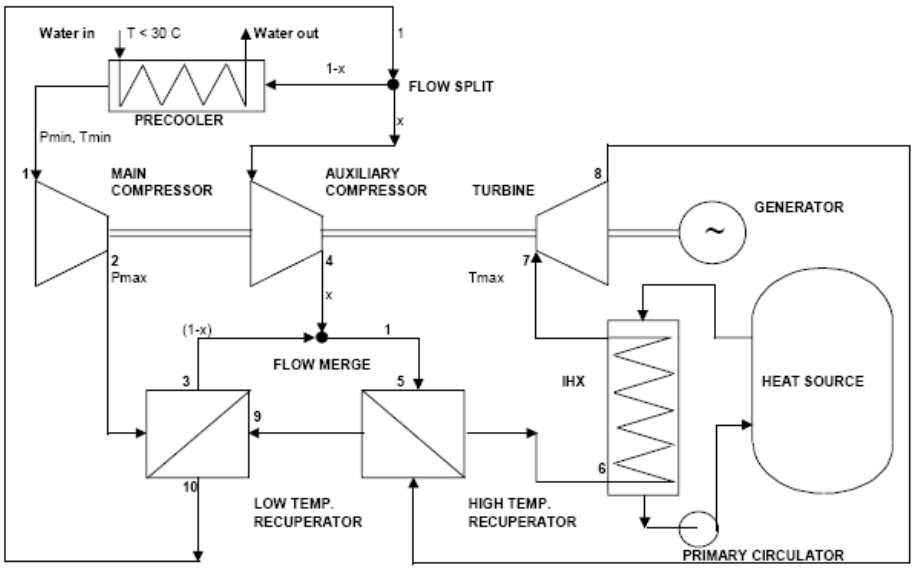


**Figure 4.1 : Supercritical-$CO_2$ re-compression cycle layout**

Several conversion cycle options have been studied for the reference pressure vessel coolant outlet temperature of 550 °C and for a proposed higher temperature of 600 °C. Cycle maximum pressures of 200 bar and 250 bar and core temperature rises of 150 °C and 200 °C were considered.

Provided the limitation conditions mentioned here above, it was found that better performance was achieved for cycles based on the higher maximum pressure. This was improved further by increasing the core temperature rise from 150 °C to 200 ° by lowering the core inlet temperature. On this basis, the temperatures at the inlet and outlet of the reactor pressure vessel have been set to 350 °C/550°C. These temperatures allow the 40% target to be exceeded easily (calculated efficiency of 43.3 %). If the accelerator power is included in the efficiency calculation, this one becomes 34.8 %.

Moreover, a provisional value of 10 % of the flow-rate was considered to by-pass the core. In the upper plenum, this by-pass flow mixes with the helium passing through the core. Consequently, one can calculate that if the pressure vessel outlet temperature is 550°C, the core outlet temperature is 572 °C.

*This document refers to work being performed by scientists and institutions involved in IP EUROTRANS, as well as the financial support of the European Commission through the contract FI6W-CT-2004-516520.*

### 4.2.2 Fuel Cladding

On the basis of the safety studies performed for the He-cooled XADS [4.4], it was shown that the limited operating temperatures associated to metallic material claddings did not allow to withstand properly all the transient events.

On the other hand, an analysis of the functions/criteria that the fuel cladding must deal with shows the following outcome:

- High melting point and stability (thermal and chemical) ;
- Reduced swelling ;
- Fission Products (FP) retention (absence of diffusion and/or cracking) ;
- Resistance to primary and secondary stresses ;
- Resistance to damage effects (fast neutron and FP).

On this basis, the material proposed for the EFIT-He cladding is Silicon Carbide (SiC). This material is under development for the Gas-Cooled Fast Reactor [4.3].

Studies conducted at CEA showed that, likewise other nitrides or carbides, SiC exhibits a high melting temperature, high mechanical characteristics and a rather good thermal conductivity. However, the main drawback of those ceramic materials is poor fracture toughness (in the range 2 to 5 $MPa.m^{1/2}$). Thus, from the mechanical point of view SiC reacts as a brittle material and the risk of failure is strongly depending on the presence of micro-cracks. To limit problems associated to this “brittle” behaviour, it was proposed to use SiC under a composite form : SiC fibres embedded in a SiC matrix ($SiC_f$/SiC). In this configuration, $SiC_f$/SiC materials with 40 % of fibres present fracture toughness of around 30 $Mpa.m^{1/2}$.

$SiC_f$/SiC materials allow manufacturing tubes which can accept some damage under mechanical loading without loosing their mechanical integrity.

According to their manufacturing process (Chemical Vapour Deposition) $SiC_f$/SiC materials are porous. Thus an internal liner is necessary to ensure the tightness of the cladding. This liner can be metallic : Re or W have been identified as the most suitable materials to .

The mechanical behaviour of $SiC_f$ /SiC materials is maintained up to 1400 °C. However, the behaviour under thermal and/or mechanical fatigue remains poorly known. Investigations have been undertaken on this issue within the CEA/GFR Program. In the safety analysis presented in chapter 6.2, provisional values have been considered for the fuel and cladding limit temperatures.

### 4.2.3 Summary of the Main He EFIT Plant Characteristics

The main characteristics of the final design of the EFIT-He plant are summarized in Table 4.1 hereafter. The optimisation was performed with Fuel and MA Compositions coming from PWR spent fuel cooled 50 years just like for the EFIT-Pb plant. 6 DHR systems are foreseen, each able to remove 50 % of decay heat to achieve a better reliability compared to the 3 x 100 % loop design which was initially considered ([4.9], [4.10] and [4.11]). The width over flats of the hexagonal S/A is fixed to 137 mm. 19 sub-assemblies (S/A) are withdrawn from the core in order to accommodate the spallation module.

*This document refers to work being performed by scientists and institutions involved in IP EUROTRANS, as well as the financial support of the European Commission through the contract FI6W-CT-2004-516520.*

| Parameter | Value | Comments |
|---|---|---|
| **PLANT GENERAL CHARACTERISTICS** | | |
| Coolant | Helium at 70 bars | |
| Core Power | 400 $MW_{th}$ | |
| Core Volumic Power | 55 $MW/m^3$ | |
| Efficiency | 43.3 % excluding acc. power<br>34.8 % including acc. power | |
| Vessel Inlet/outlet core temperatures | 350°C/550°C | 572°C for the core outlet |
| Power conversion system | Indirect S-$CO_2$ cycle with re-compression | |
| Accelerator | LINAC<br>E : 800 Mev; I : 20 mA max. | Beyond 800 MeV, the lifetime of the spallation products increases significantly |
| Spallation target | Solid target with "cold" window | Solid target : W rods cooled by helium – Target cooling separate from the core cooling |
| **CORE GENERAL CHARACTERISTICS** | | |
| Fuel pellet compo. | (Pu, Am, Cm)$O_2$ + MgO | 55 % matrix / 45 % fuel |
| Type of S/A | Hexagonal – with wrapper | Thickness : 4 mm |
| Number of S/As | Total : 366<br>2 zones with different pin diameters | 186 Inner zone (core 1)<br>180 Outer zone (core 2) |
| Fuel enrichment | 41.4 % (Pu/MA+Pu) | |
| Pin spacer system | Grids | 5 grids |
| S/A Width over flat | 137 mm | Corresponding to the withdrawal of 19 S/As to implement the spallation module |
| Total peaking factor | 1.84 | |
| Fissile Core Height | 1.25 m | |
| **FUEL PIN CHARACTERISTICS** | | |
| Cladding material | $SiC_f$/SiC | 1 mm : mini. feasible thickness with SiCf/SiC |
| Fuel/cladding gap | 100 µm for 5.8 mm pellet diameter | Evolution is proportional to the diameter |

**Table 4.1 : EFIT-He General Characteristics**

*This document refers to work being performed by scientists and institutions involved in IP EUROTRANS, as well as the financial support of the European Commission through the contract FI6W-CT-2004-516520.*

## 4.3 Description of the Accelerator and spallation target

The accelerator supplies the proton source. The maximum characteristics of the proton beam are:

$E_p$ = protons energy = 800 MeV,

I = beam intensity = 20 mA.

So, assuming that q is the proton charge (= $1.6E^{-19}$ C) and $E_p$ in Joules, the beam current (corresponding to a core power assumed to be 400 $MW_{th}$) is set to:

$$P_{beam} = \frac{I E_p}{q} = 16 \text{ MW}.$$

The spallation module is made of the following main elements:

- The target
- The window
- The thimble which is the external shell of the module

The whole spallation module is potentially removable.

The spallation target (Figure 4.2) is made of a central part and a peripheral part. The central part of the geometry corresponds to a pin bundle made of 46 staggered horizontal tungsten rod rows (35 rods per row) whereas its peripheral part is a steel ring in the thickness of which longitudinal channels are arranged allowing the helium circulation. Helium is circulating downwards in the central part and upwards in the peripheral part.

In the peripheral part, one can consider that 50 % of the ring is steel and 50 % is helium. The purpose of this arrangement is to maximize the efficiency of the target in terms of neutron production.

The central part is 69 cm high and the peripheral part is 125 cm high. Target first rods are located 65 mm above the core mid-plane. The spallation target is put in a container and a thimble, surrounded by the sub-critical core.

The target is made of tungsten and stainless steel and is cooled by a dedicated helium circuit. The height of the target is of 690 mm. A cold window is considered and placed above the reactor roof. This window is cooled by a specific circuit which has to be defined.

The thimble of the target constitutes the outer shell. The outer diameter of the thimble is 554 mm and it has a thickness of 27 mm. The thimble is suspended, fixed to the reactor roof in its upper part, and guided in its down part by the thimble axial guide. The thimble guide is clamped in the support plate.

The thimble height is about 14900 mm in the present plant lay out.

The thimble has to be designed for a temperature of 575°C.

*This document refers to work being performed by scientists and institutions involved in IP EUROTRANS, as well as the financial support of the European Commission through the contract FI6W-CT-2004-516520.*

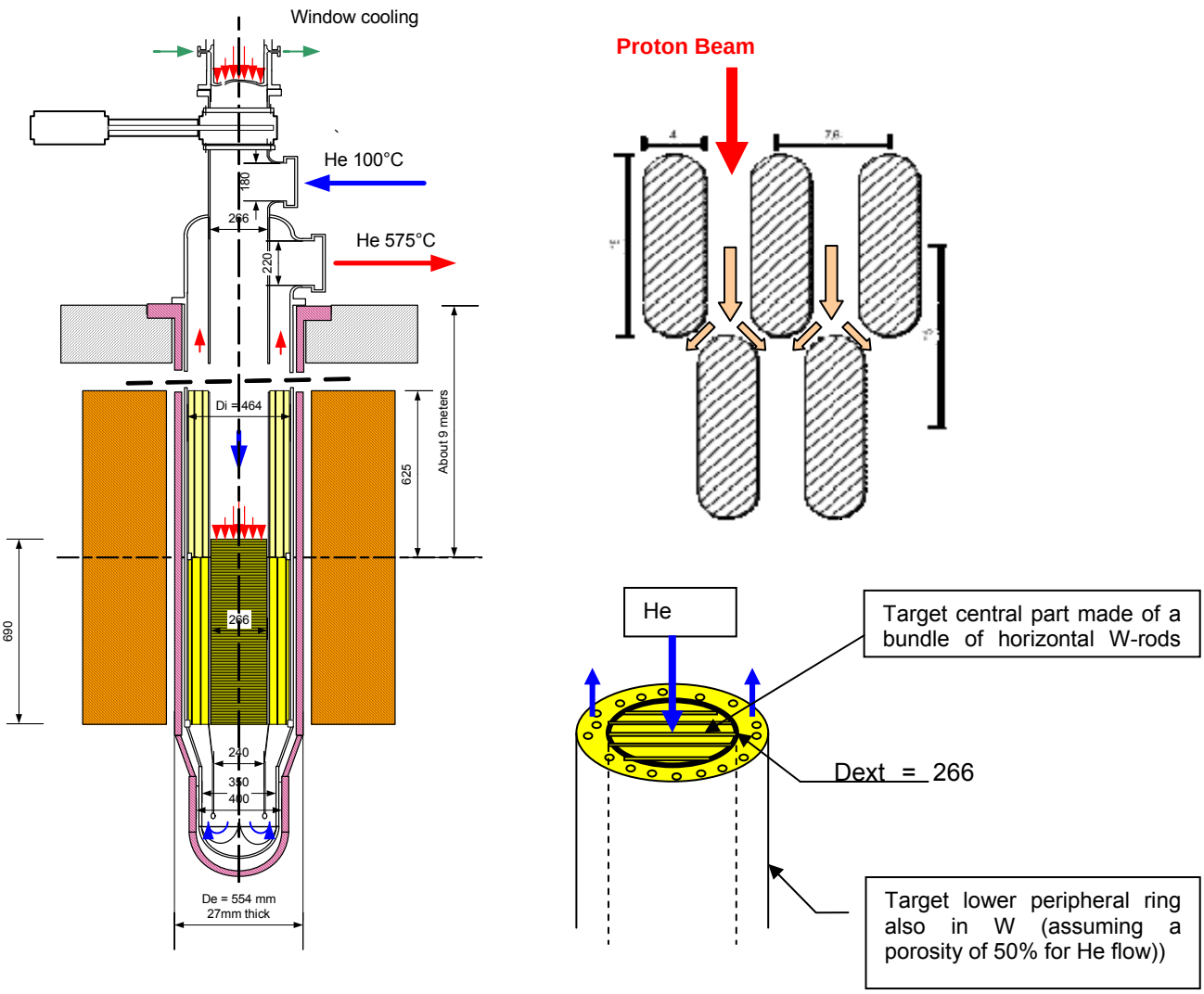


Figure 4.2 : Spallation module design

## 4.4 EFIT-He Core Design

### 4.4.1 Main Sub-Critical Core Characteristics

The EFIT core is designed for a thermal power of about 400 $MW_{th}$, aiming at transmutation performances and radial power flattening. In order to flattening the radial power distributions, a 2 fuel zone core has been finally selected ([4.12], [4.13]).

The methodology described in Chapter 3.1.1 for EFIT-Pb has been used to design the EFIT-He core. The application of this approach for the EFIT-He core is provided in chapter 4.5.

The sub-critical core is constituted by hexagonal sub-assemblies (S/As), distributed in a hexagonal scheme in concentric rows (cf. Figure 4.3). At the centre of the core, 19 S/As are removed in order to accommodate the spallation module. Each S/A is embedded in an hexagonal wrapper which ensures its sealing and is separated from the other S/As by a gap which makes possible the thermal expansion as well as the fuel handling. Each S/A includes a certain number of vertical and parallel fuel pins separated by helium channels which extract the power produced in the fuel.

*This document refers to work being performed by scientists and institutions involved in IP EUROTRANS, as well as the financial support of the European Commission through the contract FI6W-CT-2004-516520.*

In the final design of the EFIT-He plant :

- The core has a power of 400 $MW_{th}$ (with only two zones instead of three in the preliminary design) as seen in Figure 4.3 :
  - Zone 1 (inner zone): 6 rings corresponding to 186 assemblies (203.3 MW) ;
  - Zone 2 (outer zone): 3 rings corresponding to 180 assemblies (196.7 MW) ;
- The ratio of fuel/matrix volume fractions is 45/55 % (instead of 50/50 % in the preliminary design) ;
- There are 12 absorber rods at the interface of core zones 1 and 2.
- The radial reflector is made of 2 rings (150 S/As) while the radial shield consists of 3 rings (270 S/As) ;
- The plutonium and minor actinides isotopic compositions are the ones coming out of a MOX fuel irradiated at 45 GWd/t in a PWR plant and cooled during 30 years [1.2],

The hexagonal pitch is 14 cm (13.7 width for the wrapper assembly and 3 mm of inter-wrapper gap). The axial reflector and neutronic shield are both positioned at the top and the bottom of the fissile part.

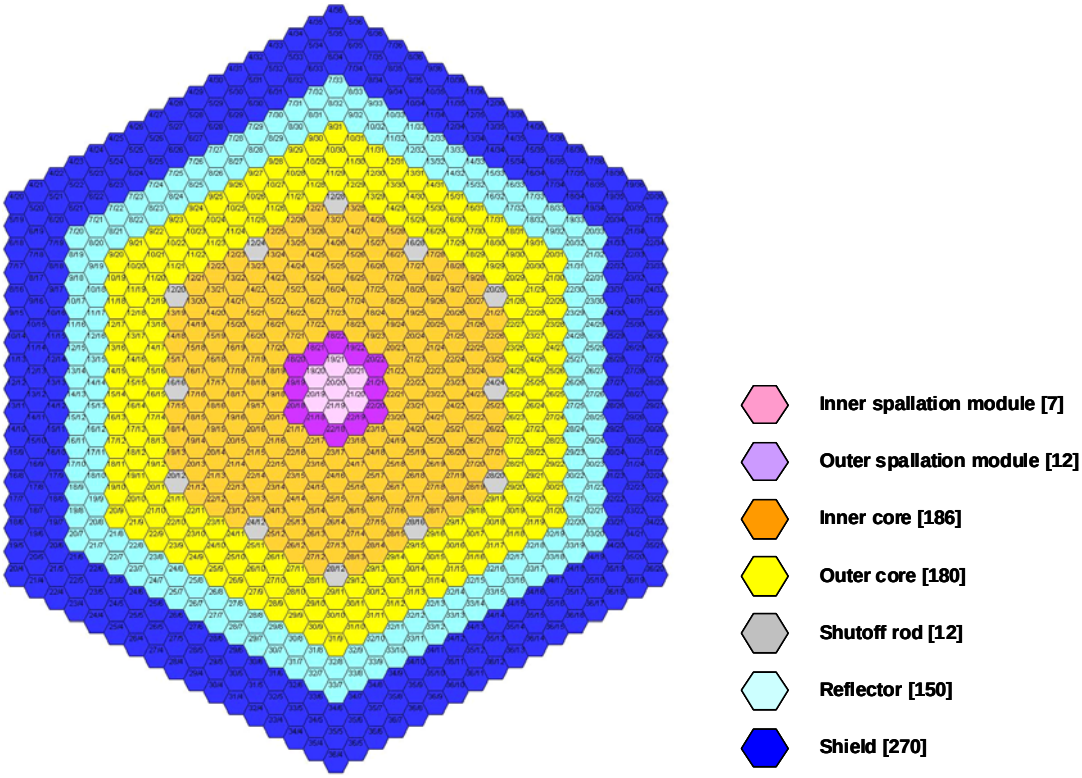


Figure 4.3 : EFIT-He Core design

The design of the S/As is widely based on the design proposed for the 600 $MW_{th}$ GCFR presented in reference [4.17].

### 4.4.2 Core Composition

Schematically, the EFIT-He core is constituted by:

- The structures of the sub-assembly : Hexagonal wrapper and internal structures ensuring the mechanical arrangement of the pin bundle Currently, the material chosen for those structures is the $SiC_f$/SiCf composite material (SiC matrix reinforced by SiC fibers) ;

*This document refers to work being performed by scientists and institutions involved in IP EUROTRANS, as well as the financial support of the European Commission through the contract FI6W-CT-2004-516520.*

- The helium coolant which circulates in the pin bundle as well as the fraction which is situated between the S/As and which does not circulate ;
- The fuel pins constituted by :
  - The CerCer ((Pu,AM)$O_2$/MgO) pellets ;
  - The liner with its adaptation material which role is to ensure the internal tightness of the cladding ;
  - The cladding made of $SiC_f$/SiC (including the external liner or seal coat) ;
  - The fuel rod plenums situated at the top of the fuel pin ;

A scheme of the fuel pin geometry (radial description) is provided in Figure 4.4.

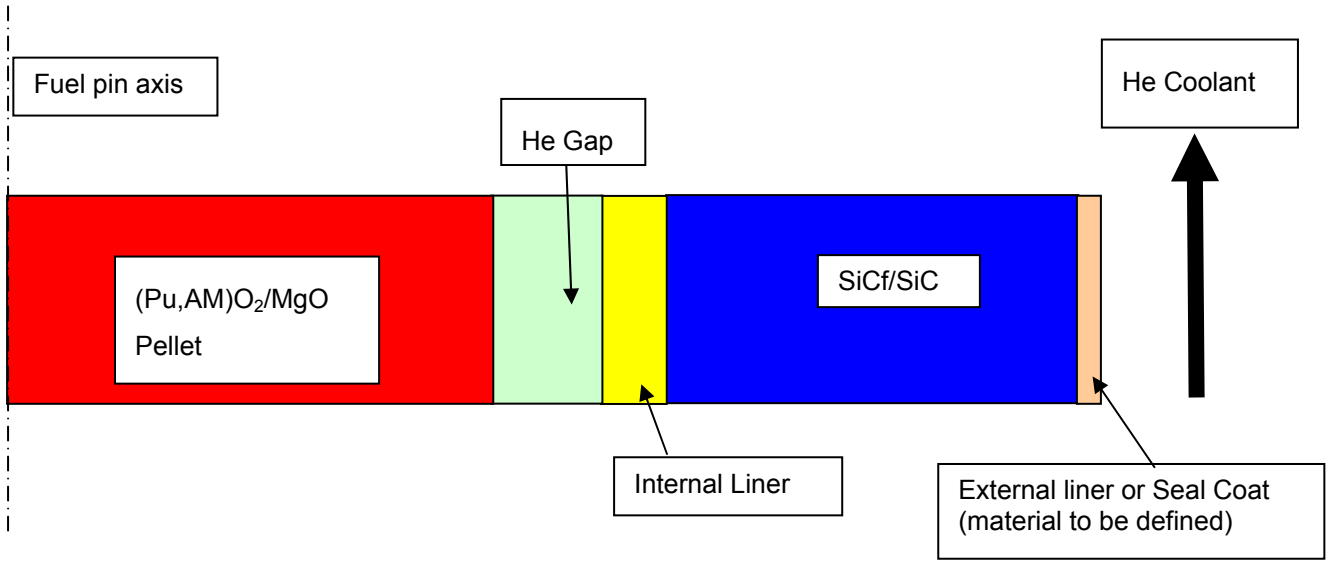


Figure 4.4: Schematic View of the EFIT-He Fuel Pin

The composition and thickness of the different materials are widely based on the experience gained in the GFR 2400 pre-conceptual design [4.14]. They are as follows :

- Internal liner : W-$Re_{14\%}$ /Thickness : 40 µm
- Adaptation Material : Re / Thickness : 10 µm
- Cladding : SiCf/SiC / Thickness : 1 mm
- External liner : “SiC-like” (transparent to neutrons) : thickness 30 µm. At the current stage of the design, this material is considered to have the SiC properties.

In the final design :

- The inter S/A gap is fixed to 3 mm ;
- The wrapper thickness is fixed to 4 mm

### 4.4.3 He EFIT core performances

Detailed results of the EFIT-He core performances can be found in references [4.15] and [4.16]. Summary of these results is given hereafter.

For safety reasons, just like for the EFIT-Pb core, it must be ensured that the core remains always sub-critical, without having to rely on shutoff or control rods. The margin to criticality is an important requirement for the core definition that leads, eventually, to define core size and reactor power.

It is assumed that a margin of 0.016 ΔK to criticality, a figure that includes allowance for measurement errors, be required at DBC, akin to standard practice for light water reactors. $K_{eff}$ shall hence not exceed

*This document refers to work being performed by scientists and institutions involved in IP EUROTRANS, as well as the financial support of the European Commission through the contract FI6W-CT-2004-516520.*

0.984 at any time during DBC. It is further assumed that $K_{eff}$ shall not be greater than 0.95 during Refuelling. Different limits in reactivity, taking in account the possible reactivity insertions have been chosen :

the safety limit of 0.99 (1% of margin to criticality) ;

the cold state limit (incidental situations) ;

the steady state limit (cold state to nominal operating conditions).

Safety limits are given in Table 4.2 (nominal state limit) and Ta ble 4.3 (cold state limit).

| | Δρ (pcm) | $K_{eff}$ |
|---|---|---|
| **Safety limit** | **-** | **0.99** |
| Core compaction | 905 | 0.9812 |
| Target removal | 82 | 0.9804 |
| Void effect | 502 | 0.9756 |
| **Hot zero power limit (100°C)** | **72** | **0.9749** |
| Fuel expansion | 169 | 0.9733 |
| Doppler (fuel) | 99 | 0.9724 |
| Doppler (structures) | -21 | 0.9726 |
| Axial expansion | -36 | 0.9729 |
| Radial expansion (diagrid) | 72 | 0.9723 |
| **Nominal state limit** | **-** | **0.9723** |

Table 4.2 – Nominal state limit setting (operating conditions)

| | Δρ (pcm) | $K_{eff}$ |
|---|---|---|
| **Safety limit** | **-** | **0.99** |
| Core compaction | 905 | 0.9812 |
| Target removal | 82 | 0.9804 |
| Void effect | 502 | 0.9756 |
| handling error | 410 | 0.9717 |
| **Cold state limit (20°C)** | **-** | **0.9717** |
| **Fuel management limit** | **-** | **0.9500** |

Table 4.3 – Cold state and management limit settings

The Δk between BOC and EOC is about 50 pcm. The ΔK of the 12 absorber rods is about 4440 pcm at BOC (Δρ = 4916 pcm). A calculation considering 87 fission products instead of global fission products gives quite similar results (less than 40 pcm at EOC).

Reactivity effects calculations show that the $K_{eff}$ value at cold state should remain below 0.9717. Otherwise, the fuel management limit at this state is set to 0.95.

Reactivity effects calculations show that the $K_{eff}$ value at operating conditions should remain below **0.9723**. The calculation for the EFIT-He actual design gives a $K_{eff}$ around this value at BOC and EOC.

It should be noted that axial expansion coefficient takes into account the axial SiC expansion and the "structure doppler" effects. All feedback coefficients are negative except for the axial expansion coefficient which is positive (probably due to SiC cladding material).

The source energetic distribution used is the one given by neutrons directly emitted from the spallation reaction on tungsten .

*This document refers to work being performed by scientists and institutions involved in IP EUROTRANS, as well as the financial support of the European Commission through the contract FI6W-CT-2004-516520.*

The source spatial distribution is built from MCNPX results with a ***plane*** radial proton source distribution instead of a spherical one.

Source burn-up calculation have been performed for a single cycle of 2790 days (frequency 1) with the neutron source inside the 19 central assemblies. The ERANOS $K_s$ and $K_{eff}$ value are presented in Figure 4.5. On this basis, the proton beam intensity required to operate the plant is almost stable and remains below 13 mA a value nearly half the one set up for designing the accelerator (cf. § 4.2).

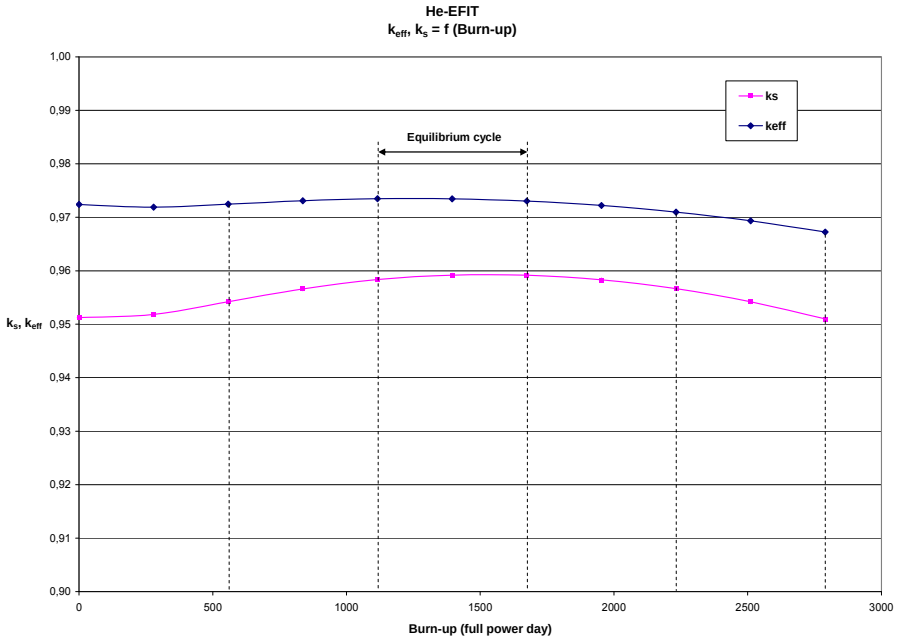


Figure 4.5: ERANOS single cycle Burn-up calculation (2790 days)

The $k_{eff}$ value obtained at BOC (0.9735) fits with safety requirements.

2D power maps (form factors) have been calculated at BOC and EOC. The maximum value for axial form factor is 1.56 (BOC, inner core) and the maximum value for radial form factor is 1.31 (outer core).

Core characterization on the final EFIT-He core design (2 zone core, Pu content of 41.4%) gave the following useful data about core configuration defined at BOC/EOC (synthesis is provided in Table 4.4). The source importance $\varphi^*$ is about 0.52 over the equilibrium cycle, a value quite low, a consequence from a rather large spallation module.

The feasibility of the system is quite resistent to uncertainties coming from nuclear data, fuel characteristics with reduced uncertainties or improved fuel management strategy. On this last item, studies have shown that this has no consequence on the BOC and EOC core characteristics including the power map distribution.

*This document refers to work being performed by scientists and institutions involved in IP EUROTRANS, as well as the financial support of the European Commission through the contract FI6W-CT-2004-516520.*

Table 4.4: Summary of EFIT-He Core Calculations

| **ERANOS calculations without source** | | |
|---|---|---|
| **Core calculations (BOC – $T_{op}$)** | | |
| ECCO | Core description | $K_{eff}$ value |
| heterogeneous | HEXZ | 0.9735 |
| **Reactivity effects (pcm)** | | |
| ECCO heterogeneous HEXZ core description | ρ effects from the steady state to the cold state (doppler & expansion effects) | 455 |
| | ρ effects from the incidental situations | 1489 |
| | ρ burn-up 1cycle | -103 |
| **ERANOS calculations with source** | | |
| **Core calculations (BOC – $T_{op}$)** | | |
| Source multiplication factor ($K_s$) ECCO heterogeneous - HEXZ core description | | 0.9583 |
| j* (MCNPX correction) | | 0.51 |
| i (mA) | | 13.1 |
| **Core calculations** | | |
| Axial form factor | | $f_{ax}$ max inner = 1.56<br>$f_{ax}$ max outer = 1.27 |
| Radial form factor | | $f_{rad}$ max inner = 1.17<br>$f_{rad}$ max outer = 1.31 |
| Transmutation rate | | 2,6 kg/TWh of Pu<br>- 50,5 kg/TWh of Am<br>5,9 kg/TWh of Cm |

The transmutation rate obtained is about 42 kg/$TWh_{th}$ of actinides while the Pu content is almost constant, as seen in Table 4.5. This figure is consistent with the objectives assigned to the plant.

Table 4.5 : Transmutation rate between BOL and EOL (2790 fpd – 400 $MW_{th}$)

| Element | m BOL (kg) | m EOL (kg) | Δm (kg) | Δm (kg/$TWh_{th}$) |
|---|---|---|---|---|
| U | 0 | 26 | 26.0 | 0.97 |
| Np | 210 | 182 | -27.8 | -1.04 |
| Pu | 3825 | 3895 | 70.0 | 2.62 |
| Am | 4970 | 3616 | -1353.2 | -50.52 |
| Cm | 233 | 391 | 158.6 | 5.92 |
| TOTAL | 9238 | 8112 | -1126.4 | -42.06 |

*This document refers to work being performed by scientists and institutions involved in IP EUROTRANS, as well as the financial support of the European Commission through the contract FI6W-CT-2004-516520.*

## 4.5 EFIT-He System Lay out

The EFIT-He plant lay-out was subject too iterations and discussed during dedicated meetings (cf. references [4.18], [4.19). The final design is described hereafter.

The coolant is pressurized helium (70 bars) and like the EFIT-Pb, the power is 400 MWth. Helium is inert and there is no corrosion issue onto metallic materials versus lead cooled EFIT reactor. The helium temperature is in a range between 350°C and 575°C.

Since the EFIT-He reactor is an alternative solution to the EFIT-Pb reactor, only a preliminary design is proposed. The PDS-XADS ($5^{th}$ framework program) is used as a reference and some elements such as the heat exchanger designs and blower are extracted from the past experience on High Temperature Reactors.

The primary system comprises a reactor vessel housing the core and internals, three separated IHX vessels connected to the core by three cross vessels including co-axial hot ducts, and six DHR vessels. The primary vessel accommodates the spallation module.

The main vessel is a pressurized vessel including a removable cover head, a cylindrical shell and an elliptical bottom head and housing the spallation module. The vessel diameter is 5.6 m and 7.5 m at the cover flange. It is almost 19 m high.

The spallation module is made of a tungsten and steel target cooled by helium, a cold window cooled by a specific circuit and a thimble which is the external shell of the module.

The three IHX vessels connected by the cross vessels (around 8 m long) comprise a 4 MW blower to run primary helium and a helical tubes heat exchanger with around 2500 tubes. The secondary fluid is supercritical $CO_2$ at 250 bars.

The DHR system is composed by six DHR vessels connected to the main vessel by means of six DHR ducts with expansion loops to accommodate the thermal expansion.

The helium flow path is formed by the main vessel and the inner vessel. The cold helium goes down by an annular gap, enters in the diagrid, and passes through the core (upwards path). At the core outlet, the helium is directed towards the hot ducts of the three cross vessels which connect the main vessel to the IHX vessels.

The cross vessel nozzles are located in the upper part of the main vessel.

The hot helium circulates in the hot leg from the main vessel to the IHX vessel. It is then, cooled by supercritical $CO_2$ in the helical heat exchanger in the IHX vessel. In the exchanger, primary helium circulates in counter current flow outside tubes from the bottom to the top. At the outlet of the exchanger bundle, the cold helium goes down in an annular gap formed by the IHX inner vessel and the IHX vessel, which allows the cooling of this later. At the bottom of the IHX vessel, the cold helium is compressed by a blower and goes in the concentric annular duct of the cross vessel.

From the cross vessel, the cold helium returns to the core via the annular gap formed by the main vessel and the inner vessel.

*This document refers to work being performed by scientists and institutions involved in IP EUROTRANS, as well as the financial support of the European Commission through the contract FI6W-CT-2004-516520.*

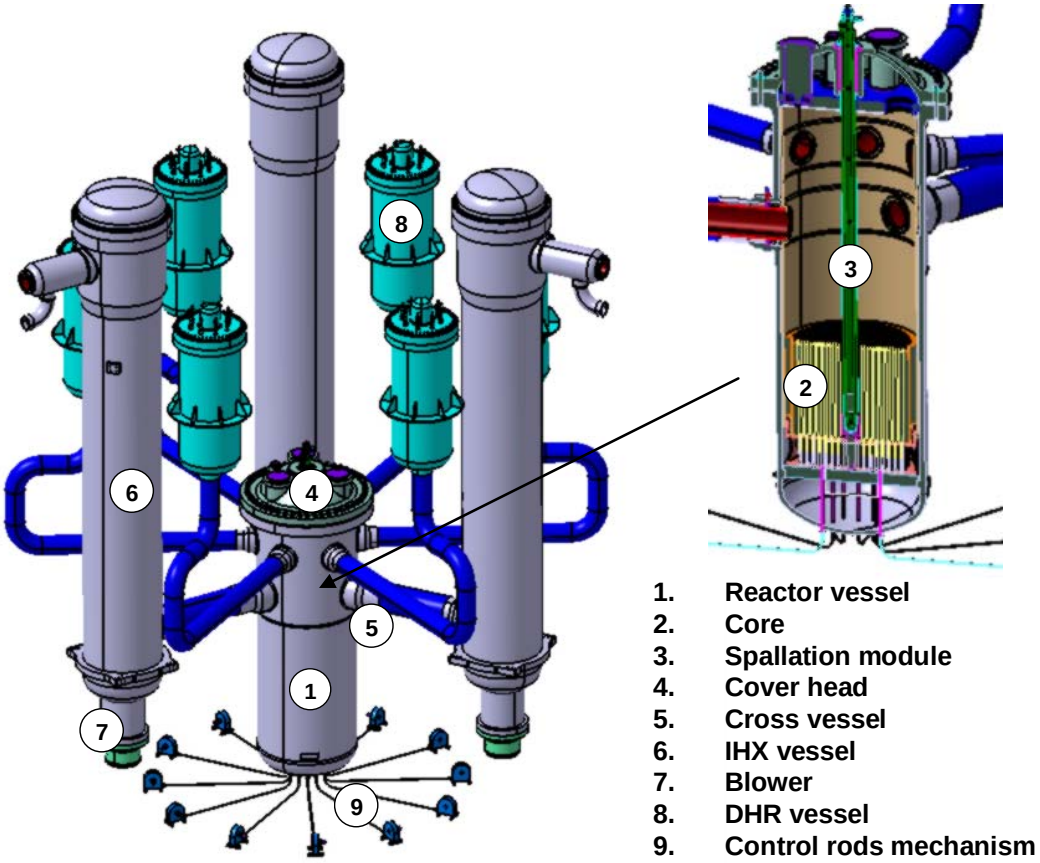


Figure 4.6: EFIT-He general architecture

The reactor parameters are exposed in the following table 4.6:

Table 4.6: Reactor parameters

| | | |
|---|---|---|
| Thermal power | 400 | $MW_{th}$ |
| Nominal helium pressure | 70 | bar |
| Core inlet temperature | 350 | °C |
| Core outlet temperature | 572 | °C |
| Primary He flow rate | 350 | kg/s |

During accidental or fuel handling conditions, the decay heat is removed by the Shutdown Cooling System composed by six DHR vessels. To enable natural circulation in some cases, the DHR vessels are located almost 20 m above the middle of the core. A concentric duct with an expansion loop runs the helium from the core to the DHR in the central hot duct and from the DHR to the core in the annular cold duct (co-axial duct).

The DHR nozzles are located above the cross vessel nozzles on the reactor main vessel.

*This document refers to work being performed by scientists and institutions involved in IP EUROTRANS, as well as the financial support of the European Commission through the contract FI6W-CT-2004-516520.*

During normal operation, the DHR vessel is closed by a passive valve so that the helium goes towards the PCS.

In case of a PCS unavailability, an active redundant flow shutter is implemented on the cold duct (in the cross vessel) in order to prevent the forced flow from the Shutdown Cooling System escaping through the breach instead of through the core. A preliminary design of this flow shutter was developed for PDS-XADS at a smaller scale and is also adopted for the EFIT-He.

## 4.6 Reactor vessel and internals

### 4.6.1 The diagrid

The diagrid is a cylindrical plenum containing the vertical shroud tubes into which the core sub-assemblies are inserted. These shroud tubes provide the positioning and support of the sub-assemblies and allow the helium feed from the diagrid through holes in the tube wall. The detail arrangement and the hydraulic of the shroud tubes have not been investigated in this project

Twelve circular lateral apertures (diameter 905 mm) on the diagrid enable the helium circulation from the cold part of the reactor to the core. The diagrid height is defined consequently at 1200 mm. The delta of pressure in the diagrid is low and a thickness of 50 mm is enough.

The thimble axial guide is located at the center of the diagrid. It provides, in its upper part, a lateral guide for the first row of sub-assemblies. In its lower part, it could guide additional modular shields (shields may be required considering the proximity of the spallation target).

### 4.6.2 The support plate

The diagrid is directly supported by the support plate, which also supports the core and the lateral baffles. The support plate must support a structure weight around 500 tons (core and lateral baffles around 410 tons and diagrid around 90 tons).

With more than 75% margin (on normal operating conditions), the thickness of the support plate is t=430 mm. An important margin is necessary to accommodate seismic conditions (additional load considering 0.5 g).

The support plate is crossed by the twelve absorber rods located outside the core during normal operation under the main vessel. The influence of these crossing rods is negligible on the plate thickness calculation. With 430 mm, the feasibility of the 316 L(N) plate is not an issue.

The support plate is supported by the main vessel on an annular flange at the bottom of the vessel cylindrical part.

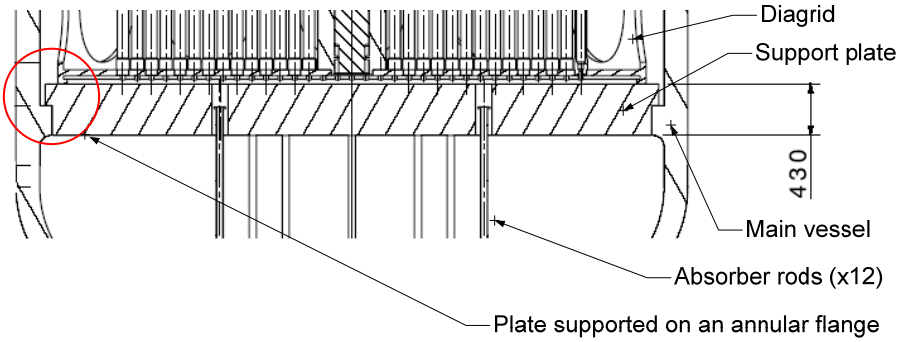


Figure 4.7: EFIT-He reactor core support plate

*This document refers to work being performed by scientists and institutions involved in IP EUROTRANS, as well as the financial support of the European Commission through the contract FI6W-CT-2004-516520.*

#### 4.6.3 Inner vessel

The cold helium comes from the intermediate heat exchangers through the cross vessel and is directed to the core via the annular gap between the main vessel and the inner vessel. In the reactor vessel, cold helium (350°C) is separated from hot helium (572°C) by the inner vessel. The inner vessel directs the major part of cold helium towards the core. A leak flow rate of cold helium is used to cool the upper part of the main vessel and the roof.

The inner vessel is suspended from a support flange which is part of the reinforced ring of the main vessel. In the lower part, metallic piston seals ensure the connection between the inner vessel and the diagrid. The thickness of the inner vessel is 50 mm and its outer diameter is 5150 mm.

#### 4.6.4 Main vessel and cover head

The reactor vessel is a classical pressure vessel including a removable cover head, a cylindrical shell and an elliptical bottom head. The peculiarity is that the main vessel houses a spallation module.

The height of the vessel is given by the core height (4250 mm) and the accommodation of the two levels nozzles (for the cross vessel and the DHR systems) and the fuel handling devices. The main vessel is about 19000 mm high.

The main vessel is formed by a cylindrical shell, an elliptical bottom and a spherical cover head whose sizing is detailed below. The main vessel thickness is 200 mm and its outer diameter is 5650 mm.

Due to the size and the temperature of the roof, a flat metallic plate would have a too large thickness. Consequently, the roof is a 170 mm thick spherical head (HTR example).

As for PDS-XADS, the bottom of the main vessel is elliptical. The choice of an elliptical bottom enables to gain on the reactor vessel height and is also more suitable for the implementation of absorber rods under the core. The thickness of the elliptical bottom is 155 mm.

### 4.7 Heat exchanger

The reactor vessel is connected to three separated vessels that house the Primary Heat Transfer System (PHTS) via cross vessels. The three IHX vessels connected by the cross vessels (around 8 m long) comprise a 4 MW blower to run primary helium and a helical tubes heat exchanger with around 2500 tubes. This type of exchanger with helium and high temperature was investigated in the frame of the HTR projects.

The helium runs towards the tubes bundle and circulates outside helical tubes upwards the tubes bundle. The cold helium circulates downwards in an annular gap around the tube bundle in order to keep the IHX vessel at 350°C.The helium passes through the blower in the lower part of the vessel and is directed toward the cross vessel to return in the core.

The supercritical $CO_2$ comes from the upper part in a concentric duct and enters tubes from above. It circulates in counter current in the helical tubes. Then the supercritical $CO_2$ goes out from the upper region of the IHX by a central duct. In the upper part, the supercritical $CO_2$ at 250 bars is separated from the primary helium at 70 bars thanks to a flat tubular plate.

The choice of the tubular flat plate comes from the HTR feedback and, in the present case, considering the large $CO_2$ pressure, the flat tubular plate may be an issue in terms of feasibility. Consequently, for this specific part of the design, the HTR IHX feedback cannot be applied and major changes need to be done.

With a large R&D program, it is possible to envisage a domed tubular plate able to resist to a large $\Delta P$ between the primary side and the secondary side. This option can be envisaged at first as its manufacturing is planned in a distant future leaving some time for this development work.

A less challenging solution for the conversion cycle is the steam cycle at 180-190 bars, which gives the same efficiency in the considered range of temperature. The steam generator should be directly designed based on HTR past experience.

*This document refers to work being performed by scientists and institutions involved in IP EUROTRANS, as well as the financial support of the European Commission through the contract FI6W-CT-2004-516520.*

The outer diameter of the IHX vessel is 4500 mm and its thickness is 250 mm. This large thickness is actually chosen to have an outer diameter large enough to implement the 4 $MW_{th}$ blower. The tube bundle height is 12800 mm and the number of tubes is 2402 which is in the feasibility field.

The total IHX vessel height is estimated around 36 m.

The following table gives the main characteristics of the tube bundle.

| | | |
|---|---|---|
| Power | 135 | $MW_{th}$ |
| Temperatures | | |
| Helium inlet temperature | 572 | °C |
| Helium outlet temperature | 350 | °C |
| $sCO_2$ inlet temperature | 332 | °C |
| $sCO_2$ outlet temperature | 525 | °C |
| Log mean temperature difference | 30.2 | |
| Pressures | | |
| Helium pressure | 70 | bar |
| $sCO_2$ pressure | 250 | bar |
| Flow rates | | |
| Helium mass flow rate | 117.2 | kg/s |
| $sCO_2$ mass flow rate | 561.2 | kg/s |
| Tubes | | |
| Tube inlet diameter | 16.6 | mm |
| Tube outlet diameter | 21 | mm |
| Number of tubes | 2402 | |
| Bundle | | |
| Bundle diameter | 3150 | mm |
| Tube length | 29940 | mm |
| Bundle height | 12800 | mm |
| Pressure losses | | |
| Helium pressure loss | 0.19 | bar |
| $sCO_2$ pressure loss | 0.82 | bar |

Table 4.8: Heat exchanger bundle characteristics

## 4.8 DHR system

The DHR system was designed by AREVA NP based on the PDS-XADS principle. A first design proposes, as for PDS-XADS, three redundant DHR vessels, each one able to evacuate 100% of the decay heat. Following a reliability study on the SCS (Shutdown Cooling System), a more reliable system with six DHR vessels, each one able to remove 50% of the decay heat is finally retained.

*This document refers to work being performed by scientists and institutions involved in IP EUROTRANS, as well as the financial support of the European Commission through the contract FI6W-CT-2004-516520.*

EFIT-He drawing presents six DHR vessels connected to the main vessel by a DHR concentric duct with an expansion loop. The duct minimum height is defined to enable the natural circulation in some working conditions (70 bars).

A passive valve is implemented at the inlet of the DHR vessel so that the DHR systems only work for shutdown, handling or accidental conditions. In normal operating conditions, the DHR vessels are filled with cold helium and do not work, the helium flows towards the PHTS (Primary Heat Transfer System).

According to safety requirements, a reliable architecture must be composed of 2 diversed systems with three redundant lines. The diversity can be ensured by two types of exchangers: plate heat exchangers and finned tubes heat exchangers. The second concept appears as the more realistic technology. The plate heat exchanger concept is more a backup solution at the present stage of the project and has not been investigated in detail.

Consequently, the present drawing of the EFIT-He will only integrate the finned tubes concept. Each of the six DHR vessels integrates finned tubes heat exchangers.

The DHR vessel architecture is based on the PDS-XADS one. It consists in eight cylindrical exchanger modules disposed in a circumferential way. The blower is located at the outlet of the exchangers system. The thickness of the DHR vessel is 150 mm, corresponding to an outer DHR vessel diameter of 3470 mm. The slab is a flat metallic plate. The thickness of the slab is 550 mm considering the pressurized case.

The main vessel is connected to a DHR vessel by means of a co-axial duct with a “L” shape and an expansion loop on the duct. The hot duct is the central part and the cold helium is returned to the core by the annular cold duct.

The “L” duct height is almost 9900 mm, this is the minimum height required to enable a start of natural circulation at 70 bars (20 m between the middle of the core and the DHR exchanger inlet) and to accommodate the layout.

The thermal insulation can be implemented inside the hot duct and can accommodate the duct elbows.

REFERENCES

[4.1] B. Giraud, “Synthesis Report of the PDS-XADS Project”, Deliverable 86 of the PDS-XADS Project

[4.2] “Gas Cooled Fast reactor Project” – Contract number 012773 – December 2004, Co-ordinator : Colin Mitchell (AMEC)

[4.3] C.Poette et al., “GFR 600MWTH design status and main characteristics“, Rapport Technique, CEA DEN/DER/SESI/LCSI/ NT DO 8 08/04/05 , 2005.

[4.4] P. Richard et al., “Technical Option Report on the Gas-Cooled XADS”, PDS-XADS Project – Deliverable D 62

[4.5] G. Rimpault, “Définition des missions détaillées de l’XT-ADS refroidi au Pb-Bi et de EFIT refroidi au Pb et de son option de repli refroidie au gaz”, Delivrable D1.1 of the EUROTRANS Project, Note Technique DER/SPRC/LEDC 05.420, Avril 2006

[4.6] P. Richard et al., “Description of plant layout and justification of core design options for the helium-cooled EFIT”, Delivrable D1.8 of the EUROTRANS Project, Note Technique CEA/DEN/CAD/DER/SESI/LCSI/NT DO 3 22/02/08

[4.7] R Thetford, V Sobolev, "Recommended properties of fuel, cladding and coolant for EFIT ", EUROTRANS CONTRACT No.: FI6W-CT-2004-516520, Deliverable No.: 3.1.4 Draft 0.2

[4.8] R. Stainsby, “Supercritical-CO2 Gas Turbine Power Conversion Systems for EFIT-He”, NNC Technical

*This document refers to work being performed by scientists and institutions involved in IP EUROTRANS, as well as the financial support of the European Commission through the contract FI6W-CT-2004-516520.*

[4.9] S. Larmignat, "EFIT-He, DHR preliminary design DHE heat exchanger and compressor design",, AREVA NP Technical document NEEL-F 2008 DC 120 A

[4.10] S. Larmignat, "EFIT-He, New DHR Preliminary Design – 6 loops at 50 %", AREVA NP Technical document NEEL-F 2009 DC 19A

[4.11] S. Larmignat, "EFIT-He, Preliminary description and drawing Reactor Vessel and Internals, IHX and cross vessel, DHR system", AREVA NP Technical document NEEL-F 2009 DC 91A

[4.12] P.Richard et al., "Description of the He-Cooled EFIT Updated Version at End April 2009", Delivrable D1.47 - Version 1 of the EUROTRANS Project, Note Technique CEA/DEN/CAD/DER/SESI/LCSI/NT DO 1 17/06/09

[4.13] P.Richard et al., "Description of the He-Cooled EFIT – Final Version at End 2009", Delivrable D1.47 - Version 2 of the EUROTRANS Project, Technical Note CEA/DEN/CAD/DER/SESI/LC4G/NT DO 1 of 22/03/10, Index 0

[4.14] P. Richard et al, "Status of GFR 2400 WMth Core Studies – Reference and Alternative Core Designs" International GFR Workshop, Paris, February 5-6, 2008

[4.15] G. Rimpault, "Caractérisation neutronique d'un avant-projet de coeur de système sous-critique refroidi à l'hélium et transmuteur de déchets" Note Technique DER/SPRC/LEDC 07.407, May 2007

[4.16] G. Rimpault, "Caractérisation neutronique del 'avant-projet de cœur de système sous-critique EFIT-He" Note Technique DEN/CAD/DER/SPRC/LEDC 09.401

[4.17] F. Morin et al., "Preliminary Study of the Irradiation of the GFR Demonstration Fuel S/A on the ETDR", Note CEA/DEN/CAD/DER/SESI/LCSI/NT DO13 10/09/07

[4.18] A. Woaye-Hune, "Minutes of the EUROTRANS EFIT GAZ (DHR component and remontage) Meeting", AREVA document NEELF-CR-09-207

[4.19] S. Esther-Vignoud, "Helium cooled EFIT Probabilistic reliability analysis of different designs of DHR system", Note technique NEPL-F 2008 DC 163 A, EUROTRANS Contract 516520 (F16W)

[4.20] MCNPX user's manual, version 2.4.0. LA-CP-02-408. LANL (2002)

[4.21] A. Koning (Ed) et al. The JEFF-3.1 nuclear data library, JEFF report 21. OECD/NEA (2006)

[4.22] Report CEA-R-6110, April 2006, "MCNP4C JEFF-3.1 based libraries" J.C. SUBLET

[4.23] J. F. Pignatel, "Etude du comportement en situations nominale et accidentelle de la première image du réacteur ADS EFIT-gaz avec le code CATHARE", CEA/DEN/CAD/DER/SESI/LCSI/NT DO17 03/12/07

[4.24] [J. F. Pignatel, " Evaluation du Cœur 2 Zones du Réacteur ADS EFIT-Gaz avec COPERNIC et CATHARE", Note technique, CEA/DEN/CAD/DER/SESI/LCSI/NT DO 2 23/06/09

[4.25] M. Schikorr et al., " Report on the results of analysis ofDBC & DEC transients in the gas cooled EFIT", Delivrable D1.44 of the EUROTRANS Project, FzK reference INR2010_006

*This document refers to work being performed by scientists and institutions involved in IP EUROTRANS, as well as the financial support of the European Commission through the contract FI6W-CT-2004-516520.*

# 5. DESCRIPTION OF THE 57 MWTH LBE-COOLED XT-ADS (MYRRHA)

## 5.1 General description of the XT-ADS plant lay out

The XT-ADS primary system is a pool-type reactor, cooled by Lead-Bismuth Eutectic (LBE) and it is designed according to current heavy metal cooled system experience [5.1]. It also takes advantage of the advantages and drawbacks of the MYRRHA draft 2 design [5.2] that SCK•CEN provided as a starting point for XT-ADS.

A liquid metal was selected as a coolant due to the desired high fast flux and the high power density. The LBE does not react with water and air like sodium and has a lower melting temperature than lead. The low LBE melting temperature (close to 125°C) allows the primary system to work at rather low temperatures which is an interesting approach to limit the corrosion issue onto metallic materials. The nominal core outlet temperature is about 400°C and the LBE core inlet temperature is 300°C.

The pool-type solution has the interest to take benefit from the thermal inertia provided by the large coolant volume. The pool system also enables to contain all the primary coolant within the main vessel, in which the primary components (pumps, heat exchanger, fuel handling tools, experimental rigs, etc…) are inserted from the top.

In order to keep a large flexibility for the experimental devices loading and because of the presence of the spallation source, the loading of fuel assemblies is foreseen to be from underneath.

The reactor plant is designed for 70 MWth but the core itself has 57 MWth power [5.3], [5.4].

Figure 5.1 presents the lay-out of the XT-ADS reactor assembly.

The spallation loop is off centered located from the core. The requirement of high flux levels leads to design a compact core and the central hole in the core to house the spallation target has to be limited dimensions (around 10 cm). Thus, the spallation loop (i.e., loop achieving the circulation of LBE used as coolant as well as spallation target) is located at the core periphery; it is connected to the central beam tube and the spallation target by two horizontal tubes, one passing above and the other one below the core.

The spallation loop contains a feed tank, a circulation pump, a heat exchanger and an auxiliary system for the control of oxygen contents and the required instrumentation.

A windowless target design is retained, i.e., without a physical separation between the accelerator beam line vacuum and the LBE. An advantage of this solution is that it enables high beam currents needed for industrial transmutation (since irradiation limitation on the window material does not exist).

In the reactor main vessel (around 6 m diameter), the hot and cold pools are separated by an inner tank. LBE circulates by means of two mechanical pumps and the power generated by the core is removed by four (2x2) LBE / water / steam primary heat exchangers (PHX).

The maximum LBE velocity in the primary circuit is 2 m/s in order to limit erosion under control onto metallic materials of all internals except the pump impeller.

The 2 pumps are axial flow pumps which operate at 300°C and supply a total flow rate of 7000 kg/s. Each pump runs the LBE from the hot pool at the level of the PHX outlet window and passes it to the cold plenum. Ongoing research programs are dedicated to find an appropriate material or coating for the pump impeller, resistant to LBE velocities up to 10 m/s.

*This document refers to work being performed by scientists and institutions involved in IP EUROTRANS, as well as the financial support of the European Commission through the contract FI6W-CT-2004-516520.*

Figure 5.1 presents the lay-out of the XT-ADS reactor assembly.

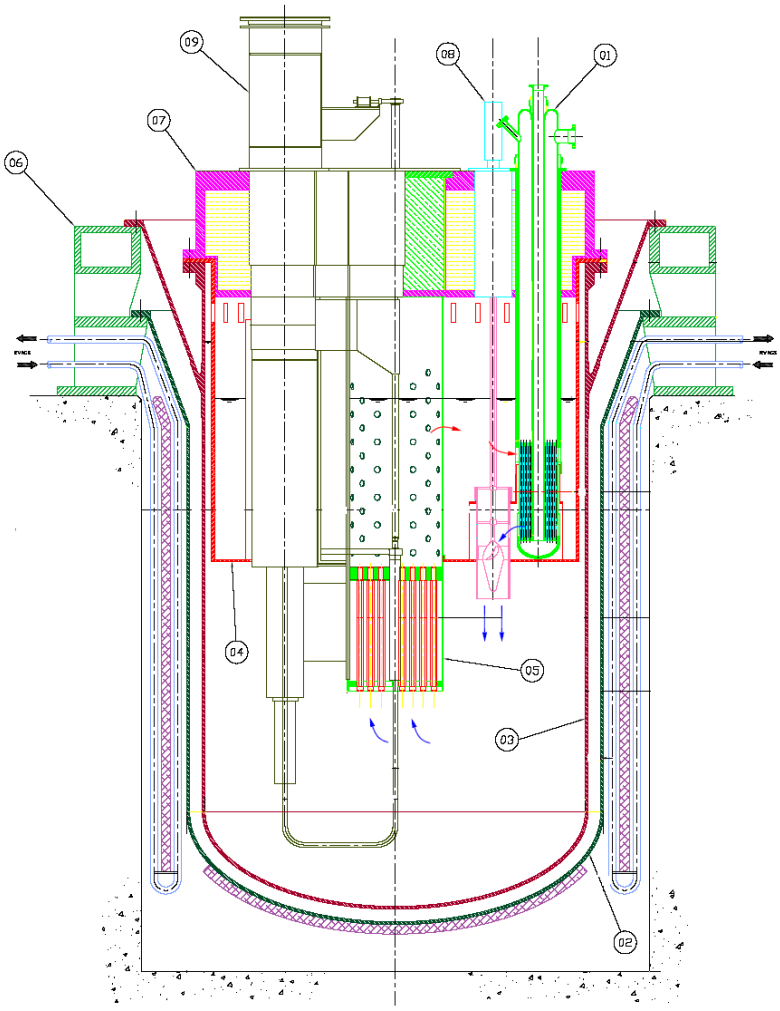


1. PHX (2X2)
2. Safety vessel
3. Reactor vessel
4. Inner vessel
5. Core Barrel
6. Support
7. Reactor Cover
8. Primary Pumps (2X1)
9. Spallation loop

Figure 5.1: XT-ADS reactor assembly

The four PHX are gathered in two circuits, each including two PHX and one pump.

The PHX is a one-through vertical evaporator which works in natural circulation on the water side. The elevation of the heat exchanger with regards to the core has been designed to achieve natural circulation capabilities.

The lower edge of the PHX inlet window remains immersed in LBE in case of a reactor vessel leakage, to ensure the primary coolant circulation and the core cooling.

*This document refers to work being performed by scientists and institutions involved in IP EUROTRANS, as well as the financial support of the European Commission through the contract FI6W-CT-2004-516520.*

The PHX is designed with the double-wall water pipes. This design aims at reducing the risk of a massive water leakage in the primary system. To meet the same goal, the PHX elliptical bottom head is reinforced.

In each circuit, saturated water enters tube side and goes out as a steam water mixture. The mixture then goes in a steam separator. The steam rising from the separator is condensed into an air condenser and the water comes back to the PHX tubes.

Two systems are provided for removing decay heat providing diversity and redundancy. For normal reactor shutdown, the decay heat removal function is ensured by the secondary cooling system using the primary LBE/ water steam heat exchanger and two independent loops.

In case of unavailability of the secondary cooling system, the safety grade reactor vault cooling system (RVACS) is used. The RVACS is placed between the guard vessel and the concrete wall.

## 5.2 XT-ADS windowless spallation target design

### 5.2.1 Spallation target boundary conditions

XT-ADS spallation target system has been designed to be compatible with the remote handling scheme envisaged for the entire XT-ADS. The full loop can be removed from the main vessel after unloading of the core. All active elements are placed in a separate sub-unit which allows servicing of these parts without removal of the spallation loop. The closed outer housing allows regular (yearly) replacement of the spallation target zone that will be required because of radiation induced embrittlement.

The main characteristics have been defined to get a flexible testing facility. Very compact target geometry has been settled to achieve sufficiently high neutron flux levels ($\phi_{Tot} \approx 3.10^{15}$ n/cm².s). The target space is created by removing three of the hexagonal fuel assemblies in the centre of the core [5.5] as it is shown on Figures 5.2-a and 5.2-b.

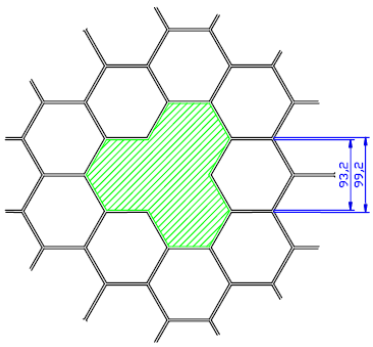


Figure 5.2-a: Three assemblies in the centre of the core are removed to make room for the spallation module (dimensions in mm).

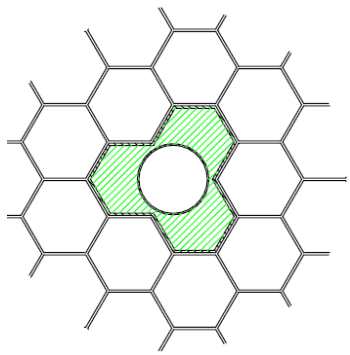

Figure 5.2-b: The hashed area indicates the space available for the LBE feeder line; the inner circle indicates the space available for the proton beam.

The needed high power proton beam, several hundreds of MeV at few mA (600 MeV and 3 mA in the reference design), is delivered by a LINAC accelerator.

The beam ingress is foreseen from the top of the vessel. One of the major reasons for that choice is strongly related to the choice made for the target unit interface. The interface being windowless, interlinking the core with an off-axis housing for all active components, beam ingress from the bottom becomes simply unfeasible (having a penetration in the reactor vessel is of course unsuitable).

In the Figures 5.3-a and 5.3-b, the global geometrical boundary conditions of the XT-ADS spallation loop and its interference with the core are shown.

*This document refers to work being performed by scientists and institutions involved in IP EUROTRANS, as well as the financial support of the European Commission through the contract FI6W-CT-2004-516520.*

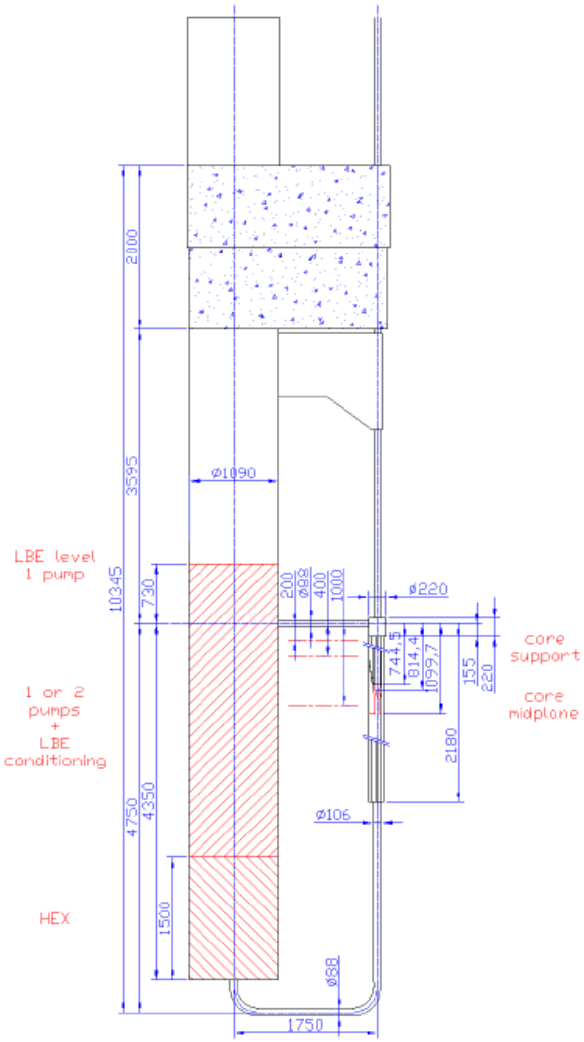


Figure 5.3-a: Global geometrical boundary conditions (outer dimensions) of the XT-ADS spallation loop.

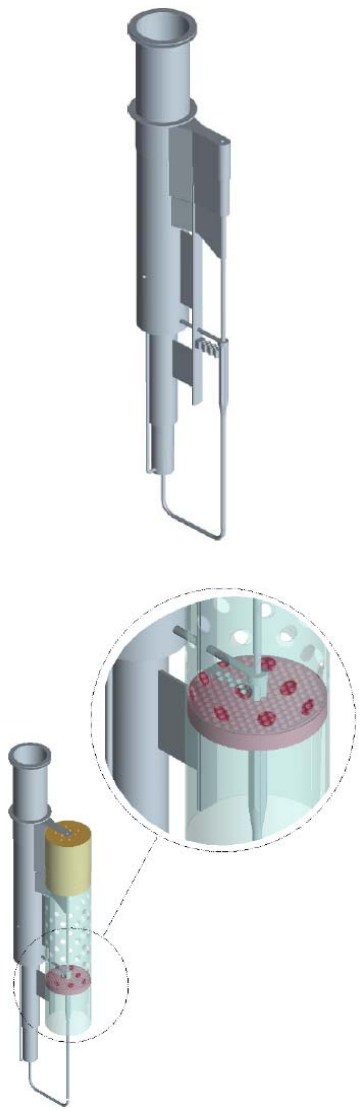

Figure 5.3-b: Spallation loop general view (upper part) and interference of the spallation loop with the core (lower part).

A replacement of the spallation target, within the envisaged lifetime of the XT-ADS, is unavoidable. Hence, the spallation target unit has been designed to survive operation within the ADS system for a sufficient amount of time (roughly one year).

### 5.2.2 Spallation loop layout

The off-axis design of the spallation loop (Figure 5.4) leaves the top and bottom of the sub-critical core accessible for fuel manipulations and the installation of irradiation experiments [5.6]. In addition the main part of the spallation loop is moved away from the high radiation zone. This arrangement is beneficial for the spallation module lifetime.

*This document refers to work being performed by scientists and institutions involved in IP EUROTRANS, as well as the financial support of the European Commission through the contract FI6W-CT-2004-516520.*

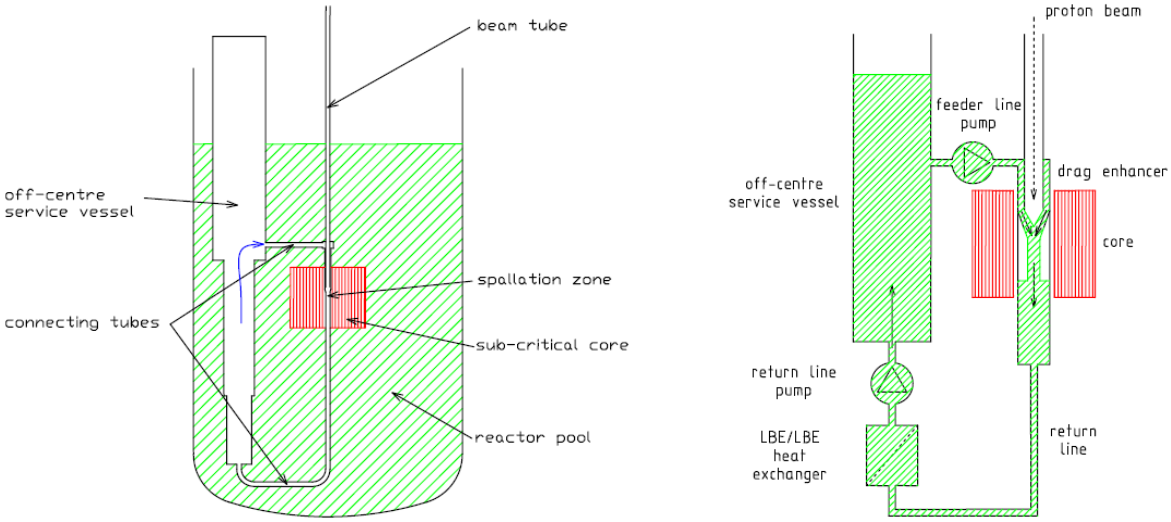


Figure 5.4: General layout showing how the spallation target is split up in a centre and an off-centre part and how the two parts are connected. Hashed area figures LBE (coolant) [left side]. Schematics of the spallation loop. Hashed area figures LBE (spallation material) [right side].

### 5.2.3 Free surface and recirculation zone

The limited space to implement the target is responsible of the choice of a vertical confluent flow as formation mechanism for the target free surface. The liquid LBE is fed to the target nozzle via a vertical three-lobed annular pipe to optimise the use of the available space in the core. Target nozzle itself is designed to ensure a stable free surface flow.

In order to achieve that stable free surface, the size of the recirculation zone, formed in the centre of the target free surface, is essential.

When the recirculation zone is too small, LBE droplets are ejected from the LBE confluent zone that may cause metal evaporation when hit by the beam. If the recirculation zone is too large, it will be directly heated by the proton beam causing the temperatures to increase very rapidly which would also lead to excessive evaporation of LBE and other volatiles.

### 5.2.4 LBE as coolant and target material

The use of LBE as core coolant allows lower working temperatures than foreseen in the lead-cooled EFIT. Liquid LBE is also used for target material as forced convection cooling is required due to the thermal energy deposited by the proton beam, both circuits are separated.

In order to limit LBE evaporation and corrosion of structural materials in the target loop, the maximal temperature allowed in the target is set at about 430°C. The lower limit of the LBE flow rate is determined by this value. Because the spallation target material is cooled by the main vessel coolant, the lowest achievable temperature during normal operation of 330°C is mainly determined by the inlet temperature of the core, 300°C.

### 5.2.5 Pumping options

The free surface level is particularly difficult to maintain under the dynamic changes caused by beam trips and during the start-up / shut-down procedures. In order to cope with these dynamics, an extra free surface is created just below the target zone. This extra free surface will act as buffer and stabilizes the target

*This document refers to work being performed by scientists and institutions involved in IP EUROTRANS, as well as the financial support of the European Commission through the contract FI6W-CT-2004-516520.*

shape. The main pump lifts the LBE that has passed the heat exchanger to the level of the second free surface. From here, the LBE flows through the feeder-line to the target nozzle by gravity.

The vertical flow in the feeder line just above the target is equipped with a drag enhancing structure, exceeding the minimum drag of 1 bar/m necessary to compensate for the hydrostatic pressure, to prevent the LBE to tear apart in the feeder line and reaching the target zone in free fall.

Several options still exist on the pumping strategy of the spallation loop [5.7]. One choice consists in implementing one pump in the return line and one smaller pump in the feeder line. The feeder pump is only required to compensate for changes in friction losses in the feeder line. If these changes in friction losses prove to be acceptable or if they can be compensated in another way it may be possible to completely remove the feeder pump from the design. This will decrease the complexity of the system thus making the system not only cheaper and easier to produce but also more reliable.

Due to lack of experimental validation, in particular for the pressure loss, it was proposed to go for the conservative option of having two pumps in the spallation loop: one big main pump in the return line; one small pump in the feeder line will be used to limit erosion/corrosion effects.

### 5.2.6 Vacuum system

The vacuum system has two essential functions. The pressure directly above the spallation target should be below the $10^{-3}$ – $10^{-4}$ mbar range to guarantee compatibility with the vacuum of the proton beam line and to avoid plasma formation caused by the interaction between the static gas above the target and the proton beam. For the confinement of volatile radioactive spallation products the vacuum system is equipped with a closed back end composed of sorption and getter pumps from where they can be batch-wise removed.

The large second free LBE surface in the servicing vessel, directly underneath the main vacuum pumps, minimises emanation of spallation products into the proton beam line.

### 5.2.7 Design support studies

### 5.2.8 MHD pump definition

A sizing of a 13 l/s – 4 bar EMP, for the return line, has been done by R. Stieglitz in [5.8]. Within this report the general electro-magnetic pump design requirements are de-scribed as well as the principle design of the MHD pump acting as a long term regulator in the return line. Based on design requirements the pump is designed, the nominal operating point of the pump is calculated together with the efficiency and other electro-magnetic parameters relevant for the following power balance of the pump.This pump could be designed and technically realized as cylindrical electromagnetic pump with overall dimensions of 0.6m in diameter and 2m long (see Figure 5.5).

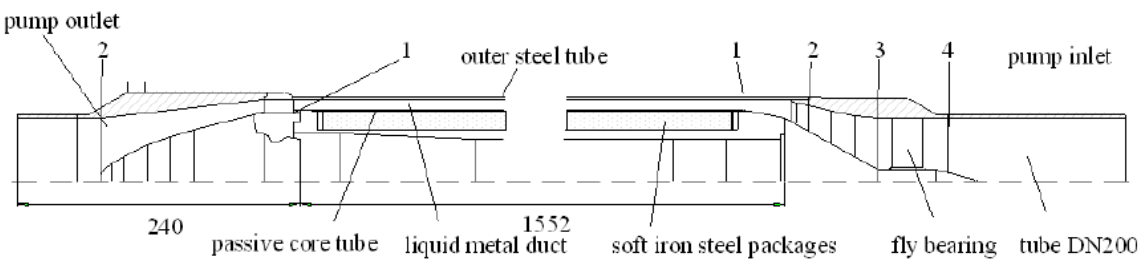


Figure 5.5: Design sketch of the biggest MHD pump in the spallation target loop.

A 4 bar EMP is able to deliver the maximally needed pressure head in a one pump scenario in transient conditions. In case of a two-pump scenario, this maximal pressure head can be distributed in a nominal pressure head of 2.5 bar for the return pump and a transient head of 1.5 bar for the feeder pump. In this case, we estimate that the return pump may be designed and technically realized in overall dimensions ø

*This document refers to work being performed by scientists and institutions involved in IP EUROTRANS, as well as the financial support of the European Commission through the contract FI6W-CT-2004-516520.*

0.4 x 1m. It can be noticed that the feeding pump is smaller due to the fact that the driving pressure is even lower.

### 5.2.9 Target nozzle

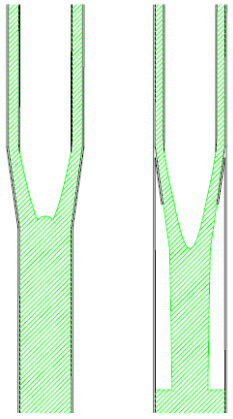

Figure 5.6: Two different nozzle principles left: without flow detachment; right: with flow detachment.

Water flow mock-up experiments performed at the Université Catholique de Louvain (UCL) have shown that a more stable flow is achieved if some detachment of the LBE flow is allowed. Further experiments with LBE at the KALLA laboratory of the Forschungszentrum Karsruhe (FzK) are planned to confirm the observations made in the water loop.

The feasibility of a target nozzle that explicitly forces flow detachment is studied. Two principally different nozzle layouts are studied (Figure 5.6). They are different by the fact that in the left nozzle the LBE flow is designed to be in contact with the walls at all times, while the right nozzle is designed to have the LBE flow separate from the walls and to form a free falling jet.

Due to its inherent stability the nozzle with flow detachment is chosen to be the reference design for further target development [5.5].

At this stage, the current hydraulic design of the target area of the XT-ADS spallation loop is shown in the Figure 5.7-a below.

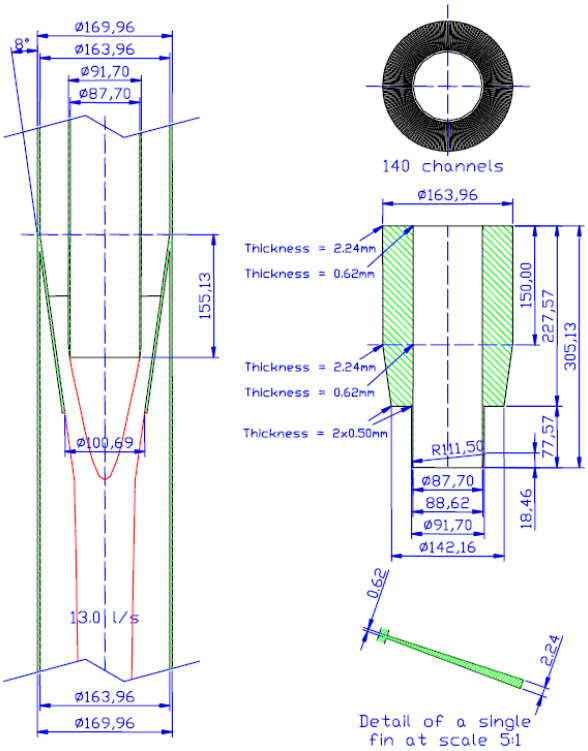


Figure 5.7-a: XT-ADS nozzle design called v0.10LBE.

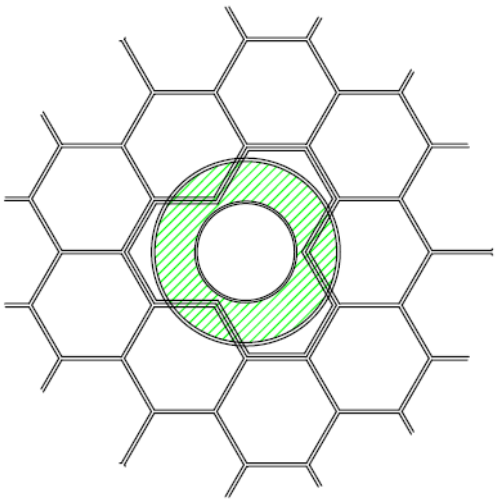

Figure 5.7-b: from a 3-feeder configuration towards an axi-symmetric design for optimisation of target formation process.

*This document refers to work being performed by scientists and institutions involved in IP EUROTRANS, as well as the financial support of the European Commission through the contract FI6W-CT-2004-516520.*

This layout has been chosen to be the reference design for numerical and experimental investigations. The detailed study of the 3-feeder option (figure 5.7-b) for the LBE downcomer, which has the advantage that optimal use is made of the available space in the ADS core, is not in the scope of the project.

### 5.2.10 Heat deposition

The proton beam footprint is designed so as to sweep around the central recirculation zone of the target, in order to avoid overheating and thus evaporation of this central recirculation zone. Given a certain beam shape and sweep profile Monte Carlo codes like MCNPX can calculate the heat deposition inside the target [5.9].

The linear heat deposition profile indicates that most of the heat is generated at the top of the target zone, see Figure 5.8.

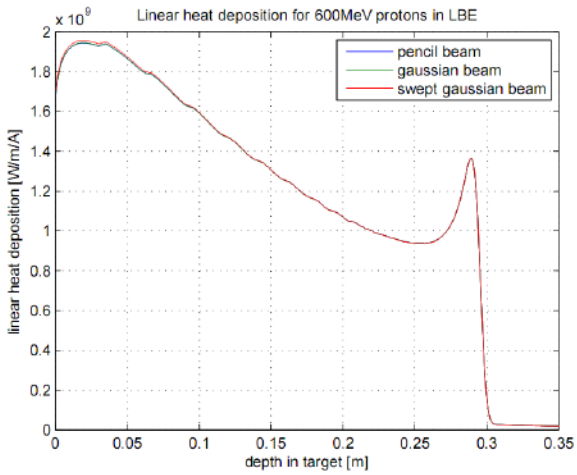


Figure 5.8: Linear heat deposition profile for a 600MeV proton beam.

At 27 cm there is a sudden rise in the linear heat deposition corresponding to the Bragg peak as expected from theory. Integrating the linear heat deposition profile results in the total heat deposition in the target: 4.16 $10^8$ W/A. As such, 69% of the total beam power is converted into heat inside the target. For 3.0 mA beam intensity, the heat deposited corresponds to roughly 125 MW.

Nuclear and neutronic assessment of the target has also been done using MCNPX. The studies mainly focussed on proton and neutron fluxes, spallation vector, evaluation of dpa in structure materials [5.10].

### 5.2.11 Thermal-hydraulics

The current hydraulic design of the spallation target area is the result of a lengthy design process accompanied by a set of full scale experiments. An experimental campaign has started for the improvement and validation of the developed numerical models. Measurement techniques are also developed for thermal-hydraulics experiments and for operational techniques in the XT-ADS. The focus is on local fluid velocity measurement, integral contactless flow meters, and free surface level sensors.

For the spallation target, particular attention has been put on characterization of the free surface flow, flow detachment, study of the 3-feeder option and development of measurement techniques for HLM flows [5.11].

*This document refers to work being performed by scientists and institutions involved in IP EUROTRANS, as well as the financial support of the European Commission through the contract FI6W-CT-2004-516520.*

Since no experiment can demonstrate the ability to transport the deposited heat in a windowless spallation target adequately, validated numerical methods are required. For this purpose, computational fluid dynamics (CFD) simulation methods are the most appropriate. This requires sufficiently accurate free surface modelling, predicting a unique (sharp) interface between LBE and beam vacuum in combination with adequate turbulence modelling. In the European 5th framework project ASCHLIM [5.12], it was demonstrated that sufficiently accurate CFD modelling of such free surface targets was not possible with the state-of-the-art methods available at that time. Within the EUROTRANS project, the development of CFD methods for the simulation of the removal of deposited heat in the LBE windowless target has progressed substantially [5.13].

The cavitations model of the commercial code STAR-CD in conjunction with a high resolution interface capturing technique has been employed to compute the flow in the XT-ADS windowless target and related experiments. The numerical scheme is capable to compute the free surface flow in the target and the experiments and can be used in design optimization and parametric studies. A HLM experiment demonstrating the feasibility of stable flow in the HLM windowless target is currently installed in KALLA [5.14].

#### 5.2.12 Beam target interaction

The purpose of the study performed by NRG is to determine whether the heating from the proton beam results in an expansion wave/pressure wave through the system resulting in LBE splashing after impact of the beam. Splashing could be an issue and is studied numerically. Although results are promising, no firm conclusions can be made at this stage.

#### 5.2.13 Safety analysis

A detailed analysis of the spallation loop behavior during operational and accidental transients using a system code is mandatory. It allows assessing in detail whether the current loop layout can accommodate these transients or whether design measures need to be taken to improve the loop response. The simulations (start-up transient, main pump failure, loss of heat sink …) were performed within the VELLA I Project of the European Commission's 6$^{th}$ Framework Program using a version of the RELAP5/Mod.3.3 code purposely modified to account for LBE properties and behavior. The conclusions of the study could be found in [5.15]. At this stage, even if the correctness of the approach for the exact simulation of the free surface levels still needs further investigation and confirmation, no showstopper were found.

Because of the space limitations, the spallation loop is closed around the sub-critical core. This increases the radio activity of the spallation unit and hence its possibility to replace it in a short period of time. Therefore, the availability of the plant is very much dependant on the possibility to remove the loop from the main vessel and its active components as well as the possibly embrittled in-core parts that would need repair or replacement. The possibility to reduce its unavailability by using a remote handling scheme must hence be considered.

## 5.3 Primary system

#### 5.3.1 Safety constraints

The primary system is designed in order for the plant to be a flexible, highly available experimental facility with a high level fast flux. In order to meet these goals, the total heat power to be extracted by the primary system is set to 70 MWth. The heat to be extracted hence includes:

- core power 57 MWth
- decay heat in storage zone(s)
- heat produced in spallation target
- heat produced by pumps

*This document refers to work being performed by scientists and institutions involved in IP EUROTRANS, as well as the financial support of the European Commission through the contract FI6W-CT-2004-516520.*

- Po heat production

LBE has been chosen as a primary coolant for its low fusion temperature while the boiling water has been chosen as the secondary coolant.

According to the policy described in Chapter 3, the advice was to choose a core inlet LBE temperature of 300°C and average outlet LBE temperature of 400°C. This recommendation is based on irradiation induced embrittlement of cladding and structural materials considerations.

Nevertheless, instead of keeping the primary system temperature constant at 300°C at the core inlet for all power levels, it is preferred from the safety point of view to reduce the primary system temperature for low power levels (down to 200°C), because that results in a more moderate secondary system pressure. It is expected that 200°C might be allowed for the chosen materials (T91 and AISI316) since a reduced temperature (down to 200°C) does not significantly affect the radiation embrittlement of the core support plate and core barrel as was extensively demonstrated in "XT-ADS Primary–System Operating Temperature" [5.16], [5.17]. Therefore, following scheme is advised for the LBE temperature at the inlet of the core:

- for power between 50 MWth and 70 MWth: 300°C.
- for power from 0 to 50 MWth : steadily increasing from 200°C to 300°C.

While LBE temperature at the outlet of the core at full power (70 MWth) is set to 400°C.

The velocity of the primary coolant is kept below 2 m/s in order to limit erosion. One notable exception are the primary pumps where this limit may be overshoot. The material for the pumps under high speed coolant has to be qualified under these condition for a given life time.

The level difference between core mid plane and PHX measures at least 2,000 mm (to ensure natural convection in case of emergency situation).

Normal Decay Heat Removal (DHR) is performed by the application of the PHX with two independent and secured safety grade secondary loops; for ultimate decay heat removal the RVCS is deployed as (two independent loops working in natural circulation – air or water cooled).

The primary system design is compatible with an off-centre spallation loop in all its aspects, i.e.:fuel handling device does not interfere with the spallation loop; sufficient NPSH for the circulation pump is provided; short response time for free surface level control.

The primary system design must include (an) in-vessel fuel storage zone(s); the storage zones is located far enough from the core to avoid neutron coupling between them; the storage zones is cooled to remove the decay heat.

Operation & Maintenance and In Service Inspection & Repair is:

- as simple as possible;
- compatible with remote handling.

Primary pumps, heat exchangers and core support structure are easily replaceable.

The spallation loop is extractable as one part, separated from the core barrel in order to allow for sufficient availability.

The primary system design is such that the instrumentation and IPS (In Pile Section) do not jeopardize the availability of the machine (the room above the core will be occupied with numerous instrumentations for the IPSs and FAs).The primary system has the capability to host irradiation rigs in the core. The primary system has the capability of easy and frequent fuel reshuffling and flexible core access for (un)loading the irradiation rigs.

The vessel is a hanging vessel, supported at the top, with an elliptical bottom. There are some arguments for this decision. Firstly, recent preliminary estimations, based on the rather smooth seismic data for the Mol

*This document refers to work being performed by scientists and institutions involved in IP EUROTRANS, as well as the financial support of the European Commission through the contract FI6W-CT-2004-516520.*

site, indicate that the seismic induced vessel stresses are more favourable than those of a flat bottom. Secondly, a standing vessel causes longitudinal thermal expansion, resulting in the need of large displacement flexible bellows for all PHX's feeding pipe connections. These bellows are not needed for a top-hanging vessel. Thirdly, in case of a standing vessel, the differential thermal expansion induces sliding between the flat bottom and its lattice support, resulting in local wear. Fourthly, an elliptical bottom is accessible for dedicated tools for ultrasonic testing. Fifthly, a flat bottom with stress reliever might cause LBE stagnant zones, while an elliptical bottom avoids sudden change of flow direction. The vessel cover is cooled by air or water to limit the main cover temperature to 100°C.The inter-space between the main vessel and the safety vessel is broad enough to allow inspection of the vessels; 150 mm is considered as a minimum for dedicated inspection tools. The primary pumps (PP) are placed downstream the PHX in the cold pool, at a sufficient low level to avoid cavitations.

### 5.3.2 Description of the primary loop

In the primary loop the pumps draw the LBE from the PHXs bottom window and pass it to the mass of the cold plenum and provide the head required for the LBE to flow through the core. The pump flow does not pass entirely through the core, so that a significant core by-pass flow is present induced by the gap among the fuel assemblies, the dummy assemblies at the periphery of the core, the spallation loop heat exchanger, the in-vessel fuel storage and diaphragm. The preliminary estimate of the core by-pass flow shows that it amounts to 2481 kg/s corresponding to about the 35% of the total flow (7000 kg/s).

When leaving the core, the LBE mixes with the mass of the hot plenum and with the colder by pass flow (the temperature drop from the core exit to the PHX's at steady state, due to thermal exchange between the hot and cold plenum, has temporarily not been taken into account, because predictably of a few degrees).The LBE flows shell-side through the four PHX's and exits into the cold plenum.

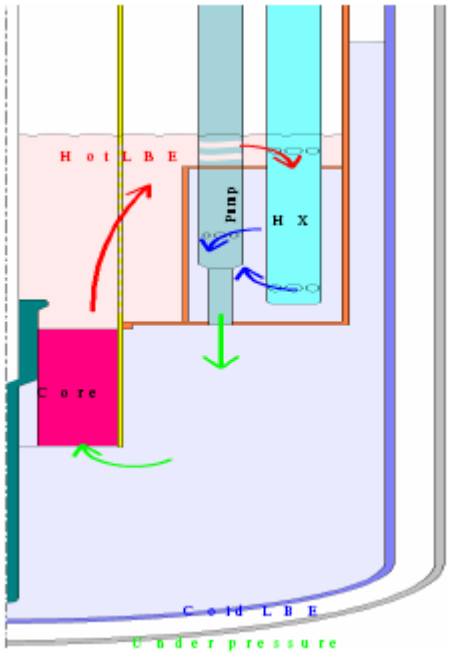


Figure 5.9: Primary system - LBE main flow path

The diaphragm has a flat bottom and is as simple as possible to facilitate the manufacturing of this huge component. The cold pool level is 1,000 mm higher than the hot pool level according to the core pressure drop of ~ 1,000 mbar. Depending on the exact primary flow pressure losses, the cold pool cover gas may

*This document refers to work being performed by scientists and institutions involved in IP EUROTRANS, as well as the financial support of the European Commission through the contract FI6W-CT-2004-516520.*

have to be slightly pressurized. The cold pool free level is at least 500 mm underneath the vessel top to limit the vessel cover temperature to 200°C. Appropriate steam detection systems must be installed on strategic locations in the reactor vessel.

In case of emergency, all cooling systems are able to operate in natural convection (primary LBE, secondary boiling water, tertiary air).

### 5.3.3 Heat exchangers

The PHXs are of the counter-flow, straight tubes type (Figure 5.10). Helicoidal tubes are considered as well, but sizing calculations demonstrated that this type of heat exchanger exhibits an unfavourable shape, i.e. very big diameter (but reduced height) which would imply a large reactor vessel diameter.

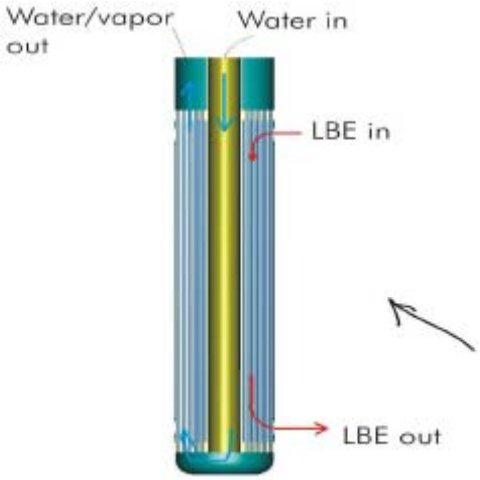


Figure 5.10: PHX lay-out

The water flows upwards inside the tubes while the LBE flows downwards outside tubes and inside the shroud. This configuration balances the pressure drops of both the water and the LBE flow. The opposite configuration would effect in excessive LBE pressure drop so that the primary pumps would have to be immersed in the LBE pool more deeply to guarantee sufficient Net Positive Suction Head (NPSH); doing so would unnecessary increase the reactor vessel height.

Boiling water flow inside parallel tubes might evoke instable flow. Therefore it must be demonstrated that the PHXs' design is such that the water/vapour flow inside the tubes is stable in all operating conditions.

The nominal power per PHX is 17.5 MWth.

LBE temperature at the outlet of the PHXs:

- for power between 50 MWth and 70 MWth: 300°C.
- for powers from 0 to 50 MWth : steadily increasing from 200°C to 300°C.

The total LBE mass flow through the PHXs is the sum of core LBE flow, the flow through the in-vessel fuel storage zones, the cooling LBE flow for the spallation target and all by-pass flows.

T91 is being used for its better thermal properties (lower thermal expansion and higher conductivity – both reduce thermal stresses as well).

*This document refers to work being performed by scientists and institutions involved in IP EUROTRANS, as well as the financial support of the European Commission through the contract FI6W-CT-2004-516520.*

### 5.3.4 Primary pumps

The pumps are vertical units, of a design very similar to the one used in fast reactors, i.e. with an impeller at the bottom end of a long shaft. The electric motor is located on the reactor cover, out of the neutron flux, at the upper end of the shaft.

The primary pumps are centrifugal pumps. For the actual rather high LBE flow together with a relatively low pressure drop over the system (core, PHXs and pool), the specific speed of the centrifugal PP is typical for an axial flow pump (>> 1).

For the required pump head (slightly more than ~ 1 bar) the maximum LBE velocity at the impeller blade will be more than the earlier mentioned maximum allowed velocity of 2 m/s. This peculiarity requires an appropriate material or surface coating to ensure an acceptable life time of ~ 3 years that can withstand LBE velocities up to ~ 10 m/s.

The primary pumps (PPs) are placed at a sufficient low level in the pool to avoid cavitation.

The pressure loss through a blocked pump propeller is rather low to favour natural convection in case of loss of flow.

### 5.3.5 Primary system auxiliaries

*Gas plenum treatment*

Gas must be circulating in the gas plenum. Its main functions are to prevent the accumulation of radioactive species in the plenum during the operation and to prevent air ingress and consequently coolant contamination.

Out of the vessel, the gas is filtered, cooled and treated in a purification unit, comprising getters, charcoals and cold traps. The gas treatment eliminates dust and chemically active species. Thereby, it minimises the amount of polonium able to escape during maintenance operations.

The gas is normally an inert one such as argon or helium. It must be possible to add a hydrogen/steam mixture, or to switch to pure hydrogen flushing gas. In this case, the gas might be circulated via sprayers at lower plenum of the vessel for PbO sludges reduction.

It is possible to pick gas anywhere in the loop and sent to an analysis station, where the presence of oxygen, moisture (from the failure of a heat exchanger tube) of fission products (from the failure of fuel pins) can be detected. Additional filters are foreseen upstream to avoid the contamination of the sensors – mainly the radiation sensors – by dust that could saturate the detector.

A plenum pressure control is foreseen to deliver to the gas plenum the amount of gas necessary to cope with an expansion of the primary cover gas plenum, due to a cool down transient, thus restoring the normal cover gas pressure.

The vessel must be protected against overpressure in the gas plenum by safety valves and discharge tank(s). The dimensioning event of those valves is the rupture of a tube of a PHX coupled with the failure-to-close of the isolation valves of the heat exchanger.

*In-vessel coolant chemistry control*

Even if the coolant is conditioned out of the reactor before the first filling, impurities and contamination will degrade its quality during operation, and mainly during the outages, when the vessel has to be openned to the outside, for the maintenance of its components. Therefore, an in-vessel conditioning system with spray tubes and electrical heaters must be foreseen.

The purification process operates with a satisfactory kinetics only above 350°C to 400°C. Therefore, heaters must be foreseen in the LBE pool and at a level as low as possible to heat the bulk up to the required temperature, at which gas (H2 or steam) is injected.

*This document refers to work being performed by scientists and institutions involved in IP EUROTRANS, as well as the financial support of the European Commission through the contract FI6W-CT-2004-516520.*

The in-vessel conditioning system will only operate during time-outs. There still is a need to continuously maintain, ensure and monitor the oxygen activity.

*Off-line coolant treatment*

This processing unit is required to continuously control the quality of the coolant and in particular the oxygen concentration.

A pump takes fluid out of the reactor and sends it to the processing unit. Before processing, low melting point impurities are separated. After processing, the fluid is re-injected in the vessel. The purification of a given quantity is completed when the quantity is passed several times in the purification system. At a rate of 30 to 40 tons/hour (i.e. 3 to 4 m³/h) it takes ~ 30 hours to circulate once the ~ 1000 tons of LBE contained in the vessel. Hence, for e.g. 5 to 10 passes, it takes between 6 and 12 days to achieve the re-conditioning and purification after opening and contamination.

Besides being used for initial conditioning of the coolant and for in-service purification, the system is used for the control of the level in the main vessel:

- the level is kept constant in spite of temperature changes in the primary loop;
- the level is raised or lowered when found convenient for the handling (compensation of the buoyancy);
- the system stores sufficient liquid to compensate for the vessel inter-space flooding after a leak.

This system is used for first filling as well. The LBE is supplied in the form of solid blocks. From manufacturing, those blocks are covered by an oxide layer that has to be removed. The blocks could possibly contain solid impurities that have to be removed as well. The treatment process is as follows:

- melting of the blocks;
- solid contaminants filtration (several filters in series, with different mesh sizes to be defined and 2 or 3 series of filters in parallel to allow filters in service replacement);
- heat-up to 300 – 400°C;
- exposition to vacuum to release volatile contaminants like gases;
- hot treatment 1: by bubbling of hydrogen and/or steam, oxides are reduced following the reaction PbO + H2 –> Pb + H2O;
- hot treatment 2: the stream is passed on a PbO pebbles bed;
- cooling down;
- control of quality and composition;
- storage;
- heat to vessel and injection in the main vessel;
- before filling, the vessel has to be assembled, tested, thoroughly cleaned from any impurities and oxygen has to be removed. During the filling of the vessel, and before the primary pumps are put into service, the vessel is heated by the electrical heaters above.

Finally, one has to consider the case that the coolant is contaminated despite all preventive measures. In this case, the coolant has to be re-conditioned when the vessel is re-closed, before putting it back into service.

## 5.4 Secondary system

The water/vapour secondary system has the function to remove the heat from the primary coolant. It is not a requisite that the secondary system would serve for generating electricity.

*This document refers to work being performed by scientists and institutions involved in IP EUROTRANS, as well as the financial support of the European Commission through the contract FI6W-CT-2004-516520.*

Each of the two secondary circuits is made of two PHXs serving as the evaporators, a steam separator of the water/steam mixture rising from the PHXs, a steam condenser, interconnecting piping, and a stack chimney (Figure 5.11).

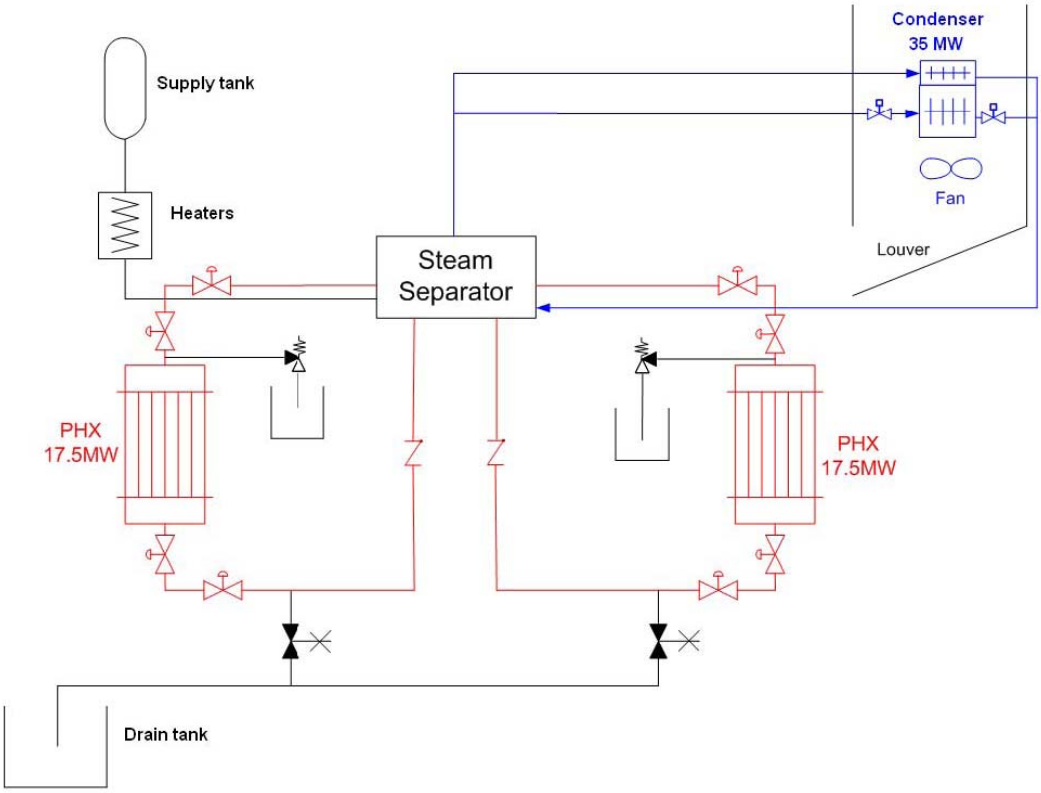


Figure 5.11: XT-ADS secondary circuit

In each circuit saturated water enters tube-side the two PHXs, operating in parallel, and leaves as a steam-water mixture. Ferruling is provided at tube inlet in order to stabilize the flow.

Steam rising from the Separator is condensed into the Air Condenser (AC) from which the condensate falls into the separator where it adds to the water plenum and feeds the PHXs, thereby closing the water circuit.

The water flows in natural circulation in the loop owing to the hydrostatic head provided by the density difference between saturated water in the inlet pipe and the steam/water mixture in the outlet pipe. The recirculation ratio is enough to prevent Direct Nuclear Boiling (DNB) and, hence, the thermal crisis. The recirculation ratio is defined as the mass flow rate of liquid water leaving the PHX compared with the mass flow rate of steam alone.

The driving force for the natural circulation is provided by the hydrostatic head difference between the hot leg and the cold leg of the circuit, achieved by arranging the separator at a sufficient elevation with respect to the PHXs. The AC performance is air-side controlled by air intake louvers and fans that provide for forced circulation and flow-rate control at the air inlet to the condenser.

The Air Condenser can be partially isolated in order not to overcool the condensate after a reactor trip.

*This document refers to work being performed by scientists and institutions involved in IP EUROTRANS, as well as the financial support of the European Commission through the contract FI6W-CT-2004-516520.*

## 5.5 Decay heat removal system

Two systems are provided for the Decay Heat Removal (DHR) function to increase diversity and redundancy, i.e.

- for normal DHR system after a reactor shutdown: the Secondary Cooling System (SCS) using the primary LBE/water&vapour heat exchangers and two independent and secured loops;
- in case of unavailability of the SCS: the safety-grade Reactor Vault Cooling System (RVCS) is called upon. The RVCS is placed between the guard vessel and the concrete pit. The system also keeps the concrete at acceptable temperature including accidental events.

This organization is retained for the XT-ADS first remontage. The PHXs are located 2m above core mid-plane for enhancing the natural circulation. Also for this reason (enhancing natural convection), the core hydraulic resistance has been kept relatively low (≤ 1 bar pressure drop in normal operation conditions).

The performances of the SCS for decay heat removal (pressure losses on primary side, need for check valves, and description of operating conditions at secondary side with boiling water) and the RVCS have been assessed and their performances verified in the frame of safety studies (cf Chapter 6.3).

## 5.6 Reactor vessels, cover and diaphragm

Both the reactor and the safety vessels are hung vessels with elliptical bottom heads. This choice is different from the MHYRRA Draft II option, where flat bottom ends are present.

An elliptical vessel bottom head has been chosen even though flat bottom heads present the benefits hereinafter reported.

1. Minimization of the LBE inventory, compared to hemispherical bottom heads;
2. easier installation of filler blocks, in order to reduce the ‘inactive’ LBE volume on the vessel bottom;
3. easier design against the high seismic loads, owing to the high mass of the coolant.

The choice has been oriented on the elliptical bottom ends for the reasons reported below:

1. a vessel with elliptical bottom would withstand the internal pressure better than the vessel with flat bottom;
2. a vessel supported on a skirt or lugs would expand upwards, resulting in the need of bellows to accommodate large displacements of the PHX's pipe connections. These bellows are not needed for a hung vessel;
3. radial expansions of the bottom-supported vessel should be absorbed by sliding of the support over plates, but this would be hardly exploitable because of the heavy load of the vessel;
4. a flat bottom head with stress reliever (local rounding in the corner) might cause LBE stagnant zones, while an elliptical bottom avoids sudden change of flow direction.
5. in case of the hung vessel, the elliptical bottom head is accessible for dedicated tools for ultrasonic testing like the free rolling vehicle of Superphenix and EFR.

Moreover the difficulties in the design of hung vessels against seismic loads are round over by the smooth seismic data for the Mol site. Preliminary estimates indicate that the seismic-induced vessel stresses are smaller than the peak stresses at the junction of the vessel wall with its bottom head in case of a flat bottom vessel.

The sketch of vessels, support system and cover is shown in Figure 5.1.

*This document refers to work being performed by scientists and institutions involved in IP EUROTRANS, as well as the financial support of the European Commission through the contract FI6W-CT-2004-516520.*

## 5.7 Core support structure

The core support assembly consists of mainly of four parts:

- the core support plate, that provides room for the fuel (or dummy) assemblies and to the In-Pile Sections (IPS) for experiments; the fuel assemblies are inserted from beneath in the holes of the support plate, and stay there by the buoyancy force even in the absence of hydrodynamic friction which is also directed upwards;
- the cylindrical core barrel, that surrounds the core and whose function is to prevent the fuel assemblies to move away from each other;
- the suspension tube, on which the core support plate and the core barrel are attached, is suspended to the reactor cover
- and the core plug that closes the suspension tube at its end and that is part of the reactor cover

The upper zone is a continuous annular ring that supports the primary vessel, the vessel cover and all the components inside the vessel. The vessel is joined to the ring by a bolted connection. The lover plate of ring is connected to an intermediate plate by 12 vertical gussets. The void space between the gussets allows the introduction of tools in the gap between the reactor vessel and the safety vessel for welds ISI during maintenance operations. The safety vessel is bolted on the intermediate plate. A second order of gussets bellow the intermediate plate connects the intermediate plate with the bottom plate that is anchored on the reactor pit edges.

The windows between the gussets are used as passage for the RVACS tubes that are vertically distributed along the walls of reactor pit.

## 5.8 In-vessel fuel storage

Spent fuel still generates decay heat and must remain in the coolant for some time after the reactor is shut down. To avoid excessive delays between two operation cycles, it was chosen to store the spent fuel at the periphery of the reactor, in a dedicated zone and let it cool there. Because of the double fuel handling system chosen, there are two such zones, at the opposite of each other, at the periphery inside the vessel.

To detect failed fuel assemblies without being obliged to take all of them out of the reactor, both storage zones are fitted with a penetration allowing the loading of a wet sipping machine. The machine is a long tube that can be opened at its lower end. A suspect fuel assembly is inserted in the machine where it is isolated from the primary coolant. The release of activity in the closed machine is the indication that at least one of the fuel pins is failed. The assembly has then to be unloaded.

The fuel storage area provides sufficient storage positions to store two core halves. The fuel assemblies are inserted in the holes of the racks and remain there until their residual heat has sufficiently decayed.

Each rack has 102 positions for the fuel assemblies storage. The same positions are also used as intermediate temporary location for new fuel assemblies during the refuelling phase.

The distance between the assembly shrouds should be sufficient to eliminate any risk of criticality. As preliminary pitch value between the fuel assemblies in the storage zone has been assumed 103 mm instead of 96.2 mm as in the core. The residual neutron flux in the storage positions was found small enough (around one thousandth of flux in the core) to make additional shielding unnecessary and still allow the decay. On the other hand, the storage zone, close to the reactor vessel, increases locally the neutron dose on the vessel, which requires some shielding.

It must be verified that there is almost no neutronic coupling between the core and the spent fuel storage zones, and therefore no modification of the Keff of the sub-critical core.

The design of the zone is such that all storage positions are within the reach of the handling system. The fuel is loaded, from underneath, in the different positions of the in-vessel fuel storage, where it stays by its

*This document refers to work being performed by scientists and institutions involved in IP EUROTRANS, as well as the financial support of the European Commission through the contract FI6W-CT-2004-516520.*

buoyancy. Per storage zone, there is one position where the fuel assemblies can be handed over to the ex-vessel fuel transfer machine.

The LBE flow in the storage zones is sized in order to let the adequate cooling flow through the assemblies, also keeping the primary pumping requirements reasonably small.

The coolant circulates through holes on the inner vessel. The cooling requirements for the storage zone and, therefore, the exact size of the different holes have to be defined.

## 5.9 In-vessel fuel handling machines

In fast reactors, the fuel is loaded and unloaded by a machine mounted on a system made of two eccentric plugs. In the XT-ADS however, the presence of the proton beam, coming from above into the reactor centre, and with the particular geometry of the spallation loop, this option is precluded. The concept of the in-vessel fuel-handling machine has to integrate several very particular requirements:

- A double machine system is required since the spallation loop, which is eccentrically placed from the core, makes a fuel assembly difficult to reach for a single handling machine installed at the opposite side of the reactor. Each fuel-handling machine will be installed at the periphery of the core.
- As already mentioned, the fuel is manipulated from underneath the core. Among several other reasons, one reason for this decision is the following.

Since the XT-ADS is a research reactor, dedicated irradiation positions are foreseen in the core. These irradiation positions could be occupied with IPSs, inserted in the core from above through penetrations in the reactor cover. These IPSs might stay several cycles in the reactor, also during core reloading. Fuel handling performed from underneath avoids the difficult and extensive handling of the IPSs if fuel handling would be performed from above the core. Another reason is the following: the LBE circulating in the spallation loop has to be cooled down and pumped back upwards. The pump impeller must be installed at sufficient depth under the free surface level, in order to avoid cavitation. It is also desirable that the fluid of the spallation loop is cooled before entering the pump, in order to avoid the enhanced corrosion problems caused by hot LBE. So, extra depth would anyway be required for the proper operation of the spallation loop, and not only for the fuel handling from underneath.

The IVFHM systems are rotating plugs with an offset arm that penetrate the reactor through the cover in two diametrically opposite sides. The arm can rotate in the rotating plug, and so has access to half of the core. The arm can move up and down by about 2.5 metre, to extract – downwards -the assemblies from the core. The extremity of the arm has a wrist, which gives the adequate orientation to the fuel assembly before its insertion into the core.

Diameters of rotating plugs and arm lengths together with IVFHM axis position must be able to reach all assemblies positions in the core and in the in vessel fuel storage zones. To satisfy this requirement with the minimum dimensions of IVFHM systems the storage zones are located near the refuelling equipments and their shape follows the limit circle of arm. To minimize the possibility of a failure a simpler rigid arm configuration has been preferred with respect to a more compact pantograph configuration of IVFHM. All electrical parts are put over the LBE level to avoid the problems connected to the use of electrical components in zones at elevated temperature.

To assure the refuelling the fuel handling system must have the movements listed below:

1. rotation around the rotating plug axis;
2. rotation around the vertical arm axis;
3. axial movement along the vertical arm axis;
4. rotation of gripper around its axis;
5. open/close gripper movement.

*This document refers to work being performed by scientists and institutions involved in IP EUROTRANS, as well as the financial support of the European Commission through the contract FI6W-CT-2004-516520.*

The IVFHM must be equipped with an ultrasonic camera and a tool to block the adjacent fuel assemblies when the assembly to be removed is gripped by the others.

The insertion in the vessel of new fuel assemblies and the extraction from the vessel of exhausted fuel assemblies is produced though a penetration located near the IVFHM rotating plug. A tube goes from the penetration to the bottom as guide for the elements.

The element to be inserted or removed are taken from or deposed on the IVFHM gripper by a tools put on the Flask used for the refuelling operations.

The XT-ADS devices envisaged are designed to ensure their suitability for remote maintenance and modification. Oxford Technologies Ltd has been defining, designing and implementing a remote handling design catalogue aimed at providing Eurotrans machine designers with information, advice and resource data in an easy to use form to ensure that their designs are fully remote handling compatible [5.26].

The resulting catalogue is a web based PC application (MENTOR™) comprising two parts – a creator and a browser or viewer. The browser part will be made freely downloadable to all registered users and with which the user can view the entire Eurotrans remote handling catalogue.

The content has been created and compiled by experienced remote handling engineers and is stored in a variety of formats including, MS Word documents, Adobe pdf documents, ProE 3D CAD files, MS Excel files, 2D image files and movie files.

Of particular note is the facility for Eurotrans design staff to identify suitable remote handling compatible standard components defined in the catalogue and then to “drag-and-drop” the component 3D model directly from the catalogue into a CAD system open on the same PC.

## 5.10 Core Design

### 5.10.1 Presentation of the core design

The fuel pin, fuel assembly and core configuration are described in [5.20]. A brief synthesis is reported here.The fuel pin (Figure 5.12) consists of a fuel pellet column of 60 cm with on both ends a neutron reflector to increase the neutron economy, a fission gas plenum and a closing cap.

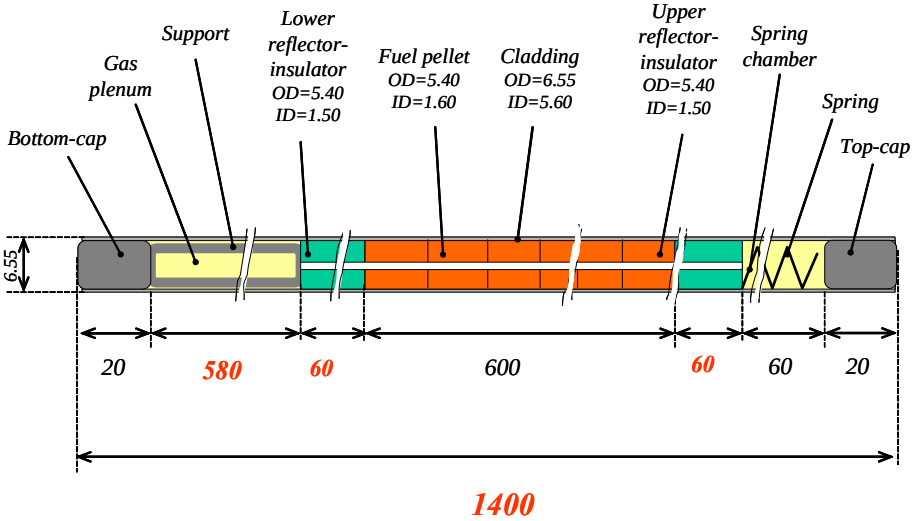


Figure 5-12: XT-ADS fuel pin [5.20]

*This document refers to work being performed by scientists and institutions involved in IP EUROTRANS, as well as the financial support of the European Commission through the contract FI6W-CT-2004-516520.*

The fuel pellets are of the hollow type (hole diameter = 1.6 mm). This reduces the centreline temperature and hence gives larger margins to fuel melting limits. The fuel assembly contains 90 of these fuel pins (diameter = 6.55 mm) in a hexagonal lattice together with one “instrumentation pin” in the centre of the assembly. The fuel pins pitch is 9.23 mm.

Mechanical calculations did show that a wall thickness of 2 mm was sufficient for the wrapper. The clearance between the assemblies was fixed to 3 mm. The final result (Figure 5.13) is an assembly of 93.2 mm (flat-to-flat) width and 96.2 mm pitch (center-to-center).

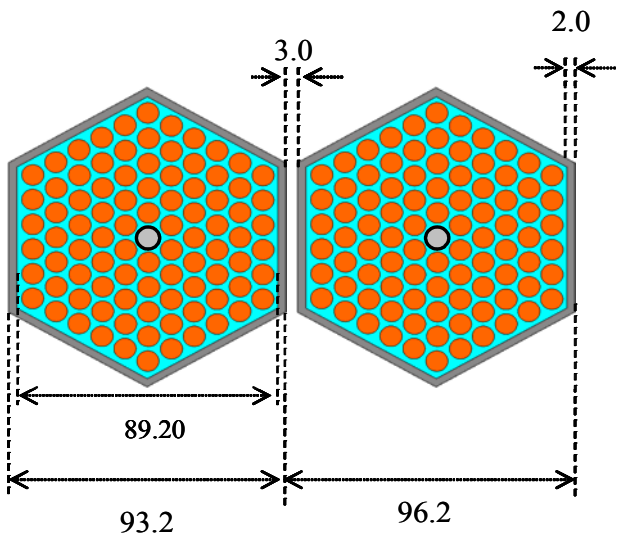


Figure 5-13: XT-ADS fuel assembly lay-out [5.20]

The core layout (Figure 5.14) for the fresh core was fixed to 68 fuel assemblies encircling a “gap” of three emptied positions to allow for the placement of the spallation target module.

In order for the XT-ADS to fulfill its mission of a flexible irradiation facility, eight positions were chosen to house irradiation devices, the so-called In-Pile-Positions. The fuel assemblies at these positions were relocated in such a way that the IPSs were all fully surrounded by fuel assemblies.

During the operation of the machine, there will be a kind of equilibrium situation relative to a chosen operational cycle. This equilibrium core needs 75 fuel assemblies to have a $K_{eff}$ around 0.95 during an operational cycle. The core power is fixed to 57 $MW_{th}$.

An estimation of the damage induced by neutron irradiation on core components, like the core barrel has led to fill up the last ring of hexagonal positions with a kind of mock-up assemblies in which fuel pins are replaced by steel pins in order to shield the core barrel. The dummy assemblies in between the active core and these steel assemblies are made up of a hexcan filled with lead-bismuth eutectic.

The core layout for 68 assemblies and 75 assemblies are shown in Figure 5-14 and Figure 5-15.

*This document refers to work being performed by scientists and institutions involved in IP EUROTRANS, as well as the financial support of the European Commission through the contract FI6W-CT-2004-516520.*

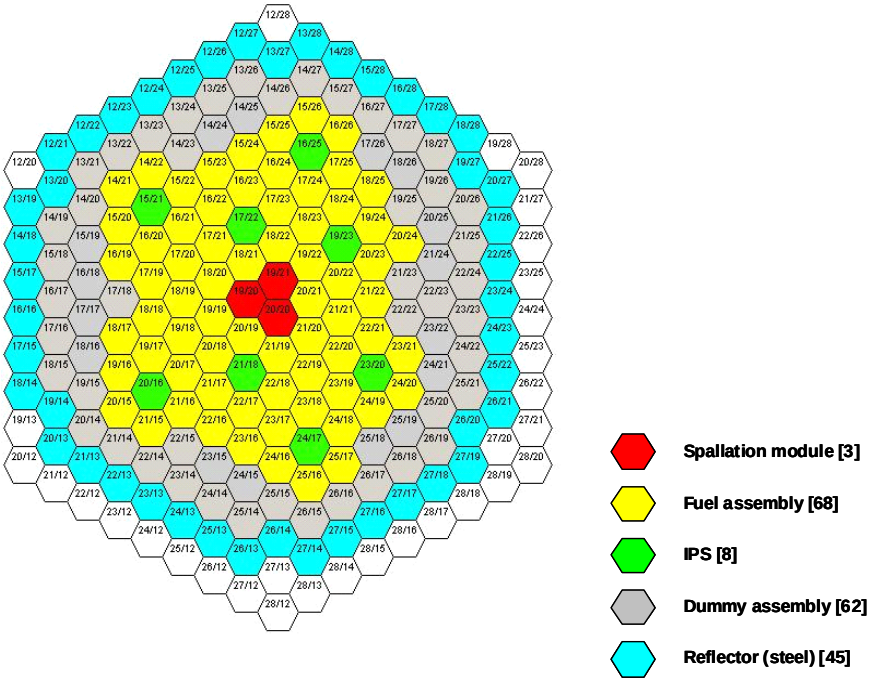


Figure 5-14: Fresh core lay-out (68 fuel assemblies)

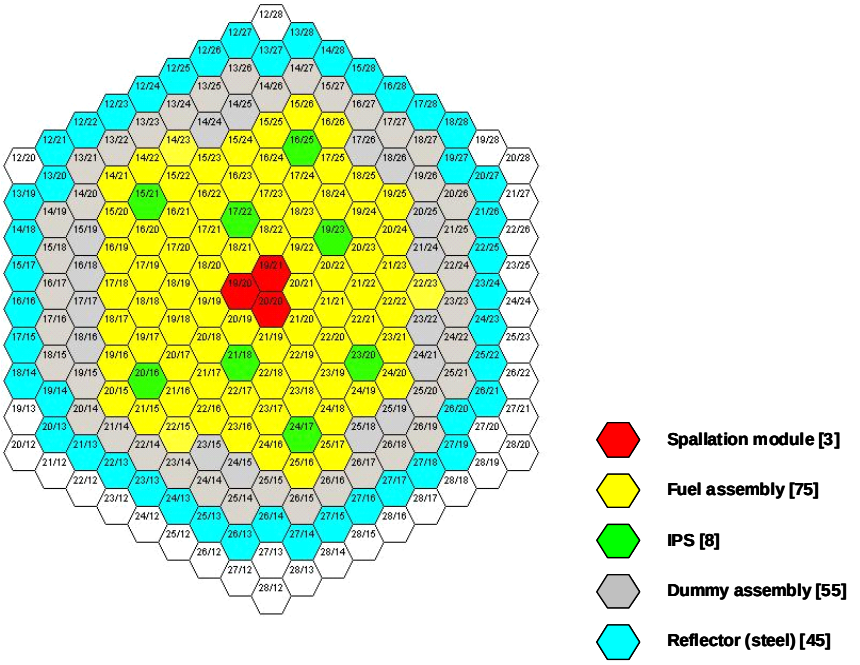


Figure 5-15: Equilibrium core lay-out (75 fuel assemblies)

Three IPS are close to the target in a high neutron flux environment and the remaining five IPS are close to the core periphery in a lower neutron flux environment.

*This document refers to work being performed by scientists and institutions involved in IP EUROTRANS, as well as the financial support of the European Commission through the contract FI6W-CT-2004-516520.*

### 5.10.2 Criticality and source calculations

The results were obtained by two codes [5.10]: ERANOS 2.1 using the JEFF3.1 neutron based library and MCNPX 2.5.0 also using the JEFF3.1 libraries [5.18]. It should be noted that ERANOS calculations are performed with a reference scheme i.e. a full 2D description of the subassemblies and a 3D description of the core in transport theory (nodal method). For the same modeling, results of ERANOS 2.1 and MCNPX 2.5.0 are very consistent.

Table 5-1 gives the multiplication factors results ($K_{eff}$) obtained for the various studied configurations. For the MCNPX calculations run at SCK•CEN [5.19], the geometry of the studied system is at cold state (densities and nuclear temperatures are at correct values, but the dimensions of the clad, S/A and core are at cold dimensions). This is, of course, not the real situation, but it allowed us to easily compare different results, independent of temperature profiles. The results from ERANOS indicated that at operational conditions, the core exhibits $K_{eff}$ a bit below the target of 0.95 at BOC. This could be possibly compensated by adding an extra S/A.

Table 5-1: Multiplication factors for various configurations

| | | Operating conditions ($T_{op}$) | Hot zero power (200°C) | Cold state (20°C) |
|---|---|---|---|---|
| CL-P0 "fresh core" (68 S/A) BOL | not linked | 0.9379 | 0.9477 | 0.9553 |
| | linked | 0.9391 | 0.9476 | 0.9553 |
| CL-P0 "equilibrium core" (75 S/A) linked | BOC | 0.9408 | 0.9489 | 0.9562 |
| | EOC | 0.9288 | 0.9367 | 0.9438 |

A series of reactivity effects has been investigated: those in normal operation (going from cold to hot conditions and vice versa) and those in incidental situations (target voiding, sub assembly voiding, core compaction).

Calculations with ERANOS have been done [5.18] on both the fresh core (68 sub assemblies) and the equilibrium core (72 sub assemblies). For going from the operational condition to the hot zero power state (200°C), Table 5.3 gives an overview of all contributions. It also gives the reactivity insertion for a hypothetical cold state of 20°C.

For what concerns accidental conditions, core compaction, target voiding and (partial) core voiding are studied. The core compaction reactivity effect is equal to 1862 pcm in those conditions. As LBE is considered as a shock absorber, this value is certainly overestimated but can be considered as envelope for reactivity insertion.

Safety limits from ERANOS calculations are given in Table 5-3. Feedback coefficients were calculated for the sake of the safety calculations although the plant, given its sub-criticality is not so sensitive to them.

*This document refers to work being performed by scientists and institutions involved in IP EUROTRANS, as well as the financial support of the European Commission through the contract FI6W-CT-2004-516520.*

Table 5-3: ERANOS reactivity balance

| | $\Delta\rho$ (pcm) | $k_{eff}$ |
|---|---|---|
| Safety limit | - | 0,99 |
| Core compaction | 1862 | 0.9721 |
| Max void effect | 439 | 0.9680 |
| Cold state limit (20°C) | - | 0.9680 |
| Hot zero power limit (200°C) | 841 | 0.9601 |
| Coolant expansion | 355 | 0.9569 |
| Fuel expansion | 181 | 0.9552 |
| Doppler (fuel) | 318 | 0.9523 |
| Doppler (structures) | 15 | 0.9522 |
| Axial expansion | 42 | 0.9518 |
| Radial expansion (diagrid) | 129 | 0.9506 |
| Nominal state limit | - | 0.9506 |

These values illustrate the safe margins this plant has concerning reactivity insertion accidents.

The optimal axial position of the spallation target free surface was investigated looking at the source efficiency and the linear power profile. One can conclude that the spallation target free surface should be at z=+5 to z=+15 cm in order to keep the source effectiveness constant and to avoid a too asymmetrical profile of the linear power.

In a first approach, a single burn-up calculation was done for a large number of operation days (450 or more) starting from a fresh core loading in the 75 S/A configuration. Of course, during the first days, this core loading is hypothetical (it starts from a $K_{eff}$ value which is much too high) but it gives us an idea of the reactivity drop per power day. It lead to an approach of a 5-step cycle: 75 S/As, after each operational cycle of 90 days, 15 S/As of fresh fuel are added, 15 old S/As are removed and the core is shuffled.

The reference approach is a 5-step shuffle out-to-in for a core loading of 75 fuel assemblies. The ERANOS results for the 5-step shuffle for $K_{eff}$ and $K_S$ are given in Figure 5.16. The same analysis has been done by FZK(KIT) using KAPROS [5.22] and SCK•CEN using MCNPX and ALEPH [5.23]. They differ only by hypothesis on the thermal expansion of the core. The average drop of reactivity for the reshuffling scheme accounts to a similar value of around 1220 pcm.

*This document refers to work being performed by scientists and institutions involved in IP EUROTRANS, as well as the financial support of the European Commission through the contract FI6W-CT-2004-516520.*

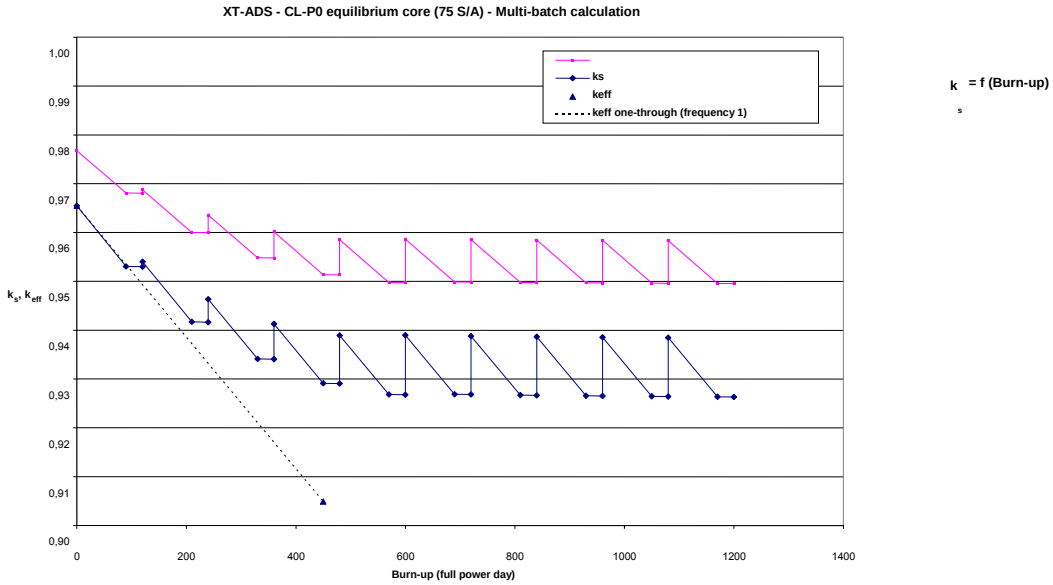


Figure 5-16: 5-step shuffle $K_{eff}$ and $K_s$ evolution

2D power maps (form factors) have been calculated at BOL. The maximum value for axial form factor is located in the sub-assembly 20/21 (closest S/A from the spallation target) and accounts for 1.21 (EOC) and the maximum value for radial form factor is 1.42 (BOL) while it is only of 1.3 at EOC.

### 5.10.3 Irradiation capabilities

The core exhibits 8 positions for IPS loadings. A number of calculations have been done to analyze the irradiation capabilities for structural materials and fuel pins in these different positions [5.24]. In Figure 5-17 below, one finds the core layout with the nomenclature used in this section for the different channels.

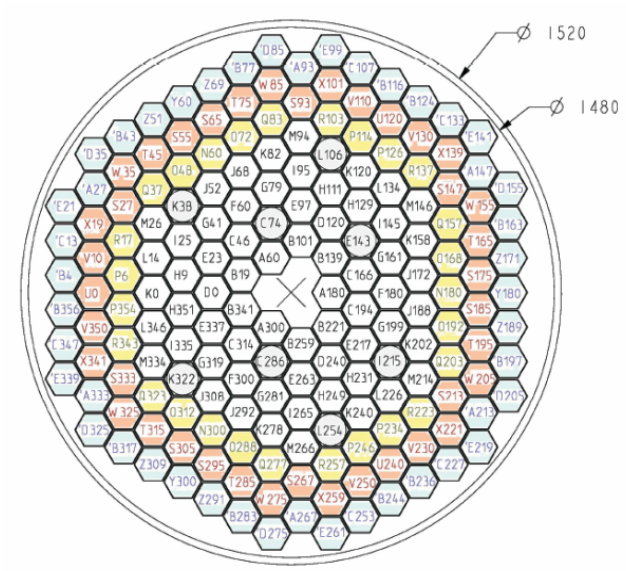


Figure 5-17: Channel nomenclature

IPS positions: L106; C74; E143; K38; I125; C286; K322; L254 Radioisotope production: O72; O288

*This document refers to work being performed by scientists and institutions involved in IP EUROTRANS, as well as the financial support of the European Commission through the contract FI6W-CT-2004-516520.*

For the irradiation rigs loaded with steel samples a 31-rod bundle has been considered. In the irradiation rigs loaded with fuel pin, the available space within the flow support tube enables to fit in 13 fuel pins. To establish mechanical stability of these two irradiation devices, there are six support pins of reduced diameter at the edges of hexagonal arrangements. The loops are loaded in C74 and K322 channels (see Figure 5-17 for the nomenclature of the channels), respectively.

Neutron fluxes inside the 8 In-Pile-Sections (except for 15/21 position) have been calculated on the core design for 2 energy groups (flux between 0.821 MeV and 20 MeV and flux below 0.821 MeV). The neutron fluxes in the IPS positions are given in Table 5-4 (the '17 22', '21 18' and '19 23' IPS are the closest positions from the target).

The neutron fluxes in Table 5-4 are given for a 57 $MW_{th}$ power at EOC, the beam current being at 3.4mA (close to the 3.5mA maximum value), with a $K_s$ value of 0.95479 and a $K_{eff}$ value of 0.93218.

Table 5-4 – IPS neutron fluxes

| S/A ERANOS position | Flux (n/cm²/s) | Flux (n/cm²/s) < 0.821 MeV | 0.821 MeV < Flux (n/cm²/s) < 20 MeV | % < 0.821 MeV | 0.821 MeV < Flux % < 20 MeV |
|---|---|---|---|---|---|
| 17 22 | 2.59E+15 | 1.81E+15 | 7.80E+14 | 70% | 30% |
| 21 18 | 2.61E+15 | 1.82E+15 | 7.90E+14 | 70% | 30% |
| 19 23 | 2.38E+15 | 1.67E+15 | 7.10E+14 | 70% | 30% |
| ***Average*** | ***2.53E+15*** | ***1.77E+15*** | ***7.60E+14*** | ***70%*** | 30% |
| 23 20 | 1.92E+15 | 1.38E+15 | 5.40E+14 | 72% | 28% |
| 16 25 | 1.65E+15 | 1.20E+15 | 4.50E+14 | 73% | 27% |
| 24 17 | 1.67E+15 | 1.21E+15 | 4.60E+14 | 73% | 28% |
| 15 21 | 1.76E+15 | 1.27E+15 | 4.90E+14 | 72% | 28% |
| 20 16 | 1.76E+15 | 1.28E+15 | 4.80E+14 | 72% | 27% |
| ***Average*** | ***1.75E+15*** | ***1.27E+15*** | ***4.80E+14*** | ***72%*** | 27% |

The neutron flux in the 3 IPS close to the target is about $2.53E^{+15}$neutrons/cm²/s and the one in the 5 IPS close to the core periphery is about $1.65E^{+15}$ to $1.92E^{+15}$ neutrons/cm²/s. It should be noted that more than 27% of the neutron flux remain above the energy of 0.821 MeV. Finally, no much difference in neutron flux exists over the cycle if the Power remains constant at 57 $MW_{th}$. Work is currently in progress in a following project to increase flux level for irradiation purposes removing some of the constraints of the current project [5.25].

REFERENCES

[5.1] F. Bianchi, C. Artioli, K. W. Burn, G. Gherardi, S. Monti, L. Mansani, L. Cinotti, D. Struwe, M. Schikorr, W. Maschek, H. Aït Abderrahim, D. De Bruyn and G. Rimpault (2005) "Status and trend of core design activities for heavy metal cooled accelerator driven system", in B. Verboomen, H. Aït Abderrahim, P. D'hondt (Eds.), ICENES 2005-Proceedings of the 12th International Conference on Emerging Nuclear Energy Systems, Brussels (Belgium), 21-26 August 2005, ISBN 907 69711 02 , Energy Conversion & Management Volume 47 (2006) pp. 2698 – 2709.

*This document refers to work being performed by scientists and institutions involved in IP EUROTRANS, as well as the financial support of the European Commission through the contract FI6W-CT-2004-516520.*

[5.2] H. Aït Abderrahim, P. D'hondt & D. De Bruyn (2007) "MYRRHA, a new fast spectrum facility", Seminar on Fission – Corsendonck Priorij, 18 – 21 September 2007, Proceedings April 2008, World Scientific, ISBN 978-981-279-105-4, pp. 207 – 221

[5.3] D. De Bruyn, D. Maes, L. Mansani & B. Giraud (2007) "From MYRRHA to XT-ADS: the design evolution of an experimental ADS system", AccApp'07 Conference, Pocatello, Idaho, July 30 – August 02, 2007, pp. 848 – 854.

[5.4] D. De Bruyn (2009) "From MYRRHA to XT-ADS: lessons learned and towards implementation", International Topical Meeting on Nuclear Research Applications and Utilization of Accelerators (AccApp09), Vienna, 04-08 May 2009

[5.5] M. Dierckx, 2009, "Target area design options for the XT-ADS spallation loop", SCK•CEN report R4649.

[5.6] M. Reale, 2009, "Description and functional sizing of main components of the reference design of XT-ADS", EUROTRANS deliverable D.1.27 – D.1.28.

[5.7] M. Dierckx, 2009, "XT-ADS spallation loop operation and pumping options, SCK•CEN report R4666"

[5.8] R. Stieglitz, 2009, "MHD-Pump for the XT-ADS design", KIT

[5.9] M. Dierckx, 2008, "Heat deposition profile in the XT-ADS target", SCK•CEN report R4567

[5.10] G. Van den Eynde, 2009, "XT-ADS Core Summary Report", EUROTRANS deliverable D.1.56

[5.11] Roelofs F., de Jager B., Class A. et al., 2008, "European research on HLM thermal-hydraulics for ADS applications", Journal of Nuclear Materials 376, 401-404

[5.12] Arien et al., 2004, "Assessment of Computational Fluid Dynamic Codes for Heavy Liquid Metals-ASCHLIM", EC Contract FIKW-CT-2001-80121-Final Rep.

[5.13] Batta A., Class A.G., Jeanmart H., 2010, "Comparative Experimental and Numerical Analysis of the Hydraulic Behaviour of Free-Surface Flow in the Water Experiment of the XT-ADS Windowless Spallation Target", Proceedings of ICAPP'10, paper-Id 10342 San Diego, CA,USA, accepted

[5.14] A.G. Class, A. Batta, 2010, "XT-ADS Windowless Target: High Resolution Interface Capturing Simulations", Proceedings of TCADS, 15-17 March 2010, Karlsruhe, Germany

[5.15] N. Forgione et al., 2009, "MYRRHA spallation target loop: RELAP 5 simulation", VELLA Deliverable, European Commission

[5.16] D. Maes, "Main requirements of the ETD XT-ADS", IP-EUROTRANS, Deliverable D1.23, SCK•CEN, May 2008.

[5.17] B. Giraud, "Review and justification of the main design options of XT-ADS", EUROTRANS DM1 Design - Workpackage 1.2, Deliverable D1.5, October 2006

[5.18] Rimpault, Gérald. Caractérisation neutronique du coeur sous-critique CL-P0 du système XT-ADS refroidi au Pb-Bi, outil d'irradiation pour des assemblages expérimentaux. 2009. CEA/DER/SPRC/LEDC/09-403.

[5.19] Nishihara, Kenji. Homogenized XT-ADS model ($K_{eff}$). 2008. SCK-CEN Calculation note. ANS/RMS/KN/B044123/825/08-13.

[5.20] Van den Eynde, Gert et al. Specification for the XT-ADS core and fuel element, Deliverable 1.7 of IP-EUROTRANS, DM1. 2007. ANS/RMS/GVdE/gvde.3910.B044123 825/07-04. Also Neutronic design of the XT-ADS core, PHYSOR 2008, International Conference on the Physics of Reactors, Casino-Kursall Conference Center, Interlaken, Switzerland, September 14-19, 2008

*This document refers to work being performed by scientists and institutions involved in IP EUROTRANS, as well as the financial support of the European Commission through the contract FI6W-CT-2004-516520.*

[5.21] Romanets, Yuriy. Radiation damage and circuit activation for XT-ADS. 2009. EUROTRANS, DM1 Design, Deliverable 1.54.

[5.22] Broeders, C.H.M, et al. KAPROS-E: Modular Program System for Nuclear Reactor Analysis. Status and Results of Selected Applications, Jahrestagung Kerntechnik Düsseldorf., 2004.

[5.23] An optimum approach to Monte Carlo Burnup. Haeck, Wim and Verboomen, Bernard. 2007, Nuclear Science and Engineernig, Vol. 156, pp. 180-196.

[5.24] Dequidt, Aline. Irradiation performance assessment for MYRRHA/XT-ADS. s.i. : Master thesis, 2008.

[5.25] P. Baeten, H. Aït Abderrahim & D. De Bruyn (2009) "The next step for MYRRHA: the Central Design Team FP7 project", International Topical Meeting on Nuclear Research Applications and Utilization of Accelerators (AccApp09), Vienna, 04-08 May 2009.

[5.26] “Design Guide for ADS Machine Hall Handling System”, Oxford Technologies LTD (OTL), TR-21 3 -REP-002-A, Deliverable D1.60 of the Workpackage 1.2 of the EUROTRANS DM1 Design.

*This document refers to work being performed by scientists and institutions involved in IP EUROTRANS, as well as the financial support of the European Commission through the contract FI6W-CT-2004-516520.*

# 6. SAFETY EVALUATION OF THE ETD CONCEPTS

## 6.1 Safety status of EFIT-Pb plant

### 6.1.1 Subcriticality margin assessment

In ADS, it is necessary to prevent, by design, nuclear flux divergence with direct consequence on power excursion both in normal operating conditions and in abnormal and accidental conditions, including Design Extension Conditions. The effective multiplication factor Keff, independent of the external neutron source, is a meaningful measure of the actual safety characteristic of the device. That is, 1-Keff is a gauge of the distance from criticality. Hence prevention of reactor power divergence is achieved if the effective multiplication factor is maintained below one with safety margins corresponding to either normal operation conditions or stand by conditions for fuel handling. The provision of an adequate level of sub-criticality can be achieved by conservatively estimating the value of all credible positive reactivity insertions and thereby choosing the allowable range of normal operating conditions, including a margin for uncertainties (see Table 3.1).

The verification of the adequacy of the selected sub-criticality level has been verified by calculating the coolant worth (total but also for credible severe safety conditions for which 7 sub-assemblies at the maximum can be voided; the rationale for that choice is explained further down), the Doppler, axial and radial structural expansion and core compaction (the gaps between assemblies are assumed to disappear).

The core compaction is generally associated to an earth-quake event during which all fuel sub-assemblies are gathered together in the center of the core. The core compaction reactivity effect is equal to 1416 pcm under those extreme conditions. Feedback effects and reactivity insertions calculations allow determining safety limits and feedback coefficients for the EFIT-Pb core design. The transition between cold and hot core states is in the range of 250 pcm, voiding of 7 subassemblies is given to 400 pcm. Most of the reactivity insertions are fuel independent since associated to geometry changes which are identical. The only significant difference comes from the void effect and this, even, is not large with core void effects in CerCer and CerMet (7884 pcm compared to 6223 pcm) and values very stable with burn up since those cores have limited reactivity swing.

With all these possible reactivity insertions, a value of 0.97 for Keff offers a safe margin including nuclear data & technology uncertainties on one side and reactivity measurements on the other side. The 0.05 distance from criticality ($K_{eff}$=0.95) is currently judged to be adequate for the controlled and continuously monitored operations involved in refueling of the reactor. In this last situation, the sub-criticality is obtained by inserting with the handling machine, absorber rods.

For the 2 situations, operating conditions and fuel handling conditions, an adequate instrumentation and signal analysis is required to monitor the reactivity (see Chapter 10.2: ECATS domain activity).

### 6.1.2 EFIT-Pb safety guidelines

For the MgO matrix, both the drastically reduced thermal conductivity in the high temperature domain ($T_{fuel}$ > 1750 °C) and the possible dissociation at temperatures in the range of 1600 °C and above (with the impact of potential fuel redistribution and recriticality [6.15]) have to be mastered. The main reasoning for recommending the CerMet fuel matrix was based on the safety performance since. The recommendation of AFTRA has also to be seen in the light of the limited knowledge on these fuels under irradiation or transient conditions.

*This document refers to work being performed by scientists and institutions involved in IP EUROTRANS, as well as the financial support of the European Commission through the contract FI6W-CT-2004-516520.*

A list of design base condition and design extension condition events was defined for the EFIT-Pb transmuter. These initiating events consist in Loss Of Flow (LOF), Transient Over Power (TOP), Loss Of Heat Sink (LOHS), Loss Of Coolant Accident (LOCA) and transients specific to the ADS, e.g. sudden beam power increase, spurious beam trip, etc. The adopted safety approach [6.10] is similar to that as employed in the XT-ADS analysis to assure consistency in the calculated system temperatures and pressures. At this stage, the innovative feature of the MgO-based MA-fuel, containing relatively large inventories of minor actinides in the core regions have to be particularly addressed. The approach adopted was to employ several safety codes such as RELAP, SIMMER, SIM-LFR, providing coverage for each of the chosen transient by at least two codes.

Most of the transients were analyzed for both protected and unprotected assumptions. Since, there is no control rod in the design for reactor shut down purpose, the protected transients implied that the accelerator could be tripped as soon as the conditions (e.g. core, temperature) for its shut-off were reached in the reactor system. The unprotected cases assumed that the accelerator shut off was failing due to inappropriate emitted, transmitted or treated signals. The unprotected transients are, thus, equivalent to the ATWS (anticipated transients without scram), which are analyzed for the LWR systems, however, they are generally defined as design extension conditions.

### 6.1.3 EFIT-Pb ULOF transient studies

In the Unprotected Loss Of Flow (ULOF) analysis of EFIT-Pb with SIMMER-III [6.13], the following boundary conditions are applied. The pressure drop in the whole system is 1.37 bars in a steady-state condition, while the primary pump stops within 1 sec for the loss of flow simulation. Figure 6.1-1 shows transients of the pump pressure and the coolant flow rate in the whole core. ULOF starts at 2 sec counting from its initial steady-state. As the pump suddenly stops within 1 second, there is a very obvious overshooting of the coolant mass flow rate in the core, 30% reversed flow can be seen in Figure 6.1-1 after the pump stops. The pump stop triggers a movement of coolant levels which causes the phenomena described in the following. The undershooting of the coolant mass flow rate leads to the overshooting of temperatures as shown in Figure 6.1-2. The coolant mass flow rate in the core is finally stabilized at 30% due to the natural convection in the system. With the 30% remained coolant heat removing capacity, the fuel, clad, and coolant peak temperatures finally stabilized at 1552 °C, 730 °C, and 685 °C, respectively. Due to the overshooting, the peak temperature of fuel, clad, and the coolant is 1687 °C, 884 °C and 858 °C, respectively. Therefore, even taking the short time overshooting into account, the clad and coolant temperatures are well below the failure limit and also the fuel peak temperature is well below the limits for melting and dissociation (1877 °C) given by the 'Fuel-Domain' AFTRA of EUROTRANS [6.14]. This is achieved with the higher decay heat load associated with the MA-based fuel [6.16], [6.17] by about 26% higher than that of conventional MOX fuel.

*This document refers to work being performed by scientists and institutions involved in IP EUROTRANS, as well as the financial support of the European Commission through the contract FI6W-CT-2004-516520.*

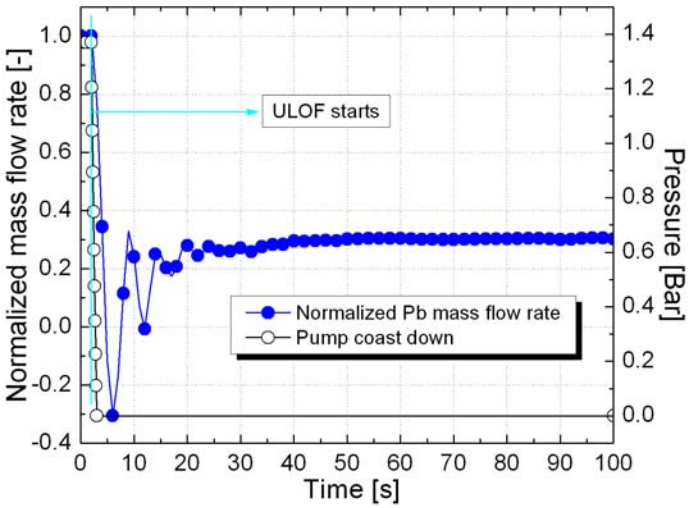


Figure 6.1-1. Pressure and coolant flow rate transients in the ULOF case

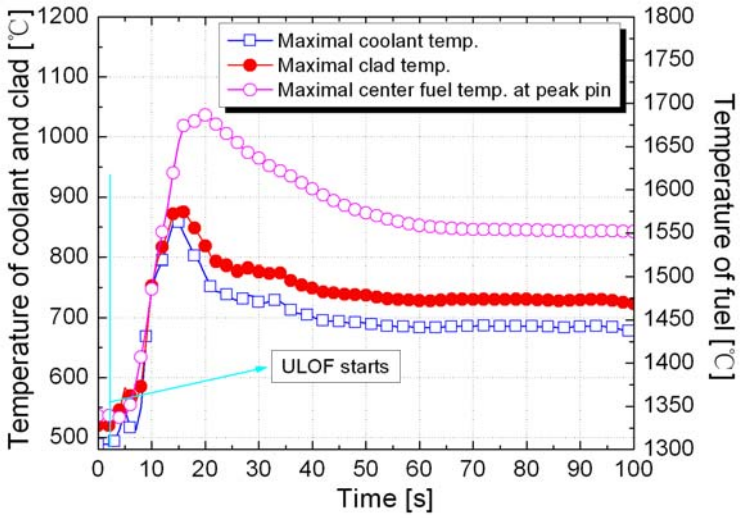


Figure 6.1-2. Temperature transients in the ULOF case

Figure 6.1-3 shows the reactivity and power transient in the ULOF condition. The power is finally stabilized at around 2% higher than its nominal value. Although the power has increased a little bit more than 8% at the overshooting point, the peak temperature shown in Figure 6.1-2 indicates that 8% power increase is acceptable with the current simulation conditions.

*This document refers to work being performed by scientists and institutions involved in IP EUROTRANS, as well as the financial support of the European Commission through the contract FI6W-CT-2004-516520.*

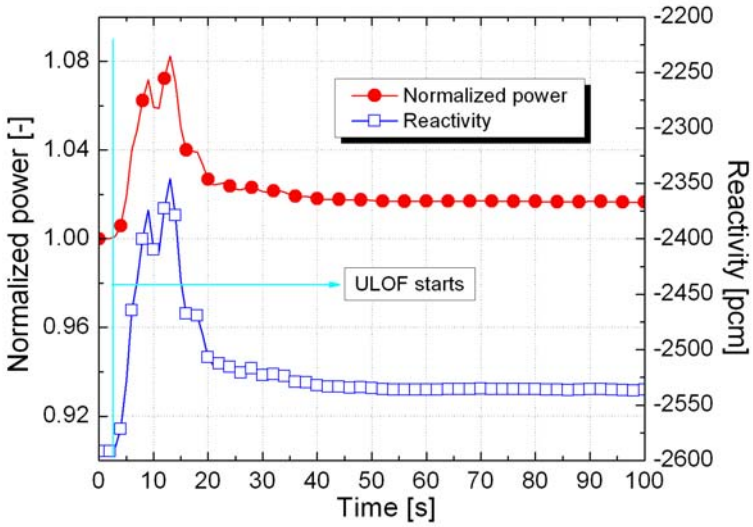


Figure 6.1-3. Power and reactivity transients in the ULOF case

### 6.1.4 Other EFIT-Pb transient studies

The response of the EFIT-Pb plant to various other transient initiators, such as loss of heat sink-LOHS, inadvertent reactivity insertions - TOP, under-cooling, etc. are summarized in Table 6.1-1 and documented in details in D1.43 [6.11]. Listed are the calculated peak temperatures of core fuel, cladding and coolant for the various transients analyzed using the RELAP5 [6.12], SIMMER [6.13], and SIM-LFR system codes.

Table 6.1-1 Peak temperatures of Materials in EFIT-Pb Transients, [ºC]

| | Fuel | Cladding | Coolant* |
|---|---|---|---|
| Steady state | 1293 | 521 | 480 |
| PLOF (all pumps stop) | 1300 | 655 | 650 |
| ULOF (all pumps stop) | 1470 | 810 | 807 |
| PLOHS and PLOHS/LOF | 1510 | 835 | 822 |
| ULOHS and ULOHS/LOF [1] | 1770 | melting | 1312 |
| UOVC (-70ºC) [2] | 1330 | 520 | 360 |
| PTOP (500 pcm) | 1441 | 536 | 513 |
| UTOP (300 pcm) | 1490 | 545 | 522 |
| PTOP (2000 pcm) | 2110 | 660 | 633 |
| UTOP (2000 pcm) | 2110 | 700 | 653 |
| PBLOCK (97.5%) | 850 | 812 | 818 |
| UBLOCK(97.5%) [3] | 1776 | 1310 | 1072 |
| UOVP (120%) | 1445[4] | 517 | 495 |
| Beam trip (10 s) [4] | 1333 | 518 | 517 |

*average coolant temperature at the core outlet

[1] at 1430 sec into ULOHS/LOF transient

[2] Lead HX primary side outlet temperature at 400 sec into UOVC

*This document refers to work being performed by scientists and institutions involved in IP EUROTRANS, as well as the financial support of the European Commission through the contract FI6W-CT-2004-516520.*

[3] at 17 sec into the UBLOCK (97.5%) transient

[4] relatively large temperature gradients of 90°C/sec and 10°C/sec for fuel and cladding respectively must be expected.

The results of these safety analyses demonstrate that the Pb-cooled EFIT plant is a very robust design ascribable to the unique combination of inherent and plant design features, which, for example are:

1. the favorable thermophysical properties of the coolant Pb
   - very high boiling temperature,
   - low vapor pressure at operating conditions,
   - high specific heat,
   - good heat transfer characteristics,
2. the high thermal inertia, or large heat sink / heat buffer characteristics associated with the coolant Pb as reflected by:
   - the large coolant mass times heat capacity in the core region,
   - the large coolant mass times heat capacity in the primary system (pool type design),
3. the large natural convection characteristics of the plant design due to:
   - the favorable sub-assembly design (pin diameter and pitch, low pressure drop),
   - the large height difference between heat source (core) and heat sink (IHX), namely ~ 3.7 meters,
4. adopting a modest linear power ratings for the 3 cores zones of EFIT-Pb thereby assuring that temperatures of the innovative MgO-MA-based fuel are below a certain upper temperature limit, namely 1380°C [6.15] under nominal conditions and 1500°C under ULOF conditions as experiments have indicated that MgO-based fuel may loose its mechanical integrity at temperatures above 1500°C, namely:

| **BOC** | Core Zone 1 | Core Zone 2 | Core Zone 3 |
|---|---|---|---|
| Average pin: avg/peak linear power [W/cm] | 148 / 169 | 140 / 161 | 138 / 148 |
| Peak pin: Avg/peak linear power [W/cm] | 183 / 210 | 162 / 186 | 170 / 202 |

| **EOC** | Core Zone 1 | Core Zone 2 | Core Zone 3 |
|---|---|---|---|
| Average pin: avg/peak linear power [W/cm] | 146 / 167 | 140 / 159 | 129 / 148 |
| Peak pin: Avg/peak linear power [W/cm] | 197 / 222 | 168 / 190 | 177 / 202 |

and,

5. a modest Po-210 accumulation in comparison to LBE-coolant.

Somewhat less favorable characteristics of the Pb as coolant are:

*This document refers to work being performed by scientists and institutions involved in IP EUROTRANS, as well as the financial support of the European Commission through the contract FI6W-CT-2004-516520.*

1. the high melting point of Pb, namely 327°C, requiring that the primary system is always operated under all plant steady state and transient conditions at temperatures in excess of 340°C to assure a safety margin of at least 13°C from the freezing point of Pb (this margin should be further enlarged in a new series of optimizations), and
2. the high corrosion rate of lead as a coolant when flowing lead is in direct contact with steel metal surfaces. This requires that all sensitive components within the primary system, in particular within the core region, are always covered by either a protective oxide layer to protect against lead-metal corrosion, or by some other protective layer, such as aluminum (GESA treatment). The thickness of this oxide layer needs to be controlled within a narrow range [optimally ~ 5 – 15 µm] by constantly controlling the oxygen concentration in the coolant. The oxide layer on the other hand should not become too thick [ > 50 - 80 µm] in order not to seriously degrade the heat transfer characteristics of the heat transfer surfaces as the poor thermal conductivity of the oxide layer [ ~ 1 W/cm/K] impedes an efficient heat transfer between the surface to be cooled and the coolant itself. Thick oxide layers could possibly lead to excessive local temperatures (clad in the core, tubes in the heat generators) in case the oxide layer should accumulate to thicknesses above 100 [um] or more (local burn-out). Of particular sensitivity are the upper core regions and the HX primary coolant inlet regions where temperatures are highest as the rate of oxide accumulation is known to increase as a function of operating temperatures.
3. The possible requirement for treating the sensitive components (such as cladding surfaces) by imparting a layer of aluminum onto these surfaces (GESA treatment) acting as a protection against the corrosion of flowing lead. GESA treatment could mitigate the requirement for a very tight oxygen control system as no oxide layering would be required, and
4. Continuous assurance of the integrity of the protective layer (either oxide or aluminum) – no spallation or cracking of the oxide layer - under all plant transient conditions in order to assure continuous fuel pin integrity, prevention of corrosive attack on heat transfer tubes and prevention of partial blockages of flow paths by local accumulation of impurities limiting operational availability factors significantly.
5. Negative impact of steam generator tube ruptures leading to potentially rapid vaporization of water. As the secondary side is pressurized at 140 bar with respect to the primary side (2 bars), any steam generator tube rupture will lead to the injection of water from the secondary into the primary side. The 335 °C water will be rapidly vaporized in the primary side. Analyses performed with SIMMER [6.14] show that though mostly directed upwards, some vapor does reach the bottom region and is swept through the core. Vapor reaches the core intermittently and leads to a void value of the core of a maximum of 4% which would correspond to a reactivity contribution of roughly 300-500 pcm. Measures based on a rupture disc system can be installed to prevent cover gas pressurization.
6. The response of the plant to potential earthquakes. Aside of issues associated with the structural integrity of the plant system (that are, however, mitigated by adopting the seismic isolators), potential reactivity insertions due to core compaction must be anticipated. Their reactivity insertion, however, have been taken into account in a very envelope way and no power excursion is hence expected.

### 6.1.5 Overall EFIT-Pb safety studies summary

The combination of the favorable features of lead as a coolant (high thermal inertia, high boiling point) assures that the integral core damage frequency is very low, and that the core and primary system temperatures for almost all transient scenarios are below the temperature limits established to avoid clad failure and thus release of radioactivity into the primary system and/or to avoid creep-fatigue failures of load carrying structures.

*This document refers to work being performed by scientists and institutions involved in IP EUROTRANS, as well as the financial support of the European Commission through the contract FI6W-CT-2004-516520.*

There were only very few transients in which the core conditions could approach clad melting and/or release of radioactivity. Principal among these was the almost complete blockage of a subassembly without accelerator trip, where detection in due time might be difficult and there may not be sufficient time available for affecting the trip manually.

The other transient of concern is that of unprotected operation with complete loss of heat sink with and/or without the operation of the primary pumps. As sub-critical systems are known to exhibit a less favorable response compared to critical systems to unprotected transient conditions (the power remains essentially unchanged in sub-critical systems whereas the power decreases significantly in critical systems), the particular design of EFIT-Pb however exhibits a relatively mellow response on account of the very large thermal inertias in combination with the large natural convection rate designed into the system (up to 30% nominal flow during ULOF conditions). During these postulated transients there will be more than half hour available for terminating the operation of the accelerator manually.

Potential positive reactivity insertions due to fuel handling errors during refueling procedures, steam generator tube rupture, or due to core voiding are enveloped by ~ +500 pcm, whereas the reactivity insertion potential for earthquake transients is enveloped under most pessimistic assumptions by ~ + 1500 pcm. Transient calculations of inserting 500 pcm under different plant state conditions (HFP, CZP) have clearly demonstrated that reactivity insertions of this magnitude have little impact on either clad or fuel temperatures as the system. All sensitive temperatures have been shown to remain below design limits. Reactivity insertions of ~ +2000 pcm will lead to fuel temperatures of ~ 2100°C (above the 1500°C operational limit) for as long as the accelerator is not tripped, but clad temperatures remain below 710°C. Clad failure is thus not expected even under these most extreme conditions, even though MgO-based fuel dissociation must be expected. This may require that the fuel may have to be replaced for continued plant operation, but no safety related issue is to be expected (unless MgO-based fuel decomposition should lead to unexpected fuel pin over-pressurization).

Potential pressure loadings on primary system structures during steam generator tube ruptures still need further design considerations as pressure loads threatening structures are considered unlikely but cannot be definitively excluded.

The effect of degraded reactivity coefficients (Doppler coefficient, reduced delayed neutron fraction to ~ 150 pcm) due to the large inventories of minor actinides (Am, Cm) has been shown to be of no impact as the system is sufficiently sub-critical ($K_{eff}$ ~ 0.9700). The consequence of practically no fuel temperature reactivity feedback (Doppler = - 31 pcm) is shown to be a positive feature under sub-critical system conditions, as no reactivity swing during plant load conditions need to be taken into account (taking the plant from HFP to CZP, or even hypothetically to ambient temperatures). The combination of fuel and core design also exhibits a very small burn-up reactivity swing that is also a positive feature as the level of sub-criticality remains essentially unchanged when going from the BOC to the EOC core state. This also simplifies the response of the EFIT-Pb plant to all transient conditions as the dynamic response of the system will be nearly the same for both BOC and EOC plant states, in particular as the reactivity coefficients have also been shown to remain essentially unchanged when going from BOC to EOC.

A concern identified was the very tight operational control requirements to be imposed on the secondary coolant conditions (feedwater inlet temperature, feedwater flow rate) in order to assure prevention of freezing of the lead coolant at the coldest location of the primary loop, namely at the outlet of the primary side of the main heat exchanger. Under nominal conditions, the primary HX outlet temperature is 400°C, well above the freezing point of Pb (327°C) while the inlet temperature of the feedwater in the secondary side of the heat exchanger is 335 °C at 140 bars. Under certain transient conditions it is conceivable that the primary Pb HX outlet temperature (nominally 400°C) decreases to

*This document refers to work being performed by scientists and institutions involved in IP EUROTRANS, as well as the financial support of the European Commission through the contract FI6W-CT-2004-516520.*

the feedwater inlet temperature 335°C, only 8 °C away from freezing of the primary lead coolant unless corrective actions are taken immediately (within several tens of seconds) by either tripping the secondary pump or assuring a continued feedwater inlet temperatures > 335°C. In addition, any sudden decrease in feedwater temperature (either by loss of the preheater, or any other cold water injection paths), or inadvertent increase in feedwater flow rate under partial load condition could lead to the rapid decrease of the primary HX outlet lead temperature to close to the freezing point of Pb.

As freezing of Pb must be avoided under all circumstances (in order to assure continued coolant flow throughout the primary system, in particular coolant flow through the core region), the control of secondary feedwater conditions (either feedwater inlet temperature, or feedwater mass flow rate) are of particular importance in all Pb-cooled systems under transient conditions.

In general, however, the safety analysis performed for the EFIT-Pb design demonstrates the very forgiving behavior of this plant design under most transient conditions. With the exception of the sub-assembly blockage transient, most unprotected transients allow sufficient grace time (~ 30 minutes) before manual corrective actions are required to avoid core melting. Even, the sub-assembly blockage event as being calculated by SIMMER does not lead to a general melt down of the core but remains limited to a few sub-assemblies. This plant behavior is almost unique when compared to most other critical reactor plant designs (LWRs, FBRs, etc.) in that these designs exhibit significantly smaller grace times under similar transient conditions. By this standard, EFIT-Pb must be judged to be a very “safe” reactor design in accordance with its mission of using a large inventory of unique minor actinide transmutation fuel (Am, Cm) with its associated large in-core actinide radionuclide inventory.

*This document refers to work being performed by scientists and institutions involved in IP EUROTRANS, as well as the financial support of the European Commission through the contract FI6W-CT-2004-516520.*

## 6.2 Safety status of EFIT-He plant

### 6.2.1 EFIT-He safety approach and PLOF transient studies

A list of design base condition and design extension condition events was defined for the EFIT-He transmuter. These initiating events consist in Loss Of Flow (LOF), Transient OverPower (TOP), Loss Of Heat Sink (LOHS), Loss Of Coolant Accident (LOCA) and transients specific to the ADS, e.g. sudden beam power increase, spurious beam trip, etc. The adopted safety approach is similar to that as employed in the XT-ADS analysis to assure consistency in the calculated system temperatures and pressures, in particular considering the innovative feature of the MgO-based MA-fuel, containing relatively large inventories of minor actinides in the core regions. The approach adopted was to employ several safety codes such as CATHARE and SIM-GFR, providing coverage for each of the chosen transients by at least two codes.

As a typical example of the transient analysis performed for EFIT-He plant could be the protected loss of flow (PLOF) transient carried out by FZK-INR using SIM-GFR code.

Two different PLOF cases were analyzed, namely:

| P-1 Transients : | Description |
|---|---|
| (PLOF-Case 1): P-1a | PLOF Reference Case, beam trip delayed **1** sec |
| (PLOF-Case 2): P-1b | PLOF Case, beam trip delayed **3** sec |

***Case 1 (P-1a): Beam trip 1 sec after pump trip (DHR totally passive – natural convection)***

The PLOF transient starts at steady state nominal conditions (HFP). At 10 sec transient time, the blowers are assumed to trip, followed by accelerator trip 1 sec after the blower trip (primary mass flow rate has decreased to ~85% during this 1 sec interval) decreasing reactor power to the decay heat level. The detailed results of this transient are shown in Figure 6.2 1.

In Figure 6.2-1a, Figure 6.2-1b, and Figure 6.2-1g the decrease in primary flow rate is shown during the first 120 sec transient time. The more detailed coast-down characteristics (pump coast-down half time = ~ 4.5 sec) of the EFIT-He primary blowers are illustrated in Figure 6.2 1k to Figure 6.2 1m.

At 120 sec transient time, when the primary mass flow rate has decreased to 3%, the PCS valves are opened, shutting off the primary system heat removal flow path. During the first 120 sec the MHX (PHX) removes all the decay heat power generated as illustrated in Figure 6.2 1g leading to a continued decrease of all core temperatures (see Figure 6.2-1e for the BOC core state and Figure 6.2-1f for EOC core state). During this time the core inlet temperature continues to decrease (see Figure 6.2-1d), due to a decreasing MHX primary outlet temperature (see Figure 6.2-1g), because of the continued nominal secondary mass flow rate throughout this transient (see Figure 6.2-1g). The core inlet temperature reaches a low temperature of 180°C at 100 sec transient time (see Figure 6.2-1d

*This document refers to work being performed by scientists and institutions involved in IP EUROTRANS, as well as the financial support of the European Commission through the contract FI6W-CT-2004-516520.*

and Figure 6.2-1e,f) as the massive diagrid (45 t) acts as a heat source at this time in the transient, reheating cold He coming from the primary outlet of the MHX (see Figure 6.2-1h) .

After opening of the PCS valves, natural He-coolant convection in the DHR is established fairly quickly as observed in Figure 6.2-1i reaching up to ~8.5 kg/s (total, for 2 DHR units) of He mass flow at 200 sec transient time after an initial overshoot after PCS-valve opening of 13 kg/s, as the water mass flow rate on the secondary side of the DHR HX is also fully established at ~150 sec transient time (at ~ 42 kg/s, not shown on the scale in Figure 6.2-1i). At 800 sec transient time, the DHR HXs are removing ~ 16 MW of decay heat in addition to ~2 MW of heat being absorbed in the heat-up of the walls of the DHR cold leg piping (now exposed to ~360°C He, see Figure 6.2-1i and Figure 6.2-1j). The DHR HXs temperature response is illustrated in Figure 6.2-1j.

After the switchover phase from the main loop to the DHR loops, all core temperatures are observed to increase again (see Figure 6.2-1e,f) due to increasing core inlet temperatures until new steady state conditions within the DHR cooling system are established. All relevant core temperatures are observed to go through a maximum of ~950°C at 1000 sec transient time. At transient times larger than 1000 sec, all core temperatures are gradually decreasing thereafter as all decay heat is being removed by the DHR system (see Figure 6.2-1i) in combination with the heat absorbed by the vessel walls and piping system of the DHR.

The above illustrates that the EFIT-He plant systems can remove decay heat in the natural convection mode. Both primary loop and the secondary side of the DHR are in natural convection modes (plant system being entirely passive at this operational point), removing successfully decay heat, under the assumption, that the primary system remains fully pressurized. During this PLOF transient, the primary system pressure reduces briefly to about 88% of nominal (~ 61 bar) between 60 and 300 sec transient time due to decreasing primary loop temperatures, recovering thereafter as core temperatures (and thus also primary/DHR loop temperatures) are increasing again (see Figure 6.2-1e).

An issue of potential concern may be the number of DHR systems in the operational mode. As the total natural convection flow rate in the primary system is distributed into the various DHR loops proportionally, the flow rate in each DHR loop will accordingly be reduced (i.e. ~ 3.5 to 4.0 kg/sec per loop in the above case – 2 DHR systems being assumed operational) corresponding to the larger the number of “active” DHR loops. With low flow rates in each loop, the flow will move into the laminar flow regime, leading to a reduced shell side (primary He flow) heat transfer coefficients (low Nusselt number), thereby leading to reduced heat transfer rates (in terms of MW removed) across the DHR HX tubes. It thus needs to be ascertained that the number of operational loops is kept to a minimum (not more than 2) during the normal decay heat mode (passive mode) during the PLOF transient.

The axial temperature profile of the peak fuel pin in EFIT-He are shown in Figure 6.2-1o during BOC core state conditions and in Figure 6.2-1q for corresponding EOC core state conditions at 2000 sec transient time, being only marginally different as thermal fuel conductivity and gap width are of no importance in the decay heat mode as relatively little power is generated in the pins (~ 4.5%). The response of the plant to the PLOF transient is essentially identical during both EOC and BOC conditions, as all core temperatures decrease rapidly after the accelerator trip.

The expected clad failure times are displayed in Figure 6.2-1n during BOC core state conditions and in Figure 6.2-1p for the corresponding EOC core state. Surprisingly clad failure time decrease down to 40 sec for both BOC and EOC core states even though the peak pins are pressurized to ~120 bar under EOC conditions. The difference is ascribable to the somewhat lower cladding temperatures experienced under EOC conditions because of lower stored fuel heat under EOC (lower fuel temperatures). This can be observed in comparing Figure 6.2-1e and Figure 6.2-1f.

***This document refers to work being performed by scientists and institutions involved in IP EUROTRANS, as well as the financial support of the European Commission through the contract FI6W-CT-2004-516520.***

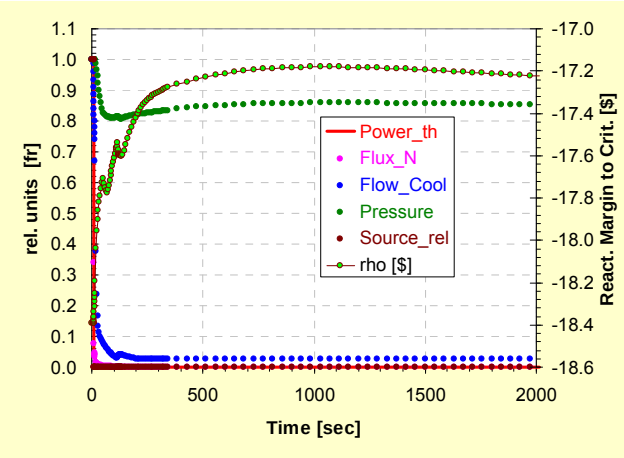


a) Relative Core Power, Flow rate, source intensity, and margin to criticality

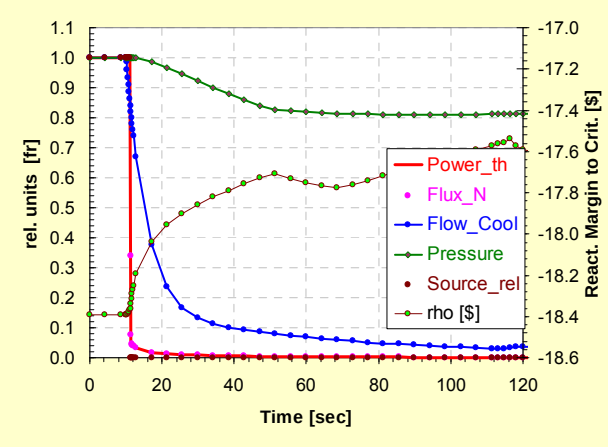


b) Relative Core Power, Flow rate, source intensity, and margin to criticality

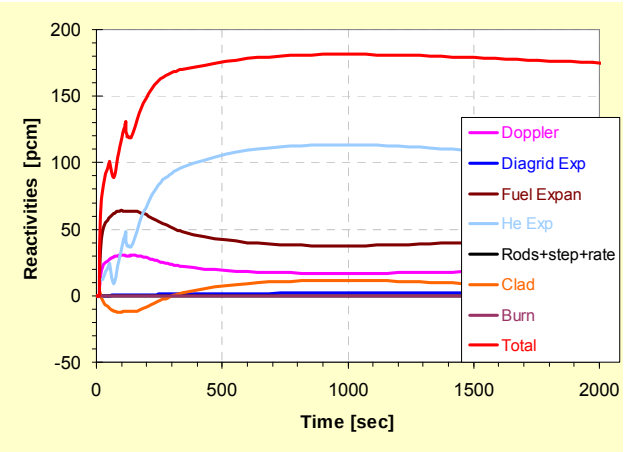


c) Reactivity Components

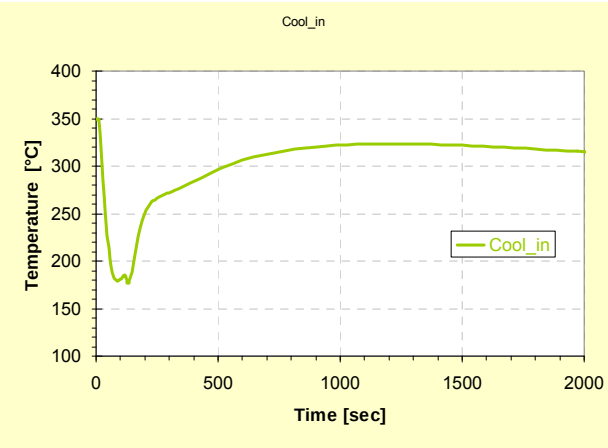


d) Core inlet temperature


***This document refers to work being performed by scientists and institutions involved in IP EUROTRANS, as well as the financial support of the European Commission through the contract FI6W-CT-2004-516520.***

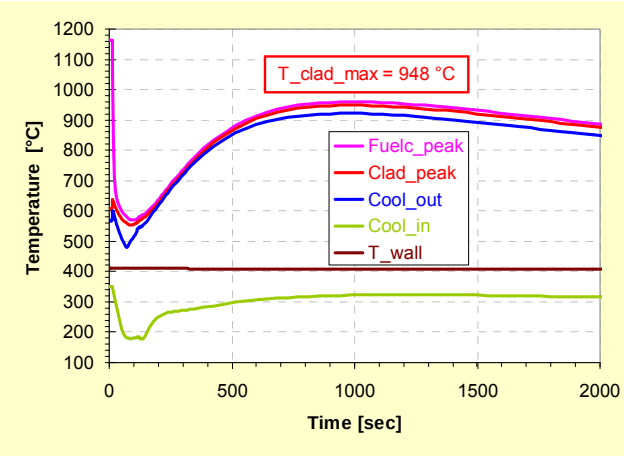


e) Peak Fuel-, Clad-, and Coolant Temperatures at **BOC**

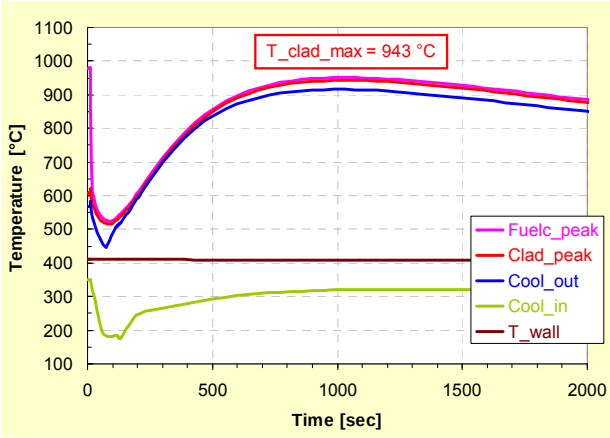


f) Peak Clad-, and Coolant Temperatures at **EOC**

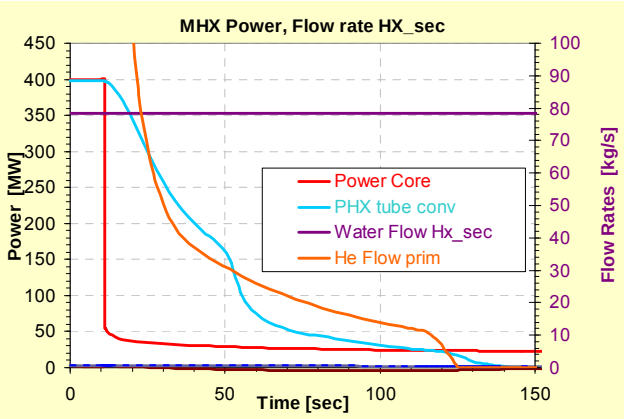


g) Core and PHX power, primary and secondary PHX flow rates

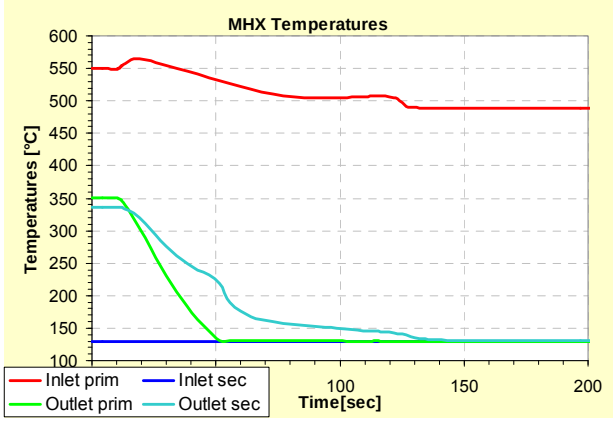


h) PHX temperatures

*This document refers to work being performed by scientists and institutions involved in IP EUROTRANS, as well as the financial support of the European Commission through the contract FI6W-CT-2004-516520.*

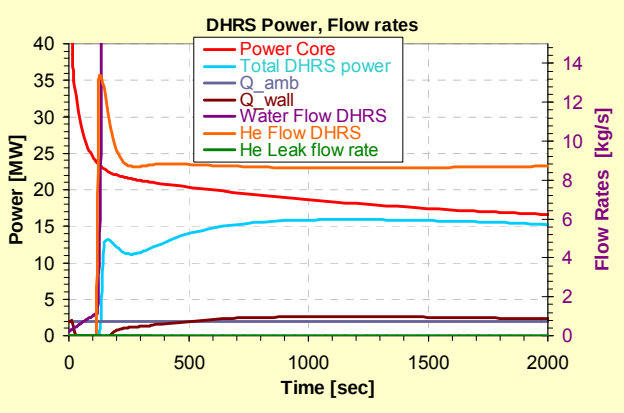


i) Core and DHR power, primary and secondary DHR flow rates

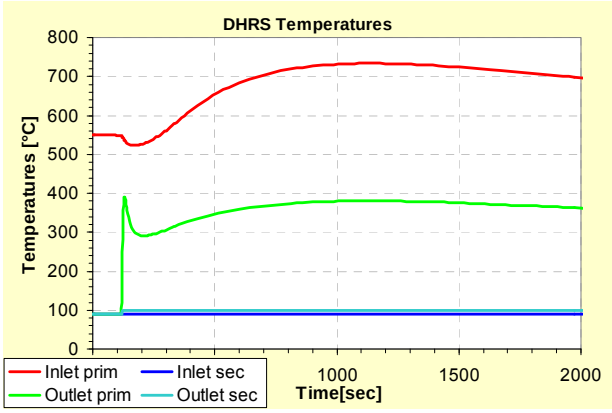


j) DHR temperatures

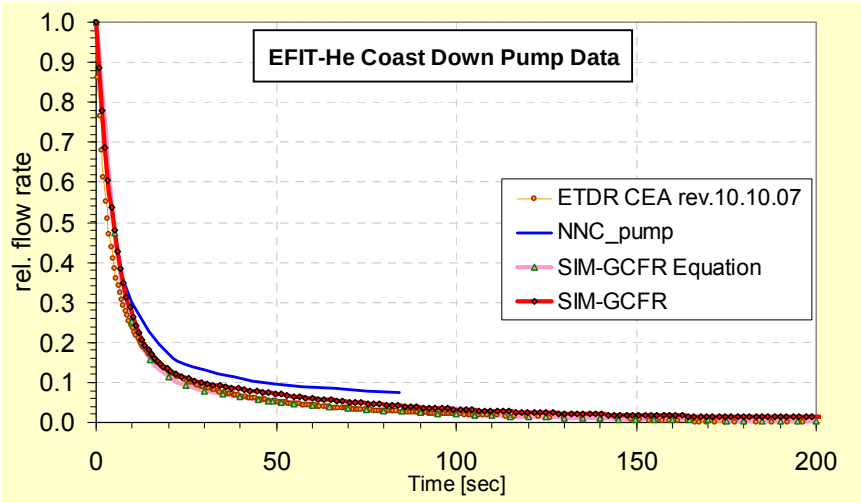


k) Coast-down characteristic for EFIT-He primary blower

*This document refers to work being performed by scientists and institutions involved in IP EUROTRANS, as well as the financial support of the European Commission through the contract FI6W-CT-2004-516520.*

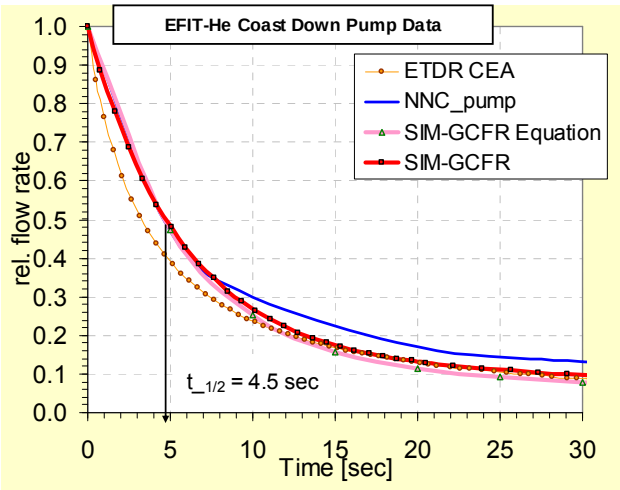


l) Coast-down characteristic for EFIT-He primary blower during first 30 sec

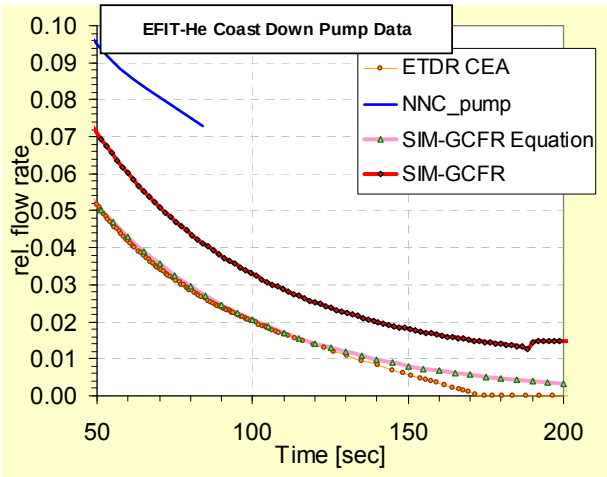


m) Coast-down characteristic for EFIT-He primary blower in low flow phase

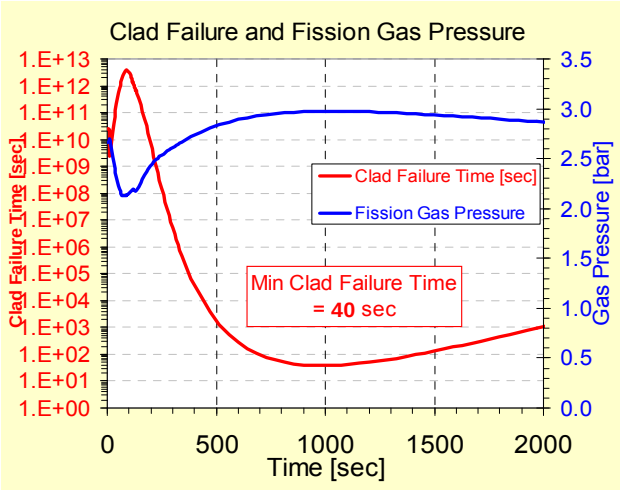


n) Axial peak pin temperature profile 350 sec into PLOF at **BOC**

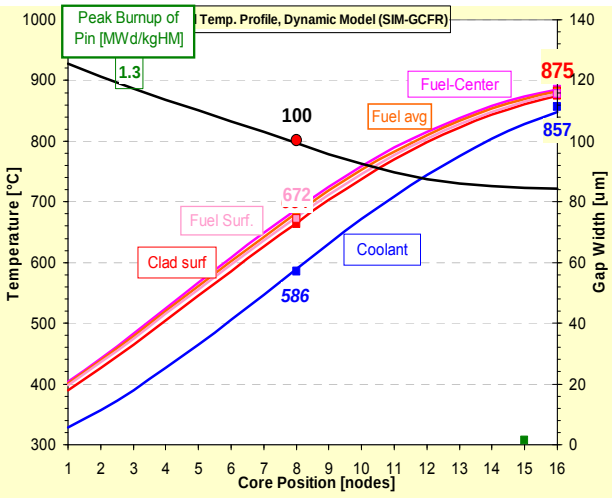


o) Axial peak pin temperature profile 350 sec into PLOF at **BOC**

*This document refers to work being performed by scientists and institutions involved in IP EUROTRANS, as well as the financial support of the European Commission through the contract FI6W-CT-2004-516520.*

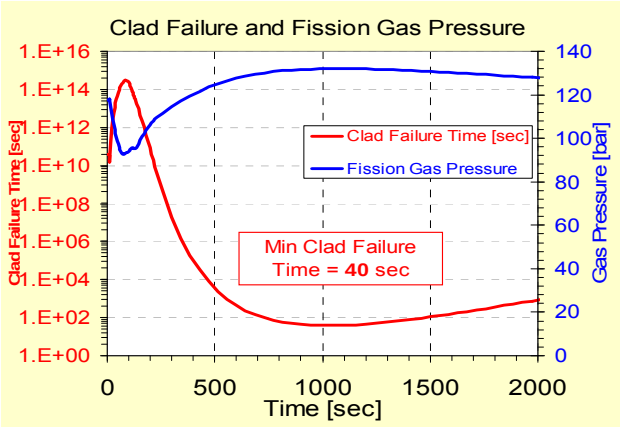


p) Axial peak pin temperature profile 2000 sec into PLOF at **EOC**

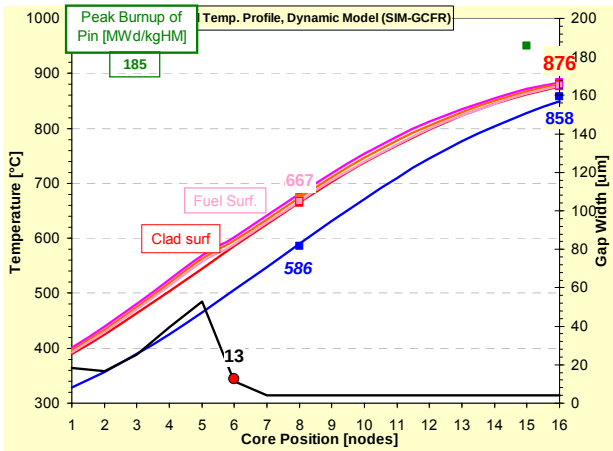


q) Axial peak pin temperature profile 2000 sec into PLOF at **EOC**

Figure 6.2-1**:** Results for P-1a: PLOF transient in EFIT-He at HFP-BOC/EOC (SIM-GFR)

Case 1: Accelerator trip **1** sec after pump trip

***Case 2 (P-1b): Beam trip 3 sec after pump trip***

The question arises what would happen in case the accelerator trip signal would be delayed (~ 3 sec) due to some malfunction during the PLOF transient.

Case 1 was rerun assuming a 3 sec time delay in the scram signal. The observed response of EFIT-He to the PLOF transient under those conditions did not have any significant effect on the transient core temperature response. The maximum fuel temperature at 1000 sec transient time was nearly identical to the case 1 documented above. Thus, the documentation of these calculational results was thus not repeated.

***Case 3: Protected Loss of Coolant Accident (PLOCA) using CATHARE***

This transient was calculated by considering only one DHR loop active.

Following the opening of a leak in the primary circuit, the helium pressure decreases from 70 bar to the containment pressure. Without a guard vessel, the containment pressure is considered to be equal to the atmospheric pressure: about 1bar. In this section, only a small leak leading to a pressure decrease from 70 bar to 1 bar in 15 minutes, is considered. This value corresponds to a depressurization usually considered in a gas-cooled reactor for a “small break”.

As for GFR reactors, the break is detected when the pressure in the plenum is lower than 85% of the initial pressure. Other criteria may activate reactor scram (clad temperature, flow of gas), but for this study, only the pressure signal has been assumed active.

When the emergency trip is actuated, the proton beam and circulator are tripped. The decrease of the primary flow corresponds to the PLOF case.

***This document refers to work being performed by scientists and institutions involved in IP EUROTRANS, as well as the financial support of the European Commission through the contract FI6W-CT-2004-516520.***

Figure 6.2-2a illustrates the depressurization of the primary system due to the leak. The blower DHR starts at the opening of DHR valves, the speed follows the evolution of pressure of the primary circuit, and the flow of the DHR loop follows the same evolution. In this case, with only one DHR loop available, the transient is relatively severe. Nevertheless, the maximum clad temperatures remain below limits (Figure 6.2-2d). The maximum temperature of the hottest assembly goes to approximately 950 °C, decreasing thereafter. The temperature of helium mixed in the upper plenum reached 600 °C before decreasing again.

The core is always properly cooled in case of LOCA with a single active DHR loop. However, it is interesting to note, as shown in Figure 6.2-2c, that for a few moments (about 400 s) the power evacuated is lower than the power generated by the fuel. This occurs when the flow from the blower reaches its minimum (900 s) and stabilizes around 6 kg/s. The rapid temperature decrease observed since from the beginning of the accident is then stopped. Keeping in mind that heat exchanges are degraded for this flow regime at low temperatures and low pressure, the clad cooling becomes insufficient to evacuate all the energy produced by the fuel. The core then starts to heat and temperatures increase. Then, when temperatures are high enough, the correlations of exchanges will restore exchange between the clad and the coolant: the trend is reversed. Having passed through a maximum, temperatures decrease again.

***This document refers to work being performed by scientists and institutions involved in IP EUROTRANS, as well as the financial support of the European Commission through the contract FI6W-CT-2004-516520.***

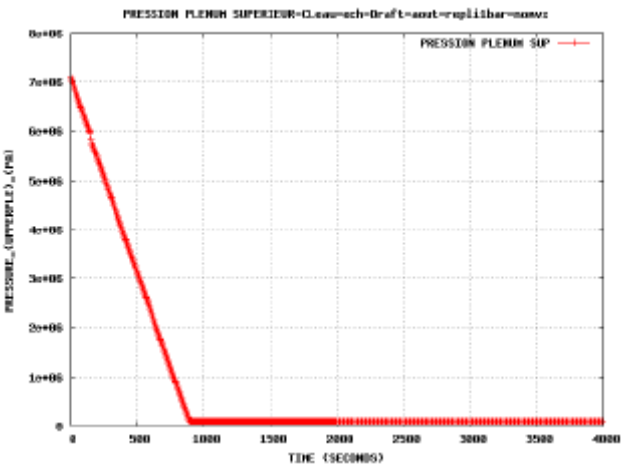


a) Pressure – LOCA - 1DHR

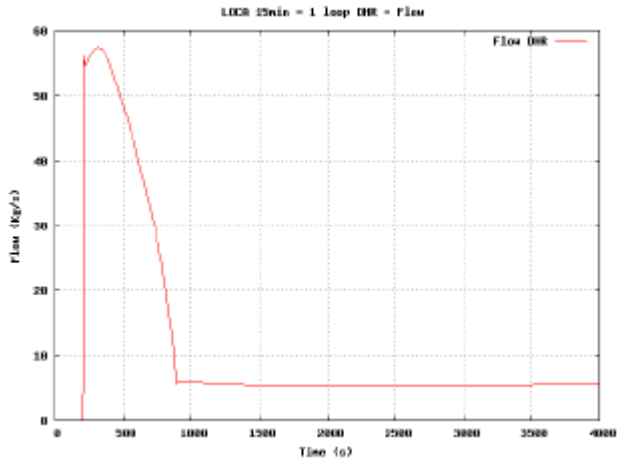


b) DHR Loop Flowrate – LOCA 1DHR

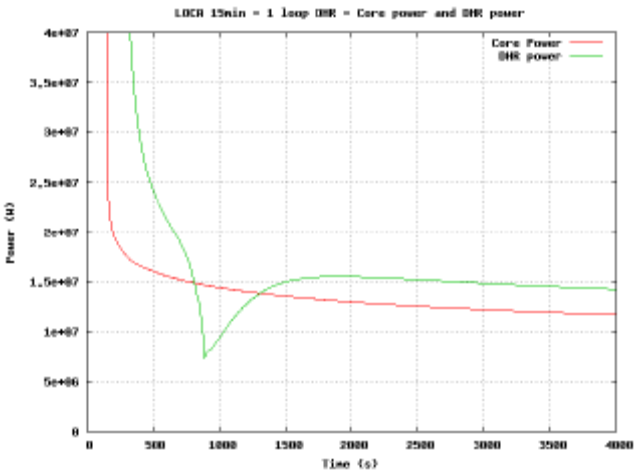


c) Core Power and Power Removed by DHR Loops- LOCA - 1 DHR

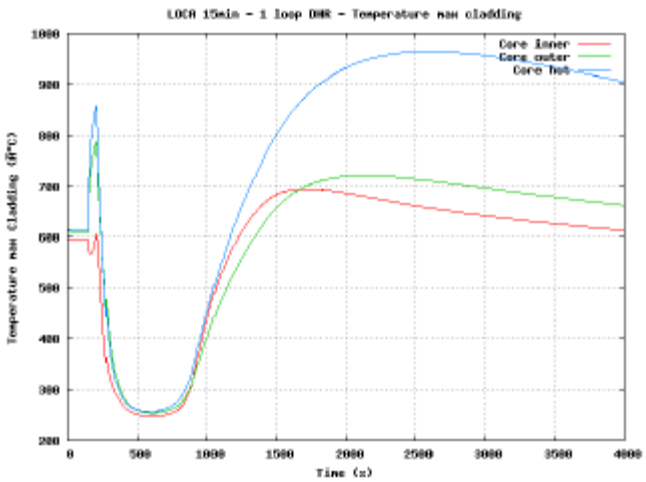


d) Max Clad Temperatures - LOCA -1 DHR

Figure 6.2-2**: Protected Loss of Coolant Accident (PLOCA) using CATHARE**

The response of the EFIT-He plant to various other transient initiators, such as loss of heat sink-LOHS, inadvertent reactivity insertions - TOP, under-cooling, etc. are summarized in Table 6.2-1 and documented in details in D1.44 [6.3]. Listed are the calculated peak temperatures of core fuel, cladding and coolant for the various transients analyzed using the CATHARE, and SIM-LFR system codes.

***This document refers to work being performed by scientists and institutions involved in IP EUROTRANS, as well as the financial support of the European Commission through the contract FI6W-CT-2004-516520.***

### 6.2.2 Other EFIT-He transient studies

The response of the EFIT-He plant to various other transient initiators, such as loss of heat sink-LOHS, inadvertent reactivity insertions - TOP, under-cooling, etc. are summarized in Table 6.2-1 and documented in details in D1.44 [6.3]. Listed are the calculated peak temperatures of core fuel, cladding and coolant for the various transients analyzed using the CATHARE, and SIM-LFR system codes.

Table 6.2 1: Peak cladding, fuel and coolant temperatures in EFIT-He Transients, [ºC]

| | Fuel | Cladding | Coolant* |
|---|---|---|---|
| Steady state BOC | 1160 | 608 | 572 |
| Steady state EOC | 978 | 608 | 572 |
| | | | |
| PLOF (DHR passive) | 950 | 950 | 920 |
| PLOHS @ 1000s | 1400 | 1400 | 1400 |
| PLOHS/LOF @ 600s | 1400 | 1400 | 1400 |
| PTOP (+1400 pcm) | 1660 | 760 | 700 |
| PLOCA: 300cm$^2$ (2 DHR active) | 611 | 605 | 576 |
| PBLOCK (95%) @ 2s trip delay | 950 | 920 | 880 |
| Beam trip (10 s) [1] | 1140 | 590 | 560 |
| | | | |
| ULOF @ 40 s | >1600 | >1400 | >1100 |
| ULOHS @ 80s | 1705 | 1312 | 1280 |
| ULOHS/LOF @ 65s | 1700 | 1403 | 1261 |
| UTOP (+900 pcm) | 1540 | 756 | 700 |
| ULOCA: 300cm$^2$ (2 DHR active) @58s | 1725 | 1400 | 1200 |
| UBLOCK(95%) @ 26s | 1640 | 1400 | 1200 |
| UOVC (-80ºC) @ 300s | 1082 | 530 | 470 |

* Average coolant temperature at the core outlet

[1] Temperature gradients of 80°C/sec and 15°C/sec for fuel and cladding respectively.

The results of the safety analyses demonstrate that the He-cooled EFIT plant as proposed by AREVA/CEA is actually a robust design as regards gas-cooled fast reactor system concepts, ascribable to the combination of plant design features, which, for example are:

1. selection of a robust, steel lined $SiC_f$/SiC fiber for cladding material allowing high cladding temperatures up to 1200 °C, thereby increasing the grace time under extreme transient conditions (i.e. S/A blockage) from a few seconds (for steel cladded pins) to a few tens of seconds (30-50 sec) before critical clad temperatures are reached,
2. a high redundancy of active DHR systems (6) of which only 2 units are required to remove the entire decay heat load of ~ 18 MW (DHR exchangers designed for a maximum helium temperature of 1000°C),
3. low linear fuel pin power rating of 160 W/cm assuring relatively low fuel temperatures,
4. a large height differential between DHR HX and core midplane of 20 m, assuring a sufficiently large natural convection mass flow rate capability in the primary system under nominal (pressurized) conditions in the decay heat mode,
5. a large volumetric primary system (~ 1723 m$^3$) with large masses of structural material providing an effective heat sink (~3000 tons) during heat-up transients (loss of heat sink transients),

*This document refers to work being performed by scientists and institutions involved in IP EUROTRANS, as well as the financial support of the European Commission through the contract FI6W-CT-2004-516520.*

6. a large He inventory of at least 6755 kg of He assuring a slow depressurization rate under LOCA conditions (primary system leakage),
7. simple in-service inspection of the primary system and internal vessel components because of the translucent nature of the coolant,
8. chemically inertness of the coolant – no corrosion products in the primary system are expected,
9. the coolant does not become activated by irradiation,
10. no possible change in phase of the gas coolant,
11. no decommissioning issues associated with the coolant,
12. Helium coolant can be operated under very high temperatures – no disassociation of helium ($CO_2$ disassociates at ~ 800 °C) allowing very high system efficiencies.

Adopting modest linear power ratings for the 2 cores zones of EFIT-He assures that maximum fuel temperatures of the innovative MgO-MA-based fuel are below 1400°C under normal operating conditions which is the limit value recommended by AFTRA (DM3 of the EUROTRANS Project).

| **BOC** | Core Zone 1 | Core Zone 2 |
|---|---|---|
| Average pin:<br>Avg/peak linear power [W/cm] | 40 / 63 | 96 / 122 |
| Peak pin:<br>Avg/peak linear power [W/cm] | 47 / 74 | 126 / 160 |

| **EOC** | Core Zone 1 | Core Zone 2 |
|---|---|---|
| Average pin:<br>Avg/peak linear power [W/cm] | 40 / 62 | 96 / 121 |
| Peak pin:<br>Avg/peak linear power [W/cm] | 47 / 72 | 126 / 159 |

Somewhat less favorable characteristics of the He as coolant are:

1. The much lower heat transfer coefficient (in comparison to liquid metals) between cladding and coolant associated with the gas coolant leading to higher cladding and fuel temperatures, and
2. The much lower thermal inertia of the gas inside the primary system in comparison to liquid metals resulting in a particular sensitivity of the core to all mass flow degradation transients (such as loss of flow, or depressurization), as the stored heat from the fuel will then have to be absorbed by the cladding material (due to the loss of coolant convection), leading by necessity to high cladding temperatures,
3. The requirement that the system must be operated under high pressure conditions (70 bar) in order to increase the density of the gas coolant,
4. The very limited natural convection capabilities under depressurized conditions. The latter mandates active cooling systems to remove the decay heat in the depressurized mode,

***This document refers to work being performed by scientists and institutions involved in IP EUROTRANS, as well as the financial support of the European Commission through the contract FI6W-CT-2004-516520.***

5. Loss of pressure can induce positive reactivity insertions due to voiding (effect is however relatively small: only +500 pcm in EFIT-He),
6. Lack of oxygen leads to triboloy related phenomena, removal of the natural oxide layer of structural materials,
7. Water/Steam ingress into primary circuit due to HX tube failure can induce significant positive reactivity insertions in addition to chemical attacks. This issue is however of limited consequences as large positive reactivity insertions are known to be inherently accommodated by sub-critical systems.

Other issues to notice are:

1. The rather badly known behaviour of the $SiC_f$/SiC fiber cladding (SiC material is brittle like other ceramic materials, but $SiC_f$/SiC as composite material might better behave which needs to be confirmed by further studies). The porous nature of the $SiC_f$/SiC cladding material requires a thin inner steel liner (tungsten, or similar very high temperature metallic materials) to assure confinement of fission products. This type of innovative cladding material and pin design must first be rigorously tested and qualified out-of-pile as well as in-pile before its large scale application can be considered feasible. This issue is being addressed in the on-going developmental activities for the critical gas-cooled reactor, that will provide information on the potential use of $SiC_f$/SiC material for the core of nuclear power plants.
2. The relatively large fuel inventory of about 9.5 tons, consisting of about 5t of Am, 3.8t of Pu, and 233 kg of Cm in addition to 210 kg of Np.
3. The impact of the MA fuel on the critical safety parameters of fast reactor systems, namely the Doppler feedback coefficient, expressed by the Doppler constant (~ -81 pcm for EFIT-He, compared to about -800pcm for a typical FBR plant) and the reduced delayed neutron fraction beta (148 pcm for the EFIT MA-fuel compared to 360 pcm for typical MOX-fueled FBRs).

### 6.2.3 EFIT-He safety studies summary

### 6.2.4 Plant behaviour under transient conditions

The safe operation of the EFIT-He system, loaded with significant quantities of minor actinide inventories, must therefore be of paramount interest. The EFIT-He system is therefore made sub-critical (because of the degraded safety coefficients, namely Doppler, and beta). Nonetheless, failure of fuel pins under normal or abnormal plant conditions should be avoided to the extent possible to prevent contamination of the primary He loop with actinide fuel.

The very positive feature of sub-critical systems is their insensitivity to very large incidental reactivity insertions (either due to fuel handling errors, voiding, core compaction, steam ingress, $CO_2$ ingress, etc.). The sub-critical level is defined in order to be immune to transients of this nature. Therefore, the monitoring of the sub-critical level is a key safety issue.

The other side of the coin however is the known unfavorable characteristics of sub-critical system to “unprotected” transients, as their power level is basically remaining at nominal conditions (~ 100%) as negative feedback reactivity effects do not have much impact in depressing the power level. Critical reactors respond much more favorable under similar transient conditions.

It is a known feature of sub-critical systems, that their transient response to “unprotected” transients is more challenging than under critical reactor conditions. For sub-critical system, negative reactivity due to the various temperature feedbacks essentially does not depress the power level. The power remains largely above 90% under “unprotected” transient conditions (for $K_{eff}$ ~ 0.97), making it particularly challenging for any reactor system to demonstrate that such transients can be accommodated.

*This document refers to work being performed by scientists and institutions involved in IP EUROTRANS, as well as the financial support of the European Commission through the contract FI6W-CT-2004-516520.*

EFIT-He however is not expected to be able to accommodate these types of transients as the nature of the gas coolant does not provide for a sufficient heat sink/heat buffer thereby effectively limiting increases in cladding temperatures. The $SiC_f$/SiC clad material is however expected to be able to sustain temperatures up to 1200°C, thereby relaxing the ~800°C temperature limit considered for steel cladding. The 1200°C temperature limit of $SiC_f$/SiC provides a significantly longer grace time for implementing diverse accelerator shut-off provision such as an effective manual (operator) intervention. Under "unprotected" LOF conditions, up to 40 sec grace time is available before clad temperatures reach ~ 1400°C. It can be considered sufficient grace time as pump speed and primary flow are decreasing during the first 10 sec of this transient to below 30% providing sufficient information to the operator in the control room to immediately activate manual reactor scram by tripping the beam.

The transients investigated in this study are intentionally taking the plant system into domains that are extremely unlikely to occur in order to investigate the intrinsic safety characteristics of the core in combination with the design of the plant. Transients, taking the fuel intentionally into the failure domain are investigated in order to determine grace time periods available for determining the likelihood of manual operator intervention.

It is judged, that the favorable features associated with He as coolant compensates the less positive features as these can be largely controlled by means of intelligent plant and system design. Not all issues however can be counterbalanced (i.e., such as the requirement for active cooling systems in the depressurized plant state, implying the assured availability of electrical power supply, e.g. by pony motors).

This study demonstrates, that core and primary system temperatures can be kept below critical failure limits for most transients as the established features, in particular the $SiC_f$/SiC cladded pins (higher thermal heat capacity of the $SiC_f$/SiC in comparison to steel, and high maximum allowable temperatures in the range of 1200°C) avoid clad failure under the more likely transient conditions, thus preventing release of radioactivity into the primary system.

The study shows, that the EFIT-He system accommodates all "protected" transients. Under normal pressurized conditions, natural convection provided by the DHR system is sufficient to maintain primary system temperatures below 1000°C.

Decay heat removal is assured by the 6 available DHR systems, only 2 of which are required for the removal of decay heat (~ 18 MW) as each DHR system is designed to reject 9 MW of heat (6x50% strategy). The DHR blowers are designed to operate (active) under all pressure conditions: from 70 bar (nominal plant conditions) to the depressurized state (ambient pressure conditions).

For the 95% SA blockage event, it was shown that the scram delay can be up to 6-7 sec without clad or fuel temperatures becoming excessive. This is significantly more grace time available than in steel cladded He-cooled systems in which this scram delay could not be more than 2 sec.

In general it was observed that the clad and fuel temperature gradients during transient conditions were significantly mellower than for conventional steel cladded MOX fuel pin. That positive feature is ascribable to the higher heat capacity of the $SiC_f$/SiC cladding material as well as the higher heat capacity of the CERCER fuel mixture in comparison to simple MOX fuel.

#### 6.2.5 Core safety features

Potential positive reactivity insertions due to fuel handling errors during refueling procedures, heat exchanger tube rupture (MHX or DHR-HX), depressurization, or earthquake induced core compaction are enveloped by a ~ +1400 pcm TOP transient. Transient calculations of inserting 900 pcm under different plant state conditions (HFP, CZP) have clearly demonstrated that reactivity insertions of this

*This document refers to work being performed by scientists and institutions involved in IP EUROTRANS, as well as the financial support of the European Commission through the contract FI6W-CT-2004-516520.*

magnitude have little impact on either clad or fuel temperatures of the system (with nominal $K_{eff}$ ~ 0.97). All sensitive temperatures have been shown to remain below design limits. Clad failure is thus not expected even under these most extreme conditions, even though MgO-based fuel decomposition must be expected. This may require that the fuel may have to be replaced for continued plant operation, but no safety related issue is to be expected (unless MgO-based fuel decomposition should lead to unexpected fuel pin overpressurization).

The effect of degraded reactivity coefficients (Doppler coefficient, reduced delayed neutron fraction to ~ 150 pcm) due to the large inventories of minor actinides (Am, Cm) has been shown to be of no impact as the system is sufficiently sub-critical ($K_{eff}$ ~ 0.9735). The effect of practically no fuel temperature reactivity feedback (Doppler = -81 pcm) is shown to be a positive feature under sub-critical system conditions, as no reactivity swing during plant load conditions need to be taken into account (taking the plant from HFP to CZP, or even hypothetically to ambient temperatures). The combination of fuel and core design also exhibits a very small burn-up reactivity swing that is also a positive feature as the level of sub-criticality remains essentially unchanged when going from the BOC to the EOC core state. This also simplifies the response of the EFIT-He plant to all transient conditions as the dynamic response of the system will be nearly the same for both BOC and EOC plant states, in particular as the reactivity coefficients have also been shown to remain essentially unchanged when going from BOC to EOC.

In general, the safety analysis performed for the EFIT-He design demonstrated that the EFIT-He can be operated safely, as long as reliance on active cooling systems can be assured under all conditions, in particular under accidental depressurized conditions.

With the exception of the total sub-assembly blockage transient, most unprotected transients allow some grace time before manual corrective actions have to be taken.

EFIT-He can be judged to be a “safe” reactor design in accordance with its mission of using a large inventory of unique minor actinide transmutation fuel (Am, Cm) with its associated large in-core actinide radionuclide inventory.

It must first, however, be demonstrated, that the combination of the innovative cladding material $SiC_f$/SiC in conjunction with a very innovative fuel (MA-MOX-MgO mixture) is a viable incore concept under realistic power generation load conditions.

## 6.3 Safety status of XT-ADS plant

### 6.3.1 Safety approach for the XT-ADS plant

Just like for the EFIT-Pb core and to be able to demonstrate the operation of an ADS plant, the XT-ADS has been designed to prevent uncontrolled nuclear flux increases both during normal operating conditions as well as during abnormal and accidental plant conditions, including Design Extension Conditions. A series of reactivity effects have been investigated. Both those present in normal operation (going from cold to hot conditions and vice versa) and those in incidental situations (target voiding, sub assembly voiding, core compaction).

The proof that this is achieved has already been presented in Section 5 and reference [5.17] on both the fresh core (68 sub assemblies) as well as the equilibrium core (72 sub assemblies). Contrary to the EFIT-Pb, going from the operational condition to the hot zero power state (200°C), gives a significant contribution because here, the Doppler effect is important. This is a bit akward since an ADS is usually designed to cope with a core without significant feedback effects just like a Doppler from a MOX core.

*This document refers to work being performed by scientists and institutions involved in IP EUROTRANS, as well as the financial support of the European Commission through the contract FI6W-CT-2004-516520.*

For what concerns accidental conditions, core compaction, target voiding and (partial) core voiding are studied. The core compaction reactivity effect is equal to 1862 pcm in those conditions. As LBE is considered as a shock absorber, this value is certainly overestimated but can be considered as envelope for reactivity insertion. Safety limits from ERANOS calculations are given in Table 5-3. With all these possible reactivity insertions, a value of 0.95 for $K_{eff}$ offers a safe margin from criticality, including nuclear data & technology uncertainties on one side and reactivity measurements on the other side. A margin of 5000 pcm from criticality has been assessed to be adequate during refueling for the controlled and continuously monitored refueling operations of the reactor. An adequate instrumentation and signal analysis is required to monitor the reactivity in all those conditions.

The scope of the transient analysis performed for XT-ADS encompasses Design Base Condition (DBC) and several Design Extension Condition (DEC) events [6.1]. The DEC events, in general, assume that the accelerator, providing the source neutrons, can not be shut off (unprotected events).

A list of design base condition and design extension condition events was defined [6.2].

The approach adopted was to employ several system computer codes, when possible. The procedure then was to compare the results obtained by the different codes to determine the consistency of the calculated temperatures and pressures of the plant, in particular the core region.

Most of the transients were analyzed for both protected and unprotected assumptions. Since there are no control rods foreseen in the XT-ADS design for the purpose of reactor shutdown, the protected transients implied that the accelerator will be tripped as soon as certain limit conditions were reached in the reactor system (e.g. source or neutron flux level, temperatures). The unprotected cases assumed that it was not possible to shut off the accelerator. The unprotected transients are, thus, equivalent to the ATWS (Anticipated Transients Without Scram), which are analyzed for the LWR systems, however, they are generally defined as design extension conditions

A typical example of the transient analysis performed for the XT-ADS plant is the unprotected loss of flow (ULOF) transient, as calculated by SCK-CEN using the RELAP5 system code [6.4], and KIT using the SIM-LFR code [6.3].

### 6.3.2 XT-ADS ULOF transient studies

At accident initiation:

- The pumps are tripped: pumps are fully stopped after 30 s.
- The air velocity in the tertiary system becomes controlled by the power released by the core and transferred to the primary coolant. The control is based on a pre-calibration (the same as for the PLOF).

The beam is not tripped. Consequently the core power and the spallation loop power are kept at their nominal values (reactivity feedback effects are neglected in RELAP5 calculations, not so in SIM-LFR which takes reactivity feedbacks into account). All condenser lines are also maintained in operation.

The power in different parts of the whole system is plotted in Figure 6.3-1:

- $P_{core}$ : power developed in the core
- $P_{sp}$ : power developed in the spallation loop
- $P_{HX}$ : power removed by the PHXs from the primary system
- $P_{cond}$ : power removed by the condensers from the secondary system

The core power $P_{core}$ and the spallation power $P_{sp}$ remain constant due to the unprotected character of the transient.

*This document refers to work being performed by scientists and institutions involved in IP EUROTRANS, as well as the financial support of the European Commission through the contract FI6W-CT-2004-516520.*

During the first phase of the transient the power $P_{HX}$ removed by the PHXs decreases very rapidly in 30 s up to 17 MW before recovering its nominal value about 520 s later. The power fall coincides with the pump coast-down: $P_{HX}$ being proportional to the primary mass flow rate, it decreases with the latter one. Later the LBE temperature in the primary system progressively rises due to the deficit of heat removal via the PHXs until a new equilibrium is reached in the energy balance between generated heat and evacuated heat.

The power transient in the PHXs is transmitted to the secondary cooling system and to the condensers, but with some softening effect.

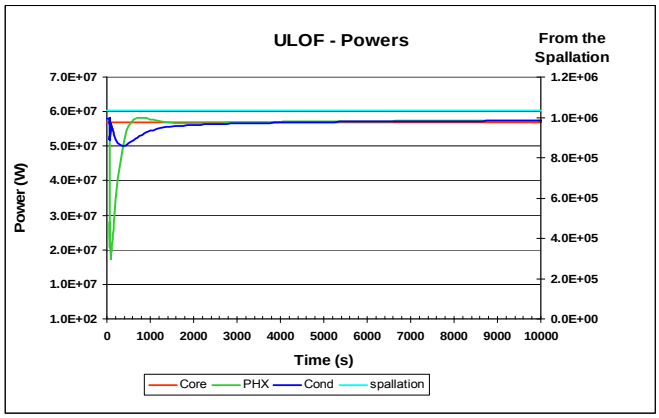


Figure 6.3-1: ULOF - Powers in the primary, secondary and tertiary systems

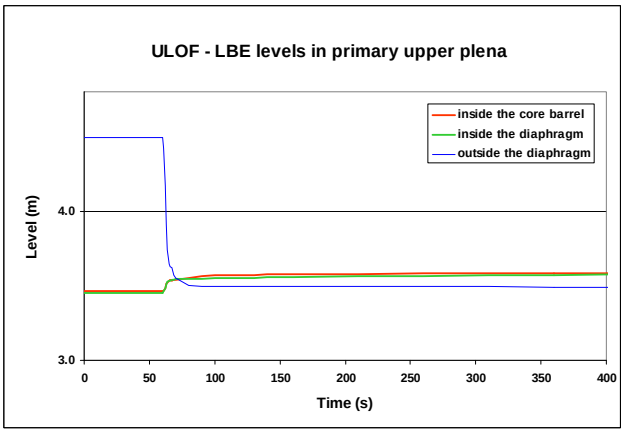


Figure 6.3-2: ULOF - LBE levels in the upper plena

The LBE levels in the different upper plena tend to equalize during the pump coast-down (see Figure 6.3 2).

The evolution of the mass flow rates in the primary system is given in Figure 6.3 3. Forty seconds after the pump trip, the total mass flow rate in the core is about 1090 kg/s (~18% of the nominal value). The distribution of the total core mass flow rate between its different components is given in Figure 6.3 4.

*This document refers to work being performed by scientists and institutions involved in IP EUROTRANS, as well as the financial support of the European Commission through the contract FI6W-CT-2004-516520.*

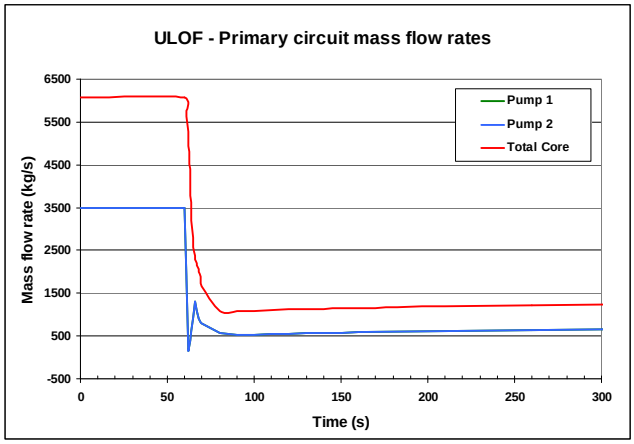


Figure 6.3-3: ULOF - Core and pump mass flow rates in the primary circuit

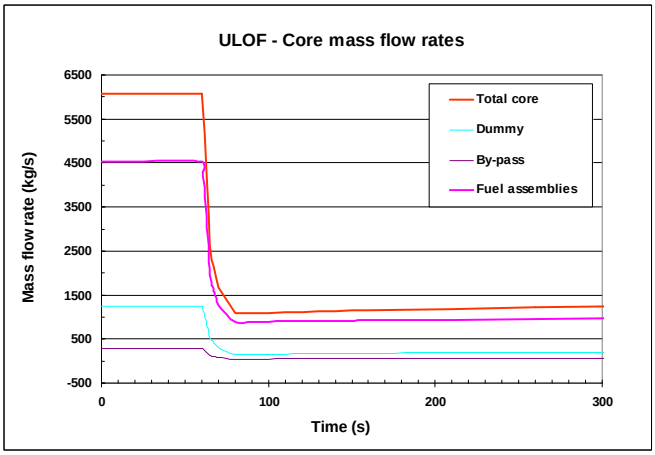


Figure 6.3-4: ULOF - Core mass flow rates

Figure 6.3 5 shows that the LBE temperature at the core outlet undergoes a relatively fast increase of about 280°C in 80 seconds, while the temperature at the core inlet practically does not change during the first phase of the transient. A small decrease (30°C) of this inlet temperature is initiated after 200 s following the pump trip; this is coherent with the LBE temperature decrease at the PHX outlet (see further), but with some delay (residence time in the lower plenum) and some attenuation (dilution effect of the lower plenum).

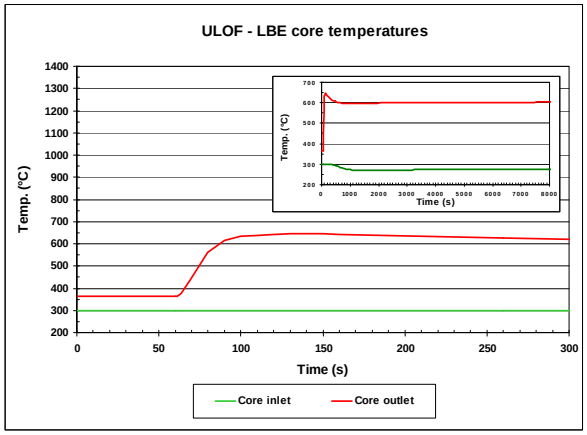


Figure 6.3-5: ULOF - LBE temperature at core inlet and outlet

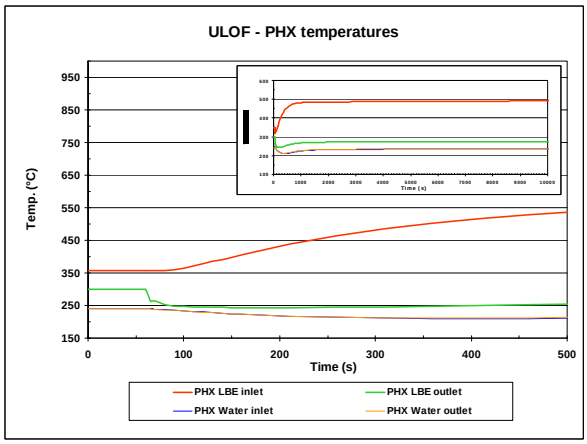


Figure 6.3-6: ULOF - LBE and water temperatures at PHX inlets and outlets

A similar observation can be made for the LBE temperature at the PHX inlet (see Figure 6.3 6). It increases like the LBE temperature at the core outlet with some delay (residence time in the upper plena) and with some attenuation (dilution effect of the upper plena). The LBE temperature at the PHX outlet first decreases because of the flow rate reduction. Later it evolves similarly to the water

*This document refers to work being performed by scientists and institutions involved in IP EUROTRANS, as well as the financial support of the European Commission through the contract FI6W-CT-2004-516520.*

temperature at the secondary side (small increase followed by a stabilization corresponding to the free convection regime).

The maximum fuel temperature, located in the centre line of the hottest fuel pin and at the level of the reactor mid-plane, does not exceed 1878 °C after 50 s of the transient, i.e. significantly below the safety criterion for the fuel (2400 °C). The maximum clad temperature however increases to 865 °C before stabilizing around 815 °C. This is above the safety criterion for the cladding (max. 800 °C not longer than 30 min.), but it concerns only the hottest fuel pin. Moreover, taking the conservative character of some assumptions, in particular a constant core power resulting from the fact that the reactivity feedback effects are neglected, we may conclude that the damages to the core - if any – would be limited to some fuel pins.

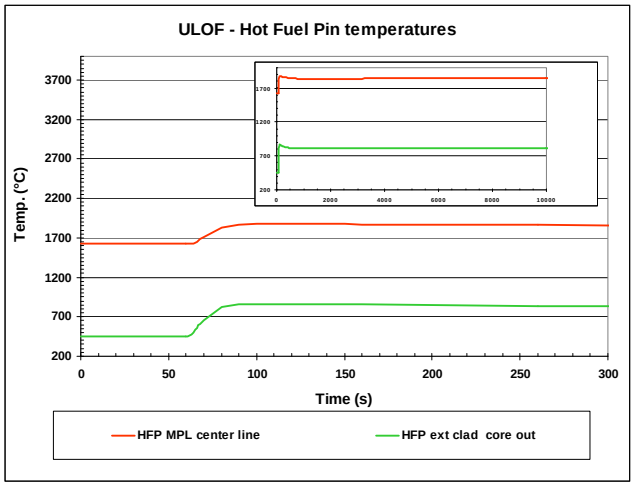


Figure 6.3-7: ULOF - Maximum fuel and clad temperatures (in hottest fuel pin)

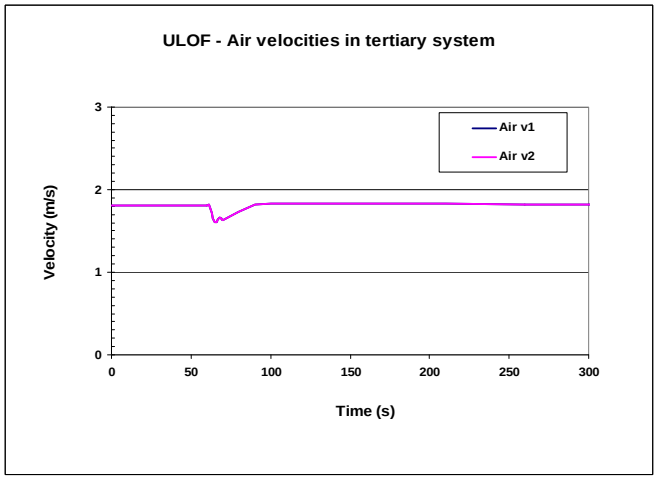


Figure 6.3-8: ULOF – Air velocities in the chimneys

As expected, the response of the primary cooling system to an unprotected loss of flow accident is much more constraining for the core, more precisely for the cladding of the fuel elements, than in the protected case. If the fuel temperatures remain much lower than the fuel safety criterion, the cladding temperatures however flirt with the maximum permitted value and even it exceeds this value in the hottest fuel elements. Nevertheless the damages to the core would be very limited and we may conclude that the core is surviving a ULOF. Owing to the fact that a ULOF in principle should not persist for a long time, the coolant temperature is fully acceptable and potential corrosion problems are not considered to be of significance.

This ULOF transient also demonstrated the very slow response of a secondary cooling system working in natural circulation mode to return to the nominal state conditions after deviation from the HFP.

### 6.3.3 XT-ADS other DBC and DEC transient studies

The response of the XT-ADS plant to various other transient initiators, such as loss of heat sink-LOHS, inadvertent reactivity insertions - TOP, under-cooling, etc. are summarized in Table 6.3-1 and documented in details in D1.42 [6.1]. Listed are the calculated peak temperatures of core fuel,

*This document refers to work being performed by scientists and institutions involved in IP EUROTRANS, as well as the financial support of the European Commission through the contract FI6W-CT-2004-516520.*

cladding and coolant for the various transients analyzed using the RELAP5 [6.4], SIMMER [6.5], TRACE/FRED [6.6] and SIM-LFR system codes [6.3]. The results as calculated by the various code systems are observed to be intrinsically consistent and in good agreement considering that each code system has its own code specific particularities, boundary conditions and modeling constraints.

Table 6.3-1 Peak temperatures of Materials in XT-ADS Transients, [ºC]

| | Transient Description | | Code System | Temperatures [°C] | | |
|---|---|---|---|---|---|---|
| | | | | **Fuel** | **Cladding** | **Coolant*** |
| | Steady state BOC | | SIM-LFR | 1385 | 440 | 421.5 |
| | Steady state BOC | | TRACE/FRED | 1343 | 433 | 416 |
| | Steady state EOC | | SIM-LFR | 1709 | 467 | 424 |
| | | | | | | |
| P-1 | PLOF | @ 2s trip delay | RELAP | nominal | < nominal | < nominal |
| P-1b | PLOF | @ 2s trip delay | SIM-LFR | nominal | 518 | 472 |
| P-1c | PLOF shaft break, | @ 2s trip delay | SIM-LFR | nominal | 862 | 854 |
| P-2 | PTOP | @ (HFP: +2500 pcm) | SIM-LFR | 2086 | 564 | 495 |
| P-3 | PTOP | @ (CZP: +1400 pcm) | SIM-LFR | 210 | 202 | 202 |
| P-4 | PLOHS | @ 2000s | RELAP | < nominal | < nominal | < nominal |
| | PLOHS | @ 2000s | SIM-LFR | 388 | 350 | 348 |
| P-5 | PLOHS/LOF | @ 2000s | RELAP | < nominal | < nominal | < nominal |
| | PLOHS/LOF | @ 2000s | SIM-LFR | 400 | 378 | 377 |
| P-7 | POVC | @ -80°C in 850s | RELAP | < nominal | < nominal | < nominal |
| | POVC | @ -150°C in 250s | SIM-LFR | 1670 | 465 | 420 |
| P-8 | PBLOCK | @ 97.5%, 2s trip delay | SIM-LFR | 1120 | 927 | 920 |
| P-10 | Beam trip (1 s) [1] | @ BOC | SIMMER | -303 °C/s | -38 °C/s | -29 °C/s |
| | Beam trip (1 s) [1] | | SIM-LFR | -190 °C/s | -17 °C/s | |
| | | | | | | |
| U-1 | ULOF | @ BOC: I = 20 / 100 kg m$^2$ | SIMMER | < 1600 | 916 / 871 | 877/829 |
| U-1 | ULOF | @ BOC | TRACE/FRED | 1488 | 987 | 904 |
| U-1 | ULOF | @ 50 s | RELAP | 1878 | 865 | |
| U-1b | ULOF | @ 40 s | SIM-LFR | 1873 | 980 | 956 |
| U-1c | ULOF shaft break | @ 22s | SIM-LFR | 1907 | 1069 | 1053 |
| U-2 | UTOP | @ BOC+HFP:+900 pcm | SIMMER | 1479 | 481 | 435 |
| | UTOP | @ EOC+HFP:+900 pcm | SIMMER | 1789 | 491 | 434 |
| | UTOP | @ BOC+HFP:+900 pcm | TRACE/FRED | 1401 | 441 | 394 |
| | UTOP | @ (HFP:+2500 pcm) | SIM-LFR | 2087 | 574 | 514 |
| | UTOP | @ BOC+HFP:+2500 pcm | TRACE/FRED | 1527 | 458 | 405 |
| U-3 | UTOP | @(CZP: +2500 pcm) | SIM-LFR | 210 | 199 | 199 |
| U-4 | ULOHS | @ 2400s | RELAP | ~2100 | ~900 | ~880 |
| | ULOHS | @ 2500s | SIM-LFR | 1744 | 891 | 856 |
| | ULOHS | @ 2500s BOC | TRACE/FRED | 1450 | 672 | 647 |
| U-5 | ULOHS/LOF | @ 1400s | RELAP | ~2100 | ~1400 | ~1260 |
| | ULOHS/LOF | @ 2500s | SIM-LFR | 1865 | 1122 | 1099 |
| | ULOHS/LOF | @ 2500s BOC | TRACE/FRED | 1593 | 1017 | 993 |
| U-7 | UOVC | @ -150°C in 400s | SIM-LFR | 1627 | 445 | 405 |
| U-8 | UBLOCK no rad ht | @ 97.5%, in 15s | SIM-LFR | 2110 | 1442 | 1428 |
| U-9 | UBLOCK rad. ht | @ 97.5%, BOC | SIMMER | SA failure remains localized, no spreading | | |
| U-11 | UBeam | @ (HFP: 120%) | SIM-LFR | 1766 | 490 | 443 |
| | UBeam | @ (HFP: 120%) BOC | TRACE/FRED | 1479 | 451 | 401 |
| | UBeam | @ (HFP: 200%) | SIMMER | 2087 | 592 | 520 |
| | UBeam | @ (HFP: 200%) BOC | TRACE/FRED | 1910 | 514 | 444 |

***This document refers to work being performed by scientists and institutions involved in IP EUROTRANS, as well as the financial support of the European Commission through the contract FI6W-CT-2004-516520.***

| | Transient Description | Code System | Temperatures [°C] | | |
|---|---|---|---|---|---|
| | | | **Fuel** | **Cladding** | **Coolant*** |
| U-12 | UBeam @ (CZP: 100%) | SIM-LFR | 1710 | 464 | 423 |

* Average coolant temperature at the core outlet.

[1] Maximum temperature gradients.

HFP = Hot Full Power

CZP = Cold Zero Power

The results of the safety analyses demonstrate that the LBE-cooled XT-ADS plant is a very robust design that is ascribable to the unique combination of inherent and plant design features, namely:

1. the favorable thermophysical properties of the coolant LBE
   - very high boiling temperature,
   - reasonable value for the melting temperature,
   - high specific heat and thermal expansion coefficient,
   - good heat transfer characteristics,
2. the high thermal inertia, or large heat sink / heat buffer characteristics associated with the coolant LBE as reflected by:
   - the large coolant mass times heat capacity in the core region,
   - the large coolant mass times heat capacity in the primary system (pool type design),
3. the large natural convection characteristics of the plant design due to:
   - the favorable sub-assembly design ( pin diameter and pitch ),
   - the large height difference between heat source (core) and heat sink (IHX), namely ~ 2 meters,
4. and modest liner power ratings:
   - peak pin averaged linear power rating = 190 W/cm,
   - peak power rating = 228.1 W/cm under BOC, or 233.6 for EOC conditions

Somewhat less favorable characteristics of the LBE as coolant which have not been studied in these transient analyses and which would require further assessment are:

1. Production of considerable amounts of radioactive $^{210}$Po and “black dust” (forming macroscopic slaggs) in the reactor cavity,
2. The high corrosion rate of LBE as a coolant. This requires that all sensitive components within the primary system, in particular within the core region, are continuously covered by a protective oxide layer ($Fe_3O_4$). The thickness of this oxide layer needs to be tightly controlled (by controlling the oxygen concentration) in order not to degrade the heat transfer characteristics of these surfaces excessively, leading possibly to local clad burnout in case the oxide layer should accumulate to thicknesses above 100 [μm]. Of particular sensitivity remains the cladding material,
3. The possible requirement for treating the sensitive components (such as cladding surfaces) by imparting a layer of aluminum onto these surfaces (GESA treatment) acting as a protection against the corrosion of flowing lead. GESA treatment could mitigate the requirement for oxide layering, and
4. Assuring the long-term integrity of the protective layer (either oxide or aluminum) under all plant transient conditions, in particular frequent beam trips,

***This document refers to work being performed by scientists and institutions involved in IP EUROTRANS, as well as the financial support of the European Commission through the contract FI6W-CT-2004-516520.***

5. Preventing excessive accumulation of lead oxide that could possibly lead to fouling and slagging of the entire primary system, potentially leading to core blockages in case the lead oxide concentration in the LBE loop is not very tightly monitored and controlled. Active and continuous removal of excessive lead oxide must be assured.

Potential positive reactivity insertions due to fuel handling errors during refueling procedures, steam generator tube rupture, or due to core voiding are enveloped by ~ +500 pcm, whereas the reactivity insertion potential for earthquake transients is enveloped under most pessimistic assumptions by ~ + 1500 pcm. Transient calculations of inserting 2500 pcm under different plant state conditions (HFP, CZP) have clearly demonstrated that reactivity insertions of this magnitude have little impact on either clad or fuel temperatures of the XT-ADS system. All sensitive temperatures have been shown to remain below design limits.

#### 6.3.4 XT-ADS overall safety assessment studies

The combination of the favorable features of LBE as a coolant assures that the core damage frequency is estimated to be very low (but probability values would have to be estimated for a safety dossier taking into account all events associated to the less favorable characteristics of the LBE as coolant) and that the core and primary system temperatures for almost all scenarios are below the temperature limits established to avoid clad failure and thus release of radioactivity into the primary system.

The transient response of the XT-ADS to the ULOF transient is as designed in that no pin failures are expected as the fission gas pressure under EOC conditions is calculated to be relatively low (24 bar) under nominal power conditions due to the low burnup (44.6 MWd/kg) of the most highly loaded pin (peak linear power rating = 234 W/cm). An issue might arise as regards a potential flow undershoot during the ULOF transient which is however expected to be quite mellow in the XT-ADS due to the particular design characteristics of the primary system.

There were only a very few transients in which the core conditions could approach clad melting or release of radioactivity. Principally among these was the almost complete blockage of a subassembly without accelerator trip, where there may be insufficient time available for affecting the trip manually as clad failure will be reached within 15 sec transient time. Instrumentation of the individual subassemblies will allow timely detection of subassembly blockages. If the trip signal is generated within 2.5 sec after excessive core outlet temperatures are reached, clad failure can be prevented.

The SIMMER analysis have also shown, that single subassembly blockage and failure will not lead to propagation to neighboring subassemblies, thereby limiting core damage to a single subassembly [6.5].

The other class of transients of concern is that of unprotected operation with complete loss of heat sink with and without the operation of the primary pumps. In these postulated transients there may be more than half hour available for terminating the operation of the accelerator manually as the primary system heatup rates of less than 10 °C/min are calculated.

As freezing of LBE must be avoided under all circumstances (in order to assure continued coolant flow throughout the primary system, in particular coolant flow through the core region), the secondary feedwater conditions (either feedwater inlet temperature, or feedwater mass flow rate) under transient conditions must be carefully monitored to assure secondary temperature above the melting point of LBE, namely 125 °C.

Theoretical limits for the release of polonium, caesium, strontium and iodine in the case of a postulated core disruptive event have been determined in the LBE-cooled XT-ADS design [6.8].

***This document refers to work being performed by scientists and institutions involved in IP EUROTRANS, as well as the financial support of the European Commission through the contract FI6W-CT-2004-516520.***

The determined upper limits are dependent on coolant temperature and the degree of contamination. In order to determine the absolute upper limits for release of radiotoxic vapours, a hypothetical case is being studied where the entire fission product inventory of a specified number of peak burn-up subassemblies has disintegrated. For the XT-ADS core, the designated reference scenario involves three peak burn-up subassemblies that are assumed to be entirely dissolved into the coolant, and the resulting volatilisation of selected radiotoxic isotopes is estimated as function of coolant temperature.

The results show that interaction with lead-bismuth strongly suppresses the release of the fission products investigated. The release of polonium is similarly suppressed, mitigating the issue of $^{210}$Po production in the coolant. Under normal operating conditions, $^{210}$Po is of course the sole important contributor to the radioactivity of the vapours over the coolant; however, assuming the dispersion of a few subassemblies into the coolant, $^{131}$I will dominate over all other isotopes by about two orders of magnitude.

The activity of $^{210}$Po might be of some concern [6.9] in the Cover Gas is strongly dependent on the LBE temperature. For high temperatures (above 1000K), high values of effective dose are mainly due to $^{210}$Po. Since it is an alpha emitter it contributes strongly to the dose due to inhalation and ingestion and the highest values are thus found with the German methodology since it takes into account both inhalation and ingestion. It must be noted that since $^{210}$Po dominates the dose, and is present in the coolant, the source term in case of accident would not depend significantly on the extent of fuel damage.

Nothing can be done to lower the activity of noble gases, but means to reduce the activity of Iodine in the containment (sprays) and to remove Polonium should be considered.

REFERENCES

[6.1] “Approach and Acceptance criteria for Safety Design of XT-ADS”, Deliverable D1.20 of the EUROTRANS project, KIT report, 2009.

[6.2] M. Schikorr, Preparation of analysis of DBC transients for XT-ADS Design, Deliverable D1.22 of the EUROTRANS project, KIT report, 2009.

[6.3] W. M. Schikorr, Assessment of the kinetic and dynamic transient behavior of subcritical systems (ADS) in comparison to critical reactor systems, Nuclear Engineering and Design 210, 95-123, 2001.

[6.4] S. Heusdains, B. Arien „ RELAP model of XT-ADS. Transient Analysis”, SCK•CEN report, February 2010.

[6.5] X.-N. Chen, D. D’Andrea, C. Matzerath Boccaccini, W. Maschek, A. Rineiski „ SIMMERIII, Steady State and Transient Calculations and Theoretical Modeling of ULOF”, Contribution to XT-ADS Deliverable D1.42, January 2010.

[6.6] K. Mikityuk “XT-ADS Transient Analysis with the TRACE/FRED Code”, Contribution to XT-ADS Deliverable D1.42, March 2010.

[6.7] M.Schikorr, E. Bubelis, Report on the results of analysis of DBC & DEC transients for XT-ADS, Deliverable D1.42 of the EUROTRANS project, KIT report, 2010.

[6.8] M.Jolkkonen, “Report on Source Term Assessment for XT-ADS”, Deliverable D1.62-64 of the EUROTRANS project, KTH report, 2009.

[6.9] R. Brucker, “Report on Containment Assessment for XT-ADS”, Deliverable D1.63 of the EUROTRANS project, EA report, 2009.

***This document refers to work being performed by scientists and institutions involved in IP EUROTRANS, as well as the financial support of the European Commission through the contract FI6W-CT-2004-516520.***

[6.10] Approach and Acceptance criteria for Safety Design of EFIT and Backup Gas option,

[6.11] Report on the results of analysis of DBC & DEC transients for the lead cooled EFIT, Deliverable D1.43 of the EUROTRANS project

[6.12] .G. Bandini, P. Meloni, M. Polidori „ Report on the Results of Analysis of DBC & DEC, Transients for the Lead-Cooled EFIT Reactor", ENEA report, March 2009;

[6.13] P. Liu, M. Flad, X-N. Chen, F. Gabrielli, W. Maschek, A. Rineiski, S. Wang „SIMMER-III Transient Calculations", Contribution to EFIT Deliverable D1.43, December 2008.

[6.14] W. Maschek et al. "Design, Safety and fuel developments for the EFIT accelerator driven system with CerCer and CerMet cores", 10th OECD Nuclear Energy Agency Information Exchange Meeting on Actinide and Fission Product Partitioning and Transmutation (IEMPT), October 6-10, 2008, Mito (Japan).

[6.15] W. Maschek, X. Chen, T. Suzuki, A. Rineiski, C. Matzerath Boccaccini, Mg. Mori , K. Morita, "A Review on Safety Issues and Analysis Tools for Accelerator Driven Systems and Transmuters", ICONE-13, Bejing, China, May 16-20, 2005.

[6.16] A. Rineiski, Decay heat production in a TRU burner, Progress in Nuclear Energy 50 (2008), pp. 377-381.

[6.17] A. Rineiski, G. Rimpault, Decay Heat Benchmark for EFIT cores, WP1.1 Non-contractual document, EUROTRANS, FI6W-CT2005-516520, October 2009

[6.18] Report on the results of analysis of DBC & DEC transients for the gas cooled EFIT, Deliverable D1.44 of the EUROTRANS project

[6.19] J. F. Pignatel "Evaluation du Coeur 2 Zones du Réacteur ADS EFIT-Gaz avec COPERNIC et CATHARE", CEA report No. CEA/DEN/CAD/DER/SESI/LCSI/NT DO2, 23 June 2009.

***This document refers to work being performed by scientists and institutions involved in IP EUROTRANS, as well as the financial support of the European Commission through the contract FI6W-CT-2004-516520.***

# 7. CONSISTENCY OF THE DIFFERENT CONCEPTS WITH THE ETD OBJECTIVES

## 7.1 EFIT-Pb design

### 7.1.1 Current features

The objective of the EFIT-Pb plant is to burn nuclear waste at the lower cost [7.1].

The design of the EFIT-Pb reactor has been proceeding with the objective of achieving an optimum transmutation rate and this with various hypotheses on technological constraints given the fact that large R&D is still pending. The long life nuclear waste, i.e. the minor actinides, has to be burned through fission in an optimum way.

The design of EFIT-Pb core has been performed so that only minor actinides (Np, Am and Cm) are burned and hence only nuclear waste from PWR spent fuel will feed the core at the equilibrium. The use of U-free fuel helps in that matter since no Pu is being produced through U238 capture but production of Pu through Cm decay should also balance the Pu disappearance through fission and capture. This final fission balance is in any case 42 kg/TWh$_{th}$, (a consequence of the fact that there is a relationship between energy produced and material destroyed though fissions; related to the fact that one fission produces 200 MeV). A three-zone core has been pre-designed and in order to achieve an optimum MA burning while keeping the power as flat as possible, a fixed Pu content has been given for the various core zones. The power flattening has been achieved through the use of different fuel volume fraction either by mean of different pitch lengths, pin diameters or matrix volume fraction within the pellet made of composite fuel [3.18].

The proof of the CerCer fuel core transmutation performance of MAs is presented in the following Table 7-1. The low reactivity burn-up swing (a consequence of the MA burning characteristics) relaxes the requirement on the power beam. The burn-up rate is of 7.9 %wt for the CerCer core. The limitation in burn up length comes from the erosion of the cladding by lead.

In this Table, one can notice the relative high inventory of Heavy Nuclides required for operating the plant. This is due to the rather limited power density (70 W/cm$^3$). The situation is even worse for the CerMet EFIT-Pb core than the CerCer EFIT-Pb one due to the rather absorbing Mo matrix even though it has been limited by enriching it in Mo92, this isotope being less absorbing than the other ones.

In the PATEROS (Partitioning and Transmutation European Roadmap for Sustainable Nuclear Energy) EU funded programme, a double strata scenario involving the CerCer EFIT-Pb core has been considered. The Scenario consider the deployment of a transmuting ADS fleet shared by the Groups of countries A (Belgium, Czech Republic, Germany, Spain, Sweden and Switzerland) and B (France). In this Scenario, the ADS will use the Plutonium of Group A and will transmute the Minor Actinides of the two Groups; the Plutonium of the Group B will be monorecycled and then stored for future deployment of Fast Reactors.

The main objectives of this Scenario are:

i) to decrease the stock of spent fuel of countries A down to 0 at the end of the century

ii) to stabilize the MA inventory of Group B within the end of the century

iii) to investigate the required number of ADS to be deployed

***This document refers to work being performed by scientists and institutions involved in IP EUROTRANS, as well as the financial support of the European Commission through the contract FI6W-CT-2004-516520.***

iv) to determine the number and capacities of the fuel cycle facilities needed

v) to stabilize the Pu inventory of Group B

Detailed descriptions of the results are given in the PATEROS report D2-2. The main outcome of that study is that for an annual electrical production of Group B of 430 TWhe, 25 EFIT-Pb (384 MWth) units are required to stabilize the MAs main stock inventory of both Groups A and B. The mass of Minor Actinides increases almost constantly until 2052, and then decreases until 2092. It reaches a more or less stable level at 0 when the last ADS reactors are deployed.

The search for optimum design within the EUROTRANS project was performed through a series of decisions which are briefly recalled in the following:

1. Define a safety strategy with the given technological constraints (Pb maximum speed flow, linear power rating, peaking factors, maximum fuel volume fraction)
2. Design the target and define its size on the basis of the outcome of the PDS-XADS Project (technological feasibility) – determined largely by the spallation heat to be removed
3. Design the core subassembly taking into account the core design constraints (Fuel composition, cladding composition, pin and sub-assembly geometry,…) : definition of the fuel (pin), sub-assembly and whole core dimensions
4. Define the number of the subassemblies in the core and hence the installed power so that $K_{eff}$ remains below 0.97 while the ratio of Minor Actinides to Heavy Nuclides is close to the 54% (it defines the efficiency of Minor Actinides burning)
5. Define the Proton Beam intensity for the proton energy of 800 MeV a value which represents a compromise between neutron production and efficiency on one side and neutron cost on the other side.
6. Arrangement of the primary system
7. Arrangement of the Balance of Plant and Containment

It answers to the Minor Actinides transmutation design objectives which were given at the start of the project (see transmutation values in table 7.1) [7.2] and these objectives are achieved under given technology constraints and a safety approach of the most recent plant designs.

***This document refers to work being performed by scientists and institutions involved in IP EUROTRANS, as well as the financial support of the European Commission through the contract FI6W-CT-2004-516520.***

Table 7.1 Detailed Characteristics of the EFIT-Pb Core (CerCer fuel 1098 fpd – 384 MWth)

EFIT-Pb Core - CerCer fuel - T91 steel cladding
Electric Power : 154 Mwe
Thermal Power : 384 MWth
Annual availability : 270 EFPdays
Annual Production : 1,00 TWhe

| **Equilibrium cycle of the 3 batch reloading scheme simulated by one-through cycle** | | **Fuel** |
|---|---|---|
| **Core** | | |
| Number of Sub Assemblies | | 180 |
| HN mass per S/A | (kg) | 29,8 |
| HN in core | (kg) | 5371 |
| Matrix (MgO) in core | (kg) | 1979 |
| Cycle length | (EFPdays) | 365 |
| Number of Cycles | | 3 |
| **Refuelling** | | |
| Number of Sub Assemblies | | 60 |
| HN mass for reloading | (kg) | 1790,3 |
| Uranium Mass | (kg) | 0,0 |
| Plutonium Mass | (kg) | 817,8 |
| Neptunium Mass | (kg) | 37,8 |
| Americium Mass | (kg) | 892,9 |
| Curium Mass | (kg) | 41,8 |
| U235 Content in the Uranium | (%) | 0,0 |
| Pu239 Equivalent Mass (MACCAO) | (kg) | 332,4 |
| Pu239 Equivalent Content in HN | (%) | 18,6 |
| Plutonium Content | (%) | 45,7 |
| Am, Cm and Np content | (%) | 54,3 |
| **Mean Irradiation (GWd/tHN)** | | 78,3 |
| at % | | 8,3 |
| Cooling time (days) | | 122 |
| **Discharge** | | |
| HN mass for discharge | (kg) | 1648,6 |
| Uranium Mass | (kg) | 1,5 |
| Plutonium Mass | (kg) | 804,9 |
| Neptunium Mass | (kg) | 33,2 |
| Americium Mass | (kg) | 731,7 |
| Curium Mass | (kg) | 77,3 |
| U235 Content in the Uranium | (%) | 1,3 |
| Pu239 Equivalent Mass (MACCAO) | (kg) | 357,4 |
| Pu239 Equivalent Content in HN | (%) | 21,7 |
| Plutonium Content | (%) | 48,8 |
| Am, Cm and Np content | (%) | 51,1 |
| Fission Product Mass | (kg) | 135,5 |
| **Balance as a function of production** (after cooling: 122 days) | | |
| Uranium | ($Kg/TWh_{th}$) | 0,4 |
| Plutonium | ($Kg/TWh_{th}$) | -3,8 |
| Neptunium | ($Kg/TWh_{th}$) | -1,4 |
| Americium | ($Kg/TWh_{th}$) | -47,8 |
| Curium | ($Kg/TWh_{th}$) | 10,5 |
| Fission Products | ($Kg/TWh_{th}$) | 40,2 |

***This document refers to work being performed by scientists and institutions involved in IP EUROTRANS, as well as the financial support of the European Commission through the contract FI6W-CT-2004-516520.***

### 7.1.2 Potential for Design Optimisation

The question raised now is the following: is the plant design, the most cost effective one?

In order to make the transmutation more cost effective, design changes could be done which concern:

- the size of the spallation module
- the core power density
- the cycle length
- the installed power of the plant

The increase in the core power density will decrease the MA inventory of the plant per unit of power hence reducing the amount of fuel to reprocess in order to load the core. This reduction will occur only for the first load and will affect the speed at which the EFIT-Pb will be deployed. It has an impact on the size of the fuel manufacturing plant.

At the equilibrium however, this design change will not affect the MA fuel flow which is mainly affected by the cycle length. Hence, increasing the cycle length will reduce the size of the manufacturing plant and of U-free fuel reprocessing plant.

Finally, the reduction of the installed power of the plant will have a direct impact of the number of plants to be deployed for burning MAs. The 10 $MW_{th}$ installed power required to burn MAs of the 430 TWe annual energy production will not be changed since there is a direct relationship between the mass of Minor Actinides being burnt and the EFIT-Pb installed power (related to the fact that one fission and hence one nuclide disappearance produces 200MeV).

It was found that the limitation in the core power density (70 $W_{th}/cm^3$) is mainly due to the limit in temperature (550°C) the cladding materials can withstand. The Russian BREST core can reach 130 $W_{th}/cm^3$ mainly because they claim their cladding material temperature limit is 620°C. A rather safe temperature limit has been set up for EFIT-Pb although not confirmed by DEMETRA tests and unless some breakthrough technology is found for the cladding material, it is not possible to increase the core power density. The other factor is the low coolant pressure drop (less than 1 bar across the core) which was requested by the safety constraints. The ability of the plant to remove heat in transients via natural circulation is a strong requirement which limits the core power density. It should be noticed that the same constraint (core pressure drop limited to 1 bar) exist for both EFIT-Pb and BREST plants. This common point of view illustrates that this safety related characteristic is unlikely to be revisited in the future. The rather low temperature limit for the fuel does not bring any additional constraints, the one on the cladding being the more limiting one.

For what concerns the limitation in the fuel residence time, it is also related to the cladding material. Although the Pb speed within the core has been limited to less than 2m/s, Pb is eroding the cladding oxide layer which protects the cladding from the Pb corrosion. The speed at which this erosion affects the cladding limits the fuel residence time.

Finally, the optimum installed power of the plant for transmutation is very much related to the source efficiency. Several aspects affect the source efficiency:

- the core power density
- the size of the spallation module
- the proton energy
- the reactivity swing

The increase in the core power density has already been discussed and will not increase without some breakthrough in cladding materials.

*This document refers to work being performed by scientists and institutions involved in IP EUROTRANS, as well as the financial support of the European Commission through the contract FI6W-CT-2004-516520.*

The size of the spallation module is bound to the energy to be delivered to the subcritical system. Of course, this could be reduced if the proton energy is increased (800MeV is almost the optimum between energy delivered and number of neutrons being produced per proton but 1 GeV could be envisaged) and if the reactivity swing is small (this is already the case for the EFIT-Pb core). Another possibility is to decide for a window design without dedicated cooling circuit. This kind of design has two main drawbacks: the temperature on the window material overpasses the 550°C temperature limit and hence is very much dependent on some breakthrough in cladding materials and the spallation products will pollute the primary circuit, a large volume of Pb where extracting them will be quite difficult. The JAEA design has chosen this type of spallation module design but the use of LBE as a coolant reduces the window material temperature limit request (inlet and outlet core temperatures are much lower). LBE has been discarded for EFIT-Pb because of limited global resources of bismuth and because limited temperatures affects the efficiency of the plant; something not to neglect when the share of EFIT-Pb (more than 7%) in the whole park is not small.

In conclusion one can say that the EFIT-Pb design is optimum for what concerns MA transmutation efficiency. The use of existing T91 cladding brings a too much stringent limitation in the core design of ETD/EFIT-Pb and hence increases the overall ETD/EFIT-Pb plant lay out MA burning cost efficiency.

Evidence of the effectiness of the reduction of MA transmutation and its reduction on the raditoxicity [7.3] [7.4] is illustrated on a double strata scenario (cf Figure 1.1) on the following Figure 7.1:

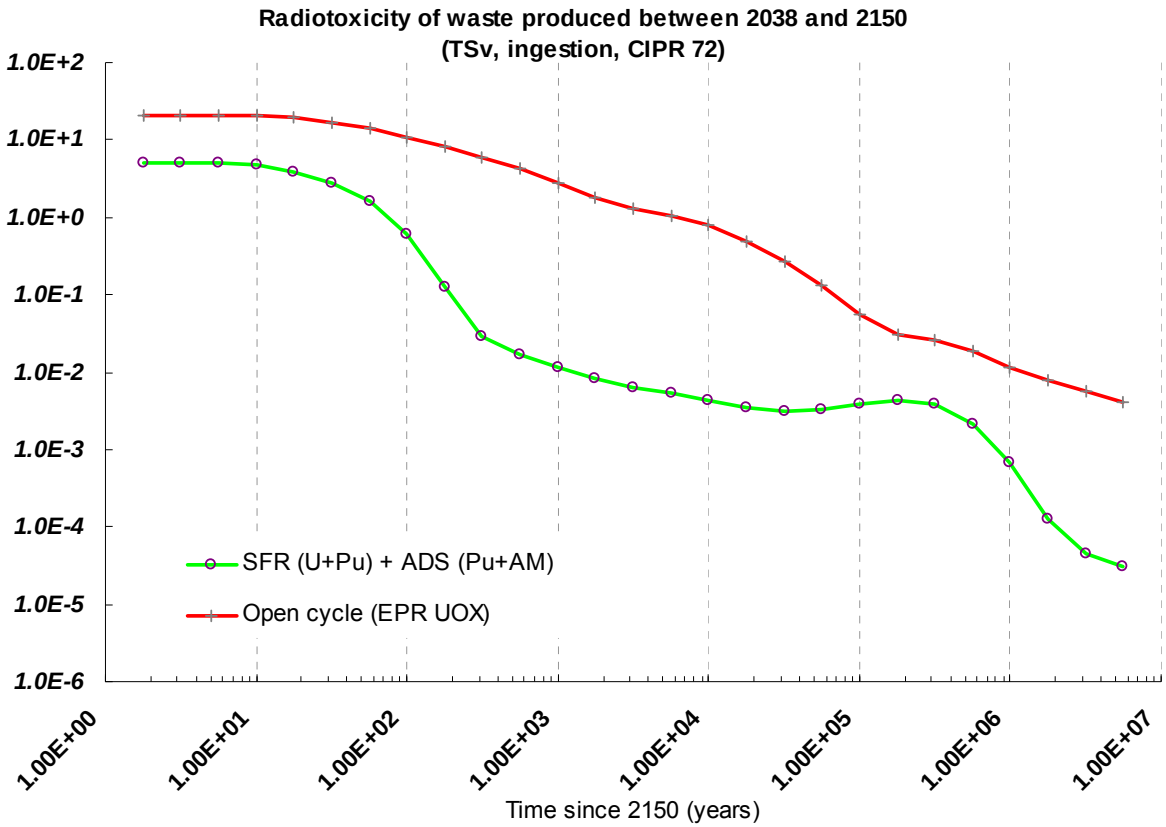


Figure 7.1 Radiotoxicity reduction with the use of EFIT-Pb in a double strata scenario

*This document refers to work being performed by scientists and institutions involved in IP EUROTRANS, as well as the financial support of the European Commission through the contract FI6W-CT-2004-516520.*

## 7.2 EFIT-He design

The objective of the EFIT-He plant is, just as the EFIT-Pb plant, to burn nuclear waste at the lower cost.

The search for EFIT-He optimum design within the EUROTRANS project was performed with the same sequence of decisions which were the ones of EFIT-Pb. Of course, because the coolants are different, the safety criteria are not the same and the decision to take SiC/SiCf as a cladding material is part of the choice of the safety strategy. The possibility to implement a solid target with a “cold” window is also a feature which is impacting the size of the spallation module is also a major difference compared to the EFIT-Pb plant. But even with these major differences, the sequence of decisions to reach the optimum transmutation rate were similar to the ones of the EFIT-Pb plant.

Hence, the EFIT-He plant exhibits a core in which only minor actinides (Np, Am and Cm) are burned and hence only nuclear waste from PWR spent fuel will feed the core at the equilibrium. In order to achieve an optimum MA burning while keeping the power as flat as possible, a fixed Pu content has been given for the two core zones. The transmutation rate obtained is about 42 kg/TWhth of actinides [7.5], as seen in Table 7.2.

Also, detailed characteristics of the plant are given in Table 7.2.

*This document refers to work being performed by scientists and institutions involved in IP EUROTRANS, as well as the financial support of the European Commission through the contract FI6W-CT-2004-516520.*

Table 7.2 Detailed Characteristics of the EFIT-He Core (CerCer fuel 2790 fpd – 400 MWth)

EFIT-He Core – CerCer fuel – SiC/SiCf cladding
Electric Power : 160 Mwe
Thermal Power : 400 MWth
Annual availability : 270 EFPdays
Annual Production : 1,04 TWhe

| **Equilibrium cycle of the 5 batch reloading scheme simulated by one-through cycle** | | **Fuel** |
|---|---|---|
| **Core** | | |
| Number of Sub Assemblies | | 366 |
| HN mass per S/A | (kg) | 25,2 |
| HN in core | (kg) | 9238,0 |
| Cycle length | (EFPdays) | 558 |
| Number of Cycles | | 5 |
| **Refuelling** | | |
| Number of Sub Assemblies | | 73 |
| HN mass for reloading | (kg) | 1847,6 |
| Uranium Mass | (kg) | 0,0 |
| Plutonium Mass | (kg) | 765,1 |
| Neptunium Mass | (kg) | 42,0 |
| Americium Mass | (kg) | 993,9 |
| Curium Mass | (kg) | 46,5 |
| U235 Content in the Uranium | (%) | 0,0 |
| Plutonium Content | (%) | 41,4 |
| Am, Cm and Np content | (%) | 58,6 |
| **Mean Irradiation (GWd/tHN)** | | 120,8 |
| | at % | 12,2 |
| Cooling time (days) | | 186 |
| **Discharge** | | |
| HN mass for discharge | (kg) | 1622,3 |
| Uranium Mass | (kg) | 5,2 |
| Plutonium Mass | (kg) | 779,1 |
| Neptunium Mass | (kg) | 36,5 |
| Americium Mass | (kg) | 723,3 |
| Curium Mass | (kg) | 78,2 |
| U235 Content in the Uranium | (%) | 0,78 |
| Plutonium Content | (%) | 48,0 |
| Am, Cm and Np content | (%) | 51,7 |
| Fission Product Mass | (kg) | 218 |
| **Balance as a function of production**<br>(after cooling: 186 days) | | |
| Uranium | ($Kg/TWh_{th}$) | 0,4 |
| Plutonium | ($Kg/TWh_{th}$) | -3,6 |
| Neptunium | ($Kg/TWh_{th}$) | -1,0 |
| Americium | ($Kg/TWh_{th}$) | -50,5 |
| Curium | ($Kg/TWh_{th}$) | 5,9 |
| Fission Products | ($Kg/TWh_{th}$) | 40,6 |

***This document refers to work being performed by scientists and institutions involved in IP EUROTRANS, as well as the financial support of the European Commission through the contract FI6W-CT-2004-516520.***

The power flattening has been achieved through the use of different fuel volume fraction by mean of different pin diameters and number of pins per sub-assembly. The matrix volume fraction within the pin has been adjusted so as to reach the optimum MA burning rate. As a consequence of this design, the reactivity swing is rather small hence limiting the requirement for the neutron beam intensity. The core power density is rather small (40 W/cm$^3$), a consequence of safety constraints related to the removal of decay heat in transients under a back up pressure. For similar safety reason, the pressure drop across the core has been limited to 1 bar.

Double strata scenario studies have not been done for this He-plant but it can be expected that limitation in power density (which affects the EFIT-He deployment in the park) would have been overbalance by the longer cycle length (quite efficient when reaching the equilibrium).

The MA transmutation would be more cost effective if design changes could be done on:

- the size of the spallation module
- the core power density
- the cycle length
- the installed power of the plant

Although the power density is small, the value for the core power density remains high (compared to HTR) as a consequence of provisions taken for the back up pressure (without the use of a guard vessel since the beam implementation limits the possibility of doing it) and a SiC/SiC$_f$ cladding that withstands high temperatures (1200°C within transients). The rather low temperature limit for the fuel does not bring any additional constraints.

The burn up is set to 12.2 at% a value 50% larger than the one of EFIT-Pb. The value cannot be increased further since the fuel residence time is limited by the cladding erosion by the Helium coolant. Technologies for impregnation of the cladding could limit that phenomenon and hence allow increasing the burning rate. The limitation might come this time from the fuel burn up, a situation which has yet been encountered due to the more stringent limitation on cladding erosion.

Finally, the installed power of the plant could be increased if the spallation neutron source efficiency could be increased. A rather innovative design has been chosen for the spallation module with tungsten (W) rods cooled by a rather low pressure (20 bar) helium. Just like for EFIT-Pb, a best estimate approach has been used for designing this spallation module with uncertainties affecting mainly the availability of the plant. It is not foreseen at the moment any improvement possible pending results of irradiation tests showing evidence of rather good behaviour of tungsten bars. There is hence rather limited chance of improving the source efficiency and increasing the plant size of this plant. The size of the various components, in particular the IHX, will limit furthermore the possibility of increasing the plant installed power.

## 7.3 XT-ADS design

The main objectives of the XT-ADS are first the demonstration of the ADS concept, second to provide a test facility for transmutation and third to provide irradiation capabilities in conditions representative of the EFIT operations [7.1].

The latter allows the use of the XT-ADS as a material testing facility as well as an aid for the fuel qualification for EFIT and for the qualification of candidate structural materials. The XT-ADS core is based on MOX fuel relatively high in Pu-content and is cooled using a Lead-Bismuth Eutectic (LBE).

***This document refers to work being performed by scientists and institutions involved in IP EUROTRANS, as well as the financial support of the European Commission through the contract FI6W-CT-2004-516520.***

The installed power of that plant (57 $MW_{th}$ for the core, 70 $MW_{th}$ for the primary system) is smaller than the one of EFIT-Pb and hence the safety approach can use more active systems than for the EFIT-Pb, rescue power supply being smaller in size.

The XT-ADS proto-type for future Accelerator Driven Systems plants will have a fast spectrum core with a spallation target module producing neutrons, allowing it to operate at a $K_{eff}$ in a safe reactivity range. This range of reactivity level unables to operate safely the system whatever the type of accidental reactivity insertion might occur. Given the experimental nature of the system, which might require to operate with not perfectly characterised test assemblies, more margins are forecast and hence, the value of $K_{eff}$ is targeted to be "around 0.95".

In order to provide a test bench for transmutation studies, XT-ADS has the possibility to house and operate with a certain number of fuel assemblies loaded with Minor Actinide (MA) fuel. The introduction of these MA fuel assemblies is intended to be done step by step: first some irradiation tests on sample size MA pieces in In-Pile-Sections (IPS), the next step might be the testing of a whole MA fuel pin in an In-Pile-Section, a controlled experimental position foreseen in XT-ADS and finally, the introduction of a full MA fuel assembly (and maybe later on, several of these) in the core.

In order to achieve a relatively high neutron flux, the core power density should be as large as possible. This is achieved as seen in the following table 7.3 presenting the core characteristics [7.6].

***This document refers to work being performed by scientists and institutions involved in IP EUROTRANS, as well as the financial support of the European Commission through the contract FI6W-CT-2004-516520.***

Table 7.3 Detailed Characteristics of the XT-ADS Core (MOX fuel 450 fpd – 57 MWth)

XT-ADS Core - T91 steel cladding
Thermal Power : 57 MWth
Annual availability : 270 EFPdays

| **Equilibrium cycle of the 5 batch reloading scheme simulated by one-through cycle** | | **Fuel** |
|---|---|---|
| **Core** | | |
| Number of Sub Assemblies | | 75 |
| HN mass per S/A | (kg) | 10,5 |
| HN in core | (kg) | 787,4 |
| Cycle length | (EFPdays) | 90 |
| Number of Cycles | | 5 |
| **Refuelling** | | |
| Number of Sub Assemblies | | 15 |
| HN mass for reloading | (kg) | 157,5 |
| Uranium Mass | (kg) | 102,3 |
| Plutonium Mass | (kg) | 55,2 |
| Neptunium Mass | (kg) | 0,0 |
| Americium Mass | (kg) | 0,0 |
| Curium Mass | (kg) | 0,0 |
| U235 Content in the Uranium | (%) | 0,4 |
| Plutonium Content | (%) | 35,0 |
| Am, Cm and Np content | (%) | 0,0 |
| **Mean Irradiation (GWd/tHN)** | | 32,6 |
| | at % | 3,55 |
| Cooling time (days) | | 30 |

The neutron flux in the In Pile Section (IPS) positions varies between 0.5 $10^{15}$ à 0.8 $10^{15}$ n/cm²/s for the fast flux (>0.821 MeV) and from 1.7 to 2.6 for the total flux. The fast flux value is smaller than the one of the Phenix reactor (5 $10^{15}$) but similar to those of the most recent SFR designs.

The XT-ADS design has been fulfilling its objectives given the design constraints which were economical and safety related ones. The XT-ADS design has allowed reaching a flux level up to $\Phi$>0.82MeV = 0,76x$10^{15}$ n.cm$^{-2}$.s$^{-1}$, the best one considering the design constraints:

- core power limited to 57 MWth,
- reduced Pu content (35%wt)
- LBE temperature increase across the core (100°C)
- small core pressure drop across the core to allow for a high natural convection flowrate
- many irradiation positions (8 IPS positions)

The most important design constraint is associated to the core power limited to 57 $MW_{th}$ while the other one was associated to the fuel technology with Pu content limited to 35%wt for allowing the use

***This document refers to work being performed by scientists and institutions involved in IP EUROTRANS, as well as the financial support of the European Commission through the contract FI6W-CT-2004-516520.***

of existing or planned fuel fabrication plants constructed for other fast reactors such as MONJU or ASTRID sodium fast reactors.

If the design can proceed without these constraints, the XT-ADS high flux level (~0.76 $10^{15}$) can be increased up to values larger than$10^{15}$ but that will require revisiting the entire plant design.

The major design criteria such as the weak core pressure loss across the core to allow for a rather passive safety, many irradiation positions (8 IPS positions), a compact core which limits the damage to the closest structures (core barrel & support plate) have to be kept.

The CDT project is presently reconsidering this design [7.7] in order to improve the irradiation efficiency of the plant aiming at a targeted fast flux level above E = 0.82 MeV of $10^{15}$ $n.cm^{-2}.s^{-1}$. To increase this flux level, an increase of the power density is necessary while in order to limit the increase of the Pu content (up to 35% with a natural uranium matrix) an increase in the installed power (from 57 $MW_{th}$ to 80 $MW_{th}$) is required. In order to be able to increase the power density an increase of the allowable temperature increment over the core from 100 °C to 130 °C or/and a decrease of the core height are necessary. The choice of the inlet and the outlet coolant temperatures will have to be chosen carefully given the cladding material to withstand embrittlement due to irradiation and LBE corrosion.

References

[7.1] G. Rimpault, Definition of the detailed missions of both the Pb-Bi cooled XT-ADS and Pb cooled EFIT and its gas back-up option, Techn. Report CEA SPRC/LEDC 05-420, December 2005; IP EUROTRANS – DM1 Design – WP 1.1 – Deliverable 1.1, Contract n° FI6W-CT-2004-516520, June 2006.

[7.2] G. Rimpault, Caracterisation Neutronique de L'avant-Projet de Coeur de Système Souscritique EFIT-Pb, Techn. Report CEA SPRC/LEDC 09-402, March 2009.

[7.3] L. Boucher and al., "COSI: the complete renewal of the simulation software for the fuel cycle analysis" Proc. Conf. ICONE 14, Miami, USA, July 17 – July 20, 2006

[7.4] Ch. Coquelet, « Comparison of different scenarios with COSI » Private communication 2010.

[7.5] G. Rimpault, Caracterisation Neutronique de L'avant-Projet de Coeur de Système Souscritique EFIT-He, Techn. Report CEA SPRC/LEDC 09-401, March 2009.

[7.6] Rimpault, Gérald. Caractérisation neutronique du coeur sous-critique CL-P0 du système XT-ADS refroidi au Pb-Bi, outil d'irradiation pour des assemblages expérimentaux.. 2009. CEA/DER/SPRC/LEDC/09-403.

[7.7] D. De Bruyn, P. Baeten, S. Larmignat, A. Woaye Hune & L. Mansani, "The FP7 Central Design Team project: Towards a fast spectrum Transmutation Experimental Facility", Proceedings of ICAPP '10 San Diego, CA, USA, June 13-17, 2010.

***This document refers to work being performed by scientists and institutions involved in IP EUROTRANS, as well as the financial support of the European Commission through the contract FI6W-CT-2004-516520.***

# 8. STRUCTURAL INTEGRITY/ROBUSTNESS

## 8.1 EFIT-Pb design

The favorable neutronic properties of the lead coolant have been duly exploited in the conceptual design of the Primary System of EFIT as illustrated by the following considerations.

The neutronic properties of lead allow designing the fuel assembly with fuel rods spaced like in the fuel assembly of a Light Water Reactor (LWR), i.e. spaced wider apart than in the case of a sodium-cooled reactor. The core designed for EFIT is accordingly a low pressure loss core, a feature that has been exploited with expected important benefits such as:

- a shorter reactor vessel, less heavy coolant mass and lower mechanical loads on the reactor vessel support system;
- lower pressure losses (of the order of one to two bars) with associated lower required primary pump power output, in spite of the high density of lead;
- the possibility of full-passive decay heat removal on loss of plant service power.

While the use of forced circulation of the primary coolant during power operation is imposed by the design goal of an industrially significant reactor power, the feature of full-passive decay heat removal in case of loss of plant service power is highly desirable to enhance its reliability and reduce the capital cost. In case the ambitious goal of DHR by full-natural circulation should not be possible, pony motors will be installed as a back-up option to enhance the natural coolant circulation to the required flowrate. However, in this case, the reliability of the DHR function should be assessed.

These design objectives i.e. the possibility to have a primary system which exhibits a strong back up natural circulation would have had a strong impact on the dimension of the plant if the plant lay out was designed just like the BREST Russian reactor [8.1]. But the EFIT-Pb plant has been designed with the primary pump in the hot leg taking advantage of the MAXSTHAL material used. This ceramic material has a quite high resistance to Pb corrosion but rather limited mechanical properties. However, the consequences on the current pump design are limited given the rather slow rotating speed of the pump. Experimental evidence of the reliability of that big component has to be addressed prior to the construction of the plant. This arrangement enables the plant to be more compact hence reducing the Lead masses of the plant compared to other designs like the BREST Russian reactor.

This reduced amount of Pb combined with appropriate anchored vessel and with a core barrel separation of the Pb free surfaces minimizes the earth quake induce effects such as the sloshing of coolant.

The selected 400 °C temperature at core inlet provides margin from the risk of lead freezing and the temperature of only 480 °C at core outlet offers many advantages in term of reduced structural material corrosion, improvement of the mechanical characteristics such as negligible creep of the structural steels, and reduced thermal shocks in transient conditions. Moreover having chosen 480°C as the average core outlet temperature, the fuel cladding temperature can be maintained below the limit of 550°C, during normal operation.

In terms of efficiency of electricity energy generation, a higher outlet core temperature would be preferable, but cannot be specified owing to the present technological limits at the higher temperatures in a molten lead environment of the known structural materials and fuel clad coating techniques are overcome by qualification of new materials and better corrosion protection techniques. Increasing the core outlet temperature significantly above 500°C would create an unjustified technological risk,

***This document refers to work being performed by scientists and institutions involved in IP EUROTRANS, as well as the financial support of the European Commission through the contract FI6W-CT-2004-516520.***

considering also that the chosen core thermal cycle and the integration of the Steam Generators in the Reactor Vessel, a key feature of the EFIT conceptual design, provide almost the same heat transfer cycle efficiency than fast reactor plants mentioned above, which have to transfer heat first to an intermediate loop.

The use of higher outlet temperatures and associated high-efficiency heat transfer cycles with proper control of the coolant chemistry and choice of cladding and structural materials remains of course a perspective to be pursued forward. The properties of existing T91 cladding bring too much stringent limitations in the design of the ETD/EFIT-Pb core and hence in the overall ETD/EFIT-Pb plant lay out.

The chance for the EFIT-Pb design performance is bound to cladding materials that could withstand operating conditions up to 600°C. As the maximum Pb speed in the EFIT-Pb core was set to 1m/s, the residence time was limited due to the clad damage (130 dpa) associated to the clad oxide layer corrosion by Pb which went to few µm. This is a serious drawback for the performance of the plant.

In general, however, the safety analysis performed for the EFIT-Pb design demonstrates the very forgiving nature of this plant design under most adverse transient conditions. With the exception of the fuel assembly blockage transient, most unprotected transients allow sufficient grace time (~ 30 minutes) before manual corrective actions are required.

However, given the somehow pre-conceptual status of the current design, some more work is required to address in a satisfactory manner several issues:

- Instrumentation and control (I&C)
- Irreversible accident scenarios driven by Pb corrosion & slag formation

For example, typical problem is that of the deposit of oxides for which the installation of filters that can interfere with the primary flow path might be of some concerns. This should be avoided because the natural convection would be no longer reliable while it remains a major asset of the concept. In principle, with a good oxygen control important deposits could be avoided. A progressive slow process of deposit in the core might be detected with thermocouples at the top of the fuel elements. Furthermore, lead in the upper part of the down comer in EFIT-Pb is stagnant. If all oxides are floating, then there will be an easy control over their formation and the cleaning of the loop.

More complicate is to foresee the behaviour of hypothetical massive slag of oxide formed in the down comer. The possibility for massive slag to reach the core could be excluded by design. This is possible if the upward speed of the slag is higher than the downward speed of lead (about 0.2 m/s), this is one of the cases for which more experimental evidence is necessary.

A summary of key challenges for EFIT-Pb as for the LFR, as seen by [8.2], is provided in Table 8.1.

***This document refers to work being performed by scientists and institutions involved in IP EUROTRANS, as well as the financial support of the European Commission through the contract FI6W-CT-2004-516520.***

Table 8.1. Key challenges of the LFR design.

| General issue | Specific issue | Proposed strategy |
|---|---|---|
| Corrosion in Lead | Tendency for material corrosion with increasing temperature | Mean core outlet temperature for the large plant is limited to 480°C[1]<br>Dissolved oxygen provides barrier against corrosion |
| | Reactor vessel | Temperature limited by design to 400°C |
| | Fuel cladding | Use of aluminized surface treatment of steels |
| | Reactor internals | Dissolved oxygen control |
| | SG tubes | Use of aluminized steels to avoid lead pollution and heat transfer degradation |
| | Pump impeller degradation[2] | Use of innovative materials |
| Seismic design | Challenge related to the large mass of lead | Use of 2D seismic isolators + short vessel design |
| SGs are installed inside the reactor vessel with risk of water ingress in lead in case of SGTR accident | Rupture of the SG collectors in lead | Eliminated by design |
| | Steam entrainment in the core in case of SGTR | Excluded by design |
| | Pressure waves inside the primary system in case of SGTR | Harmless by specific design features |
| DHR | Diversification, reliability and passive operation required[3] | Diversification and reliability by means of use of both atmospheric air and stored water |
| Refuelling in lead | High temperature makes refuelling difficult | Access to fuel assemblies is in cold cover gas |

[1] The small system operates at a higher temperature but because of the use of natural circulation cooling the erosive effect of lead is reduced
[2] Pump impeller problem is not characteristic to small system because of the use of natural circulation cooling
[3] In case of small system a simple and reliable RV air cooling system is sufficient to remove decay heat

*This document refers to work being performed by scientists and institutions involved in IP EUROTRANS, as well as the financial support of the European Commission through the contract FI6W-CT-2004-516520.*

## 8.2 EFIT-He design

### 8.2.1 DHR design strategy

It is worth pointing out a major design option choice made on the DHR strategy: due the presence of the proton beam and the spallation target (including its cooling loop) it was considered as almost impossible to implement a guard vessel around the EFIT-He primary system. In consequence, in case of accidental depressurisation, the confinement pressure will decrease from the design pressure of 70 bar to the containment pressure; namely, 2 bar approximately. The use of natural convection with a back-up pressure at 10 bar, like in the GFR DHR strategy, is no longer possible in this case. The major consequence of this choice means that one will rely on active systems to manage the accidental conditions. Consequently, this also means that blowers of the DHR loops must be designed to operate over the entire pressure range from 70 to 1 bar. From the specifications of safety systems, this means that these systems are designed with an adequate level of reliability and that redundant and independent systems are accounted in the DHR function safety analysis.

The reliability study [8.3] was carried out considering that the secondary system works in natural circulation (considering that the primary circuit is in forced circulation should not change very much the reliability study results, but this should be noticed).

Designing the secondary system so that it works in natural circulation on the water side is leading to too large height that is why a pump has been considered in the design (cf Figure 8.1). In these conditions, to a passive circuit of secondary side water (contrary to the XADS and GFR architectures) an active circuit pressurized to 8 bar, with a circulation pump was preferred.

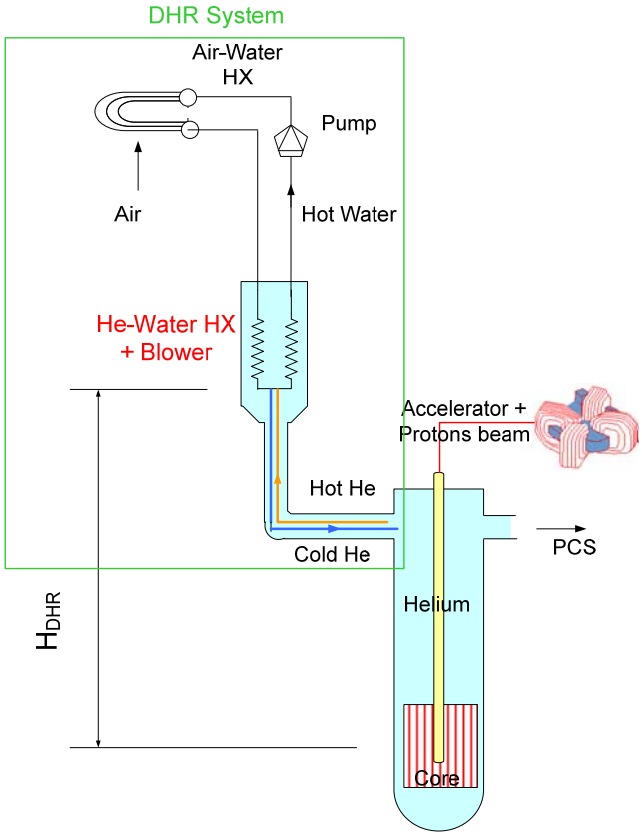


Figure 8.1: Schematic diagram of the DHR system

*This document refers to work being performed by scientists and institutions involved in IP EUROTRANS, as well as the financial support of the European Commission through the contract FI6W-CT-2004-516520.*

The scheme presented in Figure 8.1, shows the DHR principle with an air cooling system used as ultimate heat removal (in the He-cooled XADS, a water tank was the ultimate heat sink).

The DHR system will operate in natural convection when the primary system remains pressurized and in forced convection in the case of a complete depressurization. Consequently, the blowers are sized for the most penalizing accidental case; namely, the completely depressurized case at 1 bar. These assumptions lead to over-size the blowers when operating at the nominal conditions (70 bar).

The preliminary design of the SCS (Shutdown Cooling System) components similar to PDS-XADS was established on the basis of four preliminary operating conditions:

- Case 1: Bonding case of natural circulation at 70 bars

The initiating events inducing the necessity of decay heat removal, in this case, are pressurized shutdowns, a loss of power removal or other accidents for which the primary circuit remains in a pressurized state.

- Case 2: Forced Circulation at the atmospheric pressure (1 bar)

It can be a fast depressurization due to a large breach or a low one due to small breach.

- Case 4: Forced circulation 3 days after reactor shutdown during fuel handling with the reactor partially depressurized at 10 bars.
- The case 3 was equivalent to case 4 with natural circulation, but the DHR architecture shows that it is impossible to rely on natural circulation to remove the decay heat in these conditions (it would required a very large height between the core and the DHR vessel).

A valve is implemented at the inlet of the DHR vessel so that the DHR systems only work in shutdown, handling or accidental conditions. In normal operating conditions, the DHR vessels are filled with cold helium and do not work, the helium flows towards the PHTS (Primary Heat Transfer System).

As a consequence of this design, a reliability assessment was required and finally recommended a DHR configuration with 2 diverse systems (active mode) and 3 redundant lines.

Investigation of a prior study, performed within the scope of the previous European program PDS-XADS, led to suggest retaining 3 diverse systems with 100% removal capability per train to check similar safety goals. However, such extent of diversification seems very difficult to implement.

In order to manage a feasible design, other architectures had to be investigated. This study evaluated two additional architectures which have a level 2 diversification degree:

- 2 x 2 x 100% concept: 2 diverse Shutdown Cooling Systems, each one with 2 redundant lines (100% capability);
- 2 x 3 x 50% concept: 2 diverse Shutdown Cooling Systems, each one with 3 redundant lines (50% capability).

2 x 2 x 100% and 2 x 3 x 50% SCS concepts seem more feasible than 3 x 100 % concept. The study has shown that the reliability is improved.

The best configuration in terms of reliability is the 2 x 3 x 50% concept. This design is also the less sensitive to the time to repair SCS systems.

2 x 2 x 100% concept could be acceptable if it can be demonstrated that the time to repair SCS remains short (lower than 50 hours).

The study has been performed considering that core by-pass is acceptable. The possible by-passes are:

- Through PCS if flow shutter closure has failed and the primary blower is shut down,
- Through failed SCS if check valve closure has failed and the SCS blower has failed

*This document refers to work being performed by scientists and institutions involved in IP EUROTRANS, as well as the financial support of the European Commission through the contract FI6W-CT-2004-516520.*

The feasibility of these assumptions has to be assessed:

SCS circuit pressure drop (shutdown of SCS blower) must be sufficiently important with respect to core head loss but this could be penalizing for natural convection. PCS circuit pressure drop (shutdown of PCS blower) must be sufficiently important with respect to core pressure drop. Confirmation by thermal–hydraulic calculations has to be performed.

During shutdown conditions, natural convection could be not required in case of fuel handling operation at low pressure conditions:

- If 2 x 3 x 50 % concept is selected.
- If depressurized conditions are initiated after sufficient delay (about 3 days) allowing 6 x 100 % redundancy.

In the present EFIT-He architecture, six DHR vessels are considered, connected to the main vessel by means of six DHR ducts with expansion loops to accommodate the thermal expansion.

#### 8.2.2 EFIT-He design robustness

The EFIT-He plant has to be carefully designed for protected loss of flow in particular for what concerns DHR systems [8.4].

In the present EFIT-He architecture, six DHR vessels are considered, connected to the main vessel by means of six DHR ducts with expansion loops to accommodate the thermal expansion.

The proposed concept is a vessel with eight straight finned tubes heat exchangers and a helium blower. For diversity reasons, another exchanger technology should be analyzed.

The secondary fluid pressure is high (250 bars) and calls into question the feasibility of the IHX component based on the HTR technology. Major changes would be necessary to make an IHX design able to stand the large pressure. Nevertheless, an IHX design with a supercritical $CO_2$ high pressure should be feasible after a specific R&D program and design works (out of the scope of EUROTRANS framework).

A backup solution for the conversion cycle could be to consider a steam cycle at 180-190 bars which is a better known technology, with the same efficiency in the considered range of temperature. The steam generator should be directly designed based on HTR past experience.

Some component material such as the thimble material needs also to be validated by R&D considering the high temperature (572°C) and the irradiation damages.

## 8.3 XT-ADS design

#### 8.3.1 EFIT & XT-ADS common characteristics

EFIT is being designed as a transmutation demonstrator, loaded with MA fuel. It is intended to become operational many years after the XT-ADS (around 2040) and therefore to profit of the experience gained from the running European Research an Development (R&D) programs on fuel and materials and of the operation of the XT-ADS, which is to be built and operational in the near future (in operation around 2020).

EFIT and XT-ADS have some common characteristics such as:

- *Accelerator*: Superconducting LINAC CW modular accelerator; proton beam injection from the top of the vessel; windowless target type; high reliability and availability (Spurious Beam Trip < 5/y; continuous operation for < 1 s beam interruptions); 200μs holes for sub-criticality measurements.
- *Core:* Use of fuel pin spacer, wrapper-type and hexagonal fuel assembly; sub-critical by design in all operating, accidental and abnormal conditions (no control rods: ineffective for a core sustained by external neutron source); possibility to load fuel assemblies with MA in selected XT-ADS portions reproducing EFIT irradiation conditions.

*This document refers to work being performed by scientists and institutions involved in IP EUROTRANS, as well as the financial support of the European Commission through the contract FI6W-CT-2004-516520.*

- *Reactor Vessel:* Primary system integrated in the vessel (all components removable from the top for in-service inspection, maintenance and replacement); primary coolant circulation is forced in normal conditions (with mechanical pumps) and is natural in decay heat removal conditions; reactor vessel structural material 316L steel; hanged vessel and similar vessel support (EFIT has horizontal anti-seismic supports which are not required for XT-ADS since it benefits of the low seismicity of the Mol region where it should be built).
- *Heavy Liquid Metal Technology:* HLM technology experimental results are in principle applicable to LBE and Lead.
- *Fuel Handling* relies on remote handling.

While some other options differ between EFIT and XT-ADS:

- *Plant size:* XT-ADS – 75$MW_{th}$; EFIT – 384$MW_{th}$.
- *Accelerator proton energy*: XT-ADS - 600 MeV and 3 mA; EFIT - 800 MeV and 20 mA.
- *Spallation target*: XT-ADS - LBE confluent flow, off-centred; EFIT - Lead perpendicular (horizontal) flow, centred.
- *Fuel Type and Power Density*: XT-ADS - MOX; 700 W/cm³; EFIT - U-free: (Pu, AM)O2 + MgO (or Mo) matrix; 450 ÷ 650 W/cm³.
- *Primary Coolant and operating temperature*: XT-ADS - LBE (inlet T: 300°C, outlet T: 400°C); EFIT - Lead (inlet T: 400°C, outlet T: 480°C).
- *Fuel Core Loading*: XT-ADS - from bottom with horizontal fixed handling arm machine; EFIT - from top with extendible handling arm machine.
- *Secondary System*: XT-ADS - low pressure boiling water; EFIT - Superheated water cycle (Electricity production).
- *Decay heat removal systems*: XT-ADS – system 1 portion of secondary system in natural circulation and system 2 RVACS fully passive; EFIT - system 1 Isolation Condenser on secondary system and system 2 dedicate system in the reactor vessel fully passive.

### 8.3.2 Changes compared to MYRRHA Draft 2 design

In the beginning of the EUROTRANS project, SCK•CEN offered to use the "MYRRHA 2005" design file [8.6] as a starting basis for the XT-ADS design. This allowed optimizing an existing design towards the needs of XT-ADS and within the limits of the safety requirements instead of starting from a blank page. The XT-ADS primary system is a pool-type reactor, cooled by LBE. Different arrangements of the primary system for XT ADS have been compared [8.7] and it appeared that an evolution of the "MYRRHA 2005" primary system was the more viable arrangement.

In the course of this exercise, several improvements of the MYRRHA Draft 2 design were identified mainly with a view to simplify the design or make it more robust:

- Flat diaphragm,
- Reduced number of components,
- Suppression of EHX for DHR,
- Hanging vessel with elliptical bottom head,
- Accommodation of cold and hot Pb-Bi free levels in different states.

These options were retained for the remontage of XT-ADS.

The pool-type solution has the interest to take benefit from the thermal inertia provided by the large coolant volume. The pool system also enables to contain all the primary coolant within the main vessel, in which the primary components (pumps, heat exchanger, fuel handling tools, experimental rigs, etc…) are inserted by the top. In order to keep a large flexibility for the experimental devices loading and because of the presence of the spallation source, the loading of fuel assemblies is foreseen to be from underneath.

*This document refers to work being performed by scientists and institutions involved in IP EUROTRANS, as well as the financial support of the European Commission through the contract FI6W-CT-2004-516520.*

The main changes compared to MYRRHA core were driven by safety concerns, with the fuel pin has been designed with a larger gas plenum and exhibiting hollow (annular) fuel pellets. Also the fuel pin pitch has been increased to lower the pressure drop over the core (target value was one bar). The wrapper thickness has been increased and the inter-wrapper space made larger.

Based on neutronic calculations of a clean and fresh core, the decision was taken to increase the core barrel size to allow for more hexagonal positions and more distance between the last row of fuel elements and the core barrel but this was done partially without eliminating all radiation damage concerns (see next paragraph). Finally, eight positions were dedicated to house irradiation devices (In-Pile Sections, IPSs).

For the XT-ADS fuel, it has been decided to opt for a plutonium vector coming from the reprocessing of the current generation PWR spent fuel with an initial enrichment of 4.5% in 235U. The plutonium content in the MOX fuel is overpassing a little the 30% limit, a value considered as a maximum value for standard fabrication plants. The outline dimensions of the core are 1.5 m diameter by 2 m height. The sub-criticality level is around 0.95 which is considered as an appropriate level for a first of a kind medium-scale ADS. This had as a consequence the necessity to increase the core power up to 57MWth.

The spallation loop is off centered located from the core. The requirement of high flux levels leads to design a compact core and the central hole in the core to house the spallation target has to be limited dimensions (around 10 cm). Thus, the spallation loop (i.e., loop achieving the circulation of LBE used as spallation target) is located at the core periphery; it is connected to the central beam tube and the spallation target by two horizontal tubes, one passing above and the other one below the core.

The spallation loop contains a feed tank, a circulation pump, a heat exchanger and an auxiliary system for the control of oxygen contents and the required instrumentation. A windowless target design is retained, i.e., without a physical separation between the accelerator beam line vacuum and the LBE used as liquid target material. An advantage of this solution is that it enables high beam currents needed for industrial transmutation.

### 8.3.3 Dose rates of the core barrel and the upper grid plate and recommendations

The diaphragm is a large component separating the lower part (high pressure, low temperature) from the upper part (low pressure, high temperature) of the vessel inner volume. While it has a conical shape in MYRRHA, it has a flat bottom in the XT-ADS since this will simplify the diaphragm manufacturing and it offers more efficient tightness of the inserted components (PHX, PP, spallation loop, fuel manipulator, in-vessel inspection manipulators) reducing the diaphragm by-pass flows. Mechanical behaviour of the flat diaphragm is to be checked as it will involve higher bending stresses than the conical one.

The diaphragm serves as the support structure not only for already mentioned components, but also for the two in-vessel diametrically suspended fuel storages, the in-vessel recovery manipulators, the core support plate, the core barrel and for the LBE conditioning system. Some of the penetrations are fitted with guide tubes. The function of those tubes is to guide the device to be inserted through the diaphragm, to limit the LBE leakage through the diaphragm and to provide some controlled cooling along the device.

The internals exposed to irradiation are:

- Core support plate: Core support function
- Core barrel: might be used as a lateral core restraint.

The design related to shielding should lead to sufficiently low dose values of the core barrel and of the upper core support plate to argue easily for their long term integrity (10 years?) without additional measures. Since the current design is just at the limit of requested maximum dose, it is strongly recommended to reformulate the approach for demonstration of the long term integrity along the following lines:

Step 1: Specification of admissible limit values of the structure materials dependent on dose and temperature to be taken as basis for the demonstration of the structures integrity.

*This document refers to work being performed by scientists and institutions involved in IP EUROTRANS, as well as the financial support of the European Commission through the contract FI6W-CT-2004-516520.*

Step 2: Specification of a representative set of load conditions for the expected life time of the respective components i.e. start-up and shut down procedures, transients of design basis conditions, part load operation time periods, cyclic load conditions etc.

Step 3: Demonstration by calculations that the admissible limit values of the selected materials are not exceeded on a short term basis i.e. in less than 5 years and thus that the integrity of the components are not to be put into question.

Step 4: Foresee irradiation of materials samples at locations close to the structure components which are regularly investigated by destructive examination to evaluate whether the assumed materials behaviour develops over time as assumed for the theoretical evaluations (time period for testing about one year).

Step 5: Foresee a first time period of five years as the cumulative life time of the core barrel and the upper grid plate and then replace the components for intensive non-destructive investigations out side the plant. After five years of operation the cumulative dose to the structures will reach about 5 to 7 dpa NRT. Replace the components by spare components to be fabricated in due time. Only afterwards decide whether the used components can be put in place for another time period or have to be put to trash.

Step 6: Contact the respective licensing authorities in due time to evaluate whether one can get acceptance for such a procedure.

### 8.3.4 XT-ADS core support structures

The XT-ADS primary system is an evolution of the MYRRHA design with an interlinking concept for the spallation target and core loaded from the bottom.

The core support structure consists of the suspension tube, the core plug and the core support plate. The core barrel itself is the part of the suspension tube located under the core support plate. A number of holes at the suspension tube periphery, above the core level, allow the coolant circulation. It is closed at the top by a thick core plug, which is part of the reactor cover. The suspension tube is slotted over its full length to allow the insertion of the spallation loop.

Since the core is (un)loaded from underneath, the core support plate is located at the top of the core to support the fuel assemblies where they remain at their location by the buoyancy force.

Being at the top of the core, the core support plate experiences the LBE outlet temperature, which might be 400°C (72 fuelled assemblies at the centre of the core) or somewhat more than 300°C (27 dummy assemblies at the periphery of the core). This fact results in radial thermal gradients (Figure 8.2) that induce thermal stresses in the core support plate; peak concentrations of ~ 250 MPa were observed around the calibrated holes for the inter wrapper flow. Furthermore, due to the interlinking of the core and the spallation loop, a segment of the core support plate is cut away. Because the outer region of the plate is colder than the inner region, the slot in the core support plate will widen with 2.6 mm for a T91 made core support plate (Figure 8.3). Finally, a minor through thickness temperature gradient causes the core support plate to bulge (Figure 8.4).

*This document refers to work being performed by scientists and institutions involved in IP EUROTRANS, as well as the financial support of the European Commission through the contract FI6W-CT-2004-516520.*

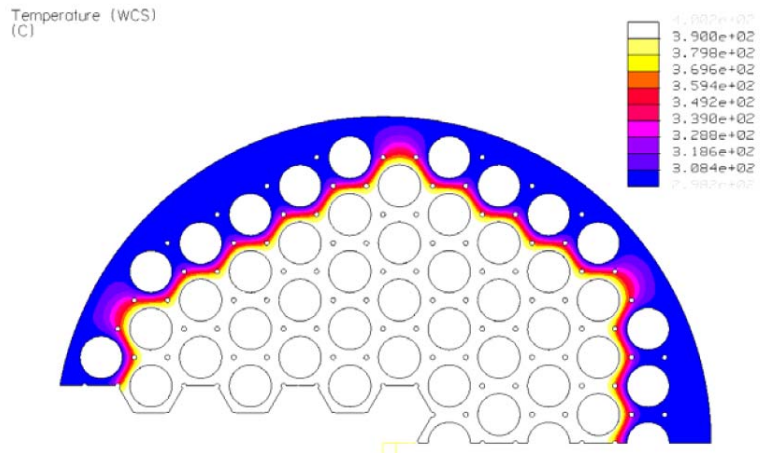


Figure 8.2. Core support plate : radial temperature distribution.

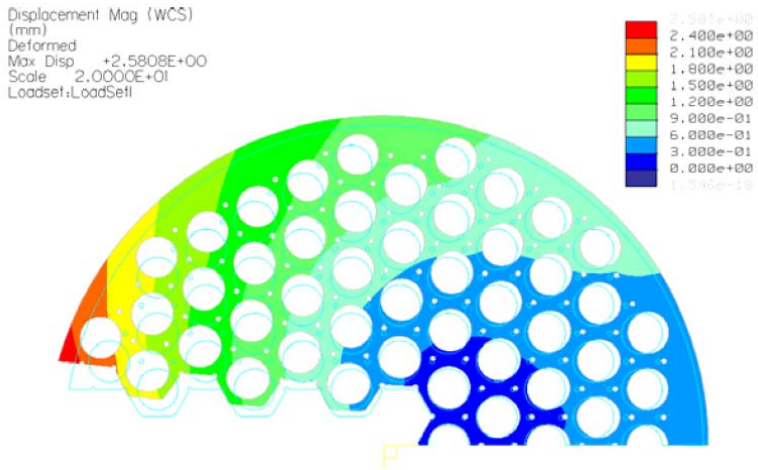


Figure 8.3 : Tangential displacement caused by radial T gradient.

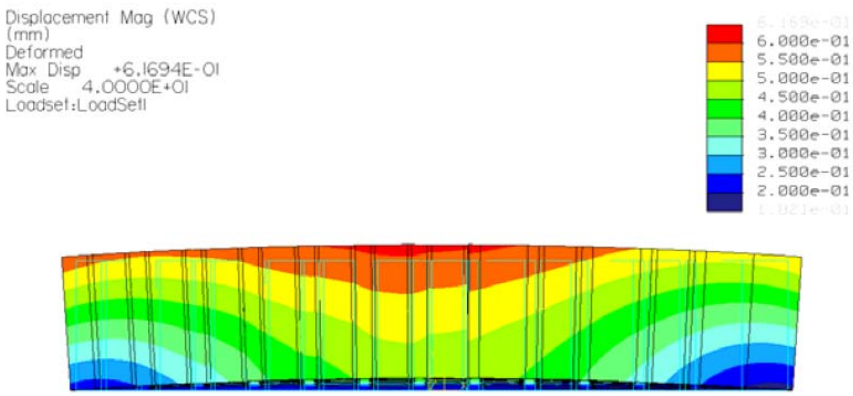


Figure 8.4: displacement caused by axial temperature distribution.

*This document refers to work being performed by scientists and institutions involved in IP EUROTRANS, as well as the financial support of the European Commission through the contract FI6W-CT-2004-516520.*

Higher thermal stress can be expected due to gradients within the core and in transient conditions.

From EFR, at saturation, values were at 2.5 at% were leading to a low ductility. The maximum irradiation is based on a swelling criteria but no data from EFR is available for T91 steel which was considered only for Steam Generator applications.

From the safety point of view [8.5], practical elimination of large failure of core support function must be excluded through the provision of sufficient lines of defence (e.g. design and operation, In Service Inspection, Leak Before Break, consideration of additional core support devices).

### 8.3.5 Fuel cladding

On the core side, the induced effects of metal corrosion by Pb-Bi might require a protective oxide layer (oxygen concentration controlled and/or protective coating by GESA treatment) on some critical parts of the core and possibly on the entire structures. DEMETRA results should also provide the LBE environment impact on the fatigue strength of basic material and/or the protective layer. Exploratory analyses complementary to the risk of local erosion by Pb-Bi at the grids/fuel clad interfaces should also be studied (local speed can reach values larger than 2 m/s and could lead to cladding erosion combined to the risk of wear per inter-structure contacts).

### 8.3.6 Recommendations towards CDT

The CDT project is presently reconsidering this design in order to improve the irradiation efficiency of the plant aiming at a targeted fast flux level above E = 0,75 MeV of $10^{15}$ $n.cm^{-2}.s^{-1}$.

Some concerns on the lower core inlet temperature of 270°C now selected for FASTEF has to be overcome if cladding material used in the core remains T91 and not AIM1. The inlet coolant temperature could be lowered provided positive answers are given to the embrittlement issue from the material specialists either in DEMETRA or GETMAT.

The study pointed out that the implications of these modifications can be accommodated by the design, but a detailed experimental confirmation is still needed.

The induced effects of metal corrosion by Pb-Bi require a protective oxide coating (oxygen concentration controlled and/or protective coating by GESA treatment) on some critical parts of the core and possibly on the entire structures. DEMETRA results should also provide the LBE environment impact on the fatigue strength of basic material and/or the protective coating. Exploratory analyses complementary to the risk of local erosion by Pb-Bi at the grids/fuel clad interfaces should also be studied (local speed can reach values larger than 2 m/s and could lead to cladding erosion combined to the risk of wear per inter-structure contacts).

These aspects for the upgrade of the design together with a progress towards an advanced engineering design level for all components have been integrated in the work programme of the FP7 project CDT [8.7, 8.8, and 8.9].

References

[8.1] A. G. Glazov , V. N. Leonov, V. V. Orlov, A. G. Sila-Novitskii, V. S. Smirnov, A. I. Filin and V. S. Tsikunov, “, Russia Brest reactor and plant-site nuclear fuel cycle “, Journal Atomic Energy, Publisher Springer New York, ISSN 1063-4258 (Print) 1573-8205 (Online), Issue Volume 103, Number 1 July, 2007 , DOI 10.1007/s10512-007-0080-5 Pages 501-508

[8.2] Cinotti L., et al., “The ELSY Project”, Paper 377, Proceeding of the International Conference on the Physics of Reactors (PHYSOR), Interlaken, Switzerland, 14-19 September, 2008.

[8.3] S. Esther-Vignoud, “Helium cooled EFIT Probabilistic reliability analysis of different designs of DHR system”, Note technique NEPL-F 2008 DC 163 A, EUROTRANS Contract 516520 (F16W)

*This document refers to work being performed by scientists and institutions involved in IP EUROTRANS, as well as the financial support of the European Commission through the contract FI6W-CT-2004-516520.*

[8.4] S. Larmignat, “EFIT-He: Preliminary Description and drawing Reactor Vessel and Internals, IHX and Cross Vessel, DHR system”, Note technique NEPL-F 2009 DC 91, EUROTRANS Contract 516520 (F16W)

[8.5] S. Esther-Vignoud,” Approach and Acceptance criteria for Safety Design of XT-ADS”, Note technique NEPL DC 06 0074, Deliverable D1.20, EUROTRANS Contract 516520 (F16W)

[8.6] H. Aït Abderrahim et al., "MYRRHA Pre-Design File – Draft 2", SCK•CEN Report R-4234, June 2005.

[8.7] B. Giraud, “Review and justification of the main design options of XT-ADS”, Note technique NEPL DC 06 0090, Deliverable D1.5, EUROTRANS Contract 516520 (F16W)

[8.8] P. Baeten, H. Ait Abderrahim & D. De Bruyn (2009) "The Next Step for MYRRHA: the Central Design Team FP7 project", International Topical Meeting on Nuclear Research Applications and Utilization of Accelerators (AccApp09), Vienna, 04-08 May 2009.

[8.9] P. Baeten, H. Ait Abderrahim & D. De Bruyn (2009), "From MYRRHA/XT-ADS to MYRRHA/FASTEF: the FP7 Central Design Team project", International Conference on Fast Reactors & Related Fuel Cycles: Challenges & Opportunities (FR09), Kyoto (Japan), 7-11 December 2009.

[8.10] D. De Bruyn, P. Baeten, S. Larmignat, A. Woaye Hune & L. Mansani, "The FP7 Central Design Team project: Towards a fast spectrum Transmutation Experimental Facility", Proceedings of ICAPP ’10 San Diego, CA, USA, June 13-17, 2010.

*This document refers to work being performed by scientists and institutions involved in IP EUROTRANS, as well as the financial support of the European Commission through the contract FI6W-CT-2004-516520.*

# 9. ECONOMICS

## 9.1 XT-ADS Cost

The cost estimation has been carried out on the following basis [9.1]:

- The plant will be constructed on a green-field site
- Costs of dismantling and decommissioning have not been considered
- Only one unit will be constructed on the site
- The cost evaluation is expressed in millions of euros based on 2008 price levels. Financial costs (comprising escalation, interest during construction and fees) are excluded
- In the case of an overall turnkey contract, the main contractor's overheads, risk & reserves, related costs and profit are not considered
- R&D costs and Owner costs are excluded
- The plant is built in a non-seismically active region governed by a regulatory body
- Insurances, taxes, duties, permits and financial costs are not considered.

Three important price figures are provided:

- The Base Price – The sum of costs incurred in manufacturing/construction, material procurement, installation and commissioning.
- The Best Estimated Price – The Base Price plus insurance, spare parts and contingency (contingency results from engineering and overlooked ambiguities, unexpected modification in costs and rates, construction problems, planning shifts, inaccurate estimations and miscellaneous unforeseen costs).
- The High/Low Price – The Best Estimate price plus/minus uncertainty (uncertainty is the accuracy with which a market price is known by March 2010).

The methodology as defined in [9.1] is following some guidelines established by the IAEA [9.2] and by GIF [9.3]. The contingency is evaluated based on the degree of maturity with which the plant is being designed. The average contingency of around 50% reflects that the design is at the end of the preliminary studies but would require two other phases such as conceptual design phase and basic engineering phase before being built.

The cost of the fuel necessary to the first two cores of system XT-ADS have been evaluated based on the marginal use of a manufacturing factory of MELOX type or in reference to a prototype workshop of manufacture for PHENIX-type fuels.

A manufacturing cost of 24.5 M€ 2008 has been retained for the first two cores of XT-ADS plant of the EUROTRANS project.

It should be noticed that these costs are based on the use of workshops of a capacity significantly higher than what is needed for the XT-ADS (195 THM/year & 10 THM/year). The costs associated to the fabrication and the operations of the manufacturing plant are hence shared between different users. If a specific workshop would have to be created (if the sodium fast reactor prototype would not be built), a multiplication by 10 of the cost should be quoted.

Furthermore, in this study, it is important to notice that the plutonium is considered as costless.

As for the other types of nuclear plants, the cost of dismantling is currently estimated at 15 % of the investment cost [9.2], in a preliminary study.

*This document refers to work being performed by scientists and institutions involved in IP EUROTRANS, as well as the financial support of the European Commission through the contract FI6W-CT-2004-516520.*

Results of that evaluation is given hereafter [9.4] with a total base cost of 784 M€ and a high price of 1265M€.

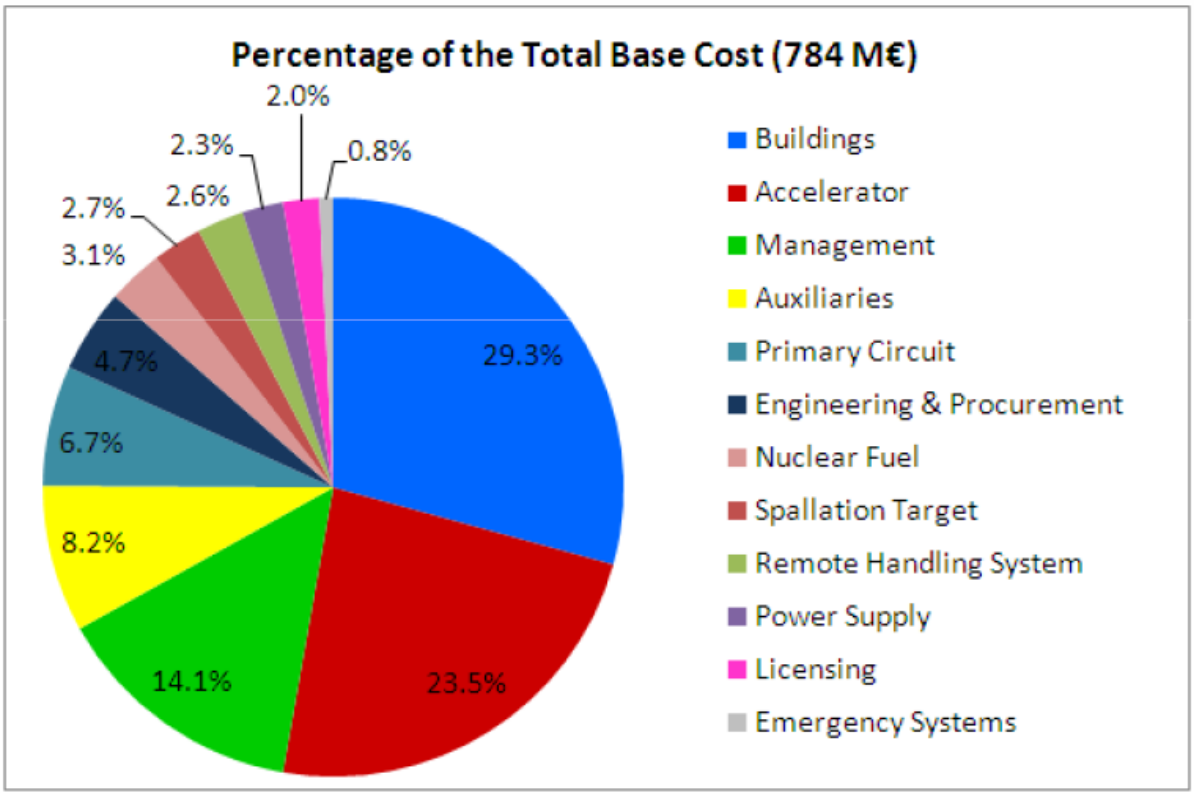


Figure 9.1: Splitting of the XT-ADS total base cost [9.4]

## 9.2 EFIT-Pb Cost

A preliminary estimate of the cost [9.5] of the EFIT Lead-cooled option has been done starting from the cost estimated for the XT-ADS [9.4]. This estimate can only be considered to be a very preliminary approximation to the final cost. A large number of the components and systems that will have an impact on the cost have not been yet developed, therefore, their costs have had to be estimated based on other references (ELSY, XT-ADS).

Concerning the CERCER fuel fabrication, the rationale is performed comparing the technical differences of the EFIT fuel with the more conventional MOX fuel as used for the XT-ADS (MYRRHA).

The parameters which guide this re-evaluation, compared to the standard workshop 10t/y for a FR prototype are:

- a cost of radiation shielding multiplied by 4;
- a cost of civil engineering and ventilation multiplied by 2;
- a cost of each stage of crushing geared down taking into account the thermal stresses;
- a size higher by a factor approximately 3, compared to the reference plant (10 t/y).

As a conclusion, for a two-core loading of 5.3 t, the unit costs are thus evaluated to be between 50 M€ (low price) and 80 M€ (high price). The best estimate value is 65 M€ (with a 5% actualisation rate).

An estimation of the cost of the EFIT Plant developed in IP-EUROTRANS has been performed. Given the early stage of development of the project, this estimate can only be considered to be a very preliminary

*This document refers to work being performed by scientists and institutions involved in IP EUROTRANS, as well as the financial support of the European Commission through the contract FI6W-CT-2004-516520.*

approximation to the final cost. A large number of the components and systems that will have an impact on the cost have not been developed at this stage of the project and therefore their costs have had to be estimated based mainly on XT-ADS [1, 2].

The Best Estimate (Base cost and Contingency) is of about 1890 M€. The overall uncertainty is of about 22% and consequently the Low/High price is 1472/2305 M€.

In the Figure 9.2 below is reported the splitting of the Best Estimate price (1890 M€) of the main groups in percentage.

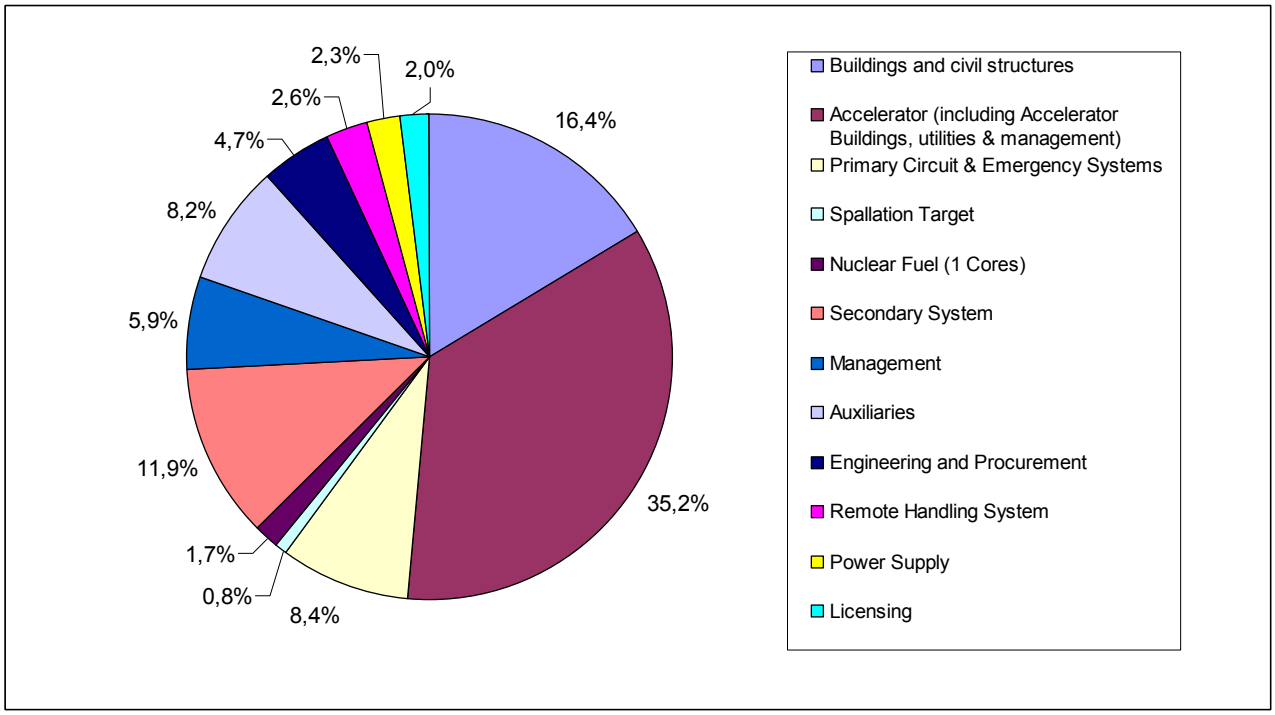


Figure 9.2: Splitting of the EFIT-Pb Best Estimate price [9.5]

## 9.3 Economic trends

The CDT project is presently reconsidering this design in order to improve the irradiation efficiency of the plant aiming at a targeted fast flux level above E = 0,75 MeV of $10^{15}$ $n.cm^{-2}.s^{-1}$ [9.6]. To increase this flux level, it is obvious that an increase in the installed power (from 57 MWth to 80 MWth,) the power density, the Pu content (up to 35% with a natural uranium matrix) and the cost of the plant will have to be increased.

Among the XT-ADS components [9.4], only a few of them have a strong dependence of the system power. Namely, these are: the fuel component storage building, the radwaste building and the cooling towers, the fuel assemblies, the primary pumps and the primary heat exchangers. As a rough estimation, the increase of cost of these components will be linear with respect to the values given for the XT-ADS [9.4]. A series of items have a slight dependence on the system parameters. A detailed evaluation of the cost should be done case-by-case. It mainly concerns the primary circuit (reactor vessels, core barrel, reactor cover…) and RVACS. Two buildings are also in this category: the reactor building and the building containing the air coolers, the central exhaust stack and the RVACS stack. All other items are practically independent of the power. In conclusion, the increase in the installed power, sufficiently well justified for allowing high flux level together with many IPS positions and the constraints on the maximum allowable Pu content in the fuel, will not induce a significant increase in price.

*This document refers to work being performed by scientists and institutions involved in IP EUROTRANS, as well as the financial support of the European Commission through the contract FI6W-CT-2004-516520.*

## 9.4 Reliability/availability

MYRRHA is to be a research reactor. Its main purpose is to accumulate neutron dose, dpa, transmutation rate or burnup on irradiated targets. Any interruption of the beam – of significant duration - translates into a reduction of the effective cycle duration and a final dose short of the objectives of the irradiation. This is certainly not what the operator desires and, regardless of the ability of the design to sustain repeated beam trips, it is of utmost importance to keep the number of beam trips to an absolute minimum.

If the restart after a beam trip is similar to the one of PHENIX (22 hours), five such beam trips would cut 5 days from a 90-days irradiation cycle. This is quite acceptable. Twenty such beam trips will reduce the effective cycle duration by almost 25%, and this is much less acceptable. At the extreme, 90 beam trips would not allow to make one single day of irradiation.

In certain cases, the interruption of the irradiation will "only" result in a final dose smaller than expected. For some applications, like the production of isotopes, repeated beam trips could simply prevent any production at all, as produced isotopes decay during the beam interruptions.

The years 2018 – 2019 would be devoted to the commissioning of XT-ADS at progressive levels of power. Four cycles at the reduced power are planned to perform:

- cycle: at about 1% of the nominal power level ($P_{nom}$) - testing main neutronic static and dynamic performances of the core;
- cycle: 1-10 % of $P_{nom}$ - testing start procedure, power control and cooling systems,…;
- cycle: 40-50 % of $P_{nom}$ – integral testing of the reactor and core reconfiguration tests after the cycle, …;
- cycle: ~80 % of $P_{nom}$ – operation of the reactor at power close to $P_{nom}$.

During the commissioning period the cooling system will operate in a special regime at the reduced input temperature (200-300°C). Lower power levels will also be repeated at every restart and shutdown of the reactor. This will require supplementary studies on the thermal-mechanical resistance of the critical elements of the core, such as the fuel cladding and the core support plate, in the region of 200-300 °C.

An operation cycle consists of three successive periods of three months each, separated by one month of minor maintenance periods, and then followed by a three months major maintenance period (Figure 9.3). The minor maintenance periods are mainly dedicated to core fuel loading and reshuffling adjustments, irradiation devices (IPS, In Pile Sections) handling, systems inspection, probe management and minor maintenance; during the major maintenance periods, particular components (e.g. the spallation loop) will be extracted from the reactor for inspection and possibly for repair (e.g. target confinement). So, the required availability of the irradiation facility is, averaged over several years, 9 irradiation months over a total cycle period of 14 months, or about 65%.

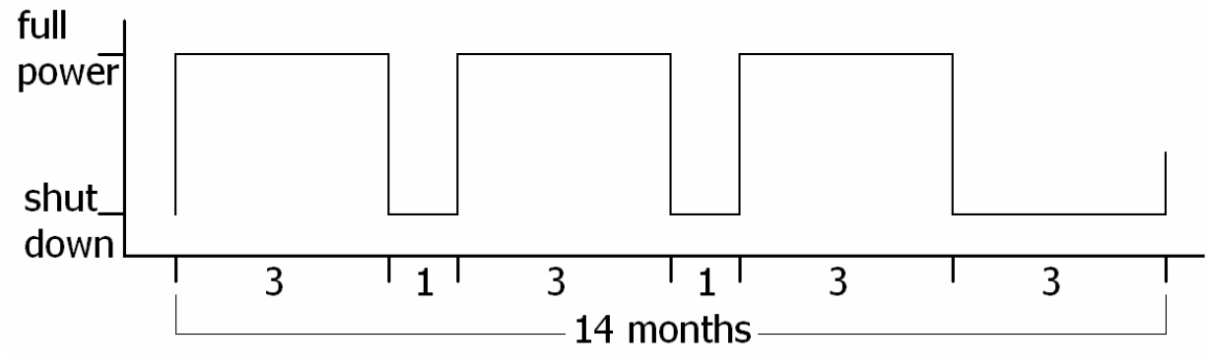


Figure 9.3: Operation regime of the XT-ADS [9.6]

*This document refers to work being performed by scientists and institutions involved in IP EUROTRANS, as well as the financial support of the European Commission through the contract FI6W-CT-2004-516520.*

- During the commissioning (the first life cycles) period, the reactor will operate at lower power (»1%, 1-10%, 40-50%, »80%) and during this period the availability obviously will be less than 65%.
- A major overhaul is foreseen every five years (four full operation periods of 14 months). Key components will be inspected and possibly repaired or replaced if required during this period (e.g. pumps, heat exchangers, inspection manipulators).
- The reactor lifetime is targeted to be more than 30 years. It is therefore required that reliable, proven equipment (including the remote handling systems) will be used in the plant design. Custom designed hardware shall not be used unless peculiar to the innovative XT-ADS concept. The equipment shall be considered proven if:
  - it has a documented and satisfactory operating experience as modules of subsystems in nuclear power plant applications or it has a documented and satisfactory operating experience in applications, other than power plants, which are similar to the use in XT-ADS;
  - it has satisfactorily completed a defined program of prototype testing which has been carried out to verify its performance in nuclear application.
- It is required that the remote handling systems guarantee the maintenance for the XTADS device during this entire lifetime and provide also the means for the complete decommissioning after its lifetime of 30 years.
- Plant reliability shall be demonstrated through a reliability analysis, the output of which shall also include recommendations for maintenance activities, spare parts, precautions and limitations, systems and components technical specifications, surveillance tests, and test intervals. Quantitative reliability performance targets shall be based on current industry available databases and on experience.
- Special relevance shall be assigned to testing operation of systems and components, so as to allow periodical check-up of their performance. Appropriate human factors principles shall be included in the design to assure that equipment configurations and test procedures will help prevent possible human errors.

Very first conservative estimations do not show stop-factors for the cladding operation at the reduced coolant input temperature of 200-300°C during the commissioning period

REFERENCES

[9.1] “Methodology for a Cost Estimate establishment”, Deliverable D1.45, Rev. 1 of the EUROTRANS project

[9.2] Technical Report Series N°396, Economic Evaluation of Bids for Nuclear Power Plants, 1999 Edition, International Atomic Energy Agency, Vienna, 2000.

[9.3] Cost Estimating Guidelines for Generation IV Nuclear Energy Systems, Revision 3, The Economic Modeling Working Group of The Generation IV International Forum, 2006.

[9.4] “Cost estimate for the XT-ADS”, Deliverable D1.68, Rev. 0, of the EUROTRANS project

[9.5] “Cost estimate for the EFIT-Pb”, Deliverable D1.79, Rev. 0, of the EUROTRANS project

[9.6] P. Baeten, H. Aït Abderrahim & D. De Bruyn (2009) "The next step for MYRRHA: the Central Design Team FP7 project", International Topical Meeting on Nuclear Research Applications and Utilization of Accelerators (AccApp09), Vienna, 04-08 May 2009

*This document refers to work being performed by scientists and institutions involved in IP EUROTRANS, as well as the financial support of the European Commission through the contract FI6W-CT-2004-516520.*

# 10. OPTION VALIDATION STATUS (R&D NEEDS)

IP EUROTRANS launched the conceptual design of a full scale transmutation demonstrator (called European Transmutation Demonstrator (ETD), loaded with transmutation dedicated fuel. This ETD would represent the first unit of a modular system of large power, which will be able to handle a large part of the high-level nuclear wastes in Europe.

The size and power of this first-of-a-kind ETD has been carefully selected based on the state of science and technology at the time of realization that is after several years of operation and R&D acquisition of the XT-ADS. This is not a simple task as too much margins based on the current knowledge could make the design unattractive either for its cost or for its transmutation potential. A reasonable set of design constraints has therefore been set up anticipating 25 years R&D development. The credibility of the final design is subject to these conditions and a sensitivity analysis to the design constraints provided as a conclusion is identifying the weakest parts of the missing R&D work.

For the XT-ADS, the material boundary limits have to be demonstrated prior to its construction and as soon as possible given the deadline (2020) given by the project. Within IP EUROTRANS, the design has been proceeding with margins taking into account the uncertainties associated to the knowledge of these boundary limits.

For this purpose, the different R&D activities within IP EUROTRANS are being summarized with in particular, development of a reliable accelerator (Chapter 10.1), the methods for reactivity measurements and start up procedure recommendation (Chapter 10.2: DM2 ECATS), the choice of fuels for EFIT and their associated characteristics (Chapter 10.3: DM3 AFTRA), the recommendations for materials under lead (Pb) and lead-bismuth eutectic coolant flows and their related technology (Chapter 10.4: DM4 DEMETRA), the nuclear data recommendation (Chapter 10.5: DM5 NUDATRA).

## 10.1 Related R&D Activities on the LINAC Accelerator

A huge R&D effort has been performed during the EUROTRANS project, including activities on the injector side and on the superconducting linac side. A brief summary of the main achievements and conclusions is proposed here after. More detailed information can be found in [10.1.1].

### 10.1.1 R&D activities on the injector

In the past years, the CEA Saclay SILHI source has been successfully used for several week-long reliability tests at currents of 30 mA, showing no beam stops and only occasional sparks in the extraction region, causing no beam interruptions [10.1.2]. In the EUROTRANS context, the 3-MeV High Intensity Proton Injector (IPHI) RFQ (Radio Frequency Quadrupole) which is the assembly of three 2-m long coupled-segments will be used. These tests are planned to be extended using the 3 MeV IPHI 4-vane 352 MHz RFQ [10.1.3] for a 2-month long-run reliability beam test. The tuning of the end regions of such accelerator with respect to the quadrupole mode, is generally made by machining the thickness of the end plates or increase of the notch in the vanes (LEDA). The dipolar modes are adjusted around the accelerator quadrupolar mode by adding dipole rods on the end plates and adjusting their length. In the case of the last IPHI RFQ segment, the achievable tuning range obtained with the possible plate thickness was not sufficient to adjust the frequency at 352 Mhz without modifying the notch depth, leading to serious engineering problem for the cooling, new thermomechanical simulations and drawings. To avoid these difficulties, the endplate thickness adjustment is replaced by a “quadrupole rod” –as opposed to the "dipole rod" - length adjustment. These rods are situated between the beam axis and the dipole rods, and the tuning range is largely

***This document refers to work being performed by scientists and institutions involved in IP EUROTRANS, as well as the financial support of the European Commission through the contract FI6W-CT-2004-516520.***

increased.The IPHI RFQ is still presently under final construction (see Figure 10.1.1), due to delays mainly due to encountered technological difficulties, especially linked with brazing procedures. Waiting for the final results of the reliability test, a preliminary conclusion on this topic is that such high frequency 4-vane RFQs are very difficult to build, and that the alternative of a 176 MHz injector based on a less demanding 4-rod RFQ should be explored.

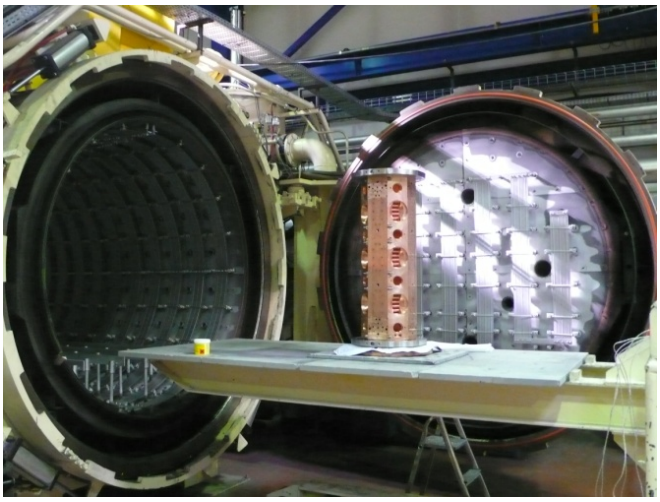

Figure 10.1.1: IPHI RFQ section 6 in vertical position at the entrance of the oven before brazing

Within the injector context, a 19-gap superconducting 352 MHz low energy CH prototype, first of its kind, has been also successfully built and tested at IAP Frankfurt in vertical cryostat, with excellent measured gradients of 7 MV/m (cf Figure 10.1.2). The cross-bar H-type (CH) cavity is a multi-gap drift tube structure based on the H-210 mode. The 19-cell, beta=0.1, 352 MHz, bulk niobium prototype cavity has been then tested in a horizontal cryostat with its associated tuners. Activities will be pursued in the following years, with the construction of a new optimized prototype cavity, its test under realistic conditions (horizontal cryostat, high RF power), and ultimately with beam at GSI. More information can be found in [10.1.4] and [10.1.5].

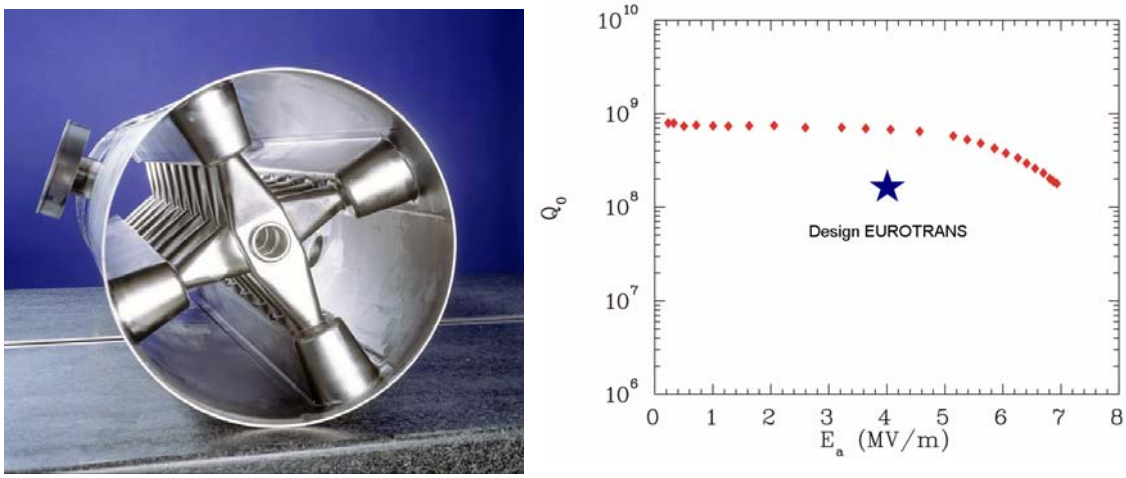


Figure 10.1.2: (left) the superconducting CH-prototype before the final welding.
(right) measurement of the Q-value as function of the accelerating gradient.

***This document refers to work being performed by scientists and institutions involved in IP EUROTRANS, as well as the financial support of the European Commission through the contract FI6W-CT-2004-516520.***

### 10.1.2 R&D activities on the main superconducting linac

Concerning the intermediate-energy section, a 352 MHz spoke cavity has been successfully tested at 4K and 2K at IPN Orsay in an "accelerator-like" horizontal cryostat configuration, fully equipped with its tuning system, magnetic shield, RF power coupler, and fed by a 10 kW 350 MHz solid-state amplifier and its associated digital LLRF loop (Figure 10.1.3). RF couplers have been successfully conditioned up to 10 kW in TW (Tertiary Winding) mode, with only a few easily processed multipacting barriers above 7.5 kW [10.1.6]. The tuning system, equipped with two piezo-actuators, has been validated together with the digital low level RF control system, reaching a field and phase stability respectively better than 1% and 0.5° at 2 $\sigma$. In the fault-recovery scenario context, preliminary experiments have also been performed to test the fast cavity detuning procedure, with very good results (~1 kHz detuning in less than 5ms). These activities will be pursued within FP7, focusing on the detailed design of a MYRRHA-like spoke cryomodule, and on the choice of the optimal operation temperature of such cavities (2 or 4K).

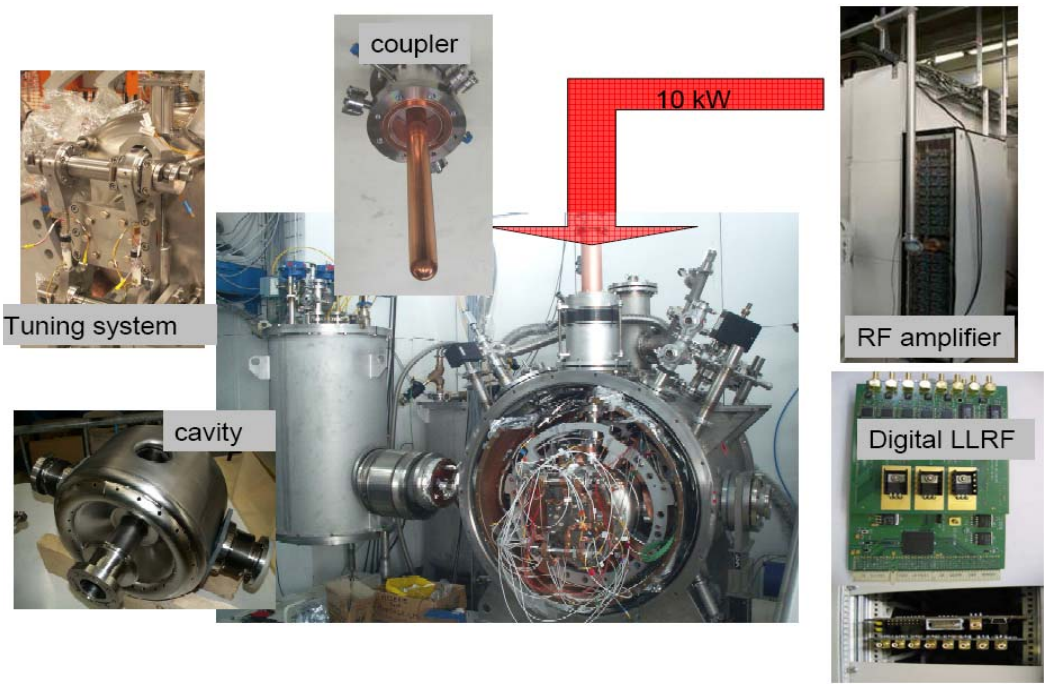


Figure 10.1.3: Pictures of the spoke test cryostat and its associated ancillaries ready for 4.2 K tests.

Concerning the high-energy section, a prototypical 700 MHz cryomodule [10.1.7], mainly funded by the EUROTRANS project, has been designed from scratch by INFN and CNRS, built and installed in a former cyclotron pit at IPN Orsay (cf Figure 10.1.4). It contains a five cell cavity ($\beta$ =0.5) elliptical superconducting, equipped with its blade tuner system, and fed by 80 kW Thales Electron Devices® IOT by means of a 150 kW power coupler and its associated door-knob transition. Part of the system has been successfully commissioned, and activities will be pursued in the following months to better evaluate the efficiency, but above all the reliability, of such an accelerating device. In particular, the capability of the piezo-based tuning system coupled with the digital low-level Radio Frequency (LLRF) I/Q (In-phase Quadrature) feedback loop and the microphonics influence on the cavity resonance

*This document refers to work being performed by scientists and institutions involved in IP EUROTRANS, as well as the financial support of the European Commission through the contract FI6W-CT-2004-516520.*

frequency will be estimated. Experimental results will be compared to MATLAB Simulink® simulations of the cavity's behaviour. Last but not least, this experiment set-up will also be able to provide a testing bench for specific sequences of the XT-ADS fast fault-recovery reference scenario that will be the focus of FP7 activities in this area [10.1.8].

Figure 10.1.4: (left) scheme of the prototypical 700 MHz cryomodule, with its dressed cavity inside. (right) The module after vacuum leak tests at the SIMIC company.

### 10.1.3 Conclusion on Accelerator R&D needs

A reliability-oriented superconducting linac has been identified as the reference solution for the European ADS concept, and an advanced design of the machine is proposed for the MYRRHA / XT-ADS Project, composed by a 17 MeV injector, possibly doubled, followed by independently-phased modular superconducting cavities with fault tolerance capability.

Numerous R&D efforts have been performed during the EUROTRANS Project, with very successful results and conclusions. These activities will be pursued within FP7, focusing on several main aspects: design consolidation, investigations on a 176 MHz injector alternative, experiments on fault recovery scenarii and several activities on system optimisation (operating cryogenic temperature, RF system optimisation with special focus on 700 MHz solid-state amplifiers, more detailed and relevant reliability analyses...). The goal is to be ready for the actual construction of MYRRHA foreseen to start in 2020.

***This document refers to work being performed by scientists and institutions involved in IP EUROTRANS, as well as the financial support of the European Commission through the contract FI6W-CT-2004-516520.***

REFERENCES

[10.1.1] J-L. Biarrotte et al., EUROTRANS DEL1.74, WP1.3 final deliverable, March 2010

[10.1.2] R. Gobin et al, “Saclay High Intensity Light Ion Source status”, Proc. EPAC 2001, Paris, France.

[10.1.3] P-Y. Beauvais, “Recent evolutions in the design of the French high intensity proton injector (IPHI)”, Proc. EPAC 2004, Lucerne, Switzerland.

[10.1.4] H. Podlech et al, “Recent developments on superconducting CH-structures and future perspectives”, Proc. LINAC 2008, Victoria, Canada.

[10.1.5] H. Podlech et al, “The 17 MeV injector for the EUROTRANS proton driver”, OECD/NEA TC-ADS workshop, Karlsruhe, Germany, March 2010.

[10.1.6] E. Rampnoux et al, “RF power coupler development for superconducting spoke cavities at IPN Orsay”, Proc. PAC 2009, Vancouver, Canada.

[10.1.7] S. Barbanotti et al., “Design of the prototypical cryomodule for the Eurotrans superconducting linac for nuclear waste transmutation”, Proc. EPAC 2008, Genoa, Italy.

[10.1.8] F. Bouly, S. Bousson et al, “Developments of 350 MHz and 700 MHz prototypical cryomodules for the EUROTRANS ADS proton linear accelerator”, OECD/NEA TC-ADS workshop, Karlsruhe, Germany, March 2010.

***This document refers to work being performed by scientists and institutions involved in IP EUROTRANS, as well as the financial support of the European Commission through the contract FI6W-CT-2004-516520.***

## 10.2 DM2 ECATS (Experimental activities on the Coupling of an Accelerator, a spallation Target and a Sub-critical blanket)

### 10.2.1 Plant Design Requirements and Experimental Objectives

From the feasibility study [10.2.1], five requirements coming from the design teams were expressed: Qualification of sub-criticality monitoring; Validation of the core power/beam current relationship; Start-up and shut-down procedures, instrumentation validation and specific dedicated experimentation; Interpretation and validation of experimental data, benchmarking and code validation activities; Safety and licensing issues of different components and for the integrated system.

In order to achieve such objectives, DM2 ECATS has been developed an extensive experimental programme to improve the knowledge about the control of an ADS and validate calculation methods, in terms of physic parameters important for safety:

- source importance,
- reaction rate (power) distributions,
- reactivity (subcriticality) measurements
- and also in terms of operational parameters:
- startup and shutdown procedures,
- subcriticality on-line monitoring,
- current/power/control rod relations (operating schemes, handling burnup swings),

After the MUSE experiment carried out within the 5$^{th}$ FP, the ECATS domain did develop the following experiments in order to fulfill the above objectives:

- The YALINA experiments in Belarus [10.2.2]. These experiments are of the MUSE type, i.e. a neutron generator is coupled to a flexible zero-power sub-critical assembly
- The RACE (Reactor Accelerator Coupled Experiment) experiments at Low Power (LP) operated in two different facilities : the TRIGA reactor of the ENEA/CASACIA named “RACE-T” [10.2.3] and the RACE sub-critical assembly of the Idaho Accelerator Center (IAC) named “RACE LP/IAC” in the USA [10.2.6].
- The GUINEVERE program, proposed by SCK-CEN [10.2.14]. In this program it is proposed to modify the critical facility VENUS located at Mol and to couple it with a dedicated GENEPI accelerator to perform the GUINEVERE experiment (Generator of Uninterrupted Intense NEutrons at the lead Venus Reactor). The way this experiment is set up is taking advantage of the experience gained with the previous experimental programmes.

### 10.2.2 The YALINA experiments

<u>Description of the YALINA-Booster facility and first reference</u>

The YALINA-Booster is a subcritical fast-thermal core coupled to a neutron generator [10.2.2]. The neutron generator uses a deuteron ion accelerator impinging on a Ti-T target to produce 14 MeV neutrons. The maximum beam current in quasi continuous mode is around 1.5 mA giving a maximum neutron yield of approximately $10^{11}$ n/s. A $^{252}$Cf neutron source with intensity of $2.56\times10^{6}$ n/s was also available for the experiments. The central fast-spectrum lead zone and the thermal-spectrum

***This document refers to work being performed by scientists and institutions involved in IP EUROTRANS, as well as the financial support of the European Commission through the contract FI6W-CT-2004-516520.***

polyethylene zone are separated by a so called thermal neutron filter, or valve zone, consisting of one layer of metallic natural uranium and one layer of boron carbide ($B_4C$), which are located in the outermost two rows of the fast zone (Figure 10.2.1). Three $B_4C$-control rods can be inserted in the thermal zone for changing the reactivity of the system by about 0.5$. The fuel in the innermost part of the booster zone could be uranium oxide of 36% enrichment or metallic uranium of 90% enrichment, whereas the rest of the fast booster zone consists of 36% enriched uranium oxide fuel. The thermal zone is loaded with uranium oxide of 10% enrichment.

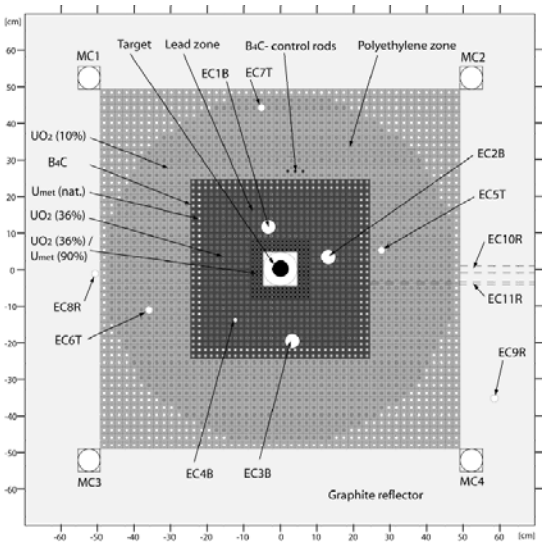


Figure 10.2.1 Schematic view of the core

| | Zone and fuel enrichment | | | | MCNP keff |
|---|---|---|---|---|---|
| | Inner booster | | Outer booster | Thermal zone | |
| | 90% | 36% | 36% | 10% | |
| SC0 | 132 | - | 563 | 1141 | 0.977 |
| SC3a | - | 132 | 563 | 1077 | 0.950 |
| SC6 | - | 132 | 563 | 726 | 0.850 |

Table 10.2.1 Core configurations studied

The main neutronics parameters of the reference assembly SC0 (Table 10.2.1) were measured (Table 10.2.2). Among the measurements, spectral index $\bar{\sigma}_f(^{238}U)/\bar{\sigma}_f(^{235}U)$ along the fuel rod in the centre of the 36% zone was achieved with solid state track detector technique, exhibiting the filter efficiency (Figure 10.2.2).

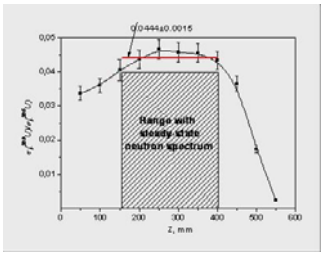


Figure 10.2.2 $\bar{\sigma}_f(^{238}U)/\bar{\sigma}_f(^{235}U)$

| PARAMETER | YALINA-BOOSTER |
|---|---|
| keff | 0.97943 |
| α | -470 s-1 |
| Λ | 56 µs |
| βeff | 738 pcm |

Table 10.2.2 Kinetic parameters of configuration SC0

*This document refers to work being performed by scientists and institutions involved in IP EUROTRANS, as well as the financial support of the European Commission through the contract FI6W-CT-2004-516520.*

YALINA results

*Calibration techniques and current to flux measurements [10.2.8]*

During a beam-trip, the prompt decay constant method can be used to determine the reactivity value. From the point kinetic model, the following expression for the reactivity can be expressed in units of β:

$$\alpha = \frac{\rho - \beta}{\Lambda} \Rightarrow \frac{\rho}{\beta} = \frac{\beta}{\Lambda}\alpha + 1$$

where α is the prompt neutron decay constant that can be determined experimentally by fitting the decay of the prompt neutron population with an exponential. The values of Λ and β can be computed. The analysis of the prompt decay constant during a beam trip is complicated by the large fraction of delayed neutrons, and to the low statistics that can be achieved using small binning time (Table 10.2.3).

| Detector | Control rods extracted | | Control rods inserted | |
|---|---|---|---|---|
| | $\alpha_{PNS}$ ($s^{-1}$) | α ($s^{-1}$) | $\alpha_{PNS}$ ($s^{-1}$) | α ($s^{-1}$) |
| EC1B | -1039 ± 12 | -1055 ± 28 | -1103 ± 5 | -1155 ± 42 |
| EC2B | --- | -1054 ± 19 | -1101 ± 3 | -1175 ± 29 |
| EC5T | -1061 ± 13 | -930 ± 51 | -1101 ± 24 | -1146 ± 51 |

Table 10.2.3 Prompt decay constant results for SC3a

The prompt decay constant method with beam trips provided coherent results with the PNS and the agreement is even better than 10% and the effect of the control rods (~$/2) is well established. These values are not corrected for spatial effect of detector locations and of the effect of the source intensity appeared in other results. The reactivity was also determined by the PNS techniques with reduced statistical uncertainties but with a reduced coherency due mainly to the spatial effect. The current mode of detection with beam trip was also tested with success to follow the reactivity effect of the control rods.

*Neutron noise measurements Rossi-α and Feynman-α [10.2.9]*

A set of neutron noise measurements was achieved in the three configurations mentioned above. The neutron noise measurements were performed with a $^{252}$Cf neutron source located in the centre of the core with the neutron generator beam tube still in place. The neutron flux was measured by two 3He-detectors located in EC5T and EC6T respectively. In the fitting procedure of the Rossi-α data, it was found that three exponentials are needed to obtain a good fit for configuration SC0 and SC3a and two exponentials for configuration SC6. The contribution of the delayed neutrons was found negligible.

***This document refers to work being performed by scientists and institutions involved in IP EUROTRANS, as well as the financial support of the European Commission through the contract FI6W-CT-2004-516520.***

The results from the fittings are summarized in Table 10.2.4.

| Case | EC | Conf | CR | Source | $\alpha_2$ [s$^{-1}$] | $\alpha_1$ [s$^{-1}$] | $\alpha_0$ [s$^{-1}$] |
|---|---|---|---|---|---|---|---|
| 1 | EC5T | SC0 | Out | INK5 | -11340 ± 426 | -2442 ± 50 | -674 ± 10 |
| 2 | | | | INK7 | | | |
| 3 | | SC3a | In | INK7 | | | -1094 ± 77 |
| 4 | | | Out | INK5 | | | -1114 ± 8 |
| 5 | | SC6 | Out | INK7 | | - | -3094 ± 113 |
| 6 | EC6T | SC0 | Out | INK7 | -6821 ± 251 | -2656 ± 71 | -746 ± 115 |
| 7 | | SC3a | In | INK7 | | | -1156 ± 86 |
| 8 | | | Out | INK5 | | | -1163 ± 7 |
| 9 | | SC6 | Out | INK7 | | - | -3042 ± 62 |

Table 10.2.4 Results of the fitting for different configurations

In the Rossi-α analysis of the data, it was found that there exists two higher eigenmodes in addition to the fundamental mode. The higher eigenmodes made the fitting procedure cumbersome and obtaining good results of the fundamental mode was challenging. For the deepest subcritical configuration SC6 one higher eigenmode coincides with or is close to the fundamental mode, thus causing problems in obtaining a good value of the fundamental mode. Although long measurement times were spent giving low statistical uncertainties in the experimental data, the accuracy of the fundamental mode after fitting was not high enough to be able to observe a reactivity difference of 0.5$. Other coherent results were obtained according to the Feynman-α formula (as the ratio variation of the variance of the counts to the mean value) they present the same features in terms of alpha modes.

### 10.2.3 The RACE experiments

The RACE experiments at Low Power (LP) were operated in two different facilities: the TRIGA reactor of the ENEA/CASACIA named “RACE-T” and the RACE LP/IAC sub-critical assembly of the Idaho Accelerator Center named “RACE-LP/IAC”.

<u>The RACE-T experiments</u>

*Description of the RACE-T facility*

The TRIGA Mark II nuclear reactor of the ENEA, is a pool thermal reactor having a core contained in an aluminium vessel and placed inside a cylindrical graphite reflector, bounded with lead shielding (Figure 10.2.3). The European experimental teams performing the different experiments operated in the February 2004–February 2006 period, on different core configurations [10.2.17]. In that period the reactor operation was exclusively in sub-critical conditions, with the exception of the critical reference core assessment at the beginning of the campaign where the maximum power was 50 W (Figure 10.2.4). This ensured that the burn-up of each fuel was constant through all measurements, allowing a whole comparison in the experimental data analysis and correction factor calculations. Two different neutron sources were used during the experiments: a pulsed generator and a 252Cf source (0.4MBq). Source jerk measurements have been performed using a “Fast Rabbit” instrumentation system. The pulsed neutron generator accelerates deuterium ions onto a tritium target and produced 108n/s 14.3MeV neutrons, at maximal frequency (150Hz).

*This document refers to work being performed by scientists and institutions involved in IP EUROTRANS, as well as the financial support of the European Commission through the contract FI6W-CT-2004-516520.*

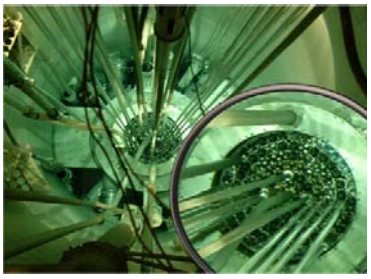

Figure 10.2.3 Top view of the ENEA/TRIGA

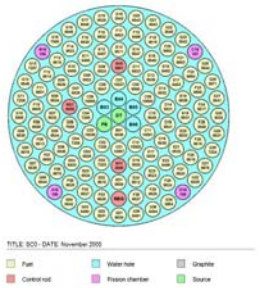

Figure 10.2.4 Reference critical (REG rod at 50% insertion)

*RACE-T results*

The main RACE-T results reported in the EUROTRANS deliverables [10.2.3] and [10.2.5] are: the characterization of the critical phase; the investigation of different sub-critical configurations with D/T generator at the core centre and specific instrumentation and acquisition systems in order to determine the sub-criticality and the relation current/power for ADS in a large scale of sub-criticality were also tested in these experiments.

*Characterization of the critical phase performed by fission rate traverses*

The radial traverses on the G13-G31 diagonal can be plotted on the same diagram, this leads to the following results (Figure 10.2.5):

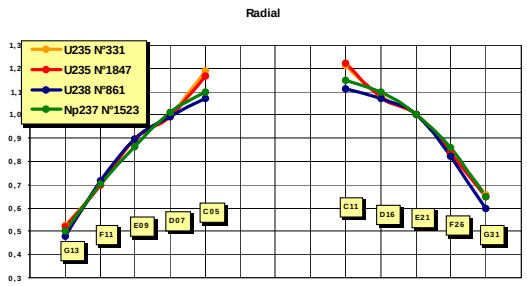


Figure 10.2.5 Normalized count rates on G13-G31 diagonal

One observes the thermal flux tilt at the centre of the core, due to the local moderation from the water in the middle of the configuration and a strong dissymmetry in the diagonal for all the radial traverses, reaching up to 20% on the peripheral fuel pins due to the presence of a tangential voided beam tube in the reflector. Axial distributions were also extracted from Au and In foil measurements and the ratio of thermal and epithermal neutron fluxes were also measured by the technique of the cadmium ratio with Au and In samples. Fast Neutron Flux was measured with Al shuttles.

*Experimental reactivity estimates of the three subcritical configurations of RACE-T*

The efficiency of various experimental techniques for assessing a sub-critical level was tested: the response to a pulsed neutron source; the transient due to a source jerk with $^{252}$Cf (SJ-Cf) or by switching off the neutron generator (SJ-Gen); the transient due to a rod drop and MSA method. The reactivity was estimated with the various methods at four core locations and for the three different subcritical core configurations, namely SC0 (~ -500pcm) SC2 (~ -2500pcm) SC3 (~ -5000pcm).

***This document refers to work being performed by scientists and institutions involved in IP EUROTRANS, as well as the financial support of the European Commission through the contract FI6W-CT-2004-516520.***

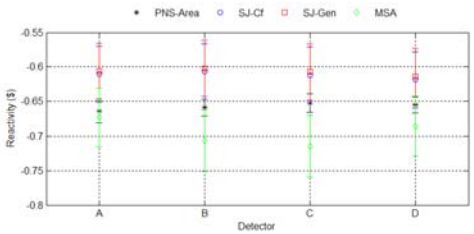


Figure 10.2.6 Comparison of techniques for the SC0 configuration

In the SC0 configuration the comparison of the techniques: PNS area-ratio method (PNS-Area), MSA method, Source jerk method by switching off the neutron generator (SJ-Gen), Source jerk method with $^{252}$Cf source (SJ-Cf). These results are displayed here with error bars for 95% of confidence.

The area-ratio method using a pulsed neutron source exhibited the best performance in terms of uncertainties and insensitivity to spatial effects (due to measurement or source location). Except the MSA, all the techniques agree in the range of 10% even for deeper sub-criticality levels.

The source multiplication method, which requires for calibration critical state and therefore is not suitable for future ADS is a well-established technique but needs large spatial correction factors far from criticality. The source jerk method (SJ-Cf) did not provide reliable results.

*The RACE LP/IAC experiments*

In the US, the first experiment of the RACE Project has been performed at the Idaho Accelerator Centre of the Idaho State University (ISU-IAC). The core of the ISU RACE sub-critical assembly is constructed of 6 modular aluminum trays each containing 25 flat plates of 20% enriched uranium-aluminum alloy with aluminum-clad (Figure 10.2.7). The sub-critical assembly is surrounded by a graphite reflector and water inside an aluminum tank that is ~1 m [10.2.6]. The $K_{eff}$ of such a sub-assembly is typically in the range of 0.90.

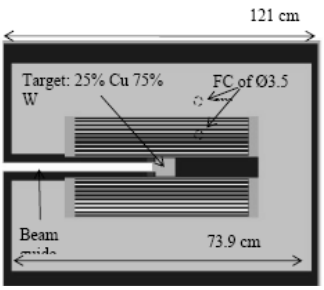


The neutron source was created by electrons produced by a LINAC and impinging a water-cooled target (75% of W and 25% Cu). The neutrons source intensity is ~ $10^9$n/s. The effective delayed neutron fractions were evaluated with MCNP by different methods, the best estimated value was equal to 768.4 ± 4.2 pcm. A methodology to calculate the spatial correcting factors for the area-ratio technique with MCNP has been developed.

Figure 10.2.7 Horizontal view of the ISU RACE assembly

The transient techniques (Inverse Kinetic and Non Linear Fitting techniques) were also applied and corrected with MCNP, these corrective factors account for both source and spatial effects [10.2.7].

***This document refers to work being performed by scientists and institutions involved in IP EUROTRANS, as well as the financial support of the European Commission through the contract FI6W-CT-2004-516520.***

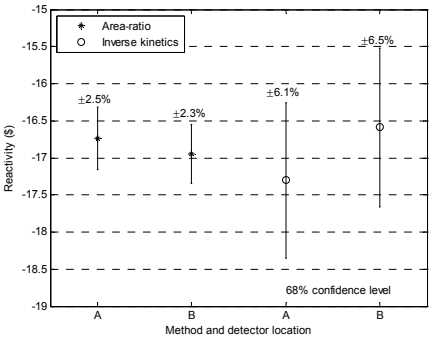


After corrections, the subassembly appears to be more subcritical than calculated (Figure 10.2.8). The area-ratio method allowed obtaining smaller overall uncertainties of 2.5% at most after correction.
The beam trip or transient techniques furnished less satisfactory results in terms of accuracy. That comes from the fact that the subassembly was so much subcritical that the transient caused by the shutdown of the pulsed neutron source was too short to successfully perform a transient analysis with the inverse kinetics method.

Figure 10.2.8 Experimental reactivity estimates

### 10.2.4 THE GUINEVERE EXPERIMENTS

On November 2006, the Scientific Consultancy Committee of EUROTRANS considered the proposed GUINEVERE experiment would be an important added value concerning the validation of the monitoring of the ADS systems. The final working plan of the DOMAIN2 was approved by the extraordinary Governing Council of EUROTRANS on December 2006. The necessary activities before the experiments concerned the modifications of VENUS the construction of the GENEPI-3C accelerator and the safety considerations [10.2.19].

*VENUS modifications:*

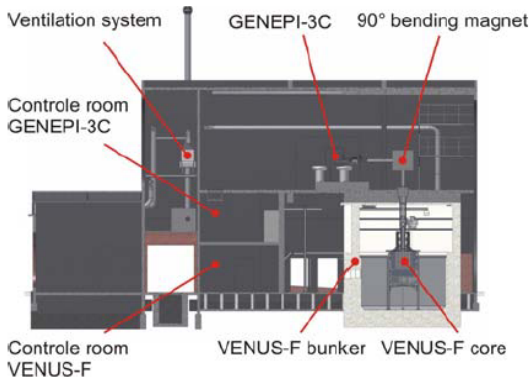


Two types of modifications were performed (Figure 10.2.9).

First, modifications are connected to the installation of the GENEPI-3C accelerator and its coupling to the core.

The second type of modifications is linked with the adaptation of the VENUS critical facility to host a fast lead-cooled core [10.2.10].

The licensing of the coupling was facilitated by the fact that the coupling of 14 MeV Pulsed Neutron Source has already been performed in the past (1960-1970) at the VENUS reactor and the experience gained during the MUSE-project.

Figure 10.2.9 The GUINEVERE facility

### *Construction of GENEPI-3C*

The GENEPI-3C neutron source is the third of a series of machines designed for reactor physics. It consists of a 250 keV deuteron accelerator producing neutrons by the D(d,n)$^3$He or T(d,n)$^4$He nuclear fusion reactions in a target.

The specifications are summed-up [10.2.11] in the following Table 10.2.5.

***This document refers to work being performed by scientists and institutions involved in IP EUROTRANS, as well as the financial support of the European Commission through the contract FI6W-CT-2004-516520.***

| | Pulsed Mode | Continuous Mode |
|---|---|---|
| Beam Energy | 140 to 240 keV | 140 to 240 keV |
| Peak Current | 40 mA | - |
| Mean Current | 190 µA at 4700 Hz | 160 µA to 1 mA |
| Pulse Rate/ Beam trip Rate | 10 up to 4700 Hz | 0,1 Hz up to 100 Hz |
| Pulse FWHM/ Beam trip Duration | 700 ns | 20 µs up to 10 ms |
| Transition time on/off | - | 1 µs |
| Spot Size | 20 mm in diameter | 20 to 40 mm in diameter |
| Source Intensity | $8\times10^{9}$ n/s (4 kHz) | $5\ 10^{10}$ n/s |

Table 10.2.5 The GENEPI specifications

The maximum beam intensity foreseen, in the continuous mode, is $I_{max}$ = 1mA. Higher current is not prohibited but it is limited by the target cooling capacity (to avoid fast Tritium desorption and target support melting). The mean intensity commonly used during the MUSE experiment was 40µA (pulsed mode at 1kHz). The maximum continuous intensity foreseen is then 25 times higher. It will provide a source strength of about $5\times10^{10}$n/s (this value might vary in time as a function of the beam charge sent onto the target)

The intensity of the beam is adjustable in the range 160µA-1mA. For the purpose of the experimental programme, in the continuous mode, beam interruptions ("beam trips") can be performed. Two neutron source monitors will be installed: the first one is a silicone detector placed upstream from the target that will detect the alpha-particles emitted in the $T(d,n)^4He$ reactions, the second will monitor directly the 14-MeV neutron at 180° thanks to a recoil proton telescope located above the vertical beam line.

### *Core specifications and experimental program [10.2.12]*

The final design of the critical core is shown in Figure 10.2.10 with the fuel pin being $U_{enriched}$ one.

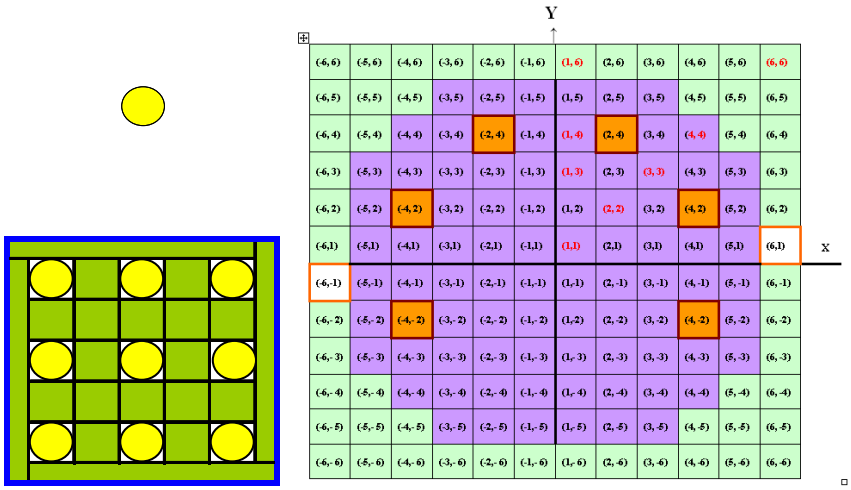


Figure 10.2.10 The GUINEVERE fuel pin, fuel sub-assembly and the core lay out

*This document refers to work being performed by scientists and institutions involved in IP EUROTRANS, as well as the financial support of the European Commission through the contract FI6W-CT-2004-516520.*

The main characteristics of the critical core are shown in Table 10.2.6.

| | |
|---|---|
| Fuel volume content | 17% |
| Critical Mass | 88 FAs |
| Keff | 1.01 |
| βeff | 748 pcm |
| Λ (prompt neutron generation time) | 3.8 $10^{-7}$ s |

Table 10.2.6 The GUENEVERE Core Characteristics

The effect of a lead buffer area, devoted to decrease the source neutron energy was investigated. Even if the effect of this buffer remains limited it was agreed to keep the corresponding slowing-down of the neutrons source. For the experimental program [10.2.14], two configurations are foreseen: a clean critical core named CR0 without the accelerator and the corresponding sub-critical configuration with the accelerator named SC1, obtained by the removal of the four central sub-assemblies. According to MCNP calculations the critical state will be reached with 88 assemblies with fuel corresponding to the pattern 5x5 with plates (82 fuels + 6 rods).The following measurements are planned to be carried out:

- Calibration of all control rods worth. These calibrations will be used to define the reference sub-criticality for MSM method.
- Axial traverses by U-235, Np-237 and U-238 fission chambers in dedicated channel of the experimental assembly. This experimental assembly will be placed in 8 different coordinates of the layout.
- Radial traverses by U235/U238 foils
- Spectral indices F238/F235, C238/F235, F239/F235, F237/F235, F240/F235, F242/F235 and F241/F235, in the core centre by activation foils and fission chambers simultaneously.
- βeff measurements by CPSD and Rossi-α technique

The SC1 configuration with a $K_{eff}$ target value of ~0.97, will be driven by the GENEPI-3C accelerator source in pulsed, continuous wave and continuous wave with beam interruptions. The same measurements as for the CR0 will be performed concerning the calibration and the axial traverses. In addition, GENEPI-3C will be operated in different modes for the sake of the foreseen experiments: PNS method, current-to-flux measurement and interim cross-checking techniques. Taking into account the time needed for fuel loading and changing the experimental devices, the necessary periods for fulfilling the experiments are 14 days for CR0 and 34 days for SC1.

### 10.2.5 Conclusion on ADS monitoring and Accelerator-Core coupling

During the FP6$^{th}$ program, ECATS provided a large panel of results concerning the ADS monitoring but also the designs of facility, accelerator and targets. New analysis methods as well as new results and theoretical considerations concerning the treatment of the harmonics with MCNP and deterministic neutronic codes can be noticed.

***This document refers to work being performed by scientists and institutions involved in IP EUROTRANS, as well as the financial support of the European Commission through the contract FI6W-CT-2004-516520.***

After the analyses of the MUSE experiments [10.2.20], some guidelines were expressed:

-an on-line and continuous sub-criticality monitoring should be established thanks to performing monitoring of the accelerator current, the intensity of the source and the power of the core,

-the comparison of critical versus sub-critical methods should be pursued,

-the ability of different techniques for measuring the absolute sub-criticality level should be confirmed. This ability should be robust and checked at different locations and different subcritical levels. The different correcting factors should be clarified (counter location, type of nuclear reaction used, with or without threshold).The associated uncertainties should be set.

The YALINA experiments allowed ensuring that techniques and analysis methods can be adapted to such complex core geometry. First experimental data with the current-power technique were obtained and confirmed the interest of the approach. Nevertheless, more experiments would have been necessary for uncertainty assessment. Main results are commented hereafter for the different techniques of reactivity measurements:

- The pulsed neutron source area-ratio technique

The spatial spread was very large and reactivity results from different detectors could differ by a factor of two. A converged result could be obtained after applying Monte Carlo correction factors [10.2.8].

- The beam trip technique

The beam trip technique obeyed the same spatial dependence as the area ratio method. The major difference, however, was the mode of functionality. The beam trip method may be used as reactivity monitoring method in a semi-continuous manner since the source is running in continuous mode with small interruptions for the reactivity measurement. The method gave the same results for detectors in pulsed and current mode operation.

- The prompt decay fitting technique

The prompt neutron decay as measured at various detector positions was found to be very close to each other. However, in the reflector a slightly slower decay was noticed. This effect became stronger at deep subcriticality.

- The Rossi-alpha technique

The neutron noise based Rossi-alpha method visualized the presence of two higher alpha-modes in addition to the fundamental mode. Most of the correlated events were occupied by the higher eigenmodes making the fundamental mode hard to obtain through fitting. As a result, the statistical accuracy in the fundamental mode was not high enough to be able to distinguish a reactivity difference of 0.5 $. Consequently, to obtain good results when higher eigenmodes are present, extremely long measurement time is needed, in particular at deep subcriticality.

- The Feynman-alpha technique

The Feynman-alpha method gave the same results as the related Rossi-alpha method, however, this method is much more sensitive to non-ideal circumstances such as non-stationary count rate and dead time effects. A consequence was that only one higher eigenmode could be obtained instead of two.

- The current-to-flux technique

This relative method is the only real monitoring technique since it can, in principle, be used at full power without beam interruptions; however, frequent beam interruptions will be necessary for

***This document refers to work being performed by scientists and institutions involved in IP EUROTRANS, as well as the financial support of the European Commission through the contract FI6W-CT-2004-516520.***

intermediate calibrations. During the experiments, it was found that in addition to the beam current and the neutron flux, it is necessary to monitor also the neutron source strength and the position of the beam impact on the target to reach full understanding of the process. The current mode electronic chain to monitor the neutron flux, the likely mode to be used in a power ADS, was also tested with success in YALINA.

During the RACE experiments consistent results with MUSE were found. In RACE-T, the area-ratio method using a pulsed neutron source exhibits the best performance in terms of uncertainties and insensitivity to spatial effects (due to measurement or source location). The source multiplication method, which requires a calibration in a critical state and therefore is not suitable for future ADS is a well-established technique but necessitates lot of heavy calculations for correcting factors often important far from criticality. In RACE-LP-ISU, the area-ratio method allowed obtaining smaller overall statistical of 2.5% at most after correction and an appropriate work on statistic errors treatment. The beam trip or transient techniques furnished less satisfactory results in terms of accuracy.

After the YALINA experiments, all the different sub-critical methods for determining the reactivity can be managed. The first trials on the on-line monitoring are satisfactory and promising. An important step towards the better comprehension of the harmonics was reached and different correcting factors were produced with Monte-Carlo codes. The discrepancies are still of the same level than in MUSE, but a great part are due to the particular conditions: multi-region system and hard conditions of measurements. After the RACE experiments, the comparison between critical method (MSM method) and sub-critical methods is still pending. The difficulties encountered with the calculations of correcting factors for these measurements are still to be addressed.

The GUINEVERE experiments have been tailored considering MUSE feed-back and conclusions. Core configurations, GENEPI-3C, materials and devices were designed to minimize all undesired effects and limitations observed during the previous programs. The progress in the calculation domain and the combined use of Monte-Carlo and deterministic codes should improve the understanding of the results and the uncertainty assessments.

The main challenges for GUINEVERE are: closing the comparison critical versus sub-critical measurements and diminishing the discrepancies between the counters and the methods which are still around 10% [10.2.21]. That is completely achievable thanks to the progress performed in the calculation of correcting factors during the YALINA and RACE experiments and the dedicated designs of the GUINEVERE core and the accelerator GENEPI-3C. All the progresses registered during the FP6$^{th}$ program on the on-line monitoring of the system (beam, source and core) will afford more accurate measurements of its behavior for any future experiments at power [10.2.15] and [10.2.16].

REFERENCES

[10.2.1] Final report on the second feasibility study including working programme with details on milestones, deliverables, time schedule, financial issues and recommendations, G. GRANGET et al., EUROTRANS deliverable D2.1

[10.2.2] Report on the core definition and characterization for YALINA, A. KIYAVTSKAYA et al., EUROTRANS deliverable D2.2

[10.2.3] Report on the RACE-T results, R. ROSA et al., EUROTRANS deliverable D2.3

[10.2.4] Report on the solid target design, P. AGOSTINI et al., EUROTRANS deliverable D2.4

***This document refers to work being performed by scientists and institutions involved in IP EUROTRANS, as well as the financial support of the European Commission through the contract FI6W-CT-2004-516520.***

[10.2.5] Analysis report of RACE-T experiments, M.CARTA et al., EUROTRANS deliverable D2.5

[10.2.6] Report on the RACE-LP/IAC results, Ch. JAMMES et al., EUROTRANS deliverable D2.6

[10.2.7] Analysis report of RACE-LP/IAC results Ch. JAMMES et al., EUROTRANS deliverable D2.7

[10.2.8] Report on the current to flux monitoring and interim calibration techniques in YALINA, D. VILLAMARIN et al., EUROTRANS deliverable D2.8

[10.2.9] Report on noise techniques applied in YALINA, C. BERGLÖF et al., EUROTRANS deliverable D2.9

[10.2.10] Report on the facility design and modifications, G. VITTIGLIO et al., EUROTRANS deliverable D2.10

[10.2.11] Report on the GENEPI design and specifications, A. BILLEBAUD et al., EUROTRANS deliverable D2.11

[10.2.12] Report on GUINEVERE core specifications, F. MELLIER et al., EUROTRANS deliverable D2.12

[10.2.13] Report on GUINEVERE safety studies, L. MERCATALI et al. , EUROTRANS deliverable D2.13

[10.2.14] Report on the GUINEVERE experimental programme definition, A. KOCHETKOV et al. , EUROTRANS deliverable D2.14

[10.2.15] Report on licensing and commissioning aspects gained with GUINEVERE to FASTEF, J.A. CARRETERO et al. , EUROTRANS deliverable D2.18

[10.2.16] Transposition of RACE and MEGAPIE experience to XT-ADS design, L. BURGAZZI et al. , EUROTRANS deliverable D2.19

[10.2.17] ECATS: an international experimental program on the reactivity monitoring of Accelerator Driven Systems - Status and progress, G. GRANGET et al. Conference, GLOBAL 2007

[10.2.18] Overview of Activities Exploring Options for Transmutation, D. STRUWE, J. SOMERS, EURADWASTE 2008

[10.2.19] The GUINEVERE project at the VENUS facility, P. BAETEN et al. Proc. HPPA'05 on Utilisation and Reliability of High Power Proton Accelerators. MOL, BELGIUM (May 2007).

[10.2.20] The MUSE experiments for sub-critical neutronics validation, F. MELLIER et al. Deliverable N°6 and 8 Contract N° FIKW-CT-2000-00063

[10.2.21] Core instrumentation and reactivity control of the He cooled eXperimental ADS (XADS), G. RIMPAULT et al., GLOBAL 2003, New Orleans, USA

***This document refers to work being performed by scientists and institutions involved in IP EUROTRANS, as well as the financial support of the European Commission through the contract FI6W-CT-2004-516520.***

## 10.3 DM3 AFTRA (Advanced Fuels for TRAnsmutation Systems )

One of the weakest parts for the demonstration of the EFIT feasibility assessment deals with the choice of the fuel because transmutation fuels are very innovative and have not been so far developed either in Europe or elsewhere. The innovation in the ADS fuel development is related to the high Minor Actinide content, the Plutonium content to control the reactivity swing of the core and the absence of Uranium to avoid any additional plutonium production. Properties data for these kinds of fuel are sparse [10.3.2]. Fuel behaviour under irradiation is unknown. Fuel modelling is not qualified too. So, the objective of Domain 3 did consist of the design, the development and the qualification in representative conditions of the most promising U-free oxide fuel concepts. The major outcome of AFTRA is the recommendation about fuel designs and fuel performances of the most promising candidates for EFIT.

### 10.3.1 TRU fuel performance assessment at normal operation conditions.

A large range of candidate fuels have been assessed according to several criteria : fabrication, reprocessing, secondary waste stream, high temperature stability, transmutation performance, thermo-mechanical performances under nominal conditions, neutronic performance under nominal conditions, margin to failure and ultimate behaviour under accident conditions.

The results of these investigations [10.3.1] indicate that composite fuels as $^{92}$Mo Ceramic-Metal fuel and MgO Ceramic-Ceramic fuel are the most promising candidates for EFIT.

Several design options for both CerCer and CerMet cores have been investigated [10.3.3],[10.3.4] and optimal designs meeting the DM1 specifications [1.2] have been found. Dealing with CerMet fuel, a first reference core design which fits DM1 criteria except a low reactivity swing, has been matured and an advanced design with lower Pu/MA ratio (from 46/54 to 35/65) and fewer pins per S/A (from 169 to 91 or 61) has been proposed as a lastest alternative. This latest design fits the whole DM1 specifications [10.3.6].

Dealing with modeling of thermo-mechanic behaviour of the fuels under irradiation, even if their thermal, mechanical and thermo-chemical properties as well as their experimental behaviour under irradiation are poorly-known, preliminary calculations have been performed with codes as TRAFIC (Serco-Assurance for NNL) and MACROS (SCK-CEN). The codes, which were initially designed to model homogeneous fuels, have been extended during the project to handle heterogeneous media. The first results from TRAFIC indicate that thermo-mechanical performances of both CerMet and CerCer fuels are acceptable for peak-linear powers around 200 W.cm$^{-1}$ up to at least a 3 year operation time [10.3.7],[10.3.8]. These promising first results remain nevertheless quite unreliable due to the lack of knowledge on basic mechanisms in these fuels and progress are still required.

### 10.3.2 Fuel safety assessment

Fuel limit temperatures for various accident conditions related to the different categories of the defence-in-depth concept have been specified [10.3.5] according to a very conservative approach owing to the limited amount of available data. The limit temperatures for Design Basis Conditions range according to the category of the event, from 1650 to 2080K for CerCer fuels and 1850-2300K for CerMet fuels. The highest limit temperatures (for Design Extension Conditions - DEC) are lower for MgO-CerCer than for Mo-CerMet because of possible MgO vaporization above 2130K whereas Mo-CerMet stability limit temperature is about 2450K.

The safety behaviour of the EFIT cores fuelled with CerCer or CerMet have been analyzed in a broad set of scenarios ranging from transient conditions, accidents and severe accidents [10.3.9], [10.3.10]. Safety analyses have shown that in both CerCer and CerMet reference cores, the most limiting conditions would come from the T91 clad and safety limits for fuel are not violated. The safety margins remains nevertheless higher for CerMet than for CerCer.

*This document refers to work being performed by scientists and institutions involved in IP EUROTRANS, as well as the financial support of the European Commission through the contract FI6W-CT-2004-516520.*

### 10.3.3 Irradiation tests

The irradiation program has investigated:

- irradiation effects on CerCer and CerMet type fuels in EFIT representative conditions with FUTURIX-FTA test in PHENIX reactor,
- helium behaviour versus temperature and microstructure with HELIOS test in HFR reactor [10.3.11],
- helium build-up and release mechanisms versus temperature in $^{10}B$ (as Am surrogate) doped fuel matrices with BODEX test in HFR reactor,
- and some PIE of nitride fuels ($Pu_{0.3}Zr_{0.7}N$) irradiated in the HFR reactor as a part of the 5$^{th}$ European Framework Program: project CONFIRM [1.11], as nitride fuels constitute a backup solution for actinide burning.

The highly radioactive materials (with Am content from 0.2 to 1.9g.cm$^{-3}$) were fabricated at lab-scale:

- The particles of Am compounds were synthesized using two processes: an oxalic co-precipitation route for CerCer [10.3.12] and a combination of external gelation and infiltration methods for CerMet and homogeneous compositions [10.3.13, 10.3.14, 10.3.15].
- The following steps of fabrication were based on conventional powder metallurgy and similar for all compositions except the HELIOS CerCer fuel whose porosity was tailored to remain open, in order to allow helium to escape [10.3.12].

The FUTURIX-FTA irradiation test is currently complete with an irradiation time of 235 EFPD and cumulative neutron fluence of respectively ~1.0x10$^{23}$ n.cm$^{-2}$ and ~1.4x10$^{23}$ n.cm$^{-2}$ for CerCer and CerMet capsules. The HELIOS irradiation started on April 29, 2009 for 300 EFPD.

Dealing with BODEX experiment which aims at investigating the He-induced swelling behaviour of inert matrices using $^{10}B$ as Am surrogate, $^{10}B$- and $^{11}B$-doped pellets as well as blank samples (without B) were fabricated [10.3.16] in order to discriminate the effects related to helium production (10B-doped samples) from irradiation (blank samples) and chemical ($^{11}B$-doped samples) ones. The boron compounds mixed with MgO, Mo (and $ZrO_2$) are $Mg_3B_2O_6$, $Mo_2B$ (and $ZrB_2$), respectively. The boron content is about 0.01 g.cm$^{-3}$ in order to be representative in helium production by Am after 2 HFR irradiation cycles. The irradiation test performed within a two-legged device in order to study the effect of two temperatures (~1073K and ~1473K) [10.3.17] has been completed. First PIE results have already shown a smaller release of He out of the Mo samples compared to MgO ones, this phenomena being linked to the open porosity in MgO tailored ceramics. Correlatively, swelling of Mo is higher than MgO one.

### 10.3.4 Out-of-pile measurements

Out-of pile measurements have aimed at gaining knowledge on the fuel thermal, mechanical and physico-chemical properties in order improve the databases with relevant and accurate data for the fuel design, fuel performance and safety modeling. Many results have been gained. Some specific points are highlighted hereafter.

Thermal conductivity experimental measurements made on FUTURIX-FTA fuels up to 2200K, have for example pointed out a significant drop at high temperatures (T>1500K) for CerCer fuels, which were not predicted by calculations based on phase mixing models [10.3.18].

Vaporization and melting temperature measurements made on CerCer fuels have confirmed the low thermal stability of MgO under vacuum and neutral atmosphere, for closed and open systems. Volatilization species and temperature ranges have been made clear too [10.3.19]: the MgO vaporization begins at 1750-1800K, increases by five orders of magnitude between 1800 and 1900K. The major gaseous species is Mg.

Chemical compatibility tests have been performed [10.3.20] at 1300 and 1800K under different atmospheres (air, Ar, Ar/$H_2$), between $PuO_2$, $AmO_2$, $Pu_{0.5}Am_{0.5}O_2$ compounds and inert matrices such as:

MgO and Mo. The results have not shown any interaction between $PuO_2$ or $Pu_{0.5}Am_{0.5}O_2$ with MgO or Mo under any atmosphere, whereas for tests involving $AmO_2$ under argon, whatever the inert matrix, undetermined X-ray diffraction peaks are observed.

There is no interaction between Pb (EFIT coolant) and T91, Mo or MgO compounds [10.3.21].

Mo is compatible with the clad T91 up to 950°C [10.3.10]. Regarding MgO case, although any interaction has been shown at 550°C, SEM/EDS analyses performed on 950°C heat treated T91/MgO sandwiches have pointed out the local presence of magnesium in the T91 area in contact with MgO. No change in the appearance or composition of MgO was nevertheless observed.

Regarding the compatibility between fissile compounds and the T91 clad, slight areas of interaction have been observed on the $Pu_xAm_{1-x}O_2$ edge opposite T91 for $x \geq 0.5$ [10.3.22]. This leads to the preliminary conclusion that the fissile particles have to be surrounded by the inert matrix to prevent interactions with the clad.

Finally experimental investigations on the Pu-Am-O phase diagram have provided relevant data to partially build the $Pu_2O_3$-$Am_2O_3$ phase diagram [10.3.23]. They have pointed out too that Am drives the reduction process in the oxygen sub-stœchiometric area.

### 10.3.5 Conclusion on U-Free fuel

Studies on fuel development, motivated by assessing the industrial practicability and transmutation of high-level nuclear wastes, have already provided a wide range of results which reinforce the interest of both MgO-CerCcer and $Mo_{enr}$-CerMet for the EFIT machine. So, the ranking between the two primary candidates seems premature without the results of PIE of HELIOS and FUTURIX-FTA fuels, which are scheduled within the FP-7 FAIRFUELS program.

Besides the results expected from on-going European programs, which concern:

- PIE as well as recalculations of temperatures and behaviour under irradiation of HELIOS and FUTURIX-FTA pins, and ab-initio calculations of helium behaviour in inert matrices, within the program FAIRFUELS,
- assessment of aqueous reprocessibility of inert matrices, including: identification of advantages/drawbacks, ranking according to criteria like partitioning performances, volume of secondary wastes,…, and proposal of relevant axes of research, within the program ACSEPT.

The EFIT fuel qualification will require additional developments to demonstrate that the “fuel product fabricated in accordance with a specification behaves as assumed or described in the applicable licensing safety case, and with the reliability necessary for economic operation of the reactor” [10.3.24]. So, next steps in R&D should include at least achievements on:

- predictive modeling of fuel behaviour under irradiation
- fabrication techniques and processes
- experiments to improve the fuel behaviour understanding in off-normal operating conditions
- fuel recycling including: reprocessability (hydro & pyro-reprocessing) and secondary waste management
- properties measurements on irradiated fuels
- irradiation tests on ADS fuel reference compositions and designs under nominal conditions of flux, temperature and doses.

REFERENCES

[10.3.1] J. Wallenius et al., 2006, Deliverable D3.7: Selection of the preliminary candidate for DM1.

*This document refers to work being performed by scientists and institutions involved in IP EUROTRANS, as well as the financial support of the European Commission through the contract FI6W-CT-2004-516520.*

[10.3.2] R. Thetford et al., 2006, Deliverable 3.4: Recommended properties of duel, cladding and coolant for EFIT predesign.

[10.3.3] P. Smith et al., 2007, D3.1: ETD/EFIT-400 reference core devoted to the comparative analysis of TRU candidate fuels.

[10.3.4] J. Wallenius et al., 2007, D3.2: Neutronic performances of EFIT-400 (AFTRA) reference cores at the beginning of operation.

[10.3.5] W. Maschek et al., 2006, D3.9: Fuel recommendation for EFIT based on transient analyses

[10.3.6] A. Rineiski et al., 2010, D3.3: Comparison of the neutronic performances of the ETD reference core loaded with the selected TRU-fuels from BOL to EOL.

[10.3.7] V. Sobolev et al., 2008, D3.5: Estimation of the thermo-mechanical performances of the fuel rods of EFIT-400 (AFTRA), loaded with the selected TRU-fuels at the beginning of operation

[10.3.8] D. Farrant et al., 2009, D3.6 part A: Thermo-mechanical performances of the rods with the selected TRU-fuels from BOL to EOL. TRAFIC Calculations.

[10.3.9] W. Maschek et al., 2007, D3.10: A comparative assessment of safety parameters and core behaviour for the CERCER and CERMET oxide fuels proposed for the EFIT

[10.3.10] W. Maschek et al., 2008, D3.11: Upadated safety assessment for EFIT with CerCer and CerMet fuels taking into account recent experimental findings.

[10.3.11] E. D'Agata et al., 2009, D3.21: Design and safety report, HELIOS irradiation of U free fuels and targets for Am transmutation in a QUATTRO rig with two sample holders at the HFR Petten.

[10.3.12] A. Jankowiak et al., 2008, Nuc. Sci. Eng., 160, 378-384: Preparation and characterization of $Pu_{0.5}Am_{0.5}O_{2-x}$-MgO Ceramic/Ceramic Composites.

[10.3.13] A. Fernandez-Carretero et al., 2006, D3.18: R&D fabrication phase of CERMET fuel (FUTURIX-FTA).

[10.3.14] A. Fernandez-Carretero et al., 2006, D3.19: Report on fabrication and characterization of the FUTURIX-FTA CEREMT fuels.

[10.3.15] A. Ferandez-Carretero et al., 2007, D3.20: HELIOS fuels and pin fabrication report.

[10.3.16] E. Tynova et al., 2008, D3.25: DODEX fabrication report.

[10.3.17] F. Klaassen et al., 2009, D3.24: EUROTRANS-BODEX doped experiment (368-D1), Design and Safety report.

[10.3.18] J.P. Ottaviani, 2008, D3.40 a: Thermal characterization of MgO+$(Pu,Am)O_2$ fuel pellets.

[10.3.19] D. Staïcu, 2007, D3.40 b: Measurement of thermophysical properties of the inert matrix fuels - CerMet and CerCer.

[10.3.20] E. Gavilan et al., 2009, D3.32: Compatibility tests between inert matrices and $(Pu_x,Am_{1-x})O_2$ compounds

[10.3.21] P. Trabuc et al. 2009, D3.35: Compatibility tests between coolant and inert matrices.

[10.3.22] E. Belval-Haltier, 2009, D3.34a: Compatibility tests between T91 cladding and $(Pu,Am)O_2$ fuel.

[10.3.23] E. Gavilan, 2009, D3.37 : Pu-Am-O system investigation

[10.3.24] D. Crawford et al., 2007, J. Nuc. Mat., 321, 232-242: An approach to fuel development and qualification.

***This document refers to work being performed by scientists and institutions involved in IP EUROTRANS, as well as the financial support of the European Commission through the contract FI6W-CT-2004-516520.***

## 10.4 DM4 DEMETRA (DEvelopment and assessment of structural materials and heavy liquid MEtal technologies for TRAnsmutation systems)

### 10.4.1 Objectives

The objectives of DEMETRA have been the development and assessment of Heavy Liquid Metal (HLM) technologies, materials characterisation in design relevant conditions, and the thermal-hydraulic experiments to support the design of the spallation target and the sub-critical core [10.4.1]. The R&D programme has been fully defined on the basis of the design needs for the XT-ADS and EFIT-Pb. The data produced within DEMETRA have enabled to:

- Assess the coolant quality control systems with focus on two main aspects, i.e. the oxygen potential measurement and adjustment and the solid impurities monitoring and removal methods from both liquid and gas phases
- Assess the behaviour of reference structural materials and corrosion protection systems in HLM and under irradiation. The selected reference structural materials are the 9Cr ferritic/martensitic steel “T91” and the austenitic steel “AISI 316L”,
- Identify heat transfer characteristics under steady state and transient conditions, the stability of free surfaces for windowless spallation target and the flow characterisation in a fuel bundle,
- Define and assess HLM instrumentation and system operation technologies, such as pumps, heat exchangers and operational measurement techniques such as flow meters, free surface detection systems etc.
- Assess the operational performances of the MEGAPIE spallation target and evaluation of the capabilities to understand and predict both the beam window and the overall target performances, in view of supporting the neutron spallation target design decisions.
- Design support and experimental validation of the windowless spallation target option.

### 10.4.2 Materials characterisation

From previous works [10.4.2] it is well known that the corrosion mechanism on the steel is oxidation if the oxygen activity in the liquid metal is kept above the oxygen potential of the magnetite formation [10.4.3].
The results obtained within DEMETRA confirm that the oxidation of the steels is dependent on the oxygen content in the HLM. Indeed, at relatively low oxygen concentration the main corrosion mechanism is dissolution of the steel elements. Moreover, dependency of the oxidation rate (expressed in terms of oxide thickness) from the flow velocity and the temperature has been as well observed [10.4.4].

The materials characterisation includes long-term corrosion tests (Figure 10.4.1), mechanical tests in HLM and irradiation experiments (Figure 10.4.2). Moreover, a corrosion protection method based on the GESA surface alloying technique is developed and characterised.

The mechanical tests (Low Cycle Fatigue, Slow Strain Rate, Tensile, Fracture Toughness and Creep-to-rupture) performed in HLM, have shown that in the low temperature range the T91 above a certain stress and wetting level is prone to Liquid Metal Embrittlement (LME). However a ductility recovery is observed for temperatures above 400°C. Indeed, in this temperature range LME is not observed but liquid metal assisted cracking might occur since this phenomena has been observed in the higher temperature range for certain stress levels.

*This document refers to work being performed by scientists and institutions involved in IP EUROTRANS, as well as the financial support of the European Commission through the contract FI6W-CT-2004-516520.*

Figure 10.4.1: Test matrix of the long-term corrosion experiments in flowing conditions. All experiments are performed at an oxygen concentration of ~ 10-6 wt % and in LBE. The experiments performed by ENEA at 500 °C are conducted in Pb.

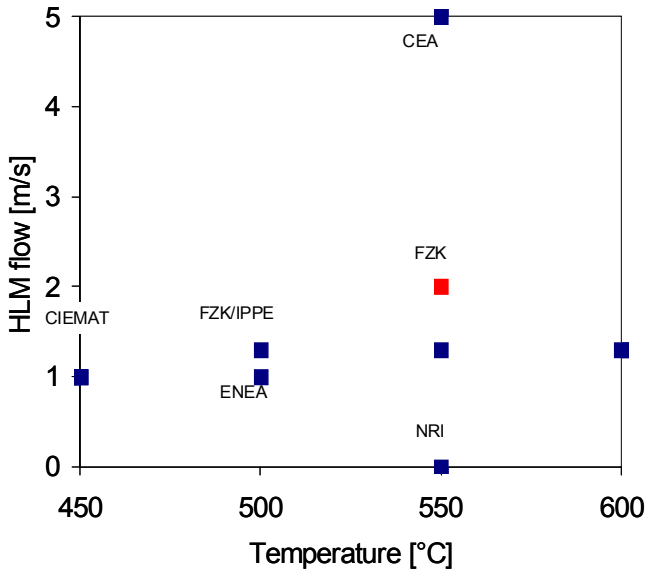


In summary, the long-term corrosion experimental results have shown that the corrosion rate depends from different parameters as e.g. the parameters acting on the corrosion rate of steels in the HLM:

- Temperature: it has been confirmed that for temperatures above 500 °C the oxide layer that can grow on the steel surface can lose its protectiveness. Moreover, the high temperature range, as expected, imposes a high oxidation rate.
- Oxygen activity: the oxygen activity in the liquid metal must be adjusted in a range where oxides can grow on the steel surface. However, it seems that an oxygen activity above a certain value (depending from the operational temperature) contribute to the build-up of a too thick oxide scale, hence leading to a reduction in fuel-coolant heat transfer.
- Flow velocity: the increase of the HLM flow velocity to values above 1.5 m/s affects the corrosion/erosion of the $Fe_3O_4$ layer, which is part of the oxide scale. The oxide scale is usually made of an internal diffusion layer, an intermediate Fe, Cr spinel oxide layer and an external $Fe_3O_4$ layer.
- Stresses: Corrosion experiments performed on pressurized tubes [10.4.4] have shown that the oxidation rate increases with increasing the hoop stress.

The occurrence of an oxide scale on the structural materials for e.g. the cladding and the heat exchanger might be beneficial to protect the steel against dissolution attack and eventual degradation of the steels mechanical properties assisted by the liquid metal [10.4.5]. However, as shown in figure 10.4.2, a too thick oxide scale can change the thermal conductivity of the materials, with consequences on the heat transfer of the system and on the thermo-mechanical resistance of the steel. Therefore the evaluation and the understanding of the parameters affecting the oxidation rate could allow defining on optimal range of them to keep the oxide scale thickness at an acceptable level.

*This document refers to work being performed by scientists and institutions involved in IP EUROTRANS, as well as the financial support of the European Commission through the contract FI6W-CT-2004-516520.*

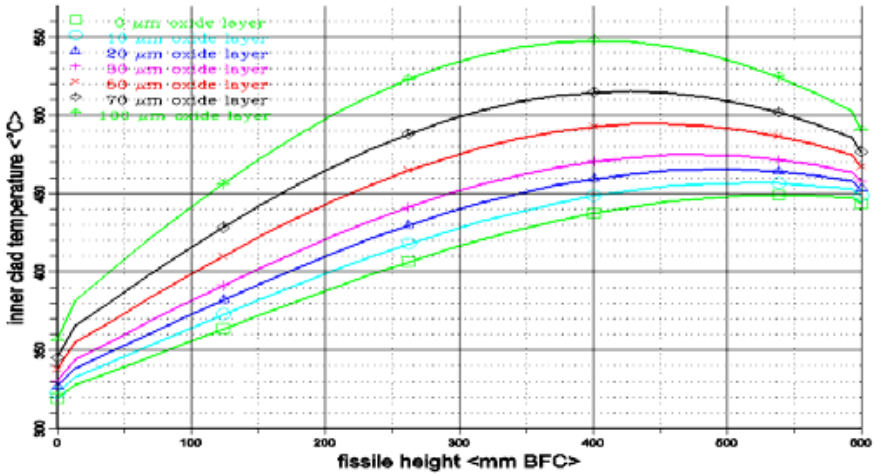


Figure 10.4.2. Temperature profile of the inner clad wall as a function of the fissile height [10.4.6]. The inner wall temperature increases with increasing oxide scale thickness.

The alternative method under assessment within DEMETRA is a corrosion protection method for the claddings (made of T91 steel) based on steel surface treatment. This method consists in spraying Fe - Al based powders on the steel surface and to treat the obtained coating with the GESA (Gepulste Elektronen Strahl Anlage) facility [10.4.4]. First results have shown that the Al content in the coating needs to be controlled in order to ensure the corrosion protection capability of the coating. Indeed, when the Al content is above ~ 4%, the corrosion tests that have been performed on the GESA treated samples in flowing HLM in the temperature range 500 - 600°C have confirmed the effectiveness of this method [10.4.4].

An experimental program has been set-up to assess the mechanical properties degradation of the two reference steels in liquid metal and to evaluate the conditions for which Liquid Metal Embrittlement (LME) can occur.
Low cycle fatigue tests have been performed on T91 steel at 300°C [10.4.7] and 550°C [10.4.8]. Several conditions of the T91 steel have been tested. The results can be summarized as follows:
At 300°C pre-oxidized T91 in LBE (the pre-oxidation has been performed at ~ 450°C with a liquid metal oxygen potential above the magnetite oxygen potential) did not exhibit any fatigue lifetime reduction. However pre-corroded T91 in LBE (pre-corrosion has been performed at ~ 450°C and low oxygen content in the liquid metal) showed a significant reduction in the fatigue lifetime.
At 550°C, both T91 samples that have been pre-oxidized in LBE and a set of samples with GESA treatment have been tested [10.4.8]. All samples showed similar fatigue resistance as the T91 tested in air.
Fracture toughness, tensile and creep-to-rupture tests have been as well performed on T91 steel in a wide temperature range and under different metallurgical conditions and surface states [10.4.9], [10.4.10]. The experimental results on tensile tests performed at slow strain have shown that the untreated steels are protected from LME by their native oxide layers and no LME could be observed.
LME can be recognized through a significant decrease in total elongation while yield stress and ultimate tensile strength of the material remain unchanged. Exposure to liquid metal and thus liquid metal corrosion plays an important role in the increase of the risk to LME. In LBE environment the initiation of a crack by means of corrosion or surface defects facilitates wetting and thus increases the susceptibility to LME.
Moreover, an increase of hardening of the materials (obtained through different heat treatment [10.4.10]), extends the temperature range for which LME can occur.
The experimental creep-to-rupture tests performed on T91 steel in air and in flowing LBE at 550°C show [10.4.11], that there is a significant reduction of creep strength of the steel when exposed to LBE. It is assumed that the onset of this phenomenon occurs at a certain threshold stress and below this threshold stress the creep properties of the steel remain unchanged. Additional R&D activities would be needed to identify the threshold stresses for a relevant temperature range.

*This document refers to work being performed by scientists and institutions involved in IP EUROTRANS, as well as the financial support of the European Commission through the contract FI6W-CT-2004-516520.*

All these experimental data show that T91 steel can be prone to LME and LMAC. However, LME can occur only when several conditions are satisfied. These conditions are:

1) high applied stress on the steel (all experimental data have shown above the elasticity limit);
2) subsistence of extended surface defects which might allow contact between LM and steel;
3) intimate contact between liquid metal and steel.

Moreover, it has been shown that LME occurs in the low temperature range, while in the high temperature range LMAC can be the preponderant phenomenon that occurs. These experimental results are valuable data to guide the designers in limiting the risk of failure of components made of T91 steel and to define surface finishing state.

### 10.4.3 Irradiation studies

The test plan to investigate irradiation effects is shown in Figure 10.4.3. The plan foresees irradiation experiments at relatively high temperature and dpa range. Indeed, in the DEMETRA program an irradiation program with a fast neutron spectrum in the Phénix reactor (at CEA, France) has been started. The objective is to reach doses in the range of 40 to ~70 dpa at temperatures between 400 and 530 °C. The materials which are irradiated are the FM steels T91 and T92 as well as the FeAl based coatings. The set of data that will be obtained from the neutron irradiation test program are of relevance for the material assessment in representative conditions of the subcritical core.

The irradiation in the proton / neutron field is performed in the high temperature and dose range. Indeed, in the SINQ facility the reference structural material is irradiated in the temperature range 400 – 600 °C with doses up to 20 dpa. The set of data which will be obtained from SINQ are of relevance for the spallation target materials assessment.

First experimental results have been obtained from the irradiation experiments performed at SINQ [10.4.12], which have been combined with the understanding of the He effect in the FM steel [10.4.13].

The interesting finding of the set of tensile data obtained from SINQ irradiation experiments is the change in fracture behavior at doses above about 16 dpa. While the specimens irradiated at lower doses exhibited a ductile fracture mode, the high dose samples were brittle and some broke in the elastic regime. It is suggested that the change of fracture behavior of the high dose specimens may be due in particular to the high helium concentrations in those specimens. Increasing the test temperature to 250 °C did not improve significantly the ductility of the specimens irradiated to the highest doses. Even at 350°C, the T91 specimen irradiated to about 20 dpa showed a brittle behavior, while recovery of ductility following annealing was observed.

These results suggest that heat treatment of structural parts of spallation devices might be beneficial. Of course, a better understanding of the phenomena occurring during the heat treatments and the conditions which enables a ductility recovery have to be defined. Moreover, the effect of re-irradiation following annealing needs to be assessed as well.

***This document refers to work being performed by scientists and institutions involved in IP EUROTRANS, as well as the financial support of the European Commission through the contract FI6W-CT-2004-516520.***

Figure 10.4.3: Test Matrix of the irradiation experiments designed and carried out within DEMETRA. The irradiation campaign comprises irradiation in a fast neutron spectrum, in a proton/neutron environment and the irradiation in a mixed spectrum in presence of LBE.

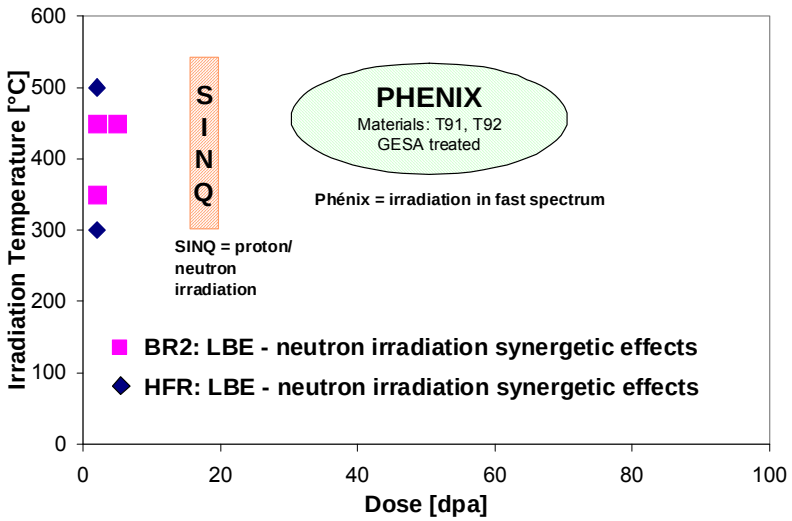


### 10.4.4 HLM Quality Control

The activities on the HLM quality control have been focused on two main items:

- The development and characterization of systems related to the solid impurities handling in both gas and liquid metal phases
- The measurement and adjustment of the oxygen potential in the liquid metal

The sources which can originate solid impurities in the liquid and gas phase have been thoroughly analyzed and a detailed plan on how to address these phenomena has been defined. Several filtering systems have been investigated for both phases.

The oxygen monitoring in the liquid metal is performed through electrochemical oxygen probes. Several oxygen probes have been designed, calibrated and tested in stagnant and in flowing conditions. At present, the reliability of oxygen sensors based on the Pt/air working electrode has been proven [10.4.14]. This type of sensor has been installed on a loop system and has operated for more than 10.000 h at temperature above 450°C.

As far as the adjustment of the oxygen activity in the liquid metal is concerned, two types of systems have been considered, i.e.(i) a solid state mass exchanger and (ii) the use of a mixture of water vapor and hydrogen. The solid state mass exchanger is based on the chemical equilibrium between Pb and PbO: at given temperature and oxygen potential of the liquid metal, PbO can dissolve in Pb thus increasing there the oxygen activity. The second system is based on the chemical equilibrium between $H_2O$ and $H_2$. Also in this case, for a given temperature and oxygen potential of the liquid metal, a certain amount of oxygen can be dissolved (or reduced) in the liquid metal. The principle of work of both systems has been proven. However, further activities are needed to implement those systems on large scale pool type configurations.

### 10.4.5 Thermal-hydraulics

The thermal-hydraulics activities within DEMETRA have been focussed on the heat transfer characterisation of a single pin and a fuel bundle mock-up as well as on some component tests in an integrated configuration. In addition, computational and experimental efforts have been put also on the

*This document refers to work being performed by scientists and institutions involved in IP EUROTRANS, as well as the financial support of the European Commission through the contract FI6W-CT-2004-516520.*

design and development of the windowless spallation target for the XT-ADS. Hereafter as examples the activities and experimental results on the fuel pin and bundle mock-up are described.

The experimental campaign on the heat transfer characteristics with a single pin has been accomplished at the TALL facility at KTH. The experimental campaign was conducted as to predict the heat exchange coefficient across the cladding with cylindrical sub-channel geometry at steady state and transient conditions. The transient experiments simulated are loss of heat sink, loss of external driving head, over power and transient from natural circulation to forced flow.

A preliminary analysis of the experimental results has shown that from the safety performance point view, the loss of heat sink, needs to be taken into account. Indeed, for this condition the temperature will increase first from the outlet of the heat exchanger rising downstream and draw the entire system. The temperature will keep rising up if no protective measures are taken to mitigate the transient.

A series of experiments has been initiated at the KArlsruhe Liquid metal Laboratory (KALLA) of FZK/KIT. In order to quantify and separate the individual phenomena occurring in the momentum and the energy transfer domain of a fuel assembly the experimental program is composed of three major experiments.

In a first step, a single electrically heated rod is placed in a hydraulically developed turbulent LBE pipe flow in the regimes of forced, mixed and buoyant convections. Radial and axial temperature fields and pressure are measured with a thermocouple rake and a movable thermal probe that also contains a Pitot tube for pressure measurements. The experimental data are compared to numerical simulations. Furthermore, this experiment allows testing the heater performance and the validation and qualification of the used measurement techniques.

The second experiment is a 19-pin hexagonal rod-bundle that is tested in a turbulent water flow. Because of the opaqueness of the liquid metal flow the rod bundle water experiment is necessary to gain information about the flow distribution and the pressure drop in the sub-channels by means of Laser Doppler Anemometry (LDA). This experiment also serves as a test for flow induced vibrations.

In the third experiment, the same rod-bundle design is placed in a hydraulically developed turbulent LBE flow. Measurements of temperature distribution and velocity fields are planned by means of UDV sensors and movable thermocouple rakes inside the rod bundle. The experimentally gained data of all three experiments serves as a numerical benchmark of sub-channel analysis codes and commercial CFD software packages.

***This document refers to work being performed by scientists and institutions involved in IP EUROTRANS, as well as the financial support of the European Commission through the contract FI6W-CT-2004-516520.***

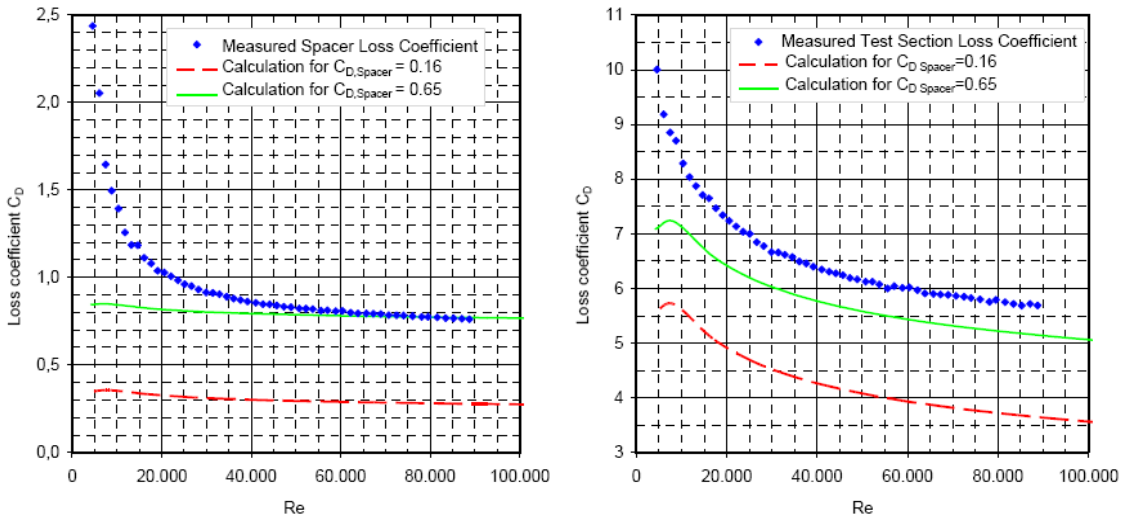


Figure 10.4.3: Comparison of numerically predicted and measured loss coefficient (the loss coefficient is proportional to the pressure loss) for one spacer (left) and for the test section area (right) as a function of Re [10.4.15].

Figure 10.4.3 (right) shows first results of pressure loss measurement performed in the water experiment. Figure 10.4.3 (left) shows that the estimated pressure loss of the spacer, for the calculated high blockage ratio, agrees almost perfectly with the measurements in the high flux region for Reynolds numbers higher than 40.000 where the flow is fully turbulent. In the transitional flow regime with Reynolds numbers between 5.000 and 35.000 the influence of the secondary flow is relatively high and leads to a rising loss coefficient.

For the complete rod bundle test section, the numerical predicted pressure loss underestimates the measurements by approximately 10% leading to a slightly lower loss coefficient. In contrast to the spacer pre-calculations, the variation stays constant also in the transitional flow regime for lower Reynolds numbers giving reasonable agreements down to Re = 10.000. One possible reason for the difference between measurement and calculation is the entrance guide at the beginning of the test section that has to be taken into account as an additional blockage for the sub channel analysis. Another reason can be found in the flow separation at the upper vessel leading to additional momentum losses.

Neutron Spallation Target

The neutron spallation target is one of the most challenging components to be developed for the ADS. Within the DEMETRA domain the evaluation of the MEGAPIE target (window configuration) has been performed in terms of neutronics, thermal-hydraulics and technologies (e.g. pumping system, measurement devices etc.). A complete report has been made available where the outcome of MEGAPIE is reported. On the other hand, experimental and computational activities are ongoing to assess the windowless configuration. At the end of the DEMETRA program, a set of data has been made available to the design teams to appreciate and assess pro and cons of the two target configurations.

A new windowless configuration has been entirely designed within the DEMETRA domain [10.4.16]. A mock-up of the proposed design has been tested in the UCL water loop. Figure10.4.4 shows the drag enhancer device as designed for the new configuration.

*This document refers to work being performed by scientists and institutions involved in IP EUROTRANS, as well as the financial support of the European Commission through the contract FI6W-CT-2004-516520.*

Figure10.4.4. Drag enhancer device for the windowless spallation target.

The drag enhancer has the aim to prevent the LBE feeder flow from free fall and stabilize the free surface.

### 10.4.6 Conclusion on Pb and LBE related technology

The structural materials investigated in DEMETRA were the Austenitic steel AISI316L and the FM (Ferro-Martensitic) steel T91. The results obtained have shown following characteristics of these two types of steels:

- AISI316L (reference material for vessel and in-vessel components):
  - The corrosion and oxidation resistance is limited to 500°C. Above this temperature the AISI316L shows severe liquid metal attack, even in oxidizing conditions.
  - The mechanical properties of the AISI316L are generally not affected by the liquid metal.
  - The irradiation resistance is very well known from past irradiation programs and in general it can be stated that at low irradiation dose the AISI316L retains radiation stability in the high temperature range.
- T91 (reference material for core components, heat exchanger and spallation target):
  - The corrosion and oxidation resistance of this steel has been observed up to 550°C. However, at this higher temperature too thick oxide scale might grow on the steel surface with several consequences as e.g. a reduction of the heat transfer capability of the material.
  - The mechanical properties of the T91 steel are affected by the liquid metal. Indeed, conditions for which LME and LMAC occurs have been defined. These conditions are of relevance for design purpose of the different components. Moreover, surface protection (oxide scale or a FeAl corrosion protection barrier) seems to reduce LME and LMAC effects.
  - Neutron irradiation experiments performed in past experimental programs have shown that hardening and embrittlement of T91 can occur at temperatures below 350°C . The irradiation resistance of the T91 steel seems to be as well poor in a spallation environment up to 350°C. A recovery of the mechanical properties has been observed upon annealing.

***This document refers to work being performed by scientists and institutions involved in IP EUROTRANS, as well as the financial support of the European Commission through the contract FI6W-CT-2004-516520.***

However, a better understanding of this phenomenon is needed to possibly address design / operational purposes of neutron spallation targets.

As for the quality control of the liquid metal, new insight of impurities sources and their management has been gained. The future step is the dimensioning of appropriate devices to remove those impurities from the liquid metal and the gas phase. In addition, oxygen probes for the measurement of the oxygen activity in the liquid metal and oxygen adjustment systems have been developed. These systems needs to be designed for pool type systems and needs to be qualified for the nuclear environment.

Finally, the thermal-hydraulics studies have been focused on the heat transfer in turbulent conditions, to validate heat transfer coefficients and relations and on the stability of free surfaces relevant for the windowless spallation target.

Supporting boundary conditions for EFIT-Pb such as those chosen by DM1 design at the start of the project was one of the major tasks of the DEMETRA programme. However, given the limited budget, the plans were rather coarse and in the end insufficient for ongoing advanced plant designs.

In DEMETRA, there are some drawbacks by experimental tests with proper core operating conditions at 550°C. Indeed, first it should be considered that T91 has a poor thermal-creep resistance at and above 550°C. This already limits the core inlet and outlet temperature for safety related issues. Moreover, long term exposition to oxidizing LBE at 550°C have shown that thick oxide scale can be produced and can spall off. Finally accelerated creep rupture at 220, 220 or 180 MPa in LBE have been observed. The GESA treatment (alumisation) might be mandatory in the high temperature range. However, a qualification program for its application might be needed. The R&D results have shown that it was maybe too early to focus on a one selected clad material. Alternative materials can still be considered. Steels developed in Russia with 1-2 wt% of Si might become brittle under irradiation even if they claim they have overcome the difficulties [10.4.17]. As far as Europe is concerned, a new R&D program should be established where new materials are developed and investigated. Several routes can be investigated as e.g. the addition of oxidation resistant elements (Al, Si, etc.) to the steel. Alternatively, focusing on the high temperature resistance the development of ODS with proper chemical composition or more conventional ODS in combination with Fe, Al coating can be also investigated. This last option is currently considered in the cross cutting project GETMAT.

REFERENCES

[10.4.1] C. Fazio, A. Alamo, A. Almazouzi, D. Gomez-Briceno, F. Groeschel, F. Roelofs, P. Turroni and J. U. Knebel, “Assessment of Reference structural materials, heavy liquid metal technology and thermal-hydraulics for European waste transmutation ADS”, Proceedings of GLOBAL, Tsukuba, Japan, Oct 9-13, 2005

[10.4.2] Handbook on Lead-bismuth Eutectic Alloy and Lead Properties, Materials Compatibility, Thermal-hydraulics and Technologies, Chapter 6. OECD-NEA 6195, 2007.

[10.4.3] G. Müller, A. Heinzel, G. Schumacher, A. Weisenburger, „Control of oxygen concentration inliquid lead and lead bismuth“, J. Nucl. Mater. Vol 321, p. 256, 2003.

[10.4.4] A. Weisenburger, A. Heinzel, G. Müller, H. Muscher, A. Rousanov, „T91 cladding tubes with and without modified FeCrAlY coatings exposed in LBE at different flow, stress and temperature conditions”. J. Nucl. Mater. 376 (2008) 274–281

[10.4.5] A. Verleene, J.-B. Vogt, I. Serre and A. Legris “Low cycle fatigue behaviour of T91 martensitic steel at 300 °C in air and in liquid lead bismuth eutectic”, International Journal of Fatigue, Volume 28, Issue 8, August 2006, Pages 843-85

[10.4.6] W. Pfrang, D. Struwe, private communication

***This document refers to work being performed by scientists and institutions involved in IP EUROTRANS, as well as the financial support of the European Commission through the contract FI6W-CT-2004-516520.***

[10.4.7] J.-B. Vogt, A. Verleene, I. Serre, F. Balbaud-Célérier, L. Martinelli, A. Terlani, “Understanding the liquid metal assisted damage sources in the T91 martensitic steel for safer use of ADS”. Engineering Failure Analysis 14 (2007) 1185–1193

[10.4.8] A. Weisenburger, A. Heinzel, C. Fazio, G. Müller, V.G. Markow, A.D. Kastanov, “Low cycle fatigue tests of surface modified T91 steel in 10-6 wt% oxygen containing Pb45Bi55 at 550 °C”. J. Nucl. Mater. 377 (2008) 261–267

[10.4.9] J. Van den Bosch, R.W. Bosch, D. Sapundjiev, A. Almazouzi, “Liquid metal embrittlement susceptibility of ferritic–martensitic steel in liquid lead alloys”. J. Nucl. Mater. 376 (2008) 322–329

[10.4.10] B. Long, Z. Tong, F. Gröschel, Y. Dai, “Liquid Pb–Bi embrittlement effects on the T91 steel after different heat treatments”. J. Nucl. Mater. 377 (2008) 219–224

[10.4.11] A. Jianu, G. Mueller, A. Weisenburger, A. Heinzel, C. Fazio, V.G. Markov, A.D Kasthanov, “Creep to rupture test of T91 steel in flowing Pb–Bi eutectic melt at 550°C”, submitted to Journal of Nuclear Materials.

[10.4.12] J. Henry, X. Averty, Y. Dai, J.P. Pizzanelli, “Tensile behaviour of 9Cr–1Mo tempered martensitic steels irradiated up to 20 dpa in a spallation environment”. J. Nucl. Mater. 377 (2008) 80–93.

[10.4.13] J. Malaplate, L. Vincent, X. Averty, J. Henry, B. Marini, “Characterization of He embrittlement of a 9Cr–1Mo steel using local approach of brittle fracture”. J. Nucl. Mater. 75 (2008) 3570–3580

[10.4.14] C. Schroer, Z. Voß, O. Wedemeyer, J. Novotny and J. Konys, „Oxidation of steel T91 in flowing lead–bismuth eutectic (LBE) at 550 °C”, J. Nucl. Mater. 356 (2006) 189-197.

[10.4.15] K. Litfin, A. G. Class, M. Daubner, S. Gnieser, R. Stieglitz, “Experimental investigation of sub channel flow distribution in a Hexagonal rod bundle experiment”, Proceedings of IEMPT10, Mito, Japan 2008.

[10.4.16] A. Batta, A. Class, K. Litfin, M. Dierckx, H. Jeanmart, F. Roelofs, P. Schuurmans, K. van Tichelen, “Numerical Study of the Water Experiment for XT-ADS Windowless Spallation Target”, Proceedings of IEMPT10, Mito, Japan 2008.

[10.4.17] Liquid Metal Cooled Reactors: Experience in Design and Operation, IAEA-TECDOC-1569, December 2007

***This document refers to work being performed by scientists and institutions involved in IP EUROTRANS, as well as the financial support of the European Commission through the contract FI6W-CT-2004-516520.***

## 10.5 DM5 NUDATRA (NUclear DAta for TRAnsmutation)

### 10.5.1 Objectives of DM5 NUDATRA

The objective of DM5 NUDATRA has been the improvement of the simulation tools for ADS core, shielding and fuel cycle design. The improvement has concerned essentially the evaluated nuclear data libraries and reaction models for materials in transmutation fuels, coolants, spallation targets, internal structures and reactor and accelerator shielding, relevant in particular for the XT-ADS and the EFIT designs.

DM5 NUDATRA addresses the improvement of the nuclear data evaluated files and models covering the following areas:

- Nuclear data uncertainty propagation in ADS fuel cycle parameters simulations and performance of sensitivity analysis to identify specific data with direct impact on the design of EFIT and XT-ADS, and definition of required data accuracies.
- Selected measurements on some $^{243}$Am, $^{244}$Cm, Pb, and Bi cross-sections in particular below 20 MeV.
- Review of the status of data and uncertainties of the calculations on decay heat, gamma-heating, dpa and gas production, respecting the peculiarities of dedicated fuels.
- Selected high-energy experiments for key elements in order to consolidate the reaction models, in particular for radioactive spallation product assessment, damage and gas production.
- Improved high energy models (INCL4 & ABLA) for implementation into MCNPX.
- Global validation of nuclear data, models and simulation tools on Integral experiments already performed in European facilities or in ISTC projects.

This work has been conducted in close contact with the JEFF project of NEA-OECD and the teams developing and using neutron transport codes.

### 10.5.2 Uncertainty propagation and data needs of ETD advanced fuel cycles

31 critical cross sections (causing an uncertainty beyond the design target accuracies) in the fuel cycle parameters (Double Strata using ETD-like ADS) have been identified. A first optimization exercise provides a list of data priorities and accuracy targets [10.5.1], [10.5.2]. However, the low quality of available covariance libraries and arbitrariness on the metric for measurements difficulties, introduce large uncertainties in the result (see Table 10.5.1) [10.5.3].

*This document refers to work being performed by scientists and institutions involved in IP EUROTRANS, as well as the financial support of the European Commission through the contract FI6W-CT-2004-516520.*

Table 10.5.1 Cross Section Target Accuracies Required for ETD advanced fuel cycles

| Isotope | Cross Section | Uncertainty (Δ%) | | EAF2007 / Target | Isotope | Cross Section | Uncertainty (Δ%) | | EAF2007 / Target |
|---|---|---|---|---|---|---|---|---|---|
| | | EAF2007 | Target | | | | EAF2007 | Target | |
| U234 | (n,γ) | 38.9 | - | | CM242 | (n,γ) | 30.0 | - | |
| U234 | (n,γ-M) | 38.9 | - | | CM243 | (n,fission) | 16.0 | - | |
| U235 | (n,fission) | 12.9 | - | | CM243 | (n,γ) | 32.0 | - | |
| NP237 | (n,γ) | 14.3 | - | | CM244 | (n,γ) | 24.6 | 14.7 | 2 |
| PU238 | (n,fission) | 12.3 | - | | CM245 | (n,fission) | 9.7 | - | |
| PU238 | (n,γ) | 14.5 | - | | CM245 | (n,γ) | 32.7 | 18.9 | 2 |
| PU239 | (n,fission) | 9.6 | - | | CM246 | (n,γ) | 28.2 | 15.1 | 2 |
| PU240 | (n,γ) | 9.3 | - | | CM247 | (n,fission) | 16.5 | - | |
| PU241 | (n,fission) | 15.6 | 13.5 | 1.2 | CM247 | (n,γ) | 32.1 | 12.6 | 3 |
| PU242 | (n,γ) | 12.6 | - | | CM248 | (n,γ) | 19.2 | 6.6 | 3 |
| AM241 | (n,γ) | 15.8 | - | | BK249 | (n,γ) | 31.7 | 8.7 | 4 |
| AM241 | (n,γ-M) | 15.8 | - | | CF249 | (n,γ) | 32.4 | 11.3 | 3 |
| AM242M | (n,fission) | 24.0 | - | | CF250 | (n,fission) | 33.0 | 17.5 | 2 |
| AM242M | (n,γ) | 32.8 | - | | CF250 | (n,γ) | 29.3 | 7.7 | 4 |
| AM243 | (n,γ-M) | 15.3 | - | | CF251 | (n,fission) | 31.6 | 11.5 | 3 |
| | | | | | CF251 | (n,γ) | 29.9 | 7.6 | 4 |

### 10.5.3 Measurements and Evaluations of cross sections

New measurements of low and intermediate energy nuclear data:

High resolution excitation functions for the inelastic scattering cross sections have been measured in Gelina [10.5.4] for Lead and Bismuth isotopes (the main components of the coolant and spallation target of both EFIT and XT_ADS). New data has been collected and analyzed for $^{206, 207, 208}$Pb and $^{209}$Bi for the reactions (n,n'γ) and (n,2n) and (n,3n) for the $^{208}$Pb. In addition the cross section and branching ratio of neutron capture by $^{209}$Bi towards either metastable or ground state $^{210}$Bi ( $^{209}$Bi(n,γ)$^{210m,g}$Bi) had been measured for several resonances beyond the thermal energies. At the same time Fe and Pb(n,xn' ) measurements performed at 100 MeV at Uppsala are being analyzed. In addition, the $^{244}$Cm neutron induced fission cross section has been investigated by $^{243}$Am($^{3}$He,pf) measurements at IPN Orsay. Finally, the measurement of the $^{243}$Am neutron capture cross section is being prepared at the CERN n_TOF facility, where a new spallation target has been built and tested in 2008.

*This document refers to work being performed by scientists and institutions involved in IP EUROTRANS, as well as the financial support of the European Commission through the contract FI6W-CT-2004-516520.*

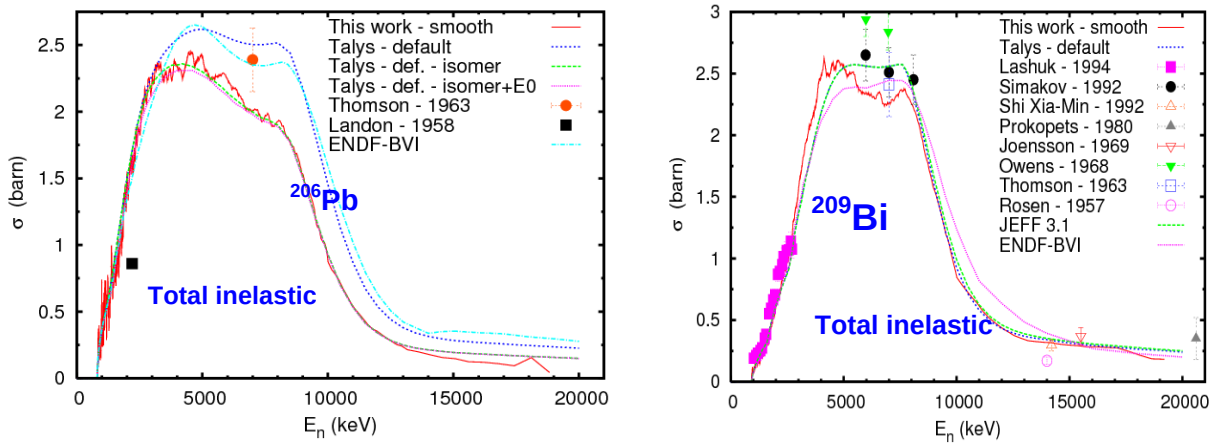


Figure 10.5.1: New measurements of $^{206}$Pb and $^{209}$Bi inelastic reaction cross sections.

<u>Improvement of low and intermediate nuclear reaction models for cross section evaluation:</u>

Several improvements have been implemented in the TALYS code including the generation of covariance libraries [10.5.5], [10.5.6]. This new version of TALYS has been made available to the international community. These enhancements had been used to reevaluate the Pb and Bi stable isotopes using the NUDATRA and previous experimental data. The resulting libraries are available for the JEFF-3.2 release and had been tested versus more than 20 cases of the international criticality benchmarks.

The Am cross section has also been re-evaluated with the improved TALYS version. As an example, the 241Am (n,2n) evaluation has been obtained by detailed models and parameters for fission, level densities and optical model (Figure 10.5.2).

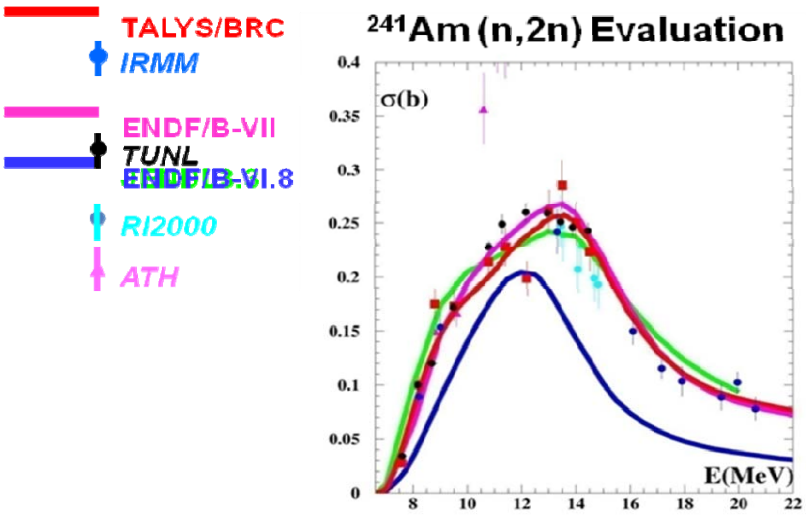


Figure 10.5.2: **$^{241}$Am (n,2n) Evaluation**

Measurement of cross sections of very difficult accessibility (very rare or radioactive samples) has been done by surrogate (transfer) reactions [10.5.7]. Different projectiles, targets and detailed channels have been used to get access to the same composite nucleus (Figure 10.5.3).

***This document refers to work being performed by scientists and institutions involved in IP EUROTRANS, as well as the financial support of the European Commission through the contract FI6W-CT-2004-516520.***

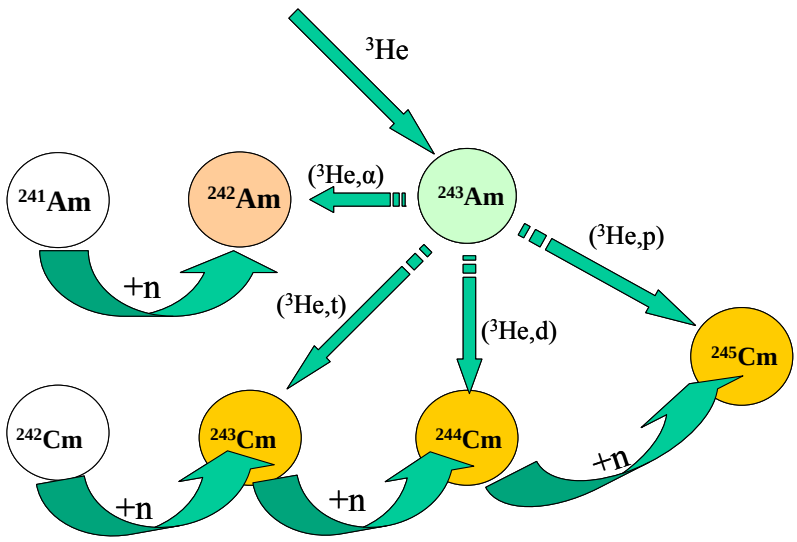


Figure 10.5.3: **$^{243}$Am Measurements by Surrogate reactions**

For $^{244}$Cm, neutron induced fission cross has been measured at Orsay: $^{244}$Cm(n,f) from $^{243}$Am($^3$He,p f). Validation and setup optimization with other output channels from the same reaction have lead to by-product results such as:

- $^{241}$Am(n,f) ($^3$He,α f)
- $^{242}$Cm(n,f) ($^3$He, $^3$H f)
- $^{243}$Cm(n,f) ($^3$He, $^2$H f)

### 10.5.4 High Energy Experiments and Modelling

During the FP5 HINDAS project [10.5.8], it was shown that the combination of the INCL4.2 version of the INCL4 cascade model combined with the standard version of the ABLA evaporation-fission model is quite successful, and generally better than widely used models, for the description of a large set of experimental data for nucleon-induced spallation reactions in an incident energy range extending from 0.2 to 2 GeV. However, some systematic shortcomings of the models were identified. In addition, sometimes conclusions were difficult to draw because of the lack of reliable experimental data. One of the deficiencies of the models concerns the prediction of light charged particles, i.e. helium and hydrogen isotopes, which is of particular importance for ADS. Indeed, build-up of gases (especially helium) can lead to swelling and embrittlement of the window separating the accelerator vacuum and the spallation target and of other structural materials, and tritium is a concern for radioprotection. Also, the production of intermediate mass fragments (IMFs), as the radioactive isotopes $^7$Be or $^{10}$Be, is generally underestimated by orders of magnitude. Finally, since some volatile radioactive fission fragments, as isotopes of Kr, I or Xe, can be released from spallation targets, it is important to have a good knowledge of fission cross-sections on materials envisaged for the targets.

The goal of NUDATRA WP4 was therefore: first, to provide new experimental data that can help understand the reaction mechanism and constrain the models, second to improve the models with special attention to the deficiencies above mentioned, third to implement the newly developed models into MCNPX and make a full calculation of a spallation target, actually the MEGAPIE target.

*This document refers to work being performed by scientists and institutions involved in IP EUROTRANS, as well as the financial support of the European Commission through the contract FI6W-CT-2004-516520.*

High-energy experiments

Within NUDATRA, ZSR has provided a systematic of excitation functions (cross sections as a function of incident energy) for the production of helium isotopes and intermediate mass fragments (residual nuclides with A < 30) for target elements from O to Bi [10.5.9]. In addition, results from the NESSI and PISA experiments at COSY-Jülich on double-differential cross-sections of hydrogen and helium isotopes, as well as of some IMFs, have been delivered by FZJ [10.5.10]. Examples of the results, one excitation function and one double differential cross-section, are shown in Figure 10.5.4. Among the interesting findings, one can cite the fact that the double differential cross-section always exhibits, even for IMFs, a high-energy tail that cannot be described by the evaporation process.

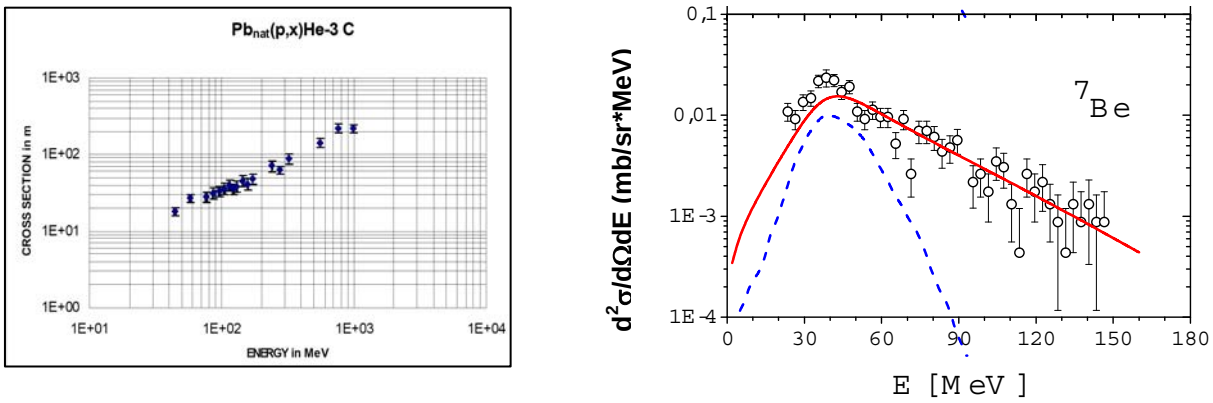


Figure 10.5.4: Left: Production cross sections of $^{3}$He (cumulative) in p+$^{nat}$Pb as a function of incident energy [10.5.9]. Right: Double differential cross section of $^{7}$Be measured by the PISA collaboration [10.5.10].The blue dotted line corresponds to the estimated evaporation contribution.

As regards data relevant for the prediction of volatile fission fragment production, absolute values of total fission cross sections of Pb and Ta at different energies have been measured at GSI Darmstadt using the reverse kinematics technique and a setup covering the full acceptance [10.5.11], [10.5.12]. The results are given in Table 10.5.2. In the case of Pb, they help solve the discrepancies found between different measurements done previously at the Fragment Separator (FRS).

Table 10.5.2. Results of the total fission cross-section measurement at GSI ([10.5.11] and [10.5.12]).

| *Reaction* | *Energy* | *Full acceptance setup* | *FRS* |
|---|---|---|---|
| *$^{208}$Pb+$^{1}$H* | *500 MeV* | *146 ± 7 mb* | *232 ± 33 mb* |
| *$^{208}$Pb+$^{1}$H* | *1000 MeV* | | *163 ± 26 mb* |
| *$^{208}$Pb+$^{2}$H* | *1000 MeV* | *203 ± 9 mb* | *175 ±31 mb* |
| *$^{181}$Ta+$^{1}$H* | *1000 MeV* | *18.5 ± 1.5 mb* | |
| *$^{181}$Ta+$^{1}$H* | *800 MeV* | *11.4 ± 0.8 mb* | |
| *$^{181}$Ta+$^{1}$H* | *500 MeV* | *5.1 ± 0.6 mb* | |
| *$^{181}$Ta+$^{1}$H* | *300 MeV* | *3.2 ± 0.7 mb* | |

High-energy model improvements

In order to cure some of the identified deficiencies, new versions of INCL4 and ABLA have been developed [10.5.13]. In the intranuclear cascade model, the main improvements in INCL4.5 [10.5.14] concern:

- the deflection of charged particles in the Coulomb field.
- the introduction of an energy and isospin dependent potential.
- a better pion dynamics.

***This document refers to work being performed by scientists and institutions involved in IP EUROTRANS, as well as the financial support of the European Commission through the contract FI6W-CT-2004-516520.***

– the extension to low energies.
– the possibility of emitting of clusters, including IMFs (up to A=10), through a mechanism of coalescence in phase space.

The latter point is particularly important since it allows reproducing the high-energy tail observed in the spectra of composite particles and IMFs.

In ABLA07 [10.5.15], a special attention has been paid to the evaporation process:

– Evaporation is no more restricted to n, p and α-particles. Parameters based on more physical grounds have been used for particle decay widths, Coulomb barriers and level densities. Change of angular momentum due to particle emission is now taken into account.
– The emission of intermediate-mass-fragments has also been introduced.
– A stage of simultaneous break-up (multifragmentation) is introduced for large excitation energy per nucleon.
– Substantial improvement of dissipation in fission was achieved. Low energy fission has been included.

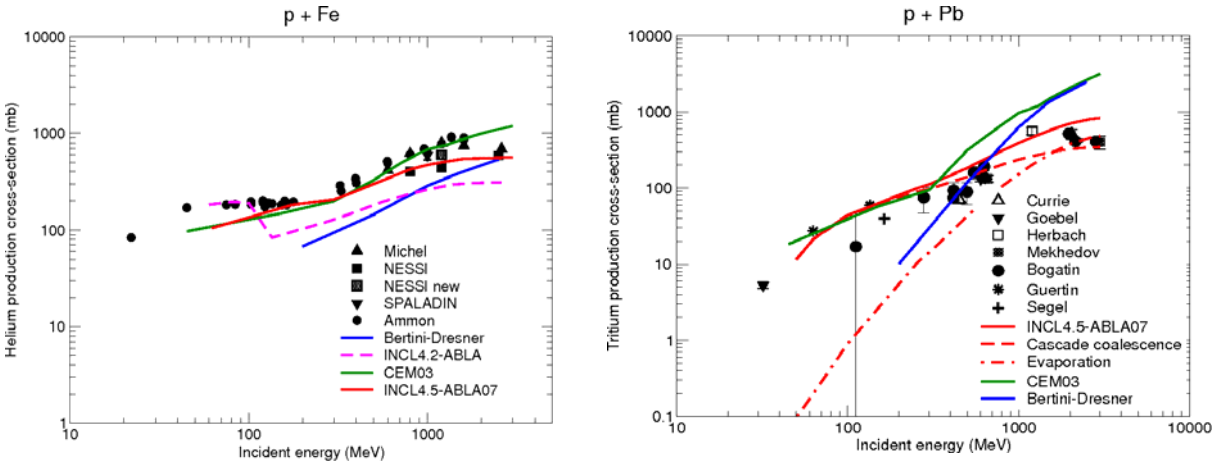


Figure 10.5.5: Left: Helium production cross-section in iron. Right: Tritium production cross-section in lead. Calculations with the INCL4.5-ABLA07 (red line), Bertini-Dresner (blue line) and of the CEM03 (green line) models. The dashed and dot-and-dashed lines give the contribution of the cascade and evaporation, respectively, in the new model. From [10.5.17].

After these modifications, INCL4.5-ABLA07 gives a very good agreement with data all over the energy range, generally better than other models in MCNPX, as it can be realized by looking at the Benchmark of Spallation Models recently organized by IAEA [10.5.16]. In particular, predictions of helium and hydrogen isotopes are much better than those from Bertini-Dresner which is the default option of MCNPX. This can be checked in Figure 10.5.5 from [10.5.17] which also shows that in the case of tritium the production is dominated by the emission during the cascade stage. Intermediate mass fragments (e.g. $^{7}$Be displayed in Figure 10.5.6 (left)) are now predicted with the right order of magnitude [10.5.13].

*This document refers to work being performed by scientists and institutions involved in IP EUROTRANS, as well as the financial support of the European Commission through the contract FI6W-CT-2004-516520.*

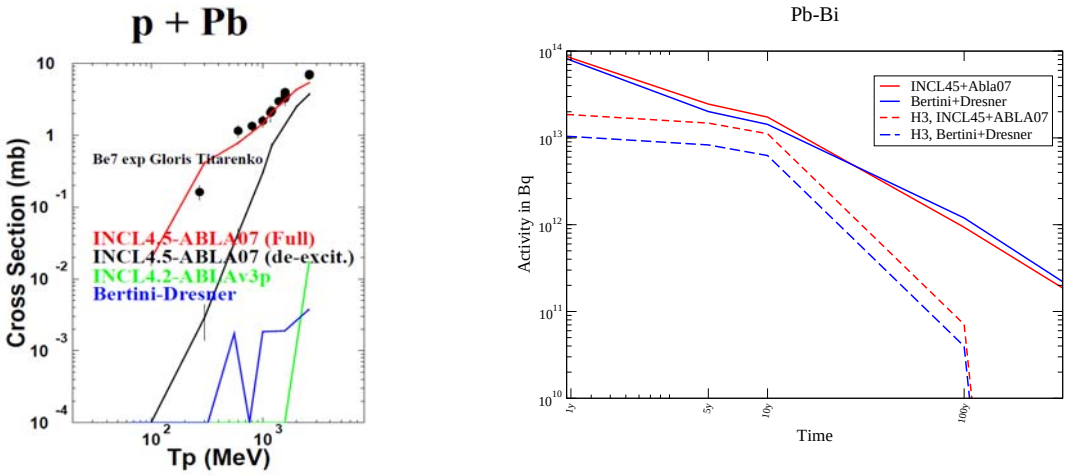


Figure 10.5.6: Left: $^{7}$Be production cross-section in lead. Right: Total activity (solid lines) and activity due to tritium (dashed lines) in the liquid Pb-Bi of the MEGAPIE target calculated with MCNPX using the INCL4.5-ABLA07 (red lines) or the Bertini-Dresner (blue lines) models. From [10.5.18].

INCL4.5-ABLA07 models have been implemented into MCNPX. This new MCNPX version will be soon available for MCNPX β-testers and to general users in the next MCNPX release, by the end of 2010. Calculations of the MEGAPIE target have been done using the new models and compared to older ones [10.5.18] done with either the old versions of the models or the default option (Bertini-Dresner). One of the main results concerns the prediction of tritium in the liquid Pb-Bi which is a factor 2 higher with INCL45-ABLA07 than with the default option of MCNPX (see Figure 10.5.6). This is not surprising since, as it can be seen in Figure 10.5.6 (Right), below 600 MeV Bertini-Dresner is always below INCL45-ABLA07 (and the experimental data). As regards helium production in the window of the MEGAPIE target (averaged over the full window volume), the new calculation leads to 147 appm/year compared to 82 appm/year with the default option. This illustrates the importance of choosing the right physics model in simulations of spallation targets.

### 10.5.5 Decay Heat in MA loaded cores

The decay heat (energy released due to decay of unstable nuclei) is a relatively small fraction (usually below 7% for conventional reactors) of reactor power at nominal conditions. But after reactor shut-down it is the most important heat source and should be properly taken into account in safety analyses. For that purpose, recommendations (decay heat relative to reactor power vs. cooling time) are available for fuels of currently operating reactors, such as UOX and MOX. The EFIT fuels, unlike UOX and MOX, contain a lot of Minor Actinides and therefore the decay heat should be assessed for EFIT.

CEA, CIEMAT, ENEA, FZK, PSI and SCK-CEN established a benchmark case [10.5.12], computed decay heat curves for EFIT fuels, for its particular components, and for a MOX-type fuel. All calculations show that the decay heat in EFIT-type fuels is appreciably higher as compared to MOX, except for short cooling times at the beginning of life conditions. This was taken into account in the design of the decay heat removal system for EFIT and in associated safety analyses.

The decay heat values for the EFIT-type and MOX fuels are within the 20% range from the average by all benchmark participants, except for cooling times between 1 month and 1 year, for which one of the participants provides decay heat curves, which are considered to be underestimated. The main contribution to the difference between MOX and EFIT fuels is due to Cm242 that builds up in EFIT-type fuels. The Cm242 content depends appreciably upon the following parameters: Am241 content in the fresh fuel, neutron flux level and irradiation time (if this time is short, e.g. less than 1 year). Therefore, unlike MOX fuel,

*This document refers to work being performed by scientists and institutions involved in IP EUROTRANS, as well as the financial support of the European Commission through the contract FI6W-CT-2004-516520.*

calculations of the Cm242 content in an EFIT-type fuel may be necessary if irradiation conditions differ appreciably from those considered in the benchmark.

The differences - between the average (of participants) decay heat values for the EFIT fuels and those for MOX - are assumed to be representative for irradiation conditions similar to those considered in the benchmark. More effort is needed to evaluate the uncertainties of the computed results.

### 10.5.6 Conclusion on DM5 NUDATRA

As a conclusion, the main results are:

- Simple sensitivity studies of fuel cycle parameters to nuclear data show that available data are good enough for single recycling but better accuracies are needed for many cross sections for multi-recycling strategies.
- Very significant improvement for Pb/Bi cross sections: measured, evaluated, disseminated (JEFF3.2) and validated.
- Improvement of some Minor Actinide cross sections: measurements of $^{243}$Am capture (EXFOR), $^{244}$Cm fission probability, evaluation of $^{241}$Am cross-section.
- Large improvement of evaluation tools (TALYS-1.0) with new capacity of cross section and uncertainty predictions under 20 MeV.
- Significant improvement on quality and completeness of nuclear data concerning light charged particles and intermediate mass fragment production cross sections. Improvement on absolute values total fission cross sections for Pb and Ta targets.
- New versions of high energy models INCL4+ABLA, now much more predictive, in particular for gas assessment and long lived intermediate mass fragment prediction, which have been implemented into MCNPX.
- Priority should be put on improving nuclear data uncertainty and covariance libraries.

With the significant improvement of some nuclear data (in particular for Pb and Bi isotopes),it should now be possible to predict the characteristics of the XT-ADS plant with reduced margins. The analysis of GUINEVERE core characteristic measurements (together with some other existing experiments) will confirm the progress made in this field.

However, nuclear data is not yet sufficiently accurate for MA and requires further experiments and studies and a long-term action plan is recommended to address these matters.

For the XT-ADS licensing dossier, a synthesis is required on the different system characteristics of relevance to the plant safety assessment, in particular an evaluation of the uncertainties associated to the potential reactivity insertions and the power peaking factors.

REFERENCES

[10.5.1] J. Sanz et al, Report on the description of selected nuclear data sensitivity methodologies for the fuel cycle and the repository parameters, Deliverable D5.11, Domain DM5 NUDATRA.

[10.5.2] G. Aliberti, G. Palmiotti, M. Salvatores, C. G. Stenberg, Transmutation Dedicated Systems: An assessment of Nuclear Data Uncertainty Impact, Nucl. Sci. Eng. 146, 13-50 (2004).

[10.5.3] Impact of different correlation structures in cross-section covariance matrices on the inventory and inventory-related parameters., N. García-Herranz, O. Cabellos, J. Sanz, J. Juan, International Conference on the Physics of Reactors “Nuclear Power: A Sustainable Resource”, Interlaken, Switzerland, September 14-19, 2008.

***This document refers to work being performed by scientists and institutions involved in IP EUROTRANS, as well as the financial support of the European Commission through the contract FI6W-CT-2004-516520.***

[10.5.4] A. Plompen, Geel Pb measurements, Deliverable D5.4, Domain DM5 NUDATRA.

[10.5.5] Status of theoretical minor actinide evaluation with TALYS, A.J. Koning , P. Romain, M. Duijvestijn, and E. Bauge, a common report from NRG - Nuclear Research and Consultancy Group, 1755 ZG Petten, The Netherlands and CEA, Service de Physique et Techniques Nucleaires, B.P. 12, F-91680 Bruyères-le-Châtel, France, November 2, 2006, NRG Report 2.1671/06.76794/P FAI/AK/MB, Deliverable D5.5, Domain DM5 NUDATRA.

[10.5.6] A.J. Koning, S. Hilaire and M.C. Duijvestijn, "TALYS: Comprehensive nuclear reaction modeling", Proceedings of the International Conference on Nuclear Data for Science and Technology - ND2004, Sep. 26 - Oct. 1, 2004, Santa Fe, USA.

[10.5.7] Minor actinide fission induced by multi-nucleon transfer reaction in inverse kinematics, EPJ Web of Conferences 2, 07001 (2010), Volume 2, 2010, CNR*09 - Second International Workshop on Compound Nuclear Reactions and Related Topics

[10.5.8] J.-P. Meulders, A. Koning and S. Leray, HINDAS EU Contract FIKW-CT-00031, final report, (available at http://www.theo.phys.ulg.ac.be/wiki/index.php/Cugnon_Joseph ).

[10.5.9] R. Michel et al., "Report on and values of helium production cross-sections in intermediate mass targets at 100/800 MeV", EUROTRANS/NUDATRA, Deliverable D5.18.

[10.5.10] F. Goldenbaum et al., "Final Report on and values of production cross sections of long-lived intermediate mass fragments (IMFs) from protons of 100 to 2500 MeV", EUROTRANS/NUDATRA, Deliverable D5.17.

[10.5.11] K.H. Schmidt, "New generation of measurements and model developments on nuclide production in spallation reactions", Proc. of the Int. Conf. on Nuclear Data for Science and Technology, Nice 2007, ed. by O. Bersillon et al, EDP Sciences, 2008, p 293.

[10.5.12] Y. Ayyad et al., "Total fission cross sections in reactions p+$^{181}$ta investigated in inverse kinematics at relativistic energies", Int. Conf. on Nuclear Data for Science and Technology 2010, Jeju, Korea, 2010.

[10.5.13] J. Cugnon et al., "Final report and code of an improved version of INCL4-ABLA", EUROTRANS deliverable D5.19

[10.5.14] J. Cugnon, A. Boudard, S. Leray, D. Mancusi, "Results obtained with INCL4", in: Proceedings of the International Topical Meeting on Nuclear Research Applications and Utilization of Accelerators, Vienna, May 4–8, 2009.

[10.5.15] A. Kelić, V. Ricciardi, K.-H. Schmidt, "Results obtained with ABLA007", in: Proceedings of the International Topical Meeting on Nuclear Research Applications and Utilization of Accelerators, Vienna, May 4–8, 2009.

[10.5.16] http://www-nds.iaea.org/spallations

[10.5.17] S. Leray et al., "Improved modelling of helium and tritium production for spallation targets", Nuclear Instruments and Methods in Physics Research B 268 (2010) 581.

[10.5.18] J.C. David et al, "A new benchmark of spallation models", Tenth meeting of the task force on Shielding Aspects of Accelerators, Targets and Irradiation Facilities, CERN, June 2-4, 2010

[10.5.19] A. Rineiski, G. Rimpault et al. Decay Heat Benchmark for EFIT cores, 18$^{th}$ International Conference on Nuclear Engineering (ICONE18), May 17-21, 2010 in Xi'an, China.

***This document refers to work being performed by scientists and institutions involved in IP EUROTRANS, as well as the financial support of the European Commission through the contract FI6W-CT-2004-516520.***

## 10.6 R&D Needs Synthesis

### 10.6.1 Pb-cooled Systems

#### 10.6.1.1 Structural materials

For the demonstration of the feasibility of a lead cooled reactor it is necessary to identify technologically viable structural and fuel cladding materials that can withstand the combined effects of high temperatures, difficult irradiation conditions and the rather corrosive/erosive operating conditions of the lead coolant.

A careful selection of steels meeting these conditions from the present nuclear materials database is required. Modified stainless steels could be used. An example of these materials is the so called 15-15 Ti stabilised steel. However, all clad-coolant interaction issues in the conditions applicable for Pb-cooled systems are still to be investigated for this material.

In situations in which no special surface protection techniques are employed, Ferritic-martensitic steels (FMS) show a higher corrosion-/oxidation rate in liquid Pb-alloys than the austenitic steels at temperatures below 550°C. They do have a better resistance to the irradiation induced swelling and creep. Therefore, taking into account the recent advancements in the development of the corrosion protection layers, they were selected as the main candidate materials for fuel cladding and structures in high neutron flux zones. An example of this class is the so-called T91 steel.

FeCrAlY coating produced with the GESA technique acts as an effective corrosion barrier at temperatures up to 600 °C in LBE with controlled oxygen activity. These results indicate that in principle a lead-cooled system with a primary system operating temperature below 500°C and fuel cladding below 600°C can be successfully developed. An industrial process for aluminization of large and non cylindrical surfaces shall be developed. At least all heat transfer surfaces (e.g. SG, heat exchanger, fuel clad, etc) shall be treated to avoid the heat transfer coefficient degradation due to the oxide layer necessary to protect the structural material. Industrial process for the surface treatment of all in-vessel components should be preferable even if more complicated.

Liquid metal embrittlement is also a known phenomenon to occur at low temperatures. Suitable out-of-pile tests in well controlled conditions need to be performed to investigate the effect of liquid metal embrittlement in combination with corrosion.

The initial R&D needs should be the extrapolation and validation of the corrosion and metallurgic test results that have been obtained for LBE in the frame of the ADS programs to the case of Pb. Out-of-pile experiments for the study of liquid metal embrittlement and corrosion will need to be pursued in the adequate temperature range. For qualification purposes, irradiation experiments of the selected materials are required in relevant conditions concerning corrosion (coolant interaction), thermal and mechanical load, temperature (400 °C – 600 °C), neutron flux intensity and neutron spectrum type. This work should also include the investigation of the boundary between the structural materials and the environment, possible changes in the composition of materials, behaviour of welds, stability of coatings, etc. In addition, the qualification experiments must involve selected incident and accident scenarios that are determined on the basis of the preliminary safety analyses of the Pb-cooled systems design.

The characterisation of other promising materials such as oxide dispersion-strengthened (ODS) steels, SiC composites and “MAX phase” materials is required on a longer timescale. In parallel, the development of advanced coatings for steel protection such as the characterization of FeCrAlY layers, which seem to be extremely promising, should be taken up.

#### 10.6.1.2 Thermal-hydraulics

The R&D efforts with respect to thermal-hydraulics are mainly concentrated on the operation of the reactor core and on the steam generator. This work should include the investigation of individual components but also the thermal-hydraulic interaction between the different components in the cooling system.

***This document refers to work being performed by scientists and institutions involved in IP EUROTRANS, as well as the financial support of the European Commission through the contract FI6W-CT-2004-516520.***

Items for research related to thermal hydraulic design of the fuel bundle should include

- Heat-transfer correlations in normal and transient conditions,
- Inter-fuel rods cross flow:
  - Full and partial power operation,
  - Influence of control assembly on sub-assembly flow.

An experimental and theoretical qualification of thermal hydraulic design (heat transfers, pressure losses) of the fuel bundle during natural convection circulation and in the transition region between natural and forced convection is needed.

Another important element is the evaluation of the heat transfer correlations in the steam generator together with the evaluation of the heat removal in the full system (core, SG, pump) in natural convection for decay heat removal.

A second important topic in the thermal-hydraulics R&D programme is the investigation of the effects that mixing a secondary coolant (water-steam) with the lead primary coolant has on the system behaviour. This mixing occurs in a severe accident scenario with the rupture of a steam generator tube. Steam ingress in the reactor core might lead to a positive void worth. It might also lead to pressure waves and sloshing of the lead pool with mechanical impact of the heavy liquid on mechanical structures. The steam formation will also lead to a pressurization of the cover gas.

Dedicated experiments need to be foreseen on a mock up representative (mainly in diameter and pitch of the tubes and their support) of the bundle of the SG for the reference configuration with perforated outer thin and main shells, immersed in a vessel. Pressure evolution inside and outside the bundle at different elevations must be measured, as well the final deformation, if any, of the bundle.

A test facility devoted to analyze core degraded configurations is needed in particular to study sub-assembly blocking events and the impact of seismic loads and sloshing tests.

#### 10.6.1.3 Reactor Components

In the innovative concept of the LFR several reactor components require development and/or qualification for operation with liquid lead as a coolant. These include the primary pumps, the steam generators (SG), and the fuel assemblies but also other items such as submerged remote handling, decay heat removal systems etc.

For the main pumps, validation of the design, functional sizing and of materials choice (mainly bearings and the impeller) during long-term operating in erosion/corrosion environment (high temperature lead at high speed) is necessary.

The steam generator in lead-cooled systems is a component with innovative feature. A validation of the SG design via the qualification of mock-up under representative conditions is needed. This includes tests on:

- Unit isolation on demand,
- Pressure drop characteristics and component behaviour under forced and natural convection.

The tests must take place in relevant conditions with a sufficiently large scale of the SG tubes and a superheated or supercritical steam cycle. The latter is advantageous for plant efficiency and better economics.

For safety reasons, the systems capability to tolerate a tube rupture accident must be tested. These experiments should include the investigation of:

- methods to detect tube leakage or rupture,
- effects of primary coolant-secondary coolant interaction (lead-water),
- measures to mitigate effects of a tube rupture incident.

When a neutronic and mechanical design of the core arrangement has been established, it must be demonstrated that the core geometry is capable of preventing core compaction without a build-up of

*This document refers to work being performed by scientists and institutions involved in IP EUROTRANS, as well as the financial support of the European Commission through the contract FI6W-CT-2004-516520.*

mechanical strain at welding or other structural material junctions. A two step approach needs to be taken, starting with a theoretical assessment including simulations, using conservative assumptions. In certain cases selected experiments in a representative mock-up may be required. Topics for investigation include:

- power operations including transients
- identification of accident initiators including those related to the removability of components
- impact of seismic loads and sloshing
- behaviour of fuel relocation after core disruption
- demonstration of fuel dispersion mechanism

A qualification programme of remote handling components submerged in the HLM coolant needs to be carried out. This programme can be conducted in synergy with the developments in LBE. In the latter, the experimental actuator/joint which is representative for the remote handling actuators are designed to operate within a vessel containing LBE heated to temperatures up to 450°C, with an inert atmosphere above the LBE surface and with a lid thermally insulated to control its surface temperature to below 50°C. Extrapolation of the results obtained in LBE to lead is most probably justified here since corrosion conditions in LBE are expected to be not better than those in liquid Pb.

Once the design of the decay heat removal system is finalised, an experimental qualification of operation modes for dip coolers and isolation condensers is needed.

For the spent fuel assembly transport cask, the material choices for the cask should be qualified and the long term behaviour and cask lifetime should be analysed. Also the operational characteristics for normal, and damaged and/or bend pins should be demonstrated.

#### 10.6.1.4 Instrumentation and coolant chemistry control

Instrumentation and coolant chemistry control is important in any liquid metal cooled reactor type. One of the main reasons for this is the fact that in order to master the corrosion properties of the structural materials, the oxygen content of the coolant must be controlled. In addition, accumulation of insoluble impurities that may block the coolant flow and the possible release of radioactive impurities must be avoided.

The measurement of variables such as level, pressure and flow of liquid lead requires measurement techniques that are somewhat different from the conventional ones. The final selection of which device(s) will eventually be used in the lead-cooled system will depend on a combination of reliability and accuracy arguments. Work in this area is needed to obtain fully validated measurement devices for the different parameters.

For long-term operations, the proposed oxygen concentration limit ($C_O=10^{-6}$ wt %) is adequate. Reduction of oxygen via $H_2$ bubbling and oxygen addition via PbO pebbles or via bubbling of a suitable $H_2/H_2O$ mixture has been successfully applied for controlling the overall $O_2$ composition of liquid lead containing experiments at laboratory scale. For application on a reactor scale it is important to quantify the Oxygen reduction rate of each process and to optimise the different methods for efficiency and speed. In addition, the extrapolation from loop applications to large scale pool applications should be made.

To monitor the oxygen concentration, sensitive electrochemical sensors are being developed. Most published results consider $Bi/Bi_2O_3$, $In/In_2O_3$ or Pt/Air as the reference electrode. Continued R&D on this topic is required. Besides the reliability issue, here also the probes need to be adapted from loop or shallow pool versions to deep pool versions.

The detection of a cladding breach in a fuel assembly can be detected by monitoring increased cover gas activity or by sensing neutrons which originates from fission products circulating in the coolant. Locating the fuel assembly containing the leaking fuel element is more difficult. The use of gas tagging is one solution to provide such identification. The principle relies on the injection of different stable gas isotopes into the fission gas plenum of each pin during manufacturing. All pins within the same fuel assembly will have the same gas isotope ratio. The defective assembly can be identified by matching the results of the cover gas

*This document refers to work being performed by scientists and institutions involved in IP EUROTRANS, as well as the financial support of the European Commission through the contract FI6W-CT-2004-516520.*

mass spectrometer analysis with the previously determined gas isotope ratio. Research on the feasibility of this technique in practice is needed. In addition it would be useful to put effort in the development of alternative detection techniques.

The opaque nature of the liquid metal coolant prohibits the use of any optical methods to inspect the internal reactor structures that are submerged in the reactor vessel. However ultrasonic visualization techniques can be used. It is envisaged to develop the ultrasonic equivalent of an optical camera.

### 10.6.2 Gas-cooled Systems

At this early stage of the EFIT-He design, some open issues remains and R&D programs must be identified to support future studies:

- The feasibility limit is reached for some components such as the helium blower technology (4 MW blowers) or the number of helical tubes (2500 tubes) in the exchanger. Those components are in the feasibility field but, considering the lack of feedback, some mock-up would be necessary.
- The secondary fluid pressure is high (250 bars) and calls into question the feasibility of the IHX component based on the HTR technology. Major changes would be necessary to make an IHX design able to stand the large pressure. Nevertheless, an IHX design with a supercritical $CO_2$ high pressure should be feasible after a dedicated R&D program and design works.
- A back-up solution for the conversion cycle is to consider a steam cycle. A steam cycle would not penalize the efficiency of the system at the level of temperature considered for the EFIT-He. The technology is better known (no need to large R&D program on the conversion cycle) and the HTR SG past experience could be used with rather minor changes.
- Some components materials such as the thimble material need to be validated by further studies considering the high temperature (572°C) and the irradiation damages.
- The demonstration of the DHR reliability, especially for what concerns the passive valve implementation is a key issue. It will deserve further assessments on the basis of a more detailed design and reliability study of the core and the SCS loops.
  Moreover, due to large pressure losses on the secondary side of the DHR exchanger, it will be difficult to assume the water natural circulation on the tertiary side.

#### 10.6.2.1 Main Components : RPV and primary circuit

At this stage, the preliminary design studies enabled possible solutions to satisfy the relatively high temperature resistance and optimized gas circulation requirements.

The main key development issues, to be further investigated, are:

- The **resistance** of the main primary structures under **severe thermal-hydraulic accidental conditions**. That concerns mainly the **pipes, the close containment and the IHX;**
- The **thermal barriers** must be carefully designed and experimental programmes in support have been undertaken with a close synergy with HTR and VHTR programmes. The specifications related to accidental situations are challenging (coolant temperature up to 1250°C), compared to HTR ones;

As the GFR has no biological protection such as water, remote manipulators must be considered.

Concerning the **Control Rod Drive Mechanisms**, the technology development seems to present no particular risk, due to “cold temperature domain” selection.

The major points still to be further studied concern:

- The design of the mechanical connections through the core, between the absorbers and the mechanisms, and the risk that these elements failure might affect the capability of absorbers to be inserted or to remain in the core;
- The reactor shutdown operating mode (fuel handling and inspection).

*This document refers to work being performed by scientists and institutions involved in IP EUROTRANS, as well as the financial support of the European Commission through the contract FI6W-CT-2004-516520.*

Concerning the specificities

- The design options for the **isolation valve** are still open: valve or check valve (either active or passive), single- or multi-element, etc. Since this isolation device has a safety classified function, further studies are required to address the technological issue, regarding the specifications such as the reference position in case of loss of instrumentation and control (to avoid core bypass), the time required for opening and closing, the associated pressure losses, etc. Feedback background from HTR and VHTR technologies (in particular the isolation valves developed for the nuclear/hydrogen plants coupling) could be used for the GFR;
- An additional **core by-pass risk** comes from the use of the cross-duct technology and the double envelope separating the hot and the cold sides (core barrel upper plenum). In the event of a double break in the cross-duct pipe or a significant internal break between the hot and the cold flow paths, the forced convection systems could become inefficient due to resulting core-bypass. Three various strategies are considered:
    - Divide the gas paths in the down-comer, in six separate sections (a section for each main or DHR loop), and use check valves to prevent the reverse flow through the down-comer
    - Demonstrate, by a leak before break approach, that in any case the pressure equilibrium subsequent to the break occurs before cross-duct full rupture ot that a micro crossing break into the hot duct cannot grow without detection until a cooling by-pass significant situation. Consequently, the flow scheme could be analyzed like a single (and limited) cold leg break.
    - Design separate hot and cold legs for all main and DHR loops, with a significant physical distance between them. In this case the double break of cold and hot legs seems to become very unlikely. Exploration of each solution is required to make a reference choice. It is worth noting that the helium transparency should be made profitable to develop adequate in-service inspection in order to limit or even to practically exclude cooling bypasses for the sensitive structures.

#### 10.6.2.2 Neutronics

The programme objective is to take advantage of the qualification of the ERANOS neutronic system codes (nuclear data and calculation procedures used, evaluation of uncertainties) which is developed to support its use for ETDR and GFR core design studies. About the physics, in addition to the coolant change, theGFR cores have particular characteristics which are significantly different from SFR cores.

The high core outlet coolant temperature which involves a temperature resistant choice of materials (mostly ceramics containing large quantities of “light” nuclei such as Carbon) used as matrix or structure elements and hence, the exclusion of usual stainless steels inside the core.

Achievement of extended or particular configurations aimed at testing particular technical solutions or studying the effects resulting from accidental gas reactor system situations.

#### 10.6.2.3 Core Thermal-hydraulics

A literature survey dealing with HTGR core thermal-hydraulic has allowed listing the various parameters influencing the heat exchange and pressure loss coefficients. A recurrent problem concerns the variation of the gas transport properties due to high gradients of temperature between walls and fluid ($T°_{wall}/T°_{bulk}$) in a Gas-cooled Fast Reactor core. The consequence is a distortion of the velocity profile within the boundary layer which has an impact on heat transfer correlations and pressure drop coefficients for the core.

Many experiments have been performed in the past with He, $CO_2$, $N_2$ or air. These experiments deal with simple geometries (internal flow in circular tubes or annular spaces). The use of classic correlations established for cylindrical tubes (without taking into account the influence of the thermal gradient in the gas) could be not conservative if the effect of the ratio $T°_{wall}/T°_{bulk}$ was confirmed for complex geometries like plates assemblies, which is the today candidate assembly concept for GFR.

The numerical friction and heat exchange coefficients have been compared to various numerical and analytical studies (laminar cases) and experimental correlations (turbulent cases). Recommendations on

*This document refers to work being performed by scientists and institutions involved in IP EUROTRANS, as well as the financial support of the European Commission through the contract FI6W-CT-2004-516520.*

friction pressure loss and heat exchange correlations proposed for the GFR Plant were taken into account for EFIT-He design studies.

To validate these recommendations and the thermal-hydraulic computations of the whole assembly, an air test section should be designed representing a portion of a typical He-EFIT pin bundle. Tests should be performed with a sufficient level of similitude conditions to support project studies. Specific Helium experimental studies should be necessary later, in particular if the clad temperature margins are low with respect of safety criteria. Helium tests are also to be carried out on a test facility which will allow performing tests up to the nominal temperature (850°C) with a helium flow rate of 100 g/s.

The EFIT-He systems transient analyses require system codes with three levels of validation:

- Validation of the physical correlations (pressure losses and heat transfer)
- Validation on components modelling such as the circulators, the heat exchangers, the core… Attention has to be paid for the modelling of axial compressors and for centrifugal compressors.
- Validation of system effects (interactions between components, coupling safety/main systems, transition from forced convection to natural convection, thermal-hydraulic/kinetic interactions…) This step of validation allows judging the consistency of the set of correlations. It also allows pointing out possible defaults of modelling.

Three existing system loops, EVOI, EVOII, PBMM are available to assess the capability of system codes to well represent the dynamic behaviour of a gas system.

In addition, the SALSA programme will add a further validation level. SALSA (a Small Air Loop for System Analysis) has been defined to represent operating conditions but will address generic issues:

- Switch from normal operation to DHR loops under Loss of flow, or Loss of Coolant conditions,
- DHR loops pre-conditioning optimization,
- DHR loops malfunction,
- Transient of power,
- Water ingress

#### 10.6.2.4 Tools for compressor/circulator modelling and studies: a multi-scale approach

The initial step involves the preliminary sizing of components. Compressor preliminary sizing modules have thus been developed, allowing confirmation of the feasibility, and size of such components, along with thermodynamic cycle performance.

With respect to reactor incidental/accidental transient analyses, the computation codes used to simulate the reactor must take into account all, or part of the energy conversion cycle. To meet this issue, of a mainly thermal–hydraulic character, a multi-scale approach (from 0D model to 3D CFD) has been implemented.

Such physical and numerical developments have to be validated by experimental data. A large amount of work has been devoted to this theme and different test cases have been treated (Fort-Saint-Vrain compressor, EVO turbomachinery, and air machines such as GHH multistage compressors, MIT 3 stage-compressor, Cambridge C106 multistage compressor).

Another possibility is to directly use measurements or 3D simulations of the complete machine (last point under investigation).

#### 10.6.2.5 Helium instrumentation:

Various Helium test facilities will be used to explore and validate different solutions (S/A equipped with thermocouples, infrared pyrometer,…) under representative conditions ( 850°C, 7 MPa, Helium velocity of 60 m/s) till the proposal of reference concepts for the thermocouple and optical solutions in 2012.

*This document refers to work being performed by scientists and institutions involved in IP EUROTRANS, as well as the financial support of the European Commission through the contract FI6W-CT-2004-516520.*

### 10.6.3 LBE-cooled Systems

Prior to the detailed design of a power plant such as the XT-ADS using Lead-Bismuth Eutectic (LBE) coolant, a series of R&D tests should be conducted to assess:

- Coolant quality control in terms of oxygen and impurities control;
- Materials compatibility in terms of corrosion, mechanical and irradiation resistance;
- Thermal-hydraulics studies related to heat transfer in turbulent conditions through dedicated experiments on a single pin, a fuel bundle and integrated component tests;
- Safety related studies through experimental and simulation studies on HLM/water interaction;
- Assessment of the windowless-neutron spallation target or the window spallation target behaviour through the post test analysis of MEGAPIE;
- Measurement and operational techniques development.

The technical work programme of DEMETRA has been answering part of these items but work still remains to be done and is being presented hereafter.

The XT-ADS system has been designed with a maximum core power of about 60 MWth and capability of the primary system corresponds to a power of 70 MWth. The coolant of XT-ADS is LBE and the core inlet and the mean outlet temperatures are 300°C and 400°C respectively. Table 10.6.3-1 summarises the operational conditions of the XT-ADS key components.

| Component/Subcomponent | Material | Replaceability Y=yes N=no | Operating Temperature (°C) | | | | Radiation Damage (dpa/365EFPD) | Local LBE Velocity (m/s) | Mechanical Stresses (MPa) |
|---|---|---|---|---|---|---|---|---|---|
| | | | Operation at Max Core Power [1] | Operation at Max Primary System Power [2] | DHR via safety system N° 1 [3 4 5] | DHR via safety systems N°2 [6] | | | |
| *Fuel Assemblies* | T91 | Y | | na | | | | | na |
| ▪ *Lower Region (up to lowermost fuel pin elevation)* | | | 300 | | 300 | 550 | | 1.3 | |
| ▪ *Hot Fuel pin (clad)* | | | 430 | | 370 | 550 | 29 | 1.6 | |
| ▪ *Fuel pin grid region* | | | 430 | | 370 | 550 | 29 | 2.3 | |
| ▪ *Upper Region (above fuel pin topmost elevation)* | | | 387 | | 365 | 550 | 30 | 1.3 | |
| **Dummy Assemblies** | T91 | Y | na | na | 365 | 550 | | 0.2 | na |
| **Core Barrel** | | Y | | na | 365 | 550 | | - | 110 |
| ▪ *Lower region (below diagrid)* | AISI316L | | 387 | | | | 2.4 | | |
| ▪ *Diagrid* | T91 | | 387 | | | | 1.4 | 0.3 | |
| ▪ *Upper region (above diagrid)* | AISI316L | | 356 | | | | | | |
| **Steam Generators** | T91 | Y | | | | | | | 247 |
| ▪ *Inlet (LBE side)* | | | 356 | 370 | 350 | 550 | 0.05 | 1.1 | |
| ▪ *Outlet (LBE side)* | | | 300 | 300 | 270 | 550 | | 1.1 | |
| **Circulation Pumps** | To be defined | Y | 300 | 300 | 270 | 550 | | | na |
| ▪ *Shaft (upstream the hub)* | MAXTHAL | | | | | | | 2 | |
| ▪ *Impeller (around the hub)* | ($Ti_3SiC_2$) [7] | | | | | | 0.1 | 9 | |
| ▪ Casing | | | | | | | | 3 | |
| **Reactor Vessel** | AISI316L | N | | | | | | | 114 |
| ▪ *Close to coolant free surface* | | | 356 | 370 | 370 | 550 | $10^{-4}$ | 0.01 | |
| ▪ *Below inner vessel (lower plenum)* | | | 300 | 300 | 300 | 550 | | 0.1 | |
| **Inner Vessel** | AISI316L | Y | 356 | 370 | 370 | 550 | 1 | 0.1 | 234 |
| **Above Core Structures (IPS)** | | | 356 | 370 | 370 | 550 | na | | na |
| **Refuelling Equipment** | AISI316L | Y | 356 | 370 | 370 | 550 | na | - | na |
| **Target** | T91 | Y | Pertinent data reported in dedicated Table 4.1-2 | | | | | | |

Table 10.6.3-1: Summary of materials selection and operational conditions of XT-ADS

A key issue to be addressed for the use of lead or lead-alloy as coolant in nuclear reactor systems is the selection and qualification of structure and clad materials. In the high-temperature operation range the molten lead and lead-alloy are corrosive towards structural materials and can induce / accelerate material failure under static loading, such as brittle fracture, and failure under time-dependent loading, such as fatigue and creep.

The main parameters impacting the corrosion rate of steels are the chemical and metallurgical features of the steel, the temperature, the liquid metal velocity and the dissolved oxygen concentration. For design purpose it is relevant to know the corrosion behaviour of the steels in a relevant range of these parameters. Moreover, one of the provisions adopted in the design to impact the corrosion resistance of the selected candidate materials (T91 and AISI316L steels) is to maintain a controlled amount of oxygen dissolved in the

melt. Therefore, oxygen control systems and strategies in pool type reactor need to be investigated and assessed.

In the high temperature range, the corrosion resistance of structural materials can be enhanced by FeAl alloy coating. This is of great interest for the fuel cladding or in general for heat exchanger tubes for which protective oxide layer thickness shall be limited so that the heat transfers characteristics are not significantly affected.

The design approach for XT-ADS has been to limit the mean core outlet temperature and to protect the T91 steel, as the construction material of the unavoidably thermally high loaded fuel cladding tubes, with Fe/Al alloy coating. However a qualification program for the use of the coatings is mandatory in order to demonstrate their mechanical stability, adhesion to the substrate etc. under relevant conditions.

Other provisions taken in the design to preserve structural material integrity against erosion phenomena have been to impose an upper limit of 2 m/s on the coolant flow velocity. Exception to this is done for the mechanical pumps where the maximum relative flow velocity is limited to 10 m/s.

Alternative structural material, for the pump impeller, resistant to this high velocity shall be identified and characterised. Promising candidates are Silicon Carbide and Titanium based alloys.

The R&D programmes including corrosion tests in flowing liquid metal (with representative parameters of the fuel cladding and in-vessel components) to estimate corrosion kinetics and to assess the long term stability of the protective layers, will confirm the design assumptions or will provide more suitable data.

In addition, the use of lead alloy for the XT-ADS concepts requires an assessment of its compatibility with structural materials under the fast neutron spectrum typical of fast reactors. The acquired experience with sodium-cooled fast reactors is not transferable to lead and lead alloys, owing to the significant differences in their physical and metallurgical properties. Therefore dedicated test plans should provide data; particularly in the higher temperature range, on tensile, creep, creep-fatigue and fracture mechanics and fatigue crack growth of the selected steels in contact with lead alloy.

***This document refers to work being performed by scientists and institutions involved in IP EUROTRANS, as well as the financial support of the European Commission through the contract FI6W-CT-2004-516520.***

# 11. GENERAL CONCLUSIONS

## 11.1 Motivation of the overall IP EUROTRANS project

The development of the ADS (Accelerator Driven Systems) is motivated by the potential which have these machines to reduce the volume and the radiotoxicity of the nuclear waste and more particularly of minor actinides generated by the operation of existing pressurized water reactors. This reduction of the volume and the radio-toxicity of such nuclear waste is obtained by transmutation and incineration (i.e. fission) of minor actinides into less active isotopes or shorter-lived by-products.

It is only within the European integrated project EUROTRANS that complete “remontages” of ADS minor actinides burners have been drawn and more particularly in the DESIGN domain which had the task to set up a pre-design of the European Transmutation Demonstrator (ETD) able to prove the feasibility of the transmutation/incineration in ADS of the long life nuclear waste.

The reference concept retained is a Lead cooled ADS for the European Transmutation Demonstrator of industrial size (EFIT for European Facility one Industrial scale Transmuter) with a back up solution of a Helium cooled ADS. The fuel selected is the CERCER $AnO_2$-MgO whereas field AFTRA studies an alternative of core using the $AnO_2$-Mo92 CERMET fuel.

The design of ETD/EFIT-Pb relies on a certain number of expected technological advances reasonably available by 2050 when such machines are likely to be built. In order to avoid misleading designs, specialists of the various disciplines were interviewed in order to get their agreement on the retained characteristics of the fuel, the metal liquid coolant and the materials necessary for this design. Finally, the safety approach is based on the one adopted for Sodium Cooled Fast Reactors. In addition to the similar constraints with those of the critical cores, specificities of the ADS resulted in developing an approach which appeared to be leading to added constraints for the design of this type of machine.

Within the integrated project EUROTRANS, design and safety analysis of the accelerator driven systems XT-ADS and EFIT have been made. XT-ADS is based on MOX fuel and LBE coolant, has a design power of 57 MWth and is mainly intended as an irradiation facility. It is also expected to prove the feasibility of coupling a high power proton accelerator with a sub-critical core. EFIT is intended as a 400 MWth prototype of an industrial facility for minor actinide burning, designed to achieve an optimal MA destruction rate of 42 kg per TWh thermal. Two coolant options have been considered in the project, the primary choice being lead, and the back-up option helium gas. In the present contribution, the objectives, the design characteristics and safety performance of these accelerator driven systems are reviewed, including design of the respective core, primary and secondary systems, spallation target and accelerator. Indications of costs for construction and operation are also provided

When transmuting minor actinides, a significant fraction will be converted to plutonium by neutron capture and decay, rather than being fissioned. In order for EFIT to perform its task as burner of minor actinides as efficiently as possible, it was decided to adopt a strategy where the net production of plutonium is zero. By simple energy balance, the net consumption of minor actinides then becomes 42 kg/TWh fission energy. An important advantage of this approach is that the burnup reactivity swing automatically becomes very small.

Since XT-ADS should act both as proof of concept and as an irradiation facility, the use of existing technology to as large extent as possible is requested, leading to the application of MOX fuel and Lead-Bismuth Eutectic (LBE) as coolant.

## 11.2 Design:EFIT-Pb

The fuel adopted for the reference design of EFIT is the ceramic-ceramic composite $(Pu,MA)O_{2-x}$ – MgO. The magnesia matrix provides thermal conductivity necessary for the highly sub-stoichiometric actinide phase to maintain margins to failure under transient conditions. This fuel type was successfully fabricated in the ATALANTE laboratory for the FUTURIX irradiation in Phénix. Since vapourisation of the MgO based

*This document refers to work being performed by scientists and institutions involved in IP EUROTRANS, as well as the financial support of the European Commission through the contract FI6W-CT-2004-516520.*

fuel was observed at T = 2130 K, an alternative solution under the form of the ceramic-metallic composite $(Pu,MA)O_{2-x}$ – $^{92}Mo$ also has been studied in EUROTRANS, to increase the margin to failure of the fuel.

The isotopic vectors of Pu and MA were taken as those from a mixture of 90% spent UOX fuel after 30 years of cooling and 10% MOX fuel after 15 years of cooling. The corresponding Pu/MA ratio yielding zero net production of plutonium (the “42-0” condition) then becomes 46/54 for the reference core. A three-zone core design was established, where the radial power peaking factor is maintained sufficiently low by a combination of varying the inert matrix fraction and the pellet diameter.

Lead coolant was adopted for the reference core, strongly reducing the concerns for coolant boiling (as compared to sodium) and reducing the production of polonium by three orders of magnitude, as compared to LBE. Its relatively high melting temperature then requires setting the core inlet temperature at 400°C. The ferritic-martensitic 9% Cr steel T91 was selected as reference cladding material in EUROTRANS, expected to exhibit a combination of good corrosion and irradiation resistance. The upper operational limit of this steel in lead is considered to be 550°C, adopting proper measures for protection from corrosion, such as surface alloying with the alumina former FeCrAlY (GESA treatment). The latter condition sets a constraint for the hot spot cladding temperature corresponding to an average core outlet temperature of 480°C.

It was decided to design the core with a pressure drop of less than one bar for the twofold purpose of reducing the pumping power and ensuring passive heat removal under transient conditions. The resulting flow rate of about 1 m/s requires a pin pitch of about 13.5 mm to maintain the hot spot cladding temperature below 550°C.

The operational K-effective was selected on the basis of maintaining a margin to criticality of at least 1000 pcm. Including a postulated measurement error margin of 600 pcm and possible design basis condition (DBC) accidents, such as earth quake induced core compaction and target flooding, a k-effective of 0.97 was arrived at. Respecting the lower limit of 50% inert matrix fraction in the outer fuel zone, the size of the core may then be obtained. The reference design feature 180 fuel assemblies with 168 fuel pins each, and a total core power of 400 $MW_{th}$, including 16 $MW_{th}$ dissipated in the spallation target.

With a power density of 300 $W/cm^3$ in the fuel, a core averaged burnup of 78 GWd/ton of actinides is achieved within 3 full power years, The reactivity swing is restricted to a few hundred pcm per year.

Figure 11.1 displays the primary system of the lead cooled EFIT, including pumps, heat exchangers and the spallation target module.

***This document refers to work being performed by scientists and institutions involved in IP EUROTRANS, as well as the financial support of the European Commission through the contract FI6W-CT-2004-516520.***

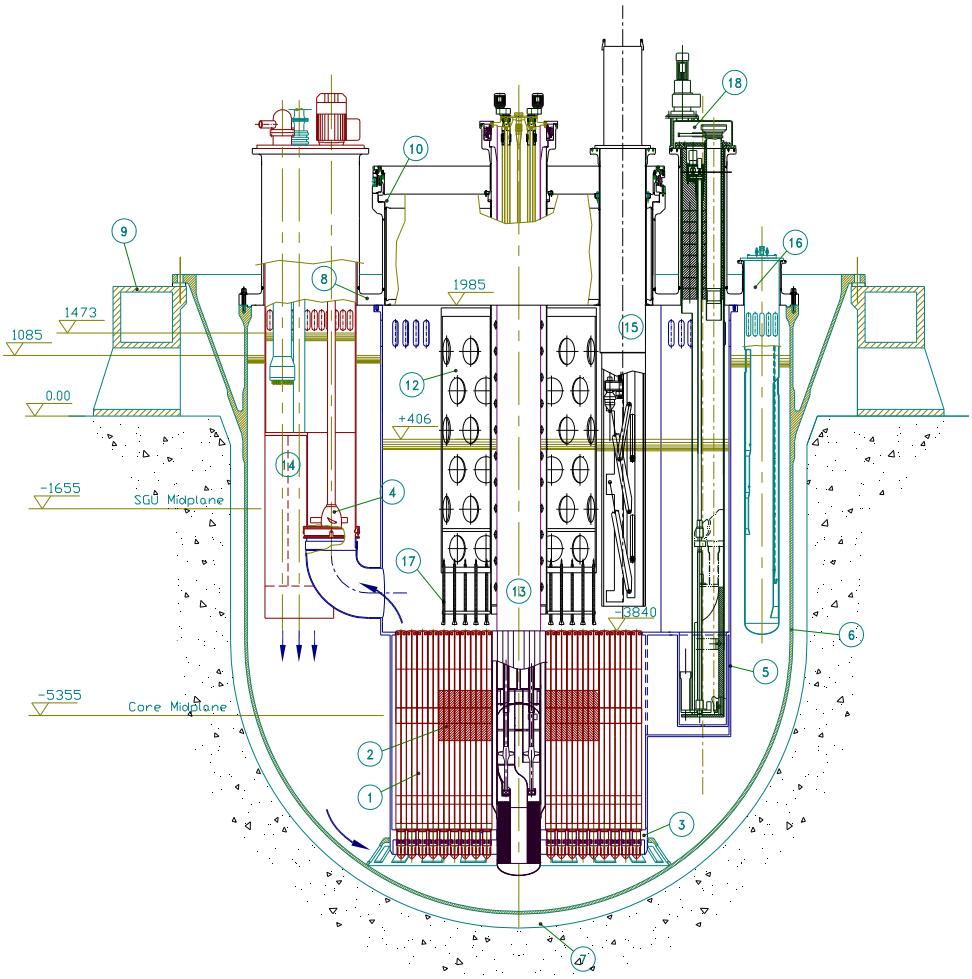


[1 Reactor Core; 2 Active Zone; 3 Diagrid; 4 Primary Pump; 5 Cylindrical Inner Vessel; 6 Reactor Vessel; 7 Reactor Cavity; 8 Reactor Roof; 9 Reactor Vessel Support; 10 Rotating Plug; 11 Thermal Shielding; 12 Above Core Structure: 13 Target Unit; 14 Steam Generator Unit; 15 Fuel Handling Machine; 16 Filter Unit; 17 Core Instrumentation; 18 Rotor Lift Machine; 19 DHR 1 Dip Cooler]

Figure 11.1: Primary system of the lead cooled EFIT

Four primary pumps are operating at the core outlet temperature of 480°C. Even when providing a relatively modest pump head of 1.37 bar, the maximum relative velocity of the impeller blades and the lead coolant reaches above 9 m/s, which gives rise to erosion problems. The availability of an erosion and corrosion resistant surface coating for the blades remains to be proven. Presently, tests are being conducted on TiSiC MAXTHAL material.

Eight steam generator units, each rated at 52 MW provide heat removal under normal operation. The units are arranged two-by-two and are co-assembled with one pump in a casing hung from the reactor vessel roof. On the secondary side, the water steam has an inlet pressure of 144 bars at 335°C and outlet pressure/temperature of 140 bars at 450-460°C.

Three systems contribute to the decay heat removal (DHR) function of EFIT: The steam generators, the direct reactor cooling (DRC) system and the isolation condenser system. The two latter are safety graded, meaning that they are mutually diverse and are designed with redundancy. The DRC system consists of dip

*This document refers to work being performed by scientists and institutions involved in IP EUROTRANS, as well as the financial support of the European Commission through the contract FI6W-CT-2004-516520.*

coolers immersed in the primary system and the isolation condensers are connected to the secondary side of the steam generators. Each system consists of four independent loops and three out of four are sufficient to perform the DHR function by removing 20 MW of decay heat. In the DRC system, vapourisation of diathermic oil provides passive heat removal. An air-cooled condenser then returns the oil to the dip cooler. In the isolation condensers, which are immersed into a pool of cold water, the lower header is connected by a valve to the main feed water line of a pair of steam generators. When called upon, the valve is opened and steam condensate is drained into the steam generator. Steam from the steam generator then may enter the upper header of the isolation condenser, where it condensates on the cold internal surface.

The spallation target unit, having a length of 14 meters and a diameter of 0.8 m is hung from the reactor roof and is supported at the bottom by a hole in the centre of the diagrid. The target configuration is windowless, where protons from the accelerator impinge on a free surface of lead exposed to vacuum. Circulation of the lead is forced by two propellers driven by motors located above the reactor roof. An heat exchanger transfers the deposited heat to a core by-pass stream of primary coolant.

## 11.3 Design: EFIT-He

The EFIT-He reactor is a concept with pressurized helium coolant (70 bars). Helium is inert and there is no corrosion issue onto metallic materials versus lead cooled EFIT reactor. The helium temperature is in a range between 350°C and 575°C.

The EFIT-He core is designed for a thermal power of about 400 $MW_{th}$, with a sub-critical core constituted of hexagonal sub-assemblies (S/As), distributed in a hexagonal pattern of 14 cm pitch with a 3 mm of inter wrapper gap. At the centre of the core, 19 S/As are removed in order to accommodate the spallation module. In order to flatten the radial power distributions, the two fuel core zones have different pin diameters but similar fuel/matrix volume ratios 45/55%. The transmutation performance of the core reaches its peak value with 42 kg/ TWth of burnt MA.

The primary system comprises a reactor vessel housing the core and internals, three separated IHX vessels connected to the core by three cross vessels including co-axial hot ducts, and six DHR vessels. The primary vessel accommodates the spallation module which is made of a tungsten and steel target cooled by helium. A cold window cooled by a specific circuit and a thimble which is the external shell of the module.

The main vessel is a pressurized vessel including a removable cover head, a cylindrical shell and an elliptical bottom head and housing the spallation module. The vessel diameter is 5.6 m and 7.5 m at the cover flange. It is almost 19 m high.

The three IHX vessels connected by the cross vessels (around 8 m long) comprise a 4 MW blower to run primary helium and a helical tubes heat exchanger with around 2500 tubes. The secondary fluid is supercritical $CO_2$ at 250 bars. A less challenging solution for the conversion cycle is the steam cycle at 180-190 bars, which gives the same efficiency in the considered range of temperature. The steam generator should be directly designed based on HTR past experience.

The DHR system is composed by six DHR vessels connected to the main vessel by means of six DHR ducts with expansion loops to accommodate the thermal expansion. Figure 11.2 displays the layout of the primary system of EFIT-He, including heat exchangers, pumps and spallation target circuit.

*This document refers to work being performed by scientists and institutions involved in IP EUROTRANS, as well as the financial support of the European Commission through the contract FI6W-CT-2004-516520.*

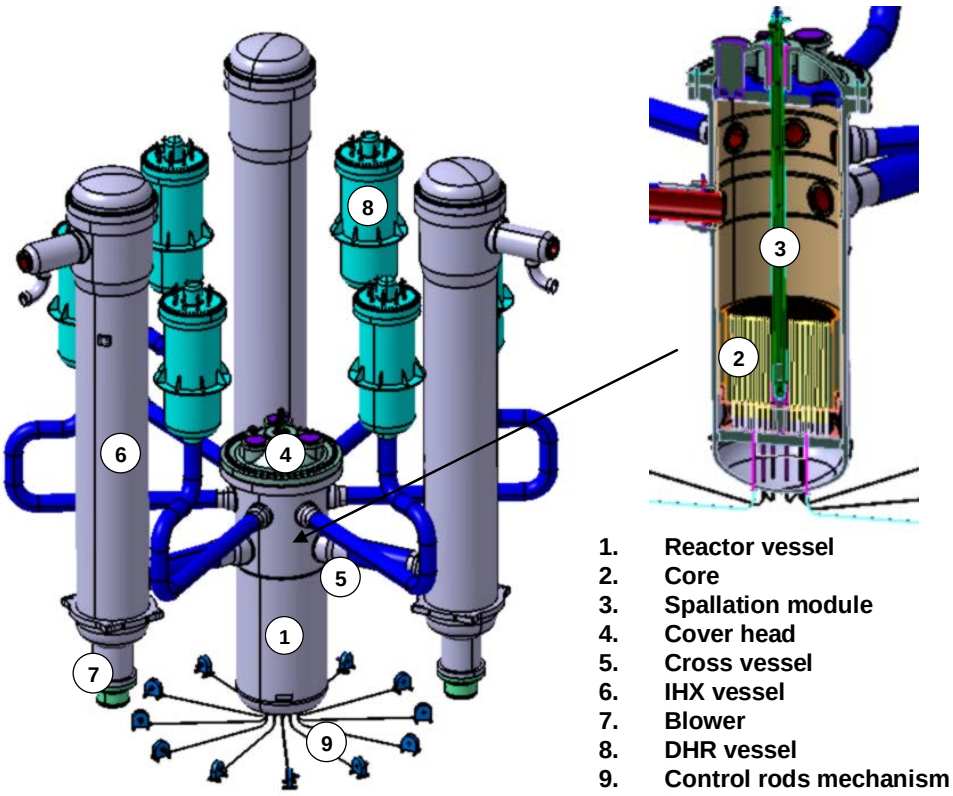


Figure 11.2: EFIT-He system layout

The feasibility of the design has been analyzed. The feasibility limit is reached for some components such as the helium blower (4 MW) or the exchanger (2500 helical tubes) as regard to the state of the art of HTR past experience.

Some open issues and future R&D needs can be noticed such as the passive behavior of the DHR system, or some components material. For instance, the thimble material needs to be validated by R&D considering the high temperature (572°C) and the irradiation damages.

## 11.4 Design: XT-ADS

The main objectives of XT-ADS are to serve as a fast neutron irradiation facility while proving the feasibility of heavy liquid metal coolants as well as the concept of coupling between accelerator and sub-critical core at high power. As such, its design is based on more conventional MOX fuel in conjunction with lead-bismuth coolant. The technology of the former is proven at industrial scale, and the latter would permit the operation at lower temperatures than pure lead does. The core contains a window-less spallation target featuring an off-centered spallation geometry (see section 11.5 below) and eight positions for experimental in-pile sections (IPS). At beginning of life, 68 fresh fuel assemblies, each with 90 fuel pins containing 35% Pu, yield a hot zero power (T=200°C) K-effective equal to 0.948. Taking temperature feedbacks into account, K-effective is reduced to 0.938 under operating conditions. The permissible operational K-effective of 0.95 is obtained by requiring at least 1000 pcm margin to criticality in the worst conceivable condition, including a core compaction effect of 1860 pcm and a maximum coolant void effect of 440 pcm. Under equilibrium conditions, 75 sub-assemblies are requested to achieve similar values for K-effective as for the fresh core. A five-step loading cycle is foreseen, where 15 sub-assemblies are replaced after 90 days of operation. A reactivity loss of 1220 pcm per cycle has been calculated, which will be compensated by increasing the proton beam current. The neutron flux in the three IPSs located closest to the target is about $1.4 \times 10^{15}/cm^2/s$

*This document refers to work being performed by scientists and institutions involved in IP EUROTRANS, as well as the financial support of the European Commission through the contract FI6W-CT-2004-516520.*

at EOC, corresponding to a maximum proton beam current of 3.4 mA for the 600 MeV accelerator of XT-ADS.

The MOX fuel pins have a an outer diameter of 6.55 mm and an active fuel column height of 600 mm. Including the gas plenum spaces, the total length of the fuel pin is 1400 mm. The pin pitch is 9.23 mm.

The coolant inlet temperature of XT-ADS has been fixed at 300°C. Postulating a coolant outlet temperature of 400°C, the required coolant channel velocity is 1.6 m/s. Since there is a significant by-pass flow through dummy-assemblies, the average inlet temperature of the primary heat exchangers is about 370°C.

Figure 11.3 displays the layout of the primary system of XT-ADS, including heat exchangers, pumps and spallation target circuit.

There are four primary heat exchangers, arranged two-by-two, each providing a heat removal of 17.5 MW. The secondary system hence is able to support a total power of 70 MW, resulting in some margin with respect to the 57 $MW_{th}$ design power of the core. As secondary coolant low pressure boiling water has been selected, the cold (T = 300°C) lead-bismuth is then directed through the two primary pumps which are co-assembled with the steam generators in a casing hung from the reactor roof. Each pump should provide a mass flow of 3500 kg/s and a pump head of 1.3 bars. The relative velocity of the impeller blades then becomes as high as 9.1 m/s, which will require the development of a highly erosion resistant surface coating on the blades. As for the case of EFIT, MAXTHAL materials (TiSiC) are considered.

Decay heat removal under normal operation conditions is provided by the redundant but non-safety graded secondary cooling system. Diversity of the decay heat removal function is provided by a safety-graded reactor vault cooling system (RVACS). The RVACS is placed between the guard vessel and the concrete pit. The RVACS consists of an annular bundle of U-pipes where atmospheric air is flowing, pipe side in natural circulation. Pipe legs connected to the air inlet manifold face the pit wall, whereas the return pipe legs face the safety vessel. Depending on outdoor temperature, the RVACS removes between 220 and 270 kW under normal operation, when the vessel wall is kept at 300°C.

***This document refers to work being performed by scientists and institutions involved in IP EUROTRANS, as well as the financial support of the European Commission through the contract FI6W-CT-2004-516520.***

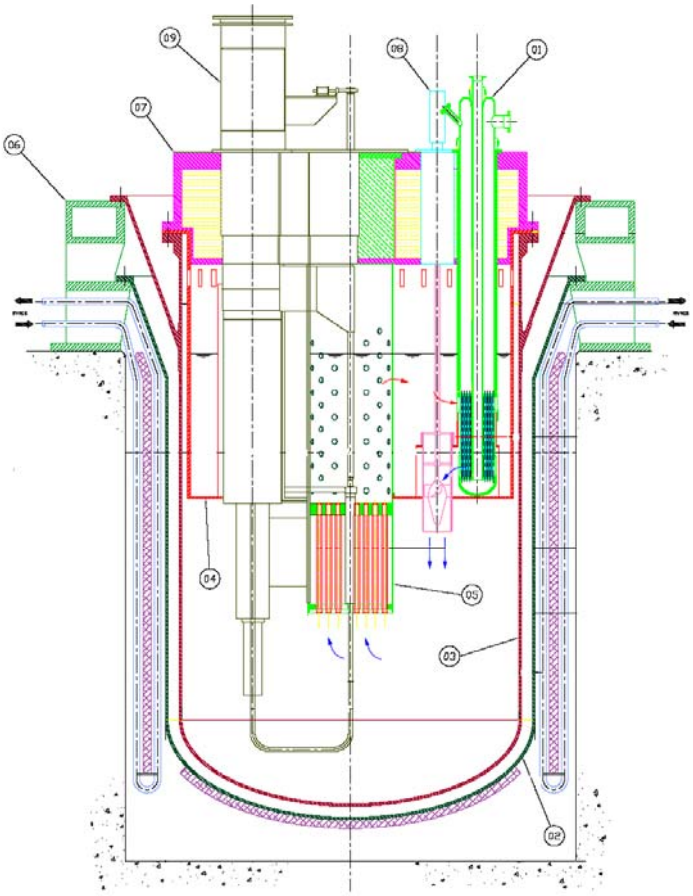

1. PHX (2X2)
2. Safety vessel
3. Reactor vessel
4. Inner vessel
5. Core Barrel
6. Support
7. Reactor Cover
8. Primary Pumps (2X1)
9. Spallation loop

Figure 11.3: XT-ADS system layout

## 11.5 Accelerator

The accelerator will deliver a proton beam to the spallation target, providing the neutron source required for driving the power production in XT-ADS and EFIT. In case of the 57 $MW_{th}$ XT-ADS, a proton energy of 600 MeV and a maximum current of 3.5 mA is foreseen, and for the latter an energy of 800 MeV and a current of 20 mA is sufficient to drive the 400 $MW_{th}$ EFIT core. These design parameters are considered to be technically well within reach. More challenging will be the requested reliability. If frequent beam trips should last longer than three seconds, the thermo-mechanical impact may become detrimental for integrity of structural components. Longer trips may demand the whole system to be shutdown, after which a lengthy restart procedure of the order of 20 hours must be undertaken, thus reducing its availability.

Following an analysis of the permitted quick and emergency stops in Phénix, less than ten beam trips lasting longer than three seconds are permitted per 90 day-cycle of XT-ADS operation. In the case of EFIT,

*This document refers to work being performed by scientists and institutions involved in IP EUROTRANS, as well as the financial support of the European Commission through the contract FI6W-CT-2004-516520.*

an even more demanding limit of three such trips per year is requested. In order to approach this high reliability, a linear accelerator operating in continuous wave (CW) mode has been selected. Low frequency 0.2 ms long beam interruptions would be applied for sub-criticality monitoring purposes.

The accelerator concept developed for XT-ADS and EFIT comprises of a dual beam injector and a fully modular superconducting LINAC. The injectors are composed of a 50 kV proton source, a 3 MeV radio frequency quadropole (RFQ), a normal conducting and a superconducting DTL structure. Here, the RFQ is designed to handle up to 30 mA CW beams and the superconducting solenoids bring the proton energy up to 17 MeV.

From 17 MeV, the superconducting LINAC accelerates the proton beam up to final energy, which for the 600 MeV XT-ADS corresponds to a length of about 240 meters. The LINAC is composed of an array of independently powered spoke and elliptical cavities with a moderate energy gain per cavity. The 25 MV/m peak field under normal operating conditions provides sufficient margin to implement fault-recovery techniques required to meet the reliability objectives defined above. The penalty in terms of accelerating length is estimated at 20%. A conservative optical design ensures low sensitivity to mismatches or current fluctuations, producing a very low emittance growth of about 5%.

The philosophy for recovery from a cavity fault consists of adjusting the accelerating gradient of neighboring cavities. Hence, the importance of operating the cavities below their design value is being stressed. Simulations show that a 20-30% rise in accelerating field can be sustained in a few (four to eight) retuned elements. The retuning can be achieved within one second using dedicated diagnostics and control instruments. Simulations show that by this approach the number of un-desired beam shutdowns might be reduced by a factor of 20, allowing to achieving the reliability goal for XT-ADS.

## 11.6 Spallation target

A major objective in the design of the spallation target of XT-ADS was to minimise its in-core footprint, for the purpose of increasing source efficiency and maximising the fast neutron flux in the experimental in-pile sections. Further, the space above the core is crowded with experimental in-pile sections. An off-centre loop was therefore designed, with pumps and heat exchanger located outside of the core (see Figure 11.2). Consequently, it was sufficient to remove three central fuel assemblies of the core lattice to host the spallation loop. A windowless design was with vertical confluent flow was adopted to make best possible use of the limited space available. Therefore, a strict control over the flow dynamics and the recirculation zone is necessary. Following mock-up experiments with water a nozzle design with flow detachment was chosen. In order to manage start-up and shutdown processes, an extra free surface was added just below the target zone, acting as a buffer.

In order to limit evaporation of the lead-bismuth from the free surface, the maximum temperature allowed in the target was set to 430°C. A two-pump solution was selected to drive the flow, one electromagnetic pump yielding a 2.5 bar pressure head in the return line, and one smaller of 1.5 bar in the feeder line.

## 11.7 Safety analysis

Safety approaches for XT-ADS and EFIT have been defined. Mission failures and combination of failures were classified as Design Basis Condition events of category II-IV (DBC), depending on their expected frequency and consequences for continued plant operation. Design Extention Conditions (DEC) consisting of DBC3 and DBC4 events combined with failure of a highly reliable mitigation system were assessed. None of these combinations should lead to the need of off-site emergency response. In addition, DEC events postulated independently of their frequency, should not exhibit any cliff-edge effect leading to severe core damage. Finally, severe accidents, where core damage is combined with loss of off-site power, should not lead to the need of off-site emergency response.

These objectives were translated into design criteria for the integrity of the fuel, its cladding, the primary vessel and the containment. The following set of enveloping transients were then analysed in protected and unprotected modes (where the unprotected mode typically corresponded to a DEC event):

*This document refers to work being performed by scientists and institutions involved in IP EUROTRANS, as well as the financial support of the European Commission through the contract FI6W-CT-2004-516520.*

- Loss Of Heat Sink (LOHS)
- Loss Of Flow (LOF)
- Loss of Direct Reactor Cooling system (Loss of DRC)
- Loss of heat sink combined with loss of flow
- Over-cooling
- Water ingress
- Sub-assembly blockage
- Transient Over Power (TOP)

It was found that the performance of the lead cooled EFIT was very robust, which may be ascribed to a combination of favourable physical properties of lead combined with the high thermal inertia, excellent natural convection characteristics and moderate power density of the particular design.

The sub-critical operation of the core obviously also contributed essentially to the stability of EFIT-lead, having a core with a detrimental combination of negligible Doppler feedback and large positive coolant temperature coefficient, as consequence of the high americium loading in the fuel.

The core was shown to remain intact for all DBC events analysed, leading to no release of radioactivity. Three DEC events were found to lead to possible concerns:

1) The combined loss of heat sink/loss of flow event, causing clad melting,
2) The unprotected blockage event, resulting in clad rupture in the blocked subassembly
3) The unprotected overcooling accident, leading to near freezing of the primary coolant.

In case (1), the containment function will have to be relied on. SIMMER analysis of the unprotected blockage could show that failure propagation to neighboring assemblies did not take place provided a few percent of coolant flow was retained, and hence no cliff-edge effect results. In order to avoid freezing of the primary coolant in case (3), tripping of the secondary pump must be assured within several tens of seconds.

Source term analysis for EFIT-lead and XT-ADS could show that heavy liquid metals have an excellent retention capability for volatiles and polonium. Even at T = 1200 K, the volatilised fraction of iodine would be less than 100 ppm and that of polonium less than 1 ppm. The low production rate of polonium in the lead cooled EFIT then means that I-131 would be the leading concern when estimating doses to the public. The containment assessment for EFIT however clarifies that the full release of iodine (and noble gases) from a single fuel assembly would not result in a dose to an infant exceeding 50 mSv, even without any containment function. The ability of the containment to retain iodine and noble gases in case (1) above would have to be of the order of 100-1000 to meet the DEC requirement of no off-site emergency response. Here, one should also note that the complete loss of heat sink is an overly conservative assumption.

A similar analysis made for XT-ADS indicates that the equilibrium inventory of Po-210 in the cover gas could give rise to a dose exceeding 700 mSv for high coolant temperatures. A filtering system able to retain at least 95% of the cover gas inventory would therefore have to be implemented, if one cannot show that LBE temperatures approaching 1200 K can be excluded under all circumstances.

## 11.8 Cost analysis

A detailed cost analysis has been performed for XT-ADS. It resulted in a base cost of 784 M€, including costs for manufacturing, construction, material procurement, installation, commissioning, insurance, spare parts and contingencies. The contingency consists of engineering and overlooked ambiguities, unexpected changes in costs and rates, construction problems, planning shifts, inaccurate estimations and unforeseen costs.

Costs for dismantling and decommissioning have not been considered. This is also the case for financial costs, such as interest during construction and governmental fees.

For EFIT-lead, the best estimated price is obtained by scaling from XT-ADS data when appropriate. References from the ELSY project have also been utilised. The analysis results in a best estimate price of 1.89 M€, with a low and high price of 1.47 /2.30 M€, respectively. The leading cost is that for the

*This document refers to work being performed by scientists and institutions involved in IP EUROTRANS, as well as the financial support of the European Commission through the contract FI6W-CT-2004-516520.*

accelerator, including accelerator buildings, utilities and management, comprising 35.2% of the total cost. Other buildings and civil structures come in second with 16.4% of the estimated costs. One may note that the primary system (including the minor actinide based fuel for the first core) constitutes only 10.1% of the total cost.

## 11.9 Perspectives

The radioactive waste which is produced in nuclear fission energy generation is mainly contained in the spent fuel, which is highly radioactive for a long time. The main concern in the disposal of this waste is related to the long-lived radionuclides, some of which will remain hazardous for tens of thousands of years.

Large efforts to resolve this issue are under way concentrating on the disposal of the nuclear waste in deep geological repositories. Parallel to this approach, the strategy of partitioning and transmutation (P&T) of the high-level nuclear waste is investigated. Even if a final repository would still be needed for the losses of the P&T strategy and for the high-level wastes which do not undergo the transmutation process, the strategy of P&T could reduce the radiotoxicity of high-level wastes and thus ease the long-term safety issue of a final repository. Any step towards the technological realisation of transmutation in Europe could have a positive influence on the improvement of public acceptance of nuclear fission electricity production. This will enhance the actual nuclear renaissance in Europe and world-wide, which in turn would reduce Europe's steadily increasing dependency on energy imports.

As EUROTRANS and their partners enhanced the direct exchange of information and results with the waste disposal community, this project considerably contributed to bringing together P&T and waste disposal, so as to produce a better common understanding.

The Integrated Project EUROTRANS has been devoted to transmutation of high-level wastes from nuclear power plants, focusing on transmutation in an Accelerator Driven System (ADS). Within EUROTRANS, the design and the feasibility assessment of an industrial ADS prototype dedicated to transmutation has been done. Although significant progresses on the R&D in the areas of fuel, technology and nuclear data have been achieved, there are still significant R&D progresses required prior to its construction. This is also the case for the XT-ADS whose construction plans are foreseen much sooner than EFIT-Pb.

Within the EURATOM Framework Programme, EUROTRANS will be followed by other programmes such as:

- Specific Targeted Research and Training Project REDIMPACT (Impact of Partitioning, Transmutation and Waste Reduction Technologies on the Final Nuclear Waste Disposal),
- Collaborative Project ACSEPT (Actinide reCycling by SEParation and Transmutation), i.e. the follow up of the FP6 Integrated Project EUROPART (EUROpean research programme for the PARTitioning of minor actinides and some long-lived fission products from high active wastes issuing the reprocessing of spent nuclear fuels),
- Network of Excellence ACTINET-6 (Network for Actinides Sciences),
- Collaborative project ANDES, Accurate Nuclear Data for nuclear Energy Sustainablity, CP-FP project, FP7-249671, a follow up of DM5 NUDATRA of the IP EUROTRANS,
- Collaborative project FAIRFUELS (FAbrication, Irradiation and Reprocessing of fuels and targets for transmutation) ", a follow up of DM3 AFTRA of the IP EUROTRANS, with Post-Irradiation Examinations of MgO-CERCER and Mo-CERMET fuels tested within the frame of FUTURIX-FTA and HELIOS irradiation experiments,
- Integrated Infrastructure Initiative VELLA (Virtual European Lead Laboratory),
- Collaborative Project CDT (Central Design Team for a Fast-spectrum Transmutation Experimental Facility),

*This document refers to work being performed by scientists and institutions involved in IP EUROTRANS, as well as the financial support of the European Commission through the contract FI6W-CT-2004-516520.*

- Collaborative Project LEADER, following the Specific Targeted Research and Training Project ELSY (European Lead Cooled System),
- Collaborative project GETMAT (GEn IV and Transmutation MATerials) ", a follow up of DM4 DEMETRA of the IP EUROTRANS.
- Collaborative project F-BRIDGE (Basic Research for Innovative fuels Design for GEN IV systems),
- Support Action EUFRAT (EUropean Facility for innovative Reactor And Transmutation neutron data) which is the follow-up of the FP6 Transnational Access Project NUDAME and the Integrated Infrastructure Initiative EFNUDAT (European Facilities for Nuclear Data Measurements).
- Collaborative project MAX "Myrrha Accelerator eXperiment, research & development programme", a follow up of WP3 of the DM1 Design of the IP EUROTRANS.
- Collaborative project FREYA "Fast Reactor Experiment for hYbrid Applications" to support the GUINEVERE experimental programme, launched within the DM2 ECATS of the IP EUROTRANS.
- And the Sustainable Nuclear Energy Technology Platform (SNETP) which puts ADS in perspective within the more general framework of a sustainable nuclear energy for Europe.

By combining the results of the above projects with those of EUROTRANS, it is expected that enough technical and economical elements will be available in order to perform a consistent and complete feasibility assessment and cost estimate between the strategy of ADS-based transmutation and other strategies, e.g. transmutation based on critical fast reactors. This assessment will be an essential input element for decision makers whether to embark on the implementation of an ADS-based transmutation in the future at the European level.

# 12. ACKNOWLEDGEMENTS

The authors appreciate the efforts of all the scientists and institutions involved in EUROTRANS, as well as the financial support of the European Commission through the contract FI6W-CT-2004-516520.